Novel drug delivery systems for *in-vitro* cancer treatment

by Meenu

Thesis submitted in fulfilment of the requirements for the degree of

Doctor of Philosophy

under the supervision of Wei Deng and Andrew Care

Certificate of Original Authorship

I, Meenu, declare that this thesis is submitted in fulfilment of the requirements for the award of Doctor of Philosophy, in the School of Biomedical Engineering, Faculty of Engineering and IT, at the University of Technology Sydney.

This thesis is wholly my own work unless otherwise referenced or acknowledged. In addition, I certify that all information sources and literature used are indicated in the thesis.

This document has not been submitted for qualifications at any other academic institution.

Production Note:
Signature: Signature removed prior to publication.

Date: 08/06/2024

Acknowledgments

First and foremost, I would like to express my deepest gratitude to my primary supervisor, Wei Deng, for her exceptional mentorship and unwavering support throughout my degree. This achievement would not have been possible without her guidance.

I am also profoundly grateful to my co-supervisor, Andrew Care, for his invaluable advice and guidance.

A special thanks to Thuy Anh Bui for her assistance and support in the lab, both inside and outside of our research activities. I am also thankful to other members of our Deng lab group Xinpu, Emily, and Haoqi for making every moment in the lab enjoyable and fun. Thanks to Sarah, Eve, and Aysha for their help throughout my PhD journey.

I extend my sincere thanks to Gyorgy Hutvagner and Jiao Jiao Li for their insightful feedback during each of my candidature assessments.

Lastly, a heartfelt thanks to my family, including my husband, Saurabh, and my children, Sartaaz and Sierra, who stood by me throughout this journey. I am also deeply thankful to my parents for their unwavering support and encouragement, which have enabled me to reach this milestone in my life.

Impact due to COVID-19 and change of supervisory panel

COVID-19

I began my PhD journey in January 2020, and the first two years of my work were significantly affected by the COVID-19 pandemic. Lockdown measures, lab closures, delays in instrument inductions, and disruptions in the shipment of chemicals and reagents were among the challenges faced. Due to the restrictions imposed by COVID-19, I had limited opportunities to work in the laboratory, with more than nine months of restricted access in 2020 and three months in 2021. This has resulted in the delay with the commencement of few project aims.

Change of Supervisor, PhD Project and School

In addition to the challenges posed by the pandemic, my Ph.D. journey also faced another challenge i.e. change in school and supervisory panel. My supervisory panel changed due to some unforeseen circumstances in 2022 (after 2 years of my PhD), and I got a transfer from the Graduate School of Health to the School of Biomedical Engineering. This transition took approximately six months, during which I commenced a new phase of my journey under the guidance of Dr. Wei Deng, starting in May 2022. This transition necessitated adapting to new academic surroundings and conducting research on a new project. Therefore, research Chapter 2 belongs to my current supervisor (Dr. Wei Deng), and Chapters 3 & 4 belong to my previous supervisor.

Despite these significant challenges, I was able to publish 3 first author papers (one review and 2 research papers)

1. **Mehta, M**., Bui, T. A., Care. A., & Deng, W. (2024). Targeted polymer lipid hybrid nanoparticles for in-vitro siRNA therapy in triple-negative breast cancer. Journal of Drug Delivery Science and Technology, 98, p. 105911. https://doi.org/10.1016/j.jddst.2024.105911.

2. **Mehta, M**., Bui, T. A., Yang, X., Aksoy, Y., Goldys, E. M., & Deng, W. (2023). Lipid-Based Nanoparticles for Drug/Gene Delivery: An Overview of the Production Techniques and Difficulties Encountered in Their Industrial Development. ACS materials Au, 3(6), 600–619. https://doi.org/10.1021/acsmaterialsau.3c00032.

3. **Mehta, M**., Malyla, V., Paudel, K. R., Chellappan, D. K., Hansbro, P. M., Oliver, B. G., & Dua, K. (2021). Berberine-loaded liquid crystalline nanostructure inhibits cancer progression in adenocarcinoma human alveolar basal epithelial cells in vitro. Journal of food biochemistry, 45(11), e13954. https://doi.org/10.1111/jfbc.13954.

Table of Contents

List of Figures and Tables

1. Literature Review

2. Targeted polymer lipid hybrid nanoparticles for *in-vitro* siRNA therapy in triple-negative breast cancer

3. Berberine-loaded liquid crystalline nanostructure inhibits cancer progression in adenocarcinomic human alveolar basal epithelial cells in vitro

4. Investigation of the anticancer potential of NFκB decoy oligonucleotide-loaded polysaccharide nanoparticles in lung cancer cells

Abstract

Breast and lung cancers collectively pose a significant global health burden, ranking among the top causes of cancer-related deaths worldwide. Triple-negative breast cancer (TNBC) stands out as an aggressive subtype of breast cancer, with limited treatment options and poor prognosis. Similarly, lung cancer is also characterized by its highly invasive and metastatic nature, leading to a poor prognosis. Standard treatment options for TNBC and lung cancer, including chemotherapy and radiation therapy, have limitations, such as significant side effects and the development of drug resistance. Hence, a treatment strategy that is both effective and safe would greatly benefit numerous cancer patients. Emerging treatment options such as plant-based and nucleic acid-based compounds show promise as safer alternatives. However, their clinical utility is hindered by challenges such as poor pharmacokinetic properties and delivery issues. Therefore, in this thesis, we have developed different nanoparticle drug delivery systems to safely deliver plant-based (berberine) and nucleic acid-based compounds (siRNA and NFκB decoy oligonucleotides (ODNs) to their target site, thereby enhancing their *in-vitro* therapeutic efficacy against both breast and lung cancer. The first research chapter focuses on developing targeted polymer hybrid nanoparticles to deliver siRNA, aiming to silence the X Box peotein-1 (XBP1) gene, a key driver of TNBC progression. Successful knockdown of the XBP1 gene with these nanoparticles significantly promoted cellular apoptosis, particularly under hypoxic conditions. The second research chapter investigates the potential of berberine-loaded liquid crystalline nanoparticles for *in-vitro* lung cancer treatment. Berberine, a natural compound with anti-cancer properties, faces challenges related to low bioavailability. Encapsulating berberine within nanoparticles improves its therapeutic effectiveness at lower doses against lung cancer cells. In the third research chapter, we explore the potential of polysaccharide-based nanoparticles to deliver NFκB decoy ODNs for inhibiting inflammation-mediated lung cancer progression. NFκB overexpression contributes to tumor aggressiveness by creating a pro-tumorigenic environment. The developed nanoparticles demonstrate high encapsulation efficiency and effectively inhibit inflammation-mediated cancer cell progression at lower doses, indicating safe and effective treatment method for lung cancer. In conclusion, by developing different nanoparticle delivery systems, this thesis offers a promising path toward more effective and safer treatments for these malignancies.

Chapter 1: Literature Review

Cancer, a multifaceted disease poses a significant health challenge, burdening both patients and healthcare systems all over the world. Breast and lung cancers are the most prevalent subtypes. Current treatment options, such as chemotherapy, radiation therapy, and surgery, have improved survival rates to some extent. However, these treatments are often accompanied by significant side effects. Furthermore, the emergence of drug resistance and tumor recurrence remain major obstacles to achieving long-term therapeutic success. Therefore, this chapter was focused on the extensive discussion of emerging advanced therapeutics, including plant-based and nucleic acid-based therapies targeting breast and lung cancer. It starts with a detailed overview of both the cancers including their prevalence, key biological features, available treatment options and their limitation, highlighting the urgent need for innovative and safe treatment methods. We further investigated emerging plant-based and nucleic acid-based therapies as potential treatment options for breast and lung cancer. In this part, we examined recent research where these therapeutic moieties have been incorporated into advanced drug delivery systems, showing effectiveness in both *in-vitro* and *in-vivo* models of breast and lung cancer. Our focus is to highlight the importance of advanced drug delivery systems in improving treatment outcomes and reducing side effects. Despite these therapies exhibiting promise in cancer treatment, they still faced some challenges that have been discussed in the last part of this chapter.

1.1 Breast cancer (BC)

BC is the most common cancer diagnosed in Australian women, accounting for 25% of all cancers diagnosed in women each year [1]. In 2023, an estimated 20,700 new breast cancer cases were diagnosed in Australian women. It is estimated that 3,220 women will die from breast cancer in 2024 [1]. The likelihood of a woman developing breast cancer increases with age and the presence of certain risk factors, such as a family history of breast cancer or specific genetic mutations [1].

1.1.1 Subtypes of BC

BC is characterized at the molecular level depending upon the expression or lack of expression of hormone receptors, i.e., estrogen receptors (ER), progesterone receptors (PR), and human epidermal growth factor receptor 2 (HER2). Based on hormonal receptor expression, breast cancer is divided into four subtypes: (1) luminal A and (2) B, which are recognized by the expression of hormonal receptors (ER+ and PR+) with or without HER2 expression, (3) basal-like cancerous cells, which lack all three hormonal receptors and are referred to as triple-negative breast cancer (TNBC), and (4) HER2+ which is characterized by overexpression of HER2

receptors (Figure 1.1). ER, a key diagnostic factor, is significantly expressed in 70-75% of invasive breast carcinomas [3]. PR, another diagnostic and prognostic biomarker, is found in over 50% of ER-positive patients and rarely in ER-negative breast cancer [2]. Both ER and PR serve as diagnostic and prognostic biomarkers [3], with higher PR levels linked to improved overall survival, time to recurrence, and treatment outcomes, while lower levels are associated with aggressive disease and poorer prognosis [4]. HER2 expression accounts for approx. 15–25% of breast cancers [5]. HER2 overexpression, an early event in breast carcinogenesis, leads to increased cancer cell growth, worse clinical outcomes, and a shorter disease-free period [6]. Serum HER2 levels are real-time markers for tumor presence or recurrence [7].

Luminal A and B

Luminal A and B are two subtypes of breast cancer, both characterized by estrogen receptor-positive (ER+) status, but they differ in several key aspects. Luminal A is the most common type of breast cancer, accounting for about 40% of all cases [8]. Luminal A breast cancer is ER and PR positive, but negative for HER2 [8]. These type of tumors are typically slow-growing and five-year survival rate is about 95% [9]. In contrast, Luminal B tumors, constituting 10–20% of luminal cases, may lack PR expression and typically have higher Ki-67 expression (>20%), indicating a faster growth rate and a less favorable prognosis [10]. Although, both subtypes respond to hormonal therapy, Luminal B tumors are more likely to require chemotherapy due to their aggressive nature. Overall, Luminal A tumors tend to have a better prognosis and slower growth compared to Luminal B tumors, reflecting their distinct molecular characteristics and clinical behavior [11, 12].

HER2 positive

The HER2-positive accounts for 10–15% of breast cancers and characterized by high levels of the HER2 protein while lacking ER and PR [13]. HER2 positivity confers more aggressive biological and clinical behavior. These subtypes have worse prognosis compared to luminal tumors. They require specific medications such as trastuzumab, trastuzumab combined with emtasin (T-DM1), pertuzumab, and tyrosine kinase inhibitors like lapatinib and neratinib targeting the HER2/neu protein along with surgery and chemotherapy [14]. They respond well to chemotherapy. These cancers often spread to the bones, and there is a higher chance of recurrence to other organs compared to the luminal subtypes [15].

TNBC

TNBC constitutes 20% of all breast cancers and lacks estrogen receptors (ER-negative), progesterone receptors (PR-negative), and HER2 (HER2-negative). It is more common in women

under the age of 40 [16]. This subtype of breast cancer is further categorized into various subgroups, including basal-like (BL1 and BL2), claudin-low, mesenchymal (MES), luminal androgen receptor (LAR), and immunomodulatory (IM), with basal-like subgroups being the most common, comprising 50–70% of cases, and claudin-low following with 20-30% of cases. Each subgroup has distinct clinical outcomes, phenotypes, and responses to pharmacological treatments [16]. The risk of developing TNBC varies with genetics, race, age, weight and obesity, breastfeeding patterns, and parity [17]. TNBC is characterized by its aggressiveness, early relapse, and a greater tendency to present in advanced stages. high proliferation rate, alteration in DNA repair genes and increased genomic instability [17]. The depletion of target receptors has resulted in a lack of effective treatments for TNBC. Therefore, chemotherapy is the only alternative which can be used to treat TNBC patients on a systemic level [18, 19].
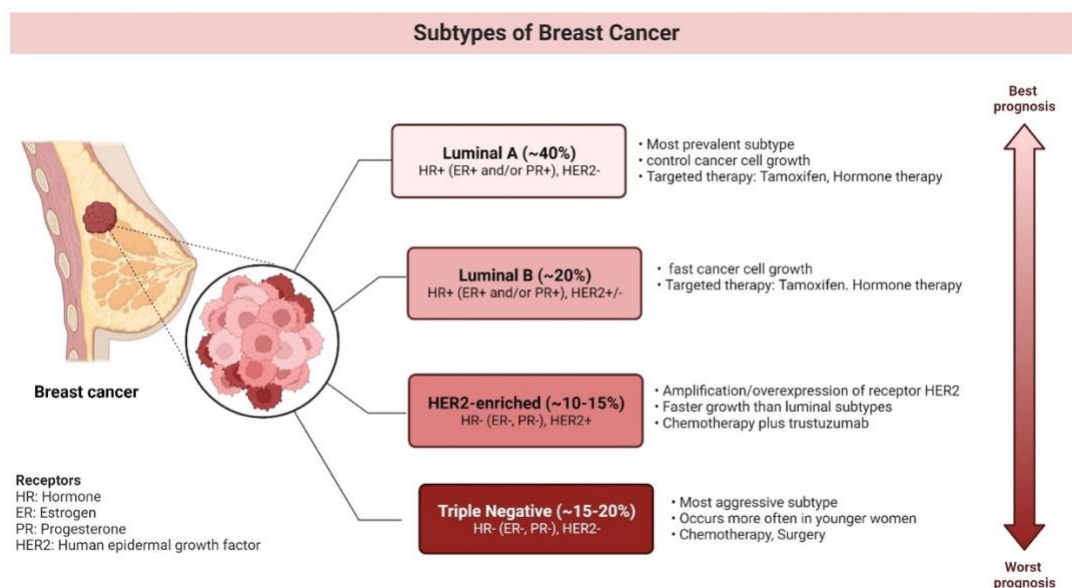
Figure 1.1: Subtypes of breast cancer

1.1.2 Currently available treatments for BC

Nowadays, the major therapeutic options for BC include surgery, chemotherapy, radiation therapy, immunotherapy, endocrine therapy and targeted therapy [20]. The choice of breast cancer treatment is influenced by many factors such as cancer type, stage, location, patient age, overall health, prior treatments, the expected benefits and side effects [20].

Surgery

Surgery serves as the primary intervention for most breast cancer patients, aiming to effectively eliminate tumors to reduce the risk of local recurrence. It plays a crucial role in minimizing cancer growth and preventing its spread to other body parts [21]. The most standard breast surgery

approaches are either total excision of the breast (mastectomy), usually followed by breast reconstruction, or breast-conserving surgery (lumpectomy). Breast-conserving surgery is frequently chosen as the initial approach, particularly due to the typically small size of most cancers. Mastectomy, considered as a secondary option, involves the removal of the entire mammary gland. Additionally, lymph node removal in the armpit region may be conducted based on individual lymph node status and the aggressiveness of the cancer in each patient [22].

Radiation therapy

Radiation therapy, or radiotherapy, employs high-energy X-rays to destroy cancer cells, preventing their continued growth. It is utilized for both primary and progressive carcinomas [23]. This treatment can be administered alone or in conjunction with other therapies such as surgery and/or chemotherapy [23]. The primary objective is to eliminate any remaining breast cancer cells that may not have been completely eradicated after surgery [24]. Radiation therapy is recommended following breast-conserving surgery, post-mastectomy for tumors exceeding 5 cm in size, or in cases where malignant cells have metastasized to the lymph nodes [24].

Chemotherapy

Chemotherapy involves the use of cytotoxic chemicals to destroy malignant cells or inhibit their growth [25]. These chemotherapeutics can be derived from natural sources or synthesized in laboratories. It is a preferred treatment for various classes of breast carcinomas. Chemotherapy can be administered either individually, with multiple anticancer drugs simultaneously, or in combination with other treatments, such as before or after surgery or radiation therapy [25].

Hormone therapy

Hormone therapy is a crucial component of breast cancer treatment, particularly for cancers that are hormone receptor-positive [26]. In this type of therapy, medications are used to block hormones like estrogen and progesterone that can fuel the growth of certain breast cancers. By inhibiting these hormonal signals, hormone therapy aims to slow down or stop the growth of cancer cells [26]. This approach is commonly employed in cases where the cancer cells have receptors for estrogen (ER-positive) or progesterone (PR-positive) [26]. Hormone therapy may be used after surgery or other primary treatments to reduce the risk of cancer recurrence and improve overall outcomes. The specific hormone therapy drugs and duration of treatment are designed to the individual characteristics of the cancer and the patient [27].

Targeted therapy

Targeted therapies refer to a treatment strategy directed towards targeting specific genes, proteins, or tissue environments associated with cancer growth and survival [28]. These therapies work

differently than chemotherapy, aiming to slow down the growth and spreading of cancer cells while minimizing harm to healthy cells [29]. For example, HER2-targeted therapies, such as trastuzumab (Herceptin), pertuzumab and ado-trastuzumab emtansine (T-DM1), work by blocking signals that promote the growth of HER2-positive cancer cells [29].

1.1.3 Limitations associated with current treatments

While these treatments demonstrate remarkable therapeutic potential, they also possess various limitations. Surgery aims to remove tumors, but it may not prevent metastasis. Chemotherapy, while effective in killing cancer cells, often leads to adverse side effects due to its impact on both cancerous and healthy cells. often do not complete the prescribed course of chemotherapies due to intolerable and severe side effects [30]. Furthermore, chemotherapy involves the administration of multiple drugs in combination to enhance pharmacological effects. However, certain drugs, like the anthracycline derivatives doxorubicin (Dox) and daunorubicin, can lead to cumulative toxicity. This toxicity may hinder patients from completing the necessary dosage, which is crucial for eradicating residual cancer cells [31]. Radiation therapy, while successful in treating local carcinomas, can cause damage to nearby healthy tissues. This happens because the radiation can directly damage the DNA of cells or create harmful molecules called free radicals, leading to cell death. Over time, this damage can cause inflammation, scarring, and impaired tissue function [32]. Additionally, radiation therapy may have long-lasting side effects such as fibrosis, damage to blood vessels, and an increased risk of developing new cancers in the treated area [33]. Targeted therapies are specific to certain molecular characteristics, limiting their applicability to subsets of patients [34]. For example, about 20% of NSCLC patients with EGFR mutations respond well to drugs like gefitinib and erlotinib [35]. Another drug, pembrolizumab, targets the programmed death-ligand 1 (PD-L1) pathway and is effective only in patients with high PD-L1 levels [36]. Moreover, the emergence of resistance to these treatments poses a significant challenge, necessitating the exploration of alternative strategies. The adverse side effects and limited efficacy in preventing metastasis underscore the urgency for innovative approaches in breast cancer therapeutics.

1.2 Lung Cancer

Lung cancer, among the most common malignant tumors affecting the respiratory system, has very high rates of morbidity and mortality [37]. Lung cancer accounts for approximately 30 of every 100 cancer-related deaths [38]. Lung cancer cases increased by over 2 lakhs just in 2022. Additionally, the same year witnessed approximately 1.3 lakh deaths from lung cancer [39]. Apart

from smoking, environmental pollution, rapid development and urbanization constitute the major causes of lung cancer across the globe [40]. Based on the morphological forms, lung cancer is divided into two main categories, NSCLC and small cell lung cancer (SCLC) [41]. NSCLC is further divided into adenocarcinoma, squamous cell carcinoma and large cell carcinoma (Figure 1.2) [41]. Adenocarcinoma is more prevalent than squamous cell carcinoma in the majority of countries worldwide [42]. In developing countries, NSCLC is very common, primarily due to smoking, and it accounts for at least 85% of cases of lung cancer, whereas SCLC accounts for the rest of the 15% of cases [43].
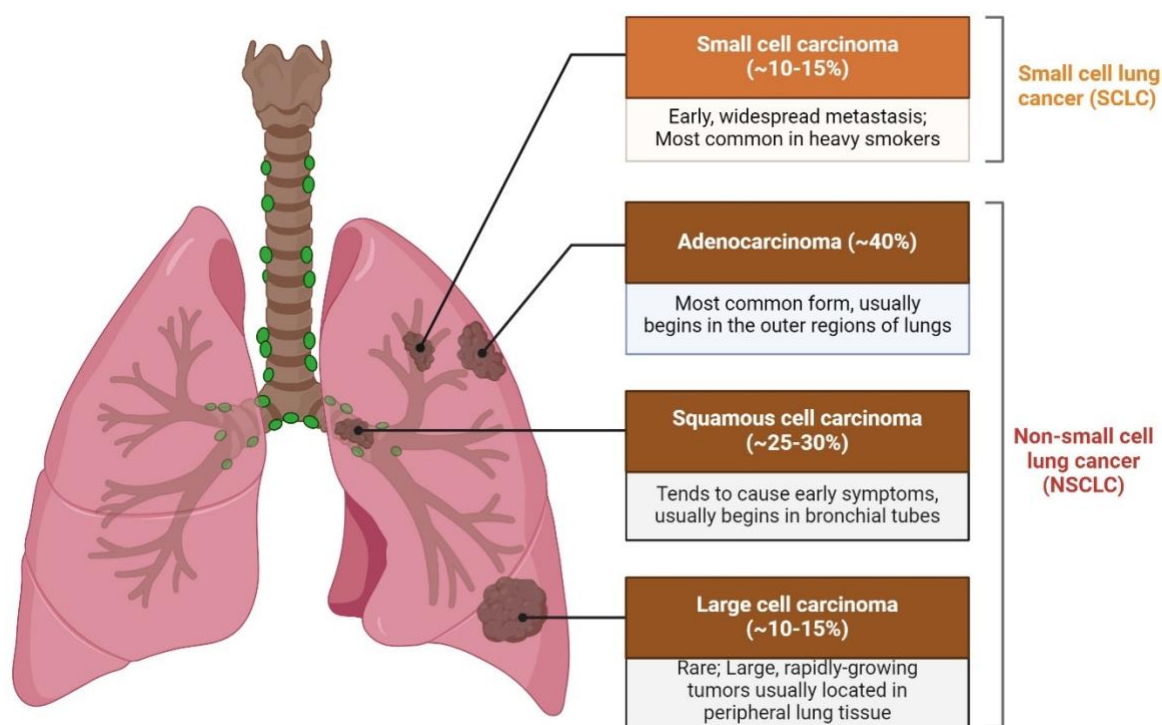
Figure 1.2: Subtypes of lung cancer

The existing treatment approaches for lung cancer primarily involve surgery, radiation, chemotherapy, immunotherapy and targeted therapy [44]. Surgical resection emerges as the most consistent and effective option, especially for patients in the early stages (I or II) of lung cancer [45]. In contrast, as the disease progresses to stage III or IV, the focus of treatment shifts toward chemotherapy or radiotherapy [46]. Chemotherapy faces various challenges such as non-specific targeting, low bioavailability and the development of drug resistance [47]. Additionally, it commonly induces adverse effects like nausea, fatigue, respiratory problems, and hair loss, limiting its effectiveness [46]. Radiotherapy induces damage to surrounding cells, leading to a considerable loss in lung functionality. Consequently, this approach may not be suitable for

patients with a severely compromised pulmonary system [48]. Immunotherapy has emerged as a revolutionary option for lung cancer treatment, by controlling the body's immune system to recognize and attack cancer cells [49]. In particular, immune checkpoint inhibitors like pembrolizumab and nivolumab have demonstrated significant success, particularly in NSCLC patients with high programmed death-ligand 1 (PD-L1) expression [50]. Targeted therapies, such as EGFR inhibitors (e.g., erlotinib) and ALK inhibitors (e.g., crizotinib), focus on specific genetic alterations within tumors, providing more specific and effective treatments for lung cancer patients [51]. Despite these emerging treatment options available for lung cancer patients, challenges still persist. These include resistance to targeted therapies and the need for personalized treatment plans [52]. While immune checkpoint inhibitors show promise, they can lead to side effects like lung inflammation or digestive issues, limiting their use for some patients. Additionally, not all patients benefit from immune checkpoint inhibitors, highlighting the need for alternative treatments [53]. Ongoing research aims to unravel the complexities of lung cancer biology, paving the way for novel therapeutic strategies and more precise interventions that consider the heterogeneity of lung tumors and individual patient profiles [51].

1.3 Drug delivery systems (DDS) for cancer treatment

The challenges of traditional cancer treatments have led to the rapid development of new methods to fight the disease [54]. One such advancement is DDS which has been developed to address several challenges associated with conventional therapies, including poor drug solubility, limited bioavailability, rapid degradation, and non-specific distribution [55]. DDS allows drugs to be enclosed in a protective carrier, ensuring their controlled release, improved stability and targeted delivery to cancer cells without harming healthy cells. This approach not only makes the treatment more effective but also allows for higher doses without increasing harmful side effects [56]. In cancer treatment, these advantages are crucial for improving patient outcomes and reducing side effects. DDS can be categorized into three main types: lipid-based, polymer-based, and inorganic-based delivery systems.

1.3.1 Lipid-based drug delivery systems

Lipid-based nanoparticles (LNPs) are a highly adaptable class of nanocarriers that have gained widespread usage in medical research and pharmacology [57]. They can encapsulate various therapeutic agents including small molecules, nucleic acids and monoclonal antibodies for a diverse range of applications [58]. LNPs offer several benefits, such as safeguarding drugs from in vivo degradation, boosting their solubility and efficacy, enabling targeted drug delivery to the disease site, regulating drug release, and altering drug biodistribution [59]. These engineered

nanocarriers hold the potential to overcome significant limitations of traditional therapeutic products such as inadequate efficacy, susceptibility to enzymatic degradation, low bioavailability, and off-target side effects [60].

LNPs typically consist of four main lipid components: phospholipids and cholesterol, which are necessary for particle formation and stability; cationic or ionizable lipids, which enable binding with negatively charged nucleic acids, thereby increasing drug loading; and PEGylated lipids, which contribute to enhanced particle stability and circulation time within the biological system . Due to their biomimetic architecture and the similarity of their lipid components to those of cell membranes, LNPs can easily cross the cell membrane to deliver nanoparticle contents to the desired intracellular sites. After crossing the cell membrane, LNPs can take advantage of the low pH environment within the target cells, promoting endosomal escape and releasing the therapeutic cargo into the cytoplasm 2.

LNPs can be categorized into five subgroups: liposomes, lipid nanoemulsions, solid lipid nanoparticles, nanostructured lipid carriers, and lipid-polymer hybrid nanoparticles. Our main interest is to explore **Lipid polymer hybrid nanoparticles (LPNs)**, a type of lipid nanoparticle that combines the advantages of lipids and polymers for various biomedical applications [61]. LPNs have polymer cores that contain therapeutic substances and lipid/lipid-PEG shells as a "stealth" coating for improved *in vivo* circulation [62]. This unique structural composition offers optimal biocompatibility and physical stability, making them an ideal vehicle for drug delivery [61]. LPNs have been successfully used to encapsulate various pharmaceuticals, including nucleic acids, for sustained release and improved stability [63, 64]. Furthermore, incorporating functional groups on the polymer surface facilitates targeted drug delivery to specific cells or tissues [63]. LPNs are gaining recognition as an advanced substitute for traditional liposomal and polymeric drug delivery systems due to their wide range of advantages, encompassing applications in combinatorial/active targeted drug deliveries, cancer gene therapy, vaccine development, and novel diagnostic imaging methods [65]. Encouraging results from Phase I and II clinical trials demonstrate the potential of LPNs in delivering the anti-cancer drug Docetaxel, particularly for lung, pancreatic, and prostate cancers

Liquid crystalline nanoparticles (LCNs) are an emerging lipid-based drug delivery system known for their ability to provide controlled, efficient, and targeted delivery of therapeutic agents [66]. Their key advantages, such as phase stability, enhanced bioavailability, and high drug-loading capacity make them particularly suitable for pulmonary delivery, especially in treating lung cancer and inflammatory diseases [66]. LCNs can passively accumulate in solid tumors through the enhanced permeability and retention (EPR) effect, leading to higher drug

concentrations at tumor sites [67]. For example, studies have shown that LCNs loaded with naringenin effectively inhibit lung cancer cell proliferation, migration, and colony formation. Notably, the encapsulation of naringenin in LCNs reduces the therapeutic dose required compared to its free form, enhancing both efficacy and safety [68]. Another study demonstrated the use of LCNs to deliver ellagic acid and Dox to A549 lung cancer cells. Surface-modified with lactoferrin, the nanocrystals targeted cancerous cells via the CD44 receptor, resulting in improved nanoparticle internalization and increased cytotoxicity [69]. Given these advantages, we have employed LCNs to encapsulate berberine, aiming for enhanced efficacy and targeted delivery in lung cancer treatment.

1.3.2 Polymer-based drug delivery system

Polymer-based drug delivery systems have garnered considerable attention over the past two decades because they offer the ability to specifically target tumor tissues and significantly improve the therapeutic window of the therapeutic [70]. For example, poly (lactic glycolic acid) (PLGA) is a biodegradable polymer that has been approved by the U.S. FDA, and several PGLA-based formulations have received clinical approval, including Decapeptyl, Suprecur MP, Lupron Depot, among others [71, 72]. These delivery systems offer key advantages such as surface adaptability, charge modification, and enhanced drug-loading capabilities, making them ideal for the controlled and sustained release of therapeutics [73, 74]. Natural polymers like chitosan and alginate are valued for their biocompatibility and biodegradability, though they often require modifications for better drug delivery performance [75].

Polymer-based nanoparticles can be engineered for passive targeting through the enhanced permeability and retention (EPR) effect, where the nanoparticles accumulate preferentially in tumor tissues due to the leaky vasculature and poor lymphatic drainage [76]. In addition to passive targeting, polymer-based nanoparticles can be functionalized with ligands such as antibodies, peptides, or folic acid to achieve active targeting, where the nanoparticles bind specifically to cancer cell receptors, increasing their therapeutic effectiveness while reducing off-target effects [77, 78]. Several studies have demonstrated the success of polymer-based nanoparticles in cancer treatment. For example, Dox-loaded PLGA nanoparticles have shown enhanced anticancer activity in breast cancer models due to their prolonged circulation and targeted drug release, reducing the systemic toxicity commonly associated with free Dox [79]. Similarly, paclitaxel (PTX) loaded PLA nanoparticles have improved therapeutic efficacy and lower side effects in lung cancer treatment [80]. These advances in polymer-based nanoparticle systems offer

significant potential for improving cancer therapy by providing targeted, controlled, and sustained drug delivery, ultimately enhancing patient outcomes while minimizing side effects.

Among the different types of polymeric systems, dextran-based nanoparticles have gained significant attention due to their unique properties and potential in cancer-targeted therapy. Dextran is an FDA-approved polysaccharide known for its high encapsulation efficiency, biodegradability, and ease of chemical modification to fine-tune drug release [81]. Acetalated dextran (AcDex) nanoparticles are especially promising because they are pH-responsive, allowing for selective drug release in acidic tumor environments [82]. Several studies highlighted the efficacy of dextran-based nanoparticles in improving drug delivery and cancer treatment. For instance, AcDex nanoparticles have been functionalized with spermine (SpAcDex) to enhance siRNA delivery to cancer cells. The study showed that nanoparticles successfully delivered siRNA to HeLa cells, leading to significant reductions in cell proliferation and migration [83]. Another study used SpAcDex nanoparticles to deliver a decoy oligodeoxynucleotide (ODN) that inhibits the NF-κB pathway in A549 cells, resulting in potent anti-cancer effects, including suppression of colony formation and tumor progression markers. Moreover, AcDex nanoparticles loaded with these drugs improve their therapeutic index by providing controlled release and targeted delivery, particularly in the lungs, where they can accumulate in cancerous tissues [84].

1.3.3 Inorganic-based drug delivery system

Inorganic-based nanocarriers offer remarkable potential in drug delivery due to their unique features, such as high surface area, tunable size and shape and ease of surface modification [85]. Additionally, they can be tailored with different ligands to enhance specificity and effectiveness for targeted treatments [85]. The main inorganic nanocarriers include gold nanocarriers, mesoporous silica nanocarriers, and magnetic nanocarriers.

Gold nanocarriers are particularly attractive for biological applications due to their ease of surface modification and lower toxicity than other metals. Some organic compounds (e.g., DNA and peptides) can be functionalized through bonds like Au–S or Au–thiol, which significantly enhances their bioavailability, making them useful in both tumor imaging and targeted drug therapy [86]. Kim et al. synthesized a radioactive iodine-labeled gold nanoparticle designed to target β integrins, which are overexpressed in tumors. Imaging results showed that the nanoparticle rapidly and efficiently targeted tumor sites within 10 minutes of injection, highlighting its strong potential for diagnostic and therapeutic applications [86].

Silica nanocarriers include silica nanoparticles, mesoporous silica nanoparticles (MSNs), hollow mesoporous silica, and silica nanotubes [87]. Among these, MSNs stand out for their high drug-loading capacity, large surface area and pore volume. Their surfaces can be easily functionalized with groups like amino and sulfhydryl, allowing for precise targeting and versatile drug delivery. An ideal MSN system ensures accurate tumor targeting, prevents drug leakage during circulation, and controls high-concentration drug release at the tumor site [88]. To achieve controlled drug release, MSNs can be modified to respond to external stimuli such as pH, enzymes, or temperature. For instance: Cheng *et al*. developed a pH-sensitive MSN system, which released Dox in acidic tumor environments, reducing toxicity to normal tissues while improving targeting efficiency and antitumor efficacy [89]. Similarly, Saini and Bandyopadhyaya designed transferrin-conjugated, chitosan-coated MSNs loaded with gemcitabine, which showed controlled release in the neutral environment but rapid drug release in the acidic tumor environment, enhancing therapeutic outcomes [90].

Magnetic nanoparticles have shown significant promise in drug delivery due to their ability to be guided to specific sites using external magnetic fields. Their biocompatibility and unique magnetic properties make them ideal for drug delivery and tumor hyperthermia. However, due to poor water solubility and aggregation, naked magnetic nanoparticles are prone to rapid clearance by the immune system. Therefore, surface modifications are essential to improve their stability and dispersion [91]. Huang *et al*. developed a nano-delivery system using superparamagnetic iron oxides coated with folic acid-modified polymers to deliver Dox. Results showed that nanoparticles effectively targeted MCF-7 breast cancer cells via folic acid receptor-mediated endocytosis and inhibited tumor growth under magnetic field guidance [92]. Wang *et al*. functionalized magnetic nanoparticles with an anti-EGFR monoclonal antibody for targeted lung cancer therapy. This modification increased the nanoparticle's specificity to tumor cells, improved the localised delivery of the drug and reduced off-target effects. Additionally, the magnetic properties of the nanoparticles enabled the use of magnetic resonance-guided focused ultrasound surgery, which further increased tissue heating in tumors and enhanced drug penetration, ultimately improving therapeutic outcomes [93].

In this thesis, three types of nanoparticles (Polymer lipid nanoparticles, liquid crystalline nanoparticles and polysaccharide-based nanoparticles) have been employed to enhance the delivery of different therapeutic agents (siRNA, berberine and NFκB decoy oligonucleotides).

Each type has been selected based on the specific challenges associated with the therapeutic agent being delivered, including its solubility and stability.

1.4 Therapeutic strategies targeting TNBC

As previously discussed, therapeutic strategies targeting TNBC encompass a variety of approaches, from traditional chemotherapy and targeted therapies to more innovative options like immunotherapy and antibody-drug conjugates., Building on these existing approaches, advanced therapeutic strategies such as RNA-based therapy have gained importance in the field of breast cancer treatment due to their ability to specifically target and manipulate the expression of genes involved in cancer development and progression [94]. Unlike traditional treatments, RNA-based therapies such as small interfering RNA (siRNA) and microRNA (miRNA) operate at the genetic level, enabling a more precise and personalized approach [94]. siRNA can selectively silence the expression of specific genes by degrading their messenger RNA. In contrast, miRNAs are involved in the regulation of gene expression by blocking the translation of specific mRNAs and lead to their degradation [95]. However, the systemic delivery of RNA-based therapies faces challenges, including susceptibility to degradation by nucleases and poor cellular uptake, which limit their therapeutic efficacy. Additionally, their large size and negative charge hinder their penetration through cellular membranes [96]. To overcome these challenges, a number of delivery systems have been developed (Figure 1.3). These delivery systems aim to protect the RNA molecules from degradation, enhance their cellular uptake and facilitate their intracellular release [97].
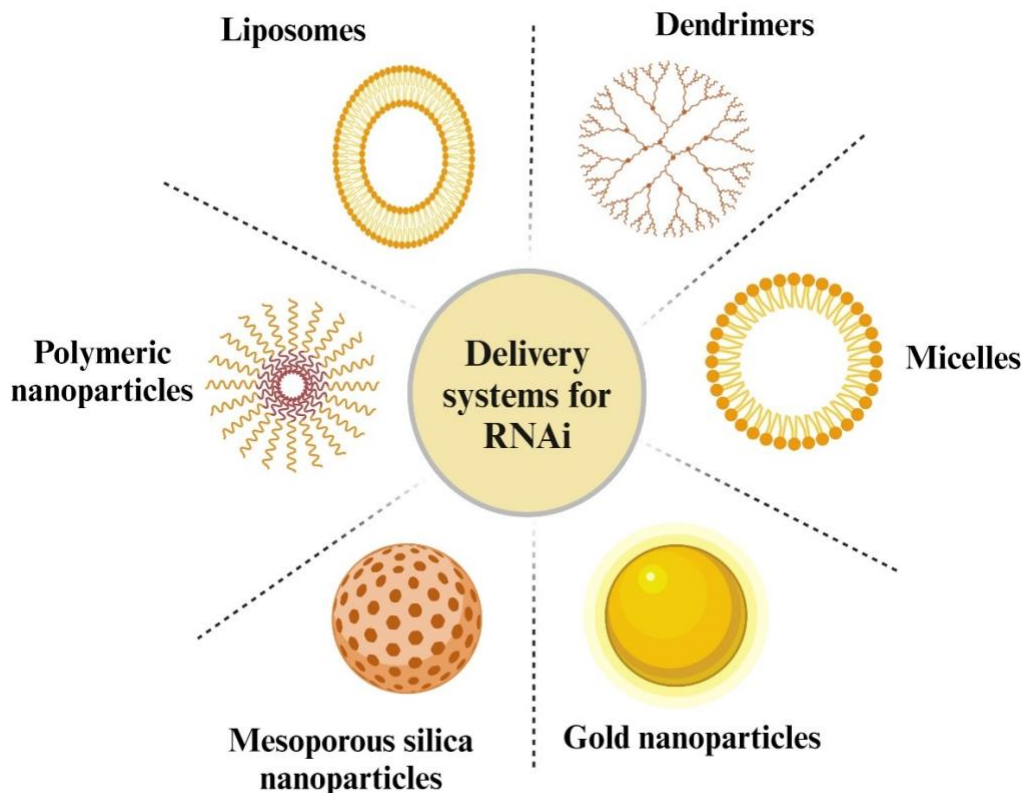
Figure 1.3: Delivery systems employed for RNA-based therapy

1.4.1 siRNA-based therapeutics

siRNA is a class of double-stranded RNA molecules that play a crucial role in gene regulation [98]. These molecules are involved in a process called RNA interference (RNAi), which is a natural mechanism for controlling gene expression. In RNAi, siRNA molecules specifically target and bind to complementary messenger RNA (mRNA) sequences, leading to their degradation and subsequent inhibition of protein synthesis (Figure 1.4a) [99]. This mechanism allows siRNA to selectively silence the expression of specific genes, offering a highly precise and targeted approach for modulating gene activity [98]. Various nanocarrier systems have been developed to optimize the delivery of siRNA for targeting TNBC (Table 1.1). Among these, liposomes are widely used as siRNA delivery vehicles due to their inherent characteristics. Their lipid bilayer structure closely resembles that of cell membranes, enhancing their compatibility with biological systems. This structural similarity facilitates a more efficient fusion of liposomes with cell membranes, thereby making them well-suited for cellular delivery. Furthermore, liposomes amphiphilic nature makes them versatile carriers for both hydrophilic and hydrophobic payloads [100]. Alshaer *et al*. utilized anti-CD44 aptamer-conjugated liposomes to achieve gene silencing

in a murine model of TNBC. In this study, the aptamer can specifically bind to CD44 receptors present in cancer cells, thereby enhancing the cancer cell targeting capability of liposomes to the tumor site. Results demonstrated effective gene silencing in both *in-vitro* and *in-vivo* models of TNBC [101]. Liposomes offer a versatile platform with the ability to encapsulate both hydrophilic and hydrophobic compounds, allowing for the co-delivery of siRNA and chemotherapeutic agents [102]. Deng *et al.* utilized cationic liposomes for the coencapsulation of PTX and siRNA, resulting in sustained drug release for up to 168 hours. This formulation not only significantly prolonged the biological half-life of PTX compared to the commercial PTX formulation but also exhibited enhanced anticancer activity [103]. Another study developed a novel redox-sensitive cationic lipid-based system that efficiently delivered both PTX and anti-survivin siRNA to target cells. *In-vitro* investigations revealed increased cellular uptake, successful endosomal escape, reduced survivin expression leading to decreased cell viability, and an elevated rate of apoptosis [104]. Deng and colleagues developed a layer-by-layer liposome-based nanocarrier for the co-delivery of siRNA and Dox to target TNBC. The combination therapy involved siRNA targeting multidrug resistance protein 1, which markedly increased *in-vitro* efficacy of Dox by 4 fold and led to an 8 fold decrease in tumor volume compared to control treatments. This system efficiently transported both the drug and siRNA to the tumor site, resulting in a substantial reduction in tumor volume without inducing toxicity, offering a safer therapeutic option for patients [105].

Table 1.1. Delivery systems used to deliver siRNA for targeting TNBC

Encapsulated drug	Delivery systems	Key findings	References
Cell death siRNA	Lipid-coated calcium phosphate nanoparticles	Successful delivery of siRNA to TNBC tumors, leading to effective gene silencing and tumor growth inhibition.	[106]
S100 calcium binding protein A4 (S100A4) siRNA	Exosomes	Enhanced stability, reduced immunogenicity, remarkable gene-silencing efficacy leading to a substantial inhibition of malignant breast cancer cell growth.	[107]

GFP siRNA	PEGylated superparamagnetic iron oxide nanoparticles functionalized with gH625 peptide, chitosan and poly-l-arginine	The gH625 peptide facilitates the internalization of nanoparticles into cancer cells, while cationic polymers offer protection to siRNA and facilitate its escape from endosomes, resulting in >73% GFP gene silencing	[108]
XBP1 siRNA+Dox	RNA nanoparticles	Reduce XBP1 expression, inhibit tumor growth upon intravenous administration, enhance sensitivity to chemotherapy	[109]
Aurora kinase A (AURKA) siRNA + PTX	Redox-sensitive hyaluronic acid-based nanoparticles	Adjustable PTX loading, selective drug release and concentration-dependent gene silencing, Successful delivery of both drug and siRNA showed synergistic effects which leads to higher antitumor efficacy	[110]
Inhibitor of nuclear factor kappa-B kinase subunit epsilon (IKBKE) siRNA+cabazitaxel	Hyaluronic acid modified lipid micelles	Enhanced cellular uptake and better tumor penetration of the encapsulated cargos, effectively inhibits invasiveness and growth of TNBC	[111]
Cell-division cycle protein 20 (CDC20) + CD44 siRNA	Hyaluronic acid-modified polymer complexes	Polymer complexes efficiently delivered siRNAs against key	[112]

		proteins involved in cell cycle regulation and phosphatase activity, effective inhibition of TNBC cell growth and migration	
Indocyanine green + PTX + survivin siRNA	Polymeric nanoparticles	Higher cellular uptake, controlled drug release, and improved antitumor efficacy due to the combined effects of photothermal therapy, gene delivery, and chemotherapy	[113]
Pyruvate kinase isozymeM2 (PKM2) siRNA	Chitosan-gold nanoparticles	The chitosan layer enhances the delivery of siRNA, allowing for efficient photothermal ablation and gene silencing, ultimately inhibiting the invasiveness and growth of TNBC cells.	[114]
Cell-penetrating peptide+EGFR siRNA	Lipid-based nanobubbles	The combination of nanobubbles and ultrasound enhances the cellular uptake of siRNA, improves the precision and effectiveness of gene silencing within TNBC cells	[115]

1.4.2 miRNA-based therapeutics

Dysregulated expression of miRNAs is frequently associated with the initiation, progression, and metastasis of breast cancer, making them attractive targets for therapeutic intervention [116]. miRNA-based therapies can be broadly categorized into two approaches: miRNA replacement therapy and miRNA inhibition therapy. In miRNA replacement therapy, synthetic miRNA mimics

are introduced to restore the levels of specific miRNAs that are downregulated in breast cancer [117]. miRNA inhibition therapy involves the use of antisense oligonucleotides, antagomirs, or other inhibitors to block the activity of overexpressed oncogenic miRNAs (Figure 1.4b) [117]. Similar to siRNA therapy, various nanocarrier delivery systems have been developed to enhance miRNA stability, protect against degradation and facilitate targeted delivery [118].

miR-34a emerges as a key player, suppressing TNBC cell proliferation, migration and invasion [119]. Wang *et al*. utilized hyaluronic acid/protamine sulfate nanocapsules to deliver miR-34a, achieving targeted inhibition of CD44 and Notch-1 signalling pathways, resulting in cellular apoptosis, reduced migration and proliferation [120]. Similarly, in another study hyaluronic acid-chitosan nanoparticles were used to codeliver Dox and miR-34a into TNBC cells. The findings revealed that chitosan nanoparticles induced an upregulation in the expression of miR-34a, resulting in reduced proliferation, migration, and invasion of MDA-MB-231 cells. Simultaneously, the inclusion of Dox exerted cytotoxic effects, thereby enhanced therapeutic efficacy [121]. Ahir *et al*. designed mesoporous silica nanoparticles (MSNs) for targeted delivery of dual miRNAs (miR-34a mimic and antisense-miR-10b), aiming to reduce TNBC metastasis. The MSNs, modified for efficient transport with a cationic basic side chain and coated with hyaluronic acid-poly (ethylene glycol)-poly (lactide-co-glycolide) polymer, demonstrated effective inhibition of tumor growth, induction of cancer cell death and delayed metastasis [122]. miR-21, associated with tumor growth and metastasis, is frequently upregulated in TNBC [123]. To address this, a miR-21 inhibitor along with Dox was encapsulated within poly(amidoamine) dendrimers, leading to successful delivery to TNBC cells. In particular, the effective miR 21 inhibitor transfection leads to the inhibition of cancer cell migration and activation of apoptosis related genes. Furthermore, co-delivery of miR21 inhibitor and Dox using dendrimer significantly improved therapeutic efficacy against cancer cells due to the synergistic effect of miR21 inhibitor and Dox treatment [124]. Another study employed metal-organic frameworks (ZIF-90 nanoparticles) to co-deliver antimiR-21 and antimir-155 along with a photosensitizing agent to target TNBC. The pH-responsive drug release was facilitated by ZIF-90 nanoparticles within the tumor microenvironment, downregulating overexpressed oncogenic miRNAs and inducing apoptosis through light-induced reactive oxygen species (ROS) production [125].

The Slug gene, contributing to aggressive behaviour and metastasis in TNBC, was specifically targeted by using miRNA-loaded liposomes functionalized with DSPE-PEG. These nanosized liposomes efficiently suppressed Slug gene expression in TNBC cells, inhibiting their invasiveness and growth while also blocking the TGF-β1/Smad pathway. In a TNBC mouse

model, the combination of functional miRNA liposomes with a chemotherapy drug showed a stronger anticancer effect. Preliminary safety tests showed no adverse effects on body weight or major organs [126].
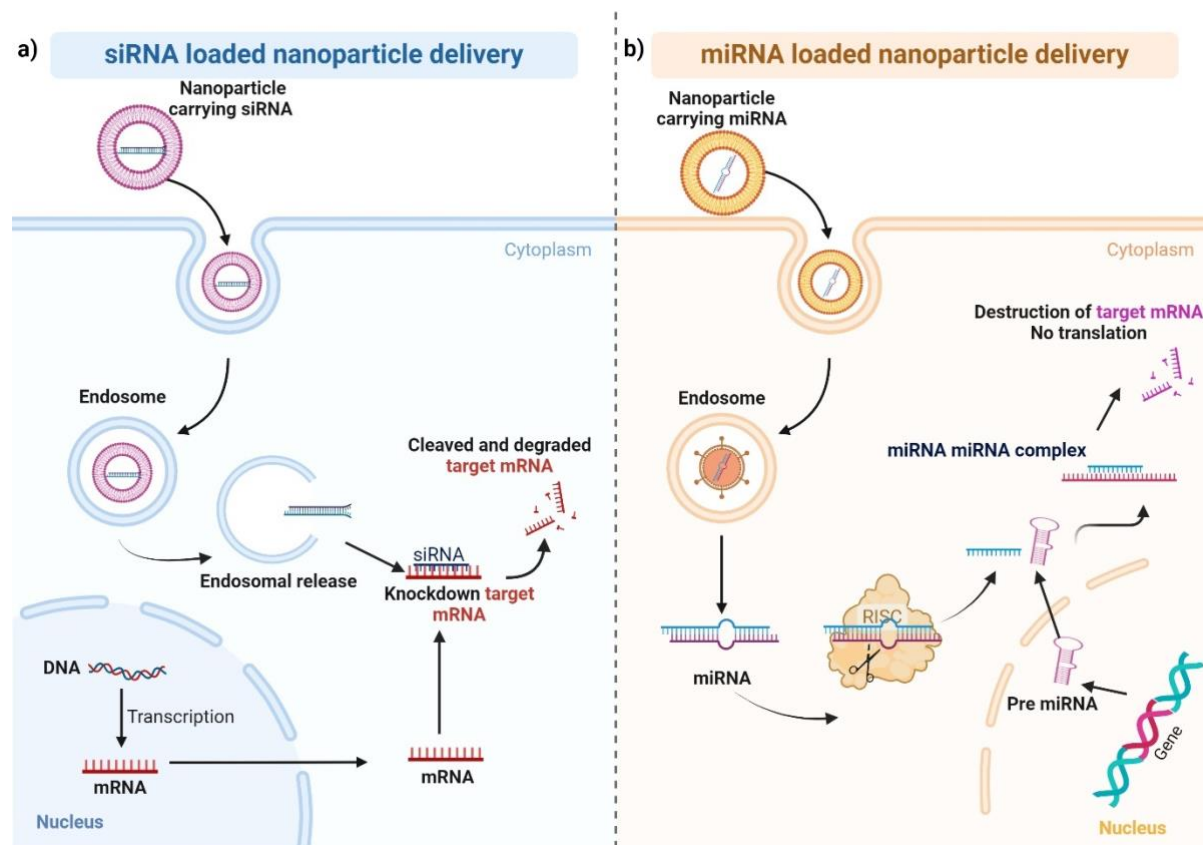
Figure 1.4 Gene silencing mechanism of a) siRNA and b) miRNA-loaded nanoparticles

1.4.3 Potential challenges associated with RNA-based therapeutics

Despite the remarkable progress in RNA therapy for cancer treatment in the preclinical stage, several challenges need to be addressed for the clinical translation of this therapeutic strategy. A key challenge is the lack of specificity of miRNA, leading to imperfect binding to target mRNA, and a single miRNA may target and degrade multiple sets of similar target mRNAs [127]. Additionally, concerns include nuclease-mediated degradation of naked siRNAs and miRNAs upon systemic injection, repulsion at the cell membrane level due to their negative charge, poor tissue penetration, and potential non-specific immune stimulation [128]. While delivery vehicles like liposomes can mitigate some challenges, but they also come with disadvantages. For instance, Dokka *et al*. demonstrated in their study that cationic lipids like DOTAP can induce pulmonary toxicity [129].

1.5 Current therapeutic strategies targeting lung cancer

Various emerging modalities are investigated to improve therapeutic outcomes in the context of current therapeutic strategies targeting lung cancer. In this section, I will discuss two highly different yet equally promising therapies, including plant-derived natural compounds and antisense oligonucleotide (ASO)-based therapeutics.

1.5.1 Plant-based therapy

Plant-derived compounds have been recognized for their diverse pharmacological properties since long time ago [130]. The investigation of these natural compounds in the context of lung cancer treatment provides a unique avenue for developing innovative and potentially less toxic therapies [131]. Several delivery systems have been developed to ensure the safe transportation of natural compounds to target sites (Table 1.2). Here I will mainly discuss liquid crystalline nanoparticles (LCNs) as delivery systems for the treatment of lung cancer [132, 133]. Berberine, derived from several plants within the papaveraceae family, is an isoquinoline alkaloid known for its anti-inflammatory and anticancer attributes. Recent studies have explored the encapsulation of berberine within LCNs for lung cancer treatment. Paudel *et al.* developed berberine-loaded LCNs and investigated their *in-vitro* antiproliferative and antimigratory effects on human lung epithelial cancer cells (A549). Results showed that these nanoparticles exhibited high entrapment efficiency and demonstrated sustained release behaviour. Berberine-loaded LCNs significantly suppressed the expression of proliferation and migration-related proteins, thereby inhibiting cancer progression [134].

Resveratrol, another natural compound with anti-inflammatory and antioxidant properties, has been encapsulated in LCNs for targeted lung cancer therapy. Abdelaziz and team explores the application of LCNs for synergistic chemo-herbal therapy in lung cancer. The findings suggest that the liquid crystalline assembly effectively facilitates the sustained release of both chemotherapeutic agents and herbal drug (resveratrol) to lung cancer cells, which decrease the systemic cytotoxicity associated with chemotherapeutic drug. Furthermore, *in-vivo* results demonstrated that this treatment method inhibited the tumor development via inhibition of angiogenesis and induction of apoptosis [135].

Paudel and team addressed the therapeutic limitations of rutin, a natural flavonoid with anti-inflammatory, antioxidant and anti-cancer properties, by encapsulating it in LCNs. This approach enhanced drug bioavailability, stability and release profile, leading to sustained release up to 24 hours. This formulation exhibited strong anti-cancer effects in the A549 cells by suppressing proliferation, migration and promoting apoptosis [136]. Zerumbone (ZER), a natural compound

from *Zingiber zerumbet,* recognized for its anti-cancer properties, faces solubility challenges. To overcome this hurdle, Manandhar *et al.* developed ZER-loaded LCNs to increase ZER's potency and effectiveness against NSCLC. The formulation exhibited substantial inhibition of cancer progression, particularly in terms of proliferation and migration, along with the downregulation of various proteins linked to cancer progression [137].

Table 1.2 Delivery systems employed for delivering plant-based bioactive compounds targeting lung cancer

Plant-based active compound	Delivery system	Key findings	References
Quercetin	Polymeric nanoparticles	Enhanced encapsulation efficiency, sustained release and improved antitumor effects	[138]
Quercetin	Cetuximab-modified chitosan nanoparticle	Targeted delivery to lung cancer cells, reduces chemoresistance and enhances the chemotherapeutic effect of PTX-based therapy	[139]
Curcumin	Chitosan-based nanoparticles	Targeted drug delivery, controlled release and effective synergistic anti-tumor outcomes were demonstrated in both *in-vitro* and *in-vivo* experiments	[140]
Silybin	Dextran based nanoparticles	Nanoparticles effectively delivered both therapeutic agents at a controlled rate and showed synergistic antitumor effect	[141]
Boswellic acids	Chitosan nanoparticles	Higher cellular uptake, sustained release and enhanced antiproliferative effect via induction of apoptosis	[142]
Taxanes	Polymeric nanoparticles	Enhance the efficacy of chemoradiation therapy.	[143]
Curcumin	Carbon nanotubes	High drug loading efficiency and sustained drug release, inhibiting the cancer cell proliferation by inducing apoptosis.	[144]

Silibinin	Magnetic nanoparticles	Enhances drug solubility and bioavailability, facilitated targeted drug delivery, Inhibited cancer cell grown and induce cell death by apoptosis	[145]

1.5.2 ASO-based therapy

ASOs are single-strand DNAs or RNAs that selectively bind to complementary mRNAs to influence gene expression and disrupt RNA functions [146]. Among ASOs, the use of decoy oligodeoxynucleotides (ODNs) presents another interesting approach. They are synthetic double-stranded DNA or RNA molecule designed to competitively bind to transcription factors, thereby inhibiting transcription factor's ability to initiate gene expression [147]. Despite promising results in preclinical studies, the advancement of ASO-based therapies into clinical trials has been constrained, largely because of the difficulties related to their pharmacokinetics, charge density and susceptibility to nucleases [148].

In response to these challenges, researchers have developed various delivery systems, including polysaccharide-based nanoparticles [149]. These nanoparticles, derived from naturally occurring polysaccharides like dextran, chitosan and alginate, offer several advantages as ASO delivery systems [149]. One of the key benefits is their biocompatibility and biodegradability. Being derived from natural sources, they are generally well-tolerated by the body, minimizing the risk of adverse reactions [149].

Dextran, an FDA-approved polysaccharide, offers high encapsulation efficiency and biocompatibility [82]. For example, Acetylated dextran (AcDex) nanoparticles demonstrated compatibility with aerosolized dry powder inhalation and pH-dependent degradation for controlled therapeutic payload release within acidic microenvironments [150]. Kannaujia *et al*. demonstrated the anticancer potential of NFκB decoy ODNs loaded AcDex nanoparticles against human lung cancer (A549) cells. The nanoparticles exhibited exceptional high encapsulation efficiency (up to 99.5%) and pH-dependent release profile of ODNs. Moreover, they display potent *in vitro* anticancer effects by inhibiting cancer cell proliferation, migration, and colony formation through the suppression of NFκB signaling pathways [84].

Nafee *et al*. developed chitosan-coated polymeric nanoparticles loaded with antisense oligonucleotide 2-O-Methyl-RNA (OMR), a telomerase inhibitor for lung cancer. The findings revealed that a specific concentration of chitosan on the nanoparticle surface is essential for a notable increase in cellular uptake. Nevertheless, excessive chitosan had a negative impact on the

transfection efficiency. These nanoparticles exhibited preferential adsorption to cell membranes and significantly reduced telomerase activity in A549 lung cancer cells, indicating their potential as an efficient treatment method [151].

In addition to polysaccharide nanoparticles, other delivery systems have been investigated for delivering ASOs to target lung cancer. Li *et al*. engineered targeted lipid-based nanoparticles for gene inhibition through ASO therapeutics in human lung cancer cells (H1299 cells) overexpressed by sigma receptor. This targeted delivery system exhibited promising results in down-regulating survivin mRNA and protein, inducing apoptosis, inhibiting tumor cell growth and enhancing chemosensitivity to anticancer drugs [152]. Another study investigates the efficacy of lipid nanoparticles loaded with an ASO gapmer targeting Bcl-2 for the treatment of lung cancer. These nanoparticles effectively deliver the gapmer to A549 cells, resulting in downregulation of Bcl-2 expression. This downregulation leads to inhibition of cancer cell proliferation, induction of apoptosis, and enhanced sensitivity to chemotherapy [153].

1.5.3 Challenges associated with plant and ASO-based therapeutics

The major challenge associated with plant-based therapeutics involves the scaling-up or commercialization of these natural compounds that meet the therapeutic requirements [138]. Other challenges include issues related to standardization, quality control, and variability in bioactive compound composition [154]. Ensuring consistent efficacy and safety across different batches of plant extracts presents a significant challenge [155]. Additionally, limited bioavailability and potential adverse effects may arise due to interactions with other prescribed medications [155]. Overcoming these hurdles necessitates careful optimization of formulation techniques and thorough clinical evaluation to ensure the efficacy, safety, and reproducibility of plant-based therapies.

The primary hurdle hindering the clinical advancement of ASO-based therapy lies in achieving effective delivery to target tissues. This is primarily due to obstacles such as biological degradation and inadequate cellular uptake [156]. Additionally, ASOs may encounter another challenge wherein they may bind to unintended mRNA targets, resulting in off-target effects that compromise therapeutic precision and may lead to adverse reactions [156]. To address these issues, several strategies have been adopted such as chemical modifications or encapsulation within delivery vehicles [157]. However, these approaches carry their own risks, including potential toxicity and activating an inflammatory immune response [156]. Addressing these challenges requires interdisciplinary efforts across fields such as pharmacology, molecular

28

biology, materials science and regulatory affairs. Innovative approaches in delivery system, formulation design and genome editing technologies are continually being developed to overcome these obstacles and harness the therapeutic potential of plant and ASO-based therapies for lung cancer treatment.

1.6 Hypothesis, aims and rationale of the thesis

Hypothesis

Nanocarriers will enhance the *in-vitro* therapeutic effect of plant-derived drugs/nucleic-acid-based drugs for the treatment of breast and lung cancer.

This hypothesis will be tested via following aims:

Aim 1: Development of targeted polymer lipid hybrid nanoparticles for in-vitro siRNA therapy in triple-negative breast cancer

Aim 2: Evaluation of anticancer potential of berberine-loaded liquid crystalline nanoparticles against lung cancer cells

Aim 3: Investigation of anticancer potential of NFκB decoy oligonucleotide loaded polysaccharide nanoparticles in lung cancer cells.

The **rationale** behind these aims have been explained in the following section.

TNBC stands as one of the most difficult challenges in oncology, affecting millions globally with its aggressive nature and limited treatment options. Conventional therapies, including chemotherapy, radiation therapy and surgery, have struggled to limit its progression, often accompanied by unbearable side effects that compromise patients' well-being. In this landscape, the emergence of siRNA therapy offers a light of hope, by targeting specific genes driving TNBC growth. However prior studies mainly explored the combined treatment of siRNA with chemodrug, which may cause toxicity associated with chemodrugs. In response, Chapter 2 (Aim 1) developed a method by targeting XBP1 gene via siRNA for TNBC treatment. XBP1 emerges as a key driver of TNBC tumor growth and recurrence, primarily by regulating the endoplasmic reticulum stress response and unfolded protein pathways, impacting cell survival, proliferation, and chemoresistance. Elevated XBP1 expression is frequently associated with TNBC, promoting these detrimental effects and contributing to a poor prognosis and treatment resistance. In this work, siXBP1 (siRNA targeting XBP1) encapsulated within polymer lipid nanoparticles. In addition, to facilitate selective cellular uptake to tumor cells, we have conjugated the nanoparticles with an EGFR antibody. Remarkably, developed targeted nanoparticles increased cellular uptake leading to enhanced gene silencing efficacy with mimimum toxicity. The findings provide the potential to develop siRNA treatment option for TNBC.

The high mortality rates associated with lung cancer underscore the urgent need for better treatment options. Conventional chemotherapy that mainly includes synthetic drugs often causes discomfort and toxicity due to high doses. Natural compounds such as berberine represent promising candidates for safer anticancer therapeutics. Natural compounds like berberine offer promise for safer anticancer therapies; however, their low bioavailability requires administration at high doses, leading to patient discomfort. Encapsulating berberine within nanoparticles presents a compelling strategy to enhance therapeutic efficacy at lower doses and mitigate adverse effects. Chapter 3 (Aim 2) of this thesis focuses on investigating the potential of berberine-loaded liquid crystalline nanoparticles against lung cancer, aiming to overcome the challenges associated with synthetic drugs and harness the benefits of natural compounds like berberine at minimal dosages. The formulated nanoparticles demonstrated significant anticancer effects at markedly reduced doses compared to previous studies, highlighting their potential to improve patient well-being and minimize associated adverse reactions if translated to clinical practice.

Further investigation into the underlying mechanisms contributing to heightened mortality rates in lung cancer cases has revealed elevated NFκB expression levels, recognized as a prognostic marker associated with advanced tumor stage, disease severity, and reduced survival rates. The accumulation of pro-inflammatory cytokines (IL-6 & IL-8) near tumor sites in malignant tissues with heightened NFκB activity significantly contributes to the pro-tumorigenic microenvironment. This observation underscores the therapeutic significance of NFκB inhibition as a viable anti-cancer strategy. Despite the potential of ASOs to prevent transcription factors from binding to target genes, their therapeutic application is limited by poor cellular uptake or short circulatory half-life. Addressing these limitations, Chapter 4 (Aim 3) was designed to encapsulate NFkB decoy ODNs into polysaccharide-based nanoparticles and evaluate their anticancer potential against a lung cancer cell line. Interestingly, the prepared nanoparticles exhibited high encapsulation efficiency (>99%) and significantly reduced the expression of pro-inflammatory cytokines, such as IL-6 and IL-8, in lung cancer cells at a much lower dose, indicating safe drug delivery to the target site and efficacy in inhibiting inflammation-mediated cancer progression in lung cancer.

Overall, the objective of the current project is the development of novel drug carriers that can deliver the drug safely to the target site with minimal toxicity, which will ultimately provide better therapeutic outcomes against cancer.

1.7 References

1. *Breast cancer statistics*. [cited 2023 22 May]; Available from: https://nbcf.org.au/about-breast-cancer/breast-cancer-stats/#:~:text=Breast%20cancer%20is%20the%20most,breast%20cancer%20in%20their%20lifetime.

2. Hicks, D.G. and S.C. Lester, *Hormone Receptors (ER/PR)*, in *Diagnostic Pathology: Breast (Second Edition)*, D.G. Hicks and S.C. Lester, Editors. 2016, Elsevier: Philadelphia. p. 430-439.

3. Nicolini, A., P. Ferrari, and M.J. Duffy, *Prognostic and predictive biomarkers in breast cancer: Past, present and future.* Semin Cancer Biol, 2018. **52**(Pt 1): p. 56-73.

4. Purdie, C.A., et al., *Progesterone receptor expression is an independent prognostic variable in early breast cancer: a population-based study.* Br J Cancer, 2014. **110**(3): p. 565-72.

5. Vaz-Luis, I., E.P. Winer, and N.U. Lin, *Human epidermal growth factor receptor-2-positive breast cancer: does estrogen receptor status define two distinct subtypes?* Ann Oncol, 2013. **24**(2): p. 283-291.

6. Iqbal, N. and N. Iqbal, *Human Epidermal Growth Factor Receptor 2 (HER2) in Cancers: Overexpression and Therapeutic Implications.* Mol Biol Int, 2014. **2014**: p. 852748.

7. Krishnamurti, U., et al., *Poor prognostic significance of unamplified chromosome 17 polysomy in invasive breast carcinoma.* Mod Pathol, 2009. **22**(8): p. 1044-8.

8. Yersal, O. and S. Barutca, *Biological subtypes of breast cancer: Prognostic and therapeutic implications.* World J Clin Oncol, 2014. **5**(3): p. 412-24.

9. *Cancer Stat Facts: Female Breast Cancer Subtypes*. c2019-2022 [cited 2024 4th Jan]; Available from: https://seer.cancer.gov/statfacts/html/breast-subtypes.html.

10. Inic, Z., et al., *Difference between Luminal A and Luminal B Subtypes According to Ki-67, Tumor Size, and Progesterone Receptor Negativity Providing Prognostic Information.* Clin Med Insights Oncol, 2014. **8**: p. 107-11.

11. Kennecke, H., et al., *Metastatic behavior of breast cancer subtypes.* J Clin Oncol, 2010. **28**(20): p. 3271-7.

12. Lafcı, O., et al., *DCE-MRI Radiomics Analysis in Differentiating Luminal A and Luminal B Breast Cancer Molecular Subtypes.* Acad Radiol, 2023. **30**(1): p. 22-29.

13. Krishnamurti, U. and J.F. Silverman, *HER2 in breast cancer: a review and update.* Adv Anat Pathol, 2014. **21**(2): p. 100-7.

14.   Figueroa-Magalhães, M.C., et al., *Treatment of HER2-positive breast cancer.* Breast, 2014. **23**(2): p. 128-136.

15.   Pulido, C., et al., *Bone metastasis risk factors in breast cancer.* Ecancermedicalscience, 2017. **11**: p. 715.

16.   Kumar, P. and R. Aggarwal, *An overview of triple-negative breast cancer.* Archives of Gynecology and Obstetrics, 2016. **293**(2): p. 247-269.

17.   Collignon, J., et al., *Triple-negative breast cancer: treatment challenges and solutions.* Breast Cancer (Dove Med Press), 2016. **8**: p. 93-107.

18.   Qattan, A., *Gene Silencing Agents in Breast Cancer*, in *Modulating Gene Expression-Abridging the RNAi and CRISPR-Cas9 Technologies*. 2018, IntechOpen.

19.   Crown, J., J. O'Shaughnessy, and G. Gullo, *Emerging targeted therapies in triple-negative breast cancer.* Ann Oncol, 2012. **23 Suppl 6**: p. vi56-65.

20.   Moo, T.-A., et al., *Overview of breast cancer therapy.* PET clinics, 2018. **13**(3): p. 339-354.

21.   Burguin, A., C. Diorio, and F. Durocher, *Breast Cancer Treatments: Updates and New Challenges.* J Pers Med, 2021. **11**(8).

22.   Schnitt, S.J., M.S. Moran, and A.E. Giuliano, *Lumpectomy Margins for Invasive Breast Cancer and Ductal Carcinoma in Situ: Current Guideline Recommendations, Their Implications, and Impact.* J Clin Oncol, 2020. **38**(20): p. 2240-2245.

23.   Boyages, J., *Radiation therapy and early breast cancer: current controversies.* Med J Aust, 2017. **207**(5): p. 216-222.

24.   Bartelink, H., et al., *Whole-breast irradiation with or without a boost for patients treated with breast-conserving surgery for early breast cancer: 20-year follow-up of a randomised phase 3 trial.* Lancet Oncol, 2015. **16**(1): p. 47-56.

25.   Montemurro, F., I. Nuzzolese, and R. Ponzone, *Neoadjuvant or adjuvant chemotherapy in early breast cancer?* Expert Opin Pharmacother, 2020. **21**(9): p. 1071-1082.

26.   El Sayed, R., et al., *Endocrine and Targeted Therapy for Hormone-Receptor-Positive, HER2-Negative Advanced Breast Cancer: Insights to Sequencing Treatment and Overcoming Resistance Based on Clinical Trials.* Front Oncol, 2019. **9**: p. 510.

27.   Davies, C., et al., *Relevance of breast cancer hormone receptors and other factors to the efficacy of adjuvant tamoxifen: patient-level meta-analysis of randomised trials.* Lancet, 2011. **378**(9793): p. 771-84.

28.   Alvarez, R.H., V. Valero, and G.N. Hortobagyi, *Emerging targeted therapies for breast cancer.* J Clin Oncol, 2010. **28**(20): p. 3366-3379.

29. Higgins, M.J. and J. Baselga, *Targeted therapies for breast cancer.* The Journal of clinical investigation, 2011. **121**(10): p. 3797-3803.

30. Yu, J., et al., *Challenges and opportunities in metastatic breast cancer treatments: Nano-drug combinations delivered preferentially to metastatic cells may enhance therapeutic response.* Pharmacology & Therapeutics, 2022. **236**: p. 108108.

31. Schneeweiss, A., E. Ruckhäberle, and J. Huober, *Chemotherapy for metastatic breast cancer–an anachronism in the era of personalised and targeted oncological therapy?* Geburtshilfe und Frauenheilkunde, 2015. **75**(06): p. 574-583.

32. Stone, H.B., et al., *Effects of radiation on normal tissue: consequences and mechanisms.* Lancet Oncol, 2003. **4**(9): p. 529-36.

33. Lin, A., et al., *Toxicity of radiotherapy in patients with collagen vascular disease.* Cancer, 2008. **113**(3): p. 648-53.

34. Masoud, V. and G. Pagès, *Targeted therapies in breast cancer: New challenges to fight against resistance.* World J Clin Oncol, 2017. **8**(2): p. 120-134.

35. Mok, T.S., et al., *Gefitinib or carboplatin-paclitaxel in pulmonary adenocarcinoma.* N Engl J Med, 2009. **361**(10): p. 947-57.

36. Reck, M., et al., *Pembrolizumab versus Chemotherapy for PD-L1–Positive Non–Small-Cell Lung Cancer.* New England Journal of Medicine, 2016. **375**(19): p. 1823-1833.

37. Khani, Y., et al., *Tobacco smoking and cancer types: a review.* Biomedical Research and Therapy, 2018. **5**(4): p. 2142-59.

38. Siegel, R.L., et al., *Cancer Statistics, 2021.* 2021. **71**(1): p. 7-33.

39. Miller, K.D., et al., *Cancer treatment and survivorship statistics, 2022.* 2022. **72**(5): p. 409-436.

40. Sharma, P., et al., *Emerging trends in the novel drug delivery approaches for the treatment of lung cancer.* Chemico-biological interactions, 2019.

41. Cheng, T.-Y.D., et al., *The international epidemiology of lung cancer: latest trends, disparities, and tumor characteristics.* Journal of Thoracic Oncology, 2016. **11**(10): p. 1653-1671.

42. Perez-Moreno, P., et al., *Squamous cell carcinoma of the lung: molecular subtypes and therapeutic opportunities.* Clin Cancer Res, 2012. **18**(9): p. 2443-51.

43. Molina, J.R., et al., *Non-small cell lung cancer: epidemiology, risk factors, treatment, and survivorship.* Mayo Clin Proc, 2008. **83**(5): p. 584-94.

44. Padinharayil, H., et al., *Advances in the Lung Cancer Immunotherapy Approaches.* Vaccines (Basel), 2022. **10**(11).

45. Port, J.L., et al., *A propensity-matched analysis of wedge resection and stereotactic body radiotherapy for early stage lung cancer.* The Annals of thoracic surgery, 2014. **98**(4): p. 1152-1159.

46. Li, Y., B. Yan, and S. He, *Advances and challenges in the treatment of lung cancer.* Biomedicine & Pharmacotherapy, 2023. **169**: p. 115891.

47. Lee, S.H., *Chemotherapy for Lung Cancer in the Era of Personalized Medicine.* Tuberc Respir Dis (Seoul), 2019. **82**(3): p. 179-189.

48. De Ruysscher, D., et al., *State of the art radiation therapy for lung cancer 2012: a glimpse of the future.* Clinical lung cancer, 2013. **14**(2): p. 89-95.

49. Steven, A., S.A. Fisher, and B.W. Robinson, *Immunotherapy for lung cancer.* Respirology, 2016. **21**(5): p. 821-833.

50. Mamdani, H., et al., *Immunotherapy in lung cancer: Current landscape and future directions.* Frontiers in immunology, 2022. **13**: p. 823618.

51. Schrank, Z., et al., *Current molecular-targeted therapies in NSCLC and their mechanism of resistance.* Cancers, 2018. **10**(7): p. 224.

52. Lahiri, A., et al., *Lung cancer immunotherapy: progress, pitfalls, and promises.* Mol Cancer, 2023. **22**(1): p. 40.

53. Yin, Q., et al., *Immune-related adverse events of immune checkpoint inhibitors: a review.* Front Immunol, 2023. **14**: p. 1167975.

54. Atlihan-Gundogdu, E., et al., *Recent developments in cancer therapy and diagnosis.* Journal of pharmaceutical investigation, 2020. **50**: p. 349-361.

55. Senapati, S., et al., *Controlled drug delivery vehicles for cancer treatment and their performance.* Signal Transduction and Targeted Therapy, 2018. **3**(1): p. 7.

56. Hong, L., et al., *Nanoparticle-based drug delivery systems targeting cancer cell surfaces.* RSC Adv, 2023. **13**(31): p. 21365-21382.

57. Gurevich, E.V. and V.V. Gurevich, *Beyond traditional pharmacology: new tools and approaches.* British Journal of Pharmacology, 2015. **172**(13): p. 3229-3241.

58. Tenchov, R., et al., *Lipid Nanoparticles─From Liposomes to mRNA Vaccine Delivery, a Landscape of Research Diversity and Advancement.* ACS Nano, 2021. **15**(11): p. 16982-17015.

59. Shah, S., et al., *Liposomes: Advancements and innovation in the manufacturing process.* Advanced Drug Delivery Reviews, 2020. **154-155**: p. 102-122.

60. Beck, H., et al., *Small molecules and their impact in drug discovery: A perspective on the occasion of the 125th anniversary of the Bayer Chemical Research Laboratory.* Drug Discov Today, 2022. **27**(6): p. 1560-1574.

61. Hadinoto, K., A. Sundaresan, and W.S. Cheow, *Lipid–polymer hybrid nanoparticles as a new generation therapeutic delivery platform: A review.* European Journal of Pharmaceutics and Biopharmaceutics, 2013. **85**(3, Part A): p. 427-443.

62. Zhang, L.I. and L. Zhang, *Lipid–Polymer Hybrid Nanoparticles: Synthesis, Characterization and Applications.* Nano LIFE, 2012. **01**(01n02): p. 163-173.

63. Zheng, Y., et al., *Transferrin-conjugated lipid-coated PLGA nanoparticles for targeted delivery of aromatase inhibitor 7α-APTADD to breast cancer cells.* International Journal of Pharmaceutics, 2010. **390**(2): p. 234-241.

64. Wang, L., B. Griffel, and X. Xu, *Synthesis of PLGA-Lipid Hybrid Nanoparticles for siRNA Delivery Using the Emulsion Method PLGA-PEG-Lipid Nanoparticles for siRNA Delivery.* Methods Mol Biol, 2017. **1632**: p. 231-240.

65. Hadinoto, K., A. Sundaresan, and W.S. Cheow, *Lipid-polymer hybrid nanoparticles as a new generation therapeutic delivery platform: a review.* Eur J Pharm Biopharm, 2013. **85**(3 Pt A): p. 427-43.

66. Chan, Y., et al., *Versatility of Liquid Crystalline Nanoparticles in Inflammatory Lung Diseases.* Nanomedicine, 2021. **16**(18): p. 1545-1548.

67. Thapa, R.K., et al., *Liquid crystalline nanoparticles encapsulating cisplatin and docetaxel combination for targeted therapy of breast cancer.* Biomater Sci, 2016. **4**(9): p. 1340-50.

68. Wadhwa, R., et al., *Anti-inflammatory and anticancer activities of Naringenin-loaded liquid crystalline nanoparticles in vitro.* Journal of Food Biochemistry, 2021. **45**(1): p. e13572.

69. Yu, X.-Y., X. Jin, and Z.-X. Shou, *Surface-engineered smart nanocarrier-based inhalation formulations for targeted lung cancer chemotherapy: a review of current practices.* Drug Delivery, 2021. **28**(1): p. 1995-2010.

70. Ding, L., et al., *Polymer-Based Drug Delivery Systems for Cancer Therapeutics.* Polymers, 2024. **16**(6): p. 843.

71. Dristant, U., et al., *An Overview of Polymeric Nanoparticles-Based Drug Delivery System in Cancer Treatment.* Technol Cancer Res Treat, 2023. **22**: p. 15330338231152083.

72. Makadia, H.K. and S.J. Siegel, *Poly lactic-co-glycolic acid (PLGA) as biodegradable controlled drug delivery carrier.* Polymers, 2011. **3**(3): p. 1377-1397.

73. Sadat Tabatabaei Mirakabad, F., et al., *PLGA-based nanoparticles as cancer drug delivery systems.* Asian Pac J Cancer Prev, 2014. **15**(2): p. 517-35.

74. Zielińska, A., et al., *Polymeric Nanoparticles: Production, Characterization, Toxicology and Ecotoxicology.* Molecules, 2020. **25**(16).

75. Fazal, T., et al., *Recent developments in natural biopolymer based drug delivery systems.* RSC advances, 2023. **13**(33): p. 23087-23121.

76. Yousefi Rizi, H.A., D. Hoon Shin, and S. Yousefi Rizi, *Polymeric Nanoparticles in Cancer Chemotherapy: A Narrative Review.* Iran J Public Health, 2022. **51**(2): p. 226-239.

77. Yan, S., et al., *Tumor-targeting photodynamic therapy based on folate-modified polydopamine nanoparticles.* Int J Nanomedicine, 2019. **14**: p. 6799-6812.

78. Sang, R., et al., *Lipid-polymer nanocarrier platform enables X-ray induced photodynamic therapy against human colorectal cancer cells.* Biomedicine & Pharmacotherapy, 2022. **155**: p. 113837.

79. Mondal, L., et al., *CD-340 functionalized doxorubicin-loaded nanoparticle induces apoptosis and reduces tumor volume along with drug-related cardiotoxicity in mice.* Int J Nanomedicine, 2019. **14**: p. 8073-8094.

80. Lee, S., et al., *Development of paclitaxel-loaded poly(lactic acid)/hydroxyapatite core–shell nanoparticles as a stimuli-responsive drug delivery system.* Royal Society Open Science, 2021. **8**(3): p. 202030.

81. Petrovici, A.R., M. Pinteala, and N. Simionescu, *Dextran Formulations as Effective Delivery Systems of Therapeutic Agents.* Molecules, 2023. **28**(3).

82. Prasher, P., et al., *Versatility of acetalated dextran in nanocarriers targeting respiratory diseases.* Materials Letters, 2022. **323**: p. 132600.

83. Cohen, J.L., et al., *Acid-Degradable Cationic Dextran Particles for the Delivery of siRNA Therapeutics.* Bioconjugate Chemistry, 2011. **22**(6): p. 1056-1065.

84. Kannaujiya, V.K., et al., *Anticancer activity of NFκB decoy oligonucleotide-loaded nanoparticles against human lung cancer.* Journal of Drug Delivery Science and Technology, 2023. **82**: p. 104328.

85. Rodrigues, C.F., et al., *Chapter 10 - Inorganic-based drug delivery systems for cancer therapy*, in *Advances and Avenues in the Development of Novel Carriers for Bioactives and Biological Agents*, M.R. Singh, et al., Editors. 2020, Academic Press. p. 283-316.

86. Kim, Y.H., et al., *Tumor targeting and imaging using cyclic RGD-PEGylated gold nanoparticle probes with directly conjugated iodine-125.* Small, 2011. **7**(14): p. 2052-60.

87.   Selvarajan, V., S. Obuobi, and P.L.R. Ee, *Silica Nanoparticles—A Versatile Tool for the Treatment of Bacterial Infections.* Frontiers in Chemistry, 2020. **8**.

88.   Giménez, C., et al., *Gated Mesoporous Silica Nanoparticles for the Controlled Delivery of Drugs in Cancer Cells.* Langmuir, 2015. **31**(12): p. 3753-3762.

89.   Cheng, W., et al., *pH-Sensitive Delivery Vehicle Based on Folic Acid-Conjugated Polydopamine-Modified Mesoporous Silica Nanoparticles for Targeted Cancer Therapy.* ACS Appl Mater Interfaces, 2017. **9**(22): p. 18462-18473.

90.   Saini, K. and R. Bandyopadhyaya, *Transferrin-Conjugated Polymer-Coated Mesoporous Silica Nanoparticles Loaded with Gemcitabine for Killing Pancreatic Cancer Cells.* ACS Applied Nano Materials, 2020. **3**(1): p. 229-240.

91.   kianfar, E., *Magnetic Nanoparticles in Targeted Drug Delivery: a Review.* Journal of Superconductivity and Novel Magnetism, 2021. **34**(7): p. 1709-1735.

92.   Huang, Y., et al., *Superparamagnetic iron oxide nanoparticles conjugated with folic acid for dual target-specific drug delivery and MRI in cancer theranostics.* Mater Sci Eng C Mater Biol Appl, 2017. **70**(Pt 1): p. 763-771.

93.   Wang, Z., et al., *Active targeting theranostic iron oxide nanoparticles for MRI and magnetic resonance-guided focused ultrasound ablation of lung cancer.* Biomaterials, 2017. **127**: p. 25-35.

94.   Kulkarni, J.A., et al., *The current landscape of nucleic acid therapeutics.* Nature Nanotechnology, 2021. **16**(6): p. 630-643.

95.   Lam, J.K., et al., *siRNA Versus miRNA as Therapeutics for Gene Silencing.* Mol Ther Nucleic Acids, 2015. **4**(9): p. e252.

96.   Ali Zaidi, S.S., et al., *Engineering siRNA therapeutics: challenges and strategies.* Journal of Nanobiotechnology, 2023. **21**(1): p. 381.

97.   Gao, K. and L. Huang, *Nonviral methods for siRNA delivery.* Mol Pharm, 2009. **6**(3): p. 651-8.

98.   Dana, H., et al., *Molecular Mechanisms and Biological Functions of siRNA.* Int J Biomed Sci, 2017. **13**(2): p. 48-57.

99.   Hu, B., et al., *Therapeutic siRNA: state of the art.* Signal Transduction and Targeted Therapy, 2020. **5**(1): p. 101.

100.   Nel, J., et al., *Functionalized liposomes for targeted breast cancer drug delivery.* Bioact Mater, 2023. **24**: p. 401-437.

101. Alshaer, W., et al., *Aptamer-guided siRNA-loaded nanomedicines for systemic gene silencing in CD-44 expressing murine triple-negative breast cancer model.* Journal of Controlled Release, 2018. **271**: p. 98-106.

102. Li, W. and F.C. Szoka, Jr., *Lipid-based nanoparticles for nucleic acid delivery.* Pharm Res, 2007. **24**(3): p. 438-49.

103. Bulbake, U., et al., *Cationic liposomes for co-delivery of paclitaxel and anti-Plk1 siRNA to achieve enhanced efficacy in breast cancer.* Journal of Drug Delivery Science and Technology, 2018. **48**: p. 253-265.

104. Chen, X., et al., *Co-delivery of paclitaxel and anti-survivin siRNA via redox-sensitive oligopeptide liposomes for the synergistic treatment of breast cancer and metastasis.* Int J Pharm, 2017. **529**(1-2): p. 102-115.

105. Deng, Z.J., et al., *Layer-by-layer nanoparticles for systemic codelivery of an anticancer drug and siRNA for potential triple-negative breast cancer treatment.* ACS Nano, 2013. **7**(11): p. 9571-84.

106. Tang, J., et al., *Enhanced delivery of siRNA to triple negative breast cancer cells in vitro and in vivo through functionalizing lipid-coated calcium phosphate nanoparticles with dual target ligands.* Nanoscale, 2018. **10**(9): p. 4258-4266.

107. Zhao, L., et al., *Exosome-mediated siRNA delivery to suppress postoperative breast cancer metastasis.* Journal of Controlled Release, 2020. **318**: p. 1-15.

108. Ben Djemaa, S., et al., *Formulation and in vitro evaluation of a siRNA delivery nanosystem decorated with gH625 peptide for triple negative breast cancer theranosis.* European Journal of Pharmaceutics and Biopharmaceutics, 2018. **131**: p. 99-108.

109. Zhang, L., et al., *Development of targeted therapy therapeutics to sensitize triple-negative breast cancer chemosensitivity utilizing bacteriophage phi29 derived packaging RNA.* Journal of Nanobiotechnology, 2021. **19**(1): p. 13.

110. Yin, T., et al., *Co-delivery of hydrophobic paclitaxel and hydrophilic AURKA specific siRNA by redox-sensitive micelles for effective treatment of breast cancer.* Biomaterials, 2015. **61**: p. 10-25.

111. Zhao, Z., et al., *Co-delivery of IKBKE siRNA and cabazitaxel by hybrid nanocomplex inhibits invasiveness and growth of triple-negative breast cancer.* Science advances, 2020. **6**(29): p. eabb0616.

112. Parmar, M.B., et al., *Combinational siRNA delivery using hyaluronic acid modified amphiphilic polyplexes against cell cycle and phosphatase proteins to inhibit growth and migration of triple-negative breast cancer cells.* Acta Biomaterialia, 2018. **66**: p. 294-309.

113. Su, S., et al., *"Triple-punch" strategy for triple negative breast cancer therapy with minimized drug dosage and improved antitumor efficacy.* Acs Nano, 2015. **9**(2): p. 1367-1378.

114. Yang, Z., et al., *Chitosan layered gold nanorods as synergistic therapeutics for photothermal ablation and gene silencing in triple-negative breast cancer.* Acta Biomater, 2015. **25**: p. 194-204.

115. Jing, H., et al., *Novel cell-penetrating peptide-loaded nanobubbles synergized with ultrasound irradiation enhance EGFR siRNA delivery for triple negative Breast cancer therapy.* Colloids Surf B Biointerfaces, 2016. **146**: p. 387-95.

116. Hwang, H. and J. Mendell, *MicroRNAs in cell proliferation, cell death, and tumorigenesis.* British journal of cancer, 2006. **94**(6): p. 776-780.

117. Mollaei, H., R. Safaralizadeh, and Z. Rostami, *MicroRNA replacement therapy in cancer.* J Cell Physiol, 2019. **234**(8): p. 12369-12384.

118. Ghafouri-Fard, S., et al., *Nanoparticle-mediated delivery of microRNAs-based therapies for treatment of disorders.* Pathology - Research and Practice, 2023. **248**: p. 154667.

119. Imani, S., et al., *MicroRNA-34a targets epithelial to mesenchymal transition-inducing transcription factors (EMT-TFs) and inhibits breast cancer cell migration and invasion.* Oncotarget, 2017. **8**(13): p. 21362-21379.

120. Wang, S., et al., *Degradable hyaluronic acid/protamine sulfate interpolyelectrolyte complexes as miRNA-delivery nanocapsules for triple-negative breast cancer therapy.* Adv Healthc Mater, 2015. **4**(2): p. 281-90.

121. Deng, X., et al., *Hyaluronic acid-chitosan nanoparticles for co-delivery of MiR-34a and doxorubicin in therapy against triple negative breast cancer.* Biomaterials, 2014. **35**(14): p. 4333-44.

122. Ahir, M., et al., *Delivery of dual miRNA through CD44-targeted mesoporous silica nanoparticles for enhanced and effective triple-negative breast cancer therapy.* Biomaterials Science, 2020. **8**(10): p. 2939-2954.

123. Dan, T., et al., *miR-21 Plays a Dual Role in Tumor Formation and Cytotoxic Response in Breast Tumors.* Cancers (Basel), 2021. **13**(4).

124. Song, C., et al., *Efficient co-delivery of microRNA 21 inhibitor and doxorubicin to cancer cells using core–shell tecto dendrimers formed via supramolecular host–guest assembly.* Journal of Materials Chemistry B, 2020. **8**(14): p. 2768-2774.

125. Shang, M., et al., *Dual antisense oligonucleotide targeting miR-21/miR-155 synergize photodynamic therapy to treat triple-negative breast cancer and inhibit metastasis.* Biomedicine & Pharmacotherapy, 2022. **146**: p. 112564.

126. Yan, Y., et al., *Nanosized functional miRNA liposomes and application in the treatment of TNBC by silencing Slug gene.* Int J Nanomedicine, 2019. **14**: p. 3645-3667.

127. Ahmadzada, T., G. Reid, and D.R. McKenzie, *Fundamentals of siRNA and miRNA therapeutics and a review of targeted nanoparticle delivery systems in breast cancer.* Biophys Rev, 2018. **10**(1): p. 69-86.

128. Sajid, M.I., et al., *Overcoming Barriers for siRNA Therapeutics: From Bench to Bedside.* Pharmaceuticals (Basel), 2020. **13**(10).

129. Dokka, S., et al., *Oxygen Radical-Mediated Pulmonary Toxicity Induced by Some Cationic Liposomes.* Pharmaceutical Research, 2000. **17**(5): p. 521-525.

130. Nasim, N., I.S. Sandeep, and S. Mohanty, *Plant-derived natural products for drug discovery: current approaches and prospects.* Nucleus (Calcutta), 2022. **65**(3): p. 399-411.

131. Yang, Y., et al., *Natural Products with Activity against Lung Cancer: A Review Focusing on the Tumor Microenvironment.* Int J Mol Sci, 2021. **22**(19).

132. Chavda, V.P., et al., *Nano-Drug Delivery Systems Entrapping Natural Bioactive Compounds for Cancer: Recent Progress and Future Challenges.* Frontiers in Oncology, 2022. **12**.

133. Chan, Y., et al., *Versatility of liquid crystalline nanoparticles in inflammatory lung diseases.* 2021, Future Medicine. p. 1545-1548.

134. Paudel, K.R., et al., *Berberine-loaded liquid crystalline nanoparticles inhibit non-small cell lung cancer proliferation and migration in vitro.* Environmental Science and Pollution Research, 2022. **29**(31): p. 46830-46847.

135. Abdelaziz, H.M., et al., *Liquid crystalline assembly for potential combinatorial chemo-herbal drug delivery to lung cancer cells.* Int J Nanomedicine, 2019. **14**: p. 499-517.

136. Paudel, K.R., et al., *Rutin loaded liquid crystalline nanoparticles inhibit non-small cell lung cancer proliferation and migration in vitro.* Life Sciences, 2021. **276**: p. 119436.

137. Manandhar, B., et al., *Zerumbone-incorporated liquid crystalline nanoparticles inhibit proliferation and migration of non-small-cell lung cancer in vitro.* Naunyn Schmiedebergs Arch Pharmacol, 2024. **397**(1): p. 343-356.

138. Baksi, R., et al., *In vitro and in vivo anticancer efficacy potential of Quercetin loaded polymeric nanoparticles.* Biomedicine & Pharmacotherapy, 2018. **106**: p. 1513-1526.

139. Wang, Y., et al., *Targeted delivery of quercetin by nanoparticles based on chitosan sensitizing paclitaxel-resistant lung cancer cells to paclitaxel.* Materials Science and Engineering: C, 2021. **119**: p. 111442.

140. Zhu, X., et al., *Chitosan-based nanoparticle co-delivery of docetaxel and curcumin ameliorates anti-tumor chemoimmunotherapy in lung cancer.* Carbohydrate Polymers, 2021. **268**: p. 118237.

141. Huo, M., et al., *Co-delivery of silybin and paclitaxel by dextran-based nanoparticles for effective anti-tumor treatment through chemotherapy sensitization and microenvironment modulation.* Journal of Controlled Release, 2020. **321**: p. 198-210.

142. Solanki, N., et al., *Antiproliferative effects of boswellic acid-loaded chitosan nanoparticles on human lung cancer cell line A549.* Future Med Chem, 2020. **12**(22): p. 2019-2034.

143. Jung, J., et al., *Polymeric nanoparticles containing taxanes enhance chemoradiotherapeutic efficacy in non-small cell lung cancer.* Int J Radiat Oncol Biol Phys, 2012. **84**(1): p. e77-83.

144. Singh, N., A. Sachdev, and P. Gopinath, *Polysaccharide Functionalized Single Walled Carbon Nanotubes as Nanocarriers for Delivery of Curcumin in Lung Cancer Cells.* J Nanosci Nanotechnol, 2018. **18**(3): p. 1534-1541.

145. Amirsaadat, S., et al., *Silibinin-loaded magnetic nanoparticles inhibit hTERT gene expression and proliferation of lung cancer cells.* Artificial Cells, Nanomedicine, and Biotechnology, 2017. **45**(8): p. 1649-1656.

146. Kole, R., A.R. Krainer, and S. Altman, *RNA therapeutics: beyond RNA interference and antisense oligonucleotides.* Nat Rev Drug Discov, 2012. **11**(2): p. 125-40.

147. Ingle, R.G. and W.J. Fang, *An Overview of the Stability and Delivery Challenges of Commercial Nucleic Acid Therapeutics.* Pharmaceutics, 2023. **15**(4).

148. Hueso, M., et al., *ncRNAs in Therapeutics: Challenges and Limitations in Nucleic Acid-Based Drug Delivery.* International Journal of Molecular Sciences, 2021. **22**(21): p. 11596.

149. Bhat, A.A., et al., *Polysaccharide-Based Nanomedicines Targeting Lung Cancer.* Pharmaceutics, 2022. **14**(12).

150. Cohen, J.L., et al., *Acid-degradable cationic dextran particles for the delivery of siRNA therapeutics.* Bioconjug Chem, 2011. **22**(6): p. 1056-65.

151. Nafee, N., et al., *Treatment of lung cancer via telomerase inhibition: self-assembled nanoplexes versus polymeric nanoparticles as vectors for 2'-O-Methyl-RNA.* Eur J Pharm Biopharm, 2012. **80**(3): p. 478-89.

152. Li, S.-D. and L. Huang, *Targeted Delivery of Antisense Oligodeoxynucleotide and Small Interference RNA into Lung Cancer Cells.* Molecular Pharmaceutics, 2006. **3**(5): p. 579-588.

153. Cheng, X., et al., *Lipid Nanoparticles Loaded with an Antisense Oligonucleotide Gapmer Against Bcl-2 for Treatment of Lung Cancer.* Pharmaceutical Research, 2017. **34**(2): p. 310-320.

154. Santana, Á.L. and G.A. Macedo, *Challenges on the processing of plant-based neuronutraceuticals and functional foods with emerging technologies: Extraction, encapsulation and therapeutic applications.* Trends in Food Science & Technology, 2019. **91**: p. 518-529.

155. Jha, S., K.K. Vaiphei, and A. Alexander, *Chapter 1 - Plant-based therapeutics: current status and future perspectives*, in *Phytopharmaceuticals and Herbal Drugs*, M.R. Singh and D. Singh, Editors. 2023, Academic Press. p. 3-11.

156. Gagliardi, M. and A.T. Ashizawa, *The Challenges and Strategies of Antisense Oligonucleotide Drug Delivery.* Biomedicines, 2021. **9**(4).

157. Juliano, R.L., *The delivery of therapeutic oligonucleotides.* Nucleic Acids Res, 2016. **44**(14): p. 6518-48.

158. Charbe, N.B., et al., *Small interfering RNA for cancer treatment: overcoming hurdles in delivery.* Acta Pharmaceutica Sinica B, 2020. **10**(11): p. 2075-2109.

159. Zhao, Y., et al., *XBP1 regulates the protumoral function of tumor-associated macrophages in human colorectal cancer.* Signal Transduction and Targeted Therapy, 2021. **6**(1): p. 357.

160. Byrd, A.E., I.V. Aragon, and J.W. Brewer, *MicroRNA-30c-2* limits expression of proadaptive factor XBP1 in the unfolded protein response.* J Cell Biol, 2012. **196**(6): p. 689-98.

161. Tiemann, K. and J.J. Rossi, *RNAi-based therapeutics-current status, challenges and prospects.* EMBO Mol Med, 2009. **1**(3): p. 142-51.

Chapter 2. Targeted polymer lipid hybrid nanoparticles for *in-vitro* siRNA therapy in triple-negative breast cancer

Meenu Mehta[1], Thuy Anh Bui[1], Andrew Care[2], Wei Deng[1*]

1. School of Biomedical Engineering, University of Technology Sydney, Ultimo, NSW 2007, Australia
2. School of Life Sciences, University of Technology Sydney, Ultimo, New South Wales 2007, Australia

Abstract

Triple-negative breast cancer (TNBC) is an aggressive subtype of breast cancer, characterised by a lack of hormone receptors and HER2 expression, resulting in limited treatment options and poor patient outcomes. This study explores a novel therapeutic approach using PLGA lipid nanoparticles loaded with siXBP1 and conjugated with an epidermal growth factor receptor (EGFR) antibody. This noncarrier will silence the XBP1 gene, which is crucial for the progression and survival of TNBC, particularly in hypoxic conditions. The conjugation of nanoparticles with the EGFR antibody improves their targeting ability to TNBC cells, as confirmed by confocal microscopy and flow cytometry. The fluorescence intensity of the targeted nanoparticles was 1.45 times higher than that of the non-targeted counterparts. These nanoparticles efficiently delivered siRNA to TNBC cells, resulting in substantial XBP1 gene silencing efficacy of 75%. Under hypoxic conditions, this gene-silencing effect significantly promoted apoptosis nearly threefold compared to normoxic conditions. These findings provide valuable insights into targeted therapies for TNBC and pave the way for further in vivo investigations to advance this approach toward clinical applications.

Keywords: Breast cancer; Gene therapy; Targeted nanoparticles; Hypoxia

2.1 Introduction

Among all breast cancer subtypes, triple-negative breast cancer (TNBC) stands out as the most aggressive, comprising approximately 15% of cases. It is characterized by the absence of human epidermal growth factor receptors 2 (HER2), progesterone receptors, and estrogen receptors [1, 2]. TNBC is associated with a high recurrence rate and limited survival, with a 40% mortality rate within five years of diagnosis [3]. After metastasis, the average survival time is just 12.2 months, and the postoperative recurrence rate is approximately 25% [4]. Chemoradiotherapy stands as the standard of care for TNBC, yet its constraints involve drug toxicity, resistance, and late morbidity linked to high-dose radiation [5]. Due to the lack of targeted therapies specific to TNBC, there is a pressing need for innovative approaches to enhance patient outcomes [6-8].

To address this challenge, XBP1 emerges as a key driver of TNBC tumor growth and recurrence, primarily by regulating the ER stress response and unfolded protein pathways, impacting cell survival, proliferation, and chemoresistance [9, 10]. Elevated XBP1 expression is frequently associated with TNBC, promoting these detrimental effects and contributing to a poor prognosis and treatment resistance [11]. Notably, a connection between XBP1 and reduced TNBC responsiveness to standard treatments is well-established [11]. Analysis of 193 TNBC patient samples revealed shorter relapse-free survival in cases with an elevated XBP1 signature [12].

Hypoxia-inducing factor 1α (HIF-1α) is known to be hyperactivated in the hypoxic microenvironment of human tumors including TNBC [13]. XBP1 has been identified to regulate tumorigenicity by controlling the HIF-1α pathway [12, 14]. It can boost the stability and activity of HIF-1α, resulting in the activation of genes that support angiogenesis, glycolysis and cell survival [12, 15]. Given the significant roles of the XBP1 gene in driving TNBC tumor growth and recurrence, specific XBP1 gene silencing is a potential therapeutic approach, particularly in hypoxic conditions.

Various strategies have been employed to achieve XBP1 gene silencing, including siRNA therapy, the CRISPR/Cas9 system, and miRNA mimics or inhibitors. siRNA offers a targeted approach by utilizing the RNA interference (RNAi) pathway to downregulate XBP1, thereby inhibiting tumor growth and improving treatment resistance [16]. Alternatively, the CRISPR/Cas9 system can permanently delete the XBP1 gene, offering a long-term solution that eliminates the need for repeated treatments. For instance: Zhao et al. demonstrated that CRISPR-mediated XBP1 silencing enhanced antitumor activity, altered cytokine expression, and promoted macrophage-mediated tumor cell clearance by disrupting self-recognition mechanisms [17]. Additionally, certain miRNAs, such as miR-30 and miR-320, have been shown to regulate XBP1 expression

[18]. Despite the potential of these gene-silencing approaches, siRNA, CRISPR, and miRNA-based therapies face significant challenges related to delivery and specificity. Off-target effects and the risk of unintended genetic alterations are major concerns with all three methods [19].

In the context of XBP1 gene knockdown, small interfering RNA (siRNA) offers a promising strategy for targeted gene silencing in TNBC treatment by leveraging the RNA interference (RNAi) pathway to selectively downregulate crucial genes, inhibiting tumor growth and overcoming treatment resistance [16]. Regarding delivery vehicles, nanoparticle-based drug delivery systems, including lipid nanoparticles with polymers like Poly (lactic-co-glycolic acid) (PLGA), are advantageous for cancer therapy [17, 18]. They are noted for their biocompatibility, controlled drug release, and capacity to encapsulate diverse therapeutic agents, such as siRNA [19, 20]. Within PLGA lipid nanoparticle, the lipid component ensures stability, biocompatibility, and enhanced cellular uptake via intracellular delivery of therapeutic contents, while the PLGA polymer enables controlled release and safeguards the encapsulated siRNA cargo [21]. Zhang *et al.* employed RNA nanoparticles to co-encapsulate the chemodrug Dox and siRNA (siXBP1) for targeting HER2+ breast cancer. The results showed that these nanoparticles provided targeted delivery and maintained structural stability. Deletion of XBP1 by RNA nanoparticles suppressed angiogenesis, inhibited cell proliferation, significantly reduced breast cancer growth, and enhanced chemotherapy sensitivity in a mouse model of HER2+ breast cancer [22]. In another study by the same team, packaging RNA derived from bacteriophage phi29 is employed as a targeted therapy approach against TNBC. The findings reveal that these RNA nanoparticles effectively reduce XBP1 expression and inhibit tumor growth upon intravenous administration. Furthermore, treatment with RNA NPs enhances sensitivity to chemotherapy and hampers angiogenesis *in-vivo* [23]. While, siXBP1 (siRNA) has been integrated into different delivery systems. However, none of the studies have investigated the delivery of siXBP1 using polymer lipid nanoparticles in TNBC cells. Therefore, the goal of this study was to devise a targeted therapeutic strategy for triple-negative breast cancer (TNBC) by engineering epidermal growth factor receptor (EGFR) antibody conjugated siXBP1 loaded PLGA lipid nanoparticles. We selected the EGFR antibody due to its elevated expression in TNBC, aiming to enhance siRNA delivery specificity [24].

To achieve this goal, we first characterized the synthesized nanoparticles for their particle size, zeta potential, and surface morphology, ensuring suitability for TNBC targeted delivery. Next, we examined the cellular uptake of the EGFR antibody-conjugated PLGA lipid nanoparticles in TNBC cells (MDA-MB-231) using confocal microscopy and flow cytometry as assessment of

nanoparticle internalization. We confirmed EGFP gene silencing in HEK293-EGFP cells by encapsulating EGFP siRNA for confocal microscopy analysis prior to validation of XBP1 gene silencing in MDA-MB-231 cells with siXBP1-loaded PLGA lipid nanoparticles by qRT-PCR and Western Blot. Finally, we evaluated the effect of XBP1 gene knockdown with EGFR antibody-siXBP1-loaded PLGA lipid nanoparticles on cell survival and apoptosis in MDA-MB-231 cells under hypoxic conditions, highlighting the potential of our nanoparticles as a promising therapeutic approach for TNBC.

2.2 Materials

Poly(D,L-lactide-co-glycolide) acid terminated, lactide:glycolide 50:50 (PLGA) (719870-5G), Mw 24000-38000, Poly vinyl alcohol (PVA) (P8136), MW 30,000-70,000, Coumarin-6 (C-6) (442631-1G) were purchased from Sigma-Aldrich Pty Ltd (Australia). DOTAP (890890P-200mg) and 1,2-distearoyl-sn-glycero-3-phosphoethanolamine-N-[maleimide(polyethylene glycol)-2000] (ammonium salt) (DSPE-PEG2000-Mal) (880126p-25mg) were purchased from Avanti Polar Lipids. Chloroform (C2432–500 mL), Dichloromethane (270997-1 L), Phosphate buffered saline (P4417-50 TAB) were also purchased from Sigma-Aldrich Pty Ltd (Sydney, Australia). Human anti-EGFR antibody (cetuximab, C225) was purchased from Assay Matrix Pty Ltd (Melbourne, Australia). Scramble siRNA (siScr -SIC001) was purchased from Merck, Australia and siRNA targeting EGFP (siGFP-51-01-05-06) was purchased from Integrated DNA Technologies, Australia. siRNA targeting XBP1 (s14913), Lipofectamine RNAiMax transfection reagent (13778075), Opti-Minimal Essential Medium (Opti-MEM; reduced serum medium; product, 31985062), Pierce™ Coomassie (Bradford Protein Assay Kit) (23200) were purchased from (Thermo Fisher Scientific, Australia). MTT (3-[4,5-dimethylthiazol-2-yl]-2,5-diphenyl tetrazolium bromide), Dimethyl sulfoxide (DMSO), DAPI were purchased from Sigma-Aldrich, St. Louis, MO, USA. FITC Annexin V Apoptosis Detection Kit I (cat. no. 556547) was purchased from BD Biosciences (San Jose, CA, USA). The antibodies to XBP1 and β-actin were purchased from Abcam. All the remaining chemical reagents and solvents were purchased from Sigma-Aldrich unless stated.

Cell culture

MDA-MB-231 and MCF-7 cell lines were a kind gift from Prof. Majid Ebrahimi Warkiani lab, School of Biomedical Engineering, University of Technology Sydney, Australia. These cells were cultured in Dulbecco′s Modified Eagle′s Medium (DMEM) (Sigma-Aldrich Pty Ltd, Australia) with 10% heat-inactivated Fetal Bovine Serum (Thermo Fisher Scientific, Australia) at 37°C at

5% CO_2 in a humidified atmosphere. Human mammary epithelial cells (HMEC) and Human embryonic kidney 293 cells expressing EGFP (HEK 293-EGFP) were a kind gift from Prof. Ewa Goldys lab, School of Biomedical Engineering, University of New South Wales, Australia. HMEC were cultured in HMEC growth medium while HEK 293-EGFP cells were cultured in DMEM with10% heat-inactivated Fetal Bovine Serum under standard conditions (37°C, 5% CO_2) in a humidified incubator. All cells were frequently tested for the presence of mycoplasma, and all experiments were carried out in mycoplasma negative cells.

2.3 Methods

2.3.1 Preparation of PLGA lipid nanoparticles

PLGA lipid nanoparticles were prepared using the double emulsion-solvent evaporation technique [19]. The formulation was optimized including the particle size, zeta potential and polydispersity index (PDI) based on DOTAP/PLGA ratio, sonication time and polyvinyl alcohol (PVA) concentration. In brief, 200 pmole of siRNA was added dropwise to 500 µl of PLGA/DOTAP mixture (mole ratio of 7:3) in dichloromethane (DCM). This mixture was emulsified using probe sonication over an ice bath at 40 % amp for 30 s (3 times) to form the primary emulsion. Subsequently, 6 ml of 1% (w/v) PVA containing 0.3 mg of DSPE-PEG2000-Mal was added to the primary emulsion, followed by sonication at 40 % amp for 30 s (3 times) over an ice bath. This process resulted in the formation of the secondary water-in-oil-in-water emulsion, which was left under agitation for 3h at room temperature to evaporate organic solvent. Afterwards, the dispersion was centrifuged for 12 min at 4°C and 18,000×g. The supernatant was discarded, and the pellet containing the nanoparticles was re-dispersed in phosphate buffer saline (PBS). This process of centrifugation and re-dispersion was repeated three times to ensure the removal of PVA before further characterisation. We employed the same method to prepare various types of PLGA lipid nanoparticles, by encapsulating different cargoes (coumarin-6 (a dye), EGFP siRNA, scramble siRNA). The formulation details are listed in table 2.1:

Table 2.1. Composition of different PLGA lipid nanoparticles

S.No.	Formulation	Cargo amount	PLGA/DOTAP ratio (w/w)	PVA (% w/v)	DSPE-PEG2000-Mal (mg)
1.	Blank PLGA lipid nanoparticles	-	7:3	1	0.3
2.	Coumarin-6 loaded nanoparticles (C-6 NPs)	17.5 µg	7:3	1	0.3

3.	EGFP siRNA loaded nanoparticles (siEGFP NPs)	100 pmole	7:3	1	0.3
4.	Scramble siRNA loaded nanoparticles (Scr NPs)	200 pmole	7:3	1	0.3
5.	siXBP1 (siRNA) loaded nanoparticles	200 pmole	7:3	1	0.3

Antibody conjugation to nanoparticles

Antibody conjugation to nanoparticles was achieved through a thiol-maleimide reaction [22]. Initially, 10 µl EGFR antibody (1mg/ml stock solution in PBS) was diluted with 990 µl of PBS (pH 7.4). Simultaneously, 1mg of N-Succinimidyl S-Acetylthioacetate (SATA) was dissolved in 0.5 ml of dimethyl sulphoxide (DMSO) just before the reaction. The EGFR antibody solution was then mixed with SATA solution at a molar ratio of 8:1 (SATA: antibody) and incubated at room temperature for 30 min. To facilitate SATA crosslinking with maleimide groups, the sulfhydryl groups were deacetylated by mixing the SATA/antibody solution with 100 µl of hydroxylamine solution (0.5M Hydroxylamine, 25mM EDTA in PBS, pH 7.2-7.5) and incubated for 1 h at room temperature. Subsequently, conjugation was initiated by combining nanoparticles with the SATA/antibody solution at a molar ratio of 1:10 (nanoparticles: SATA/antibody solution) and incubated at room temperature for 2 h, followed by overnight incubation at 4°C. Unbound antibody was removed through centrifugation, and the nanoparticle pellet was redispersed in PBS for further applications.

Quantification of EGFR antibody conjugated onto the surface of nanoparticles

The amount of EGFR antibody conjugated to the nanoparticle surface was confirmed by Bradford assay, which was based on the binding of coomassie brilliant blue dye (Bradford reagent) to proteins, resulting in a color change proportional to the protein concentration. Following the manufacturer's protocol, various concentrations of the protein standard solution, ranging from 25 µg/mL to 2000 µg/mL, were prepared in PBS buffer. Next, 5 µL of each standard or nanoparticle suspension was carefully transferred to the appropriate wells of a microplate. Subsequently, 250 µL of the Bradford reagent was added to each well, and the plate was incubated for 10 min. at room temperature. The absorbance was measured at 595 nm using a Tecan plate reader. The amount of conjugated antibody was determined by assessing the absorbance intensity and subsequently calculating its concentration using the standard curve of free protein solution.

2.3.2 Nanoparticle characterization

Particle size, polydispersity index (PDI), and zeta potential measurements were carried out using Dynamic Light Scattering (Malvern Zetasizer Nano ZS). Before analysis, the nanoparticle suspension was resuspended, sonicated, and vortexed. For particle size and PDI measurement, diluted samples were placed in clear disposable cuvettes, while zeta cells were utilized for zeta potential measurement. All measurements were performed in triplicate at 25°C. The surface morphology of nanoparticles was examined by using Scanning Electron Microscopy (SEM, Zeiss Supra 55 VP). For SEM imaging, nanoparticles were suspended in nuclease-free water (100 µl/ml) and sonicated for 30 s. A drop of this suspension was deposited on a silicon wafer and allowed to air dry for 24 h under ambient conditions. The silicon wafer was then attached to a stub using double-sided carbon tape. To ensure conductivity, the nanoparticles were sputtered with gold/palladium using the Leica Coater prior to image acquisition.

Entrapment Efficiency (EE)

The amount of coumarin-6 (C-6) encapsulated within the nanoparticles was determined by assessing the fluorescence intensity of the C-6-loaded nanoparticles (C-6 NPs) (Ex/Em: 450 nm/505 nm) and subsequently calculating its concentration using the standard curve derived from a free C-6 solution.

The entrapment efficiency of siRNA loaded inside the nanoparticles was determined using RediPlate 96 Ribogreen RNA Kit (Thermo Fisher Scientific, Australia). The RiboGreen® reagent specifically reacts with free siRNA, producing a fluorescent compound with an emission maximum at 535 nm (λex = 485 nm). Thus, to assess entrapment efficiency, the prepared nanoparticle suspension was centrifuged, and the supernatant was collected. The unloaded siRNA in the supernatant was then measured using the Ribogreen RNA Kit and compared to the initial siRNA concentration used in the nanoparticle preparation.

In details, various concentrations of pure siRNA solution (ranging from 5 ng/mL to 200 ng/mL) were prepared using TE buffer. Subsequently, 20 µL pure siRNA solution and the supernatant were added to wells of a microplate, followed by thorough pipetting. The microplate was incubated for 20 min. at room temperature, shielded from light. After incubation, fluorescence was measured using a microplate reader (Ex/Em: 480 nm/535 nm). The concentration of siRNA

in the supernatant was determined by comparing it to the standard curve of a free siRNA solution. The entrapment efficiency was calculated using the following equation:

$$\%EE = \frac{(\text{RNA amount used for formulation} - \text{RNA amount present in supernatant})}{\text{RNA amount used for formulation}} x100$$

2.3.3 Cellular uptake activity

Cellular uptake activity was assessed by using C-6 NPs and EGFR antibody conjugated C-6 nanoparticles (EGFR Ab-C-6 NPs). Briefly, MDA-MB-231 cells were cultured overnight in glass-bottom petri dishes and incubated with nanoparticle suspension (200 µg/ml) for 1 and 2 h, respectively. Subsequently, the cells were thoroughly washed with DPBS (pH 7.4) three times to eliminate any unbound nanoparticles and then fixed using 4% paraformaldehyde (100 µl) at room temperature. After fixation, the cells were stained with DAPI (Sigma) reagent, and the internalization of nanoparticles was visualized using a Nikon A1 inverted confocal microscope system. Additionally, flow cytometry analysis was performed after the nanoparticle incubation. The cells were washed, trypsinized, collected, and their fluorescence was quantitatively analyzed using a CytoFLEX LX flow cytometer (Beckman Coulter).

2.3.4 XBP1 expression level in normal vs breast cancer cell lines and under hypoxia conditions

To evaluate XBP1 gene expression, we selected two breast cancer cell lines, MDA-MB-231 and MCF-7, along with one normal mammary epithelial cell line (HMEC). To induce hypoxia, MDA-MB-231 cells were placed in hypoxic chamber for 24 h or 48 h. After each incubation period, RNA and proteins were isolated from cells and analyzed for XBP1 gene expression.

RNA extraction

RNA samples were isolated using the Trizol® method [25]. Initially, the cells underwent a brief wash in PBS, followed by transfer into nuclease-free Eppendorf tubes. Subsequently, they were centrifuged at 12,000 xg at 4°C for 10 min. The resulting cell pellets were then combined with 1ml of Trizol® (Invitrogen), and 300 µl was added, after which the mixture was incubated at room temperature for 3 min. After this, the samples were subjected to phase separation by centrifuging at 12,000×g at 4°C for 10 min. The upper aqueous layer, containing the RNA, was carefully transferred to new tubes containing 600 µl of ice-cold isopropanol (Sigma, Australia). RNA precipitation was facilitated by centrifuging for 30 min at 12,000×g and 4°C. The RNA pellets were briefly washed in 1ml of 70% ethanol and again centrifuged at 12,000×g at 4°C for

10 min. Following this step, the ethanol was removed, and the RNA pellet was dried on a 37°C heat block for 5 min. Finally, the resulting RNA pellet was resuspended in 40μl of nuclease-free water. RNA concentration was measured via absorbance at 260nm by Nanodrop™ One Microvolume UV-Vis spectrophometer (Thermo Fisher Scientific, Australia).

qRT-PCR

All the primers utilized in the quantitative PCR reactions for this study were purchased from Sigma-Aldrich. In summary, a quantity of RNA samples less than 1μg was employed for both cDNA conversion and the qPCR reaction, employing the Luna® Universal One-Step RT-qPCR Kit from New England Biolabs. The qPCR reactions were conducted according to the manufacturer's protocol. The primer sequences used for these reactions are detailed in Table 2.2.

Table 2.2: Primer sequences used for qRT-PCR

Primer	Sequence
XBP1 - Forward	5′- AGGAGTTAAGACAGCGCTTGGGGATGGAT-3′
XBP1 - Reverse	5'-CTGAATCTGAAGAGTCAATACCGCCAGAAT-3′
Beta actin – Forward	5'-CCTGTACGCCAACACAGTGC-3′
Beta actin – Reverse	5'-ATACTCCTGCTT GCTGATCC-3′

Protein extraction

Cell samples were gathered in RIPA Lysis buffer, which included Halt™ Protease Inhibitor Cocktail (Thermo Fisher Scientific, Australia). They were left to incubate on ice for 20 min. before undergoing a short 15-second sonication. Subsequently, the cell lysates were subjected to centrifugation at 12,000×g at 4°C for 20 min to eliminate cellular debris. The protein concentration of each sample was assessed via absorbance at 280nm using the NanoDrop™ Microvolume UV-Vis Spectrophotometer (Thermo Fisher Scientific, Australia).

Western Blot assay

Briefly, 30μg of each protein lysate was combined with 5 μl of NuPAGE LDS Sample Buffer and heated at 70°C for 10 min. All prepared samples were subsequently loaded into NuPAGE 4-12% Bis-Tris 1.5mm Mini Protein Gels secured within the XCell SureLock™ Mini-Cell. The loaded protein samples were then separated in 1× NuPAGE MOPS SDS Running Buffer at 125V for 90 min.

After the gel electrophoresis, the protein samples were transferred onto a 0.2μm PVDF Transfer Membrane using the XCell Blot Module and 1× NuPAGE Transfer Buffer at 30V for 120 min.

The membranes were subsequently immersed in a blocking solution (3% w/v Bovine Serum Albumin from Sigma in TTBS buffer, which consists of 0.01M Tris Base, 0.05M NaCl, and 0.1% Tween20) for 1 h at room temperature to prevent non-specific binding.

Membrane incubation with primary antibodies (XBP1 or Beta-actin from Abcam, each at a 1:1000 dilution in TTBS) was carried out at 4°C overnight. After three 5-min washes in TTBS buffer, the membranes were incubated in an anti-rabbit horse peroxidase-conjugated secondary antibody (CST, diluted at 1:5000 in TTBS) on an orbital shaker at room temperature. Following this, the membranes were washed in TTBS buffer for 5 min. each and then visualized using PierceTM ECL Western Blotting Substrate (Thermo Fisher Scientific, Australia) under a ChemiDoc MP System (Biorad, USA).

2.3.5 Assessment on *in vitro* EGFP and XBP1 knockdown via siRNA-loaded nanoparticles

HEK293-EGFP cells were cultured at a density of 5×10^4 in glass-bottom petri dishes and then incubated with the siGFP-loaded nanoparticle suspension for 24 and 48 h. Subsequently, the cells were imaged under a confocal microscope to assess EGFP fluorescence signal. Additionally, flow cytometry analysis was performed as indicated in the above section.

MDA-MB-231 cells were seeded at a density of 1×10^5 cells per well in a 6-well plate and incubated for 24 h. Following this, the cells were treated with various conditions for an additional 48 h. The treatment conditions included: cells only, free siRNA alone, siRNA transfected with RNAiMax transfection reagent, EGFR antibody conjugated siRNA-loaded nanoparticles (EGFR Ab-siXBP1 NPs) and EGFR antibody conjugated siScr-loaded nanoparticles (EGFR Ab-Scr NPs). All these samples contain 25 nM siXBP1 or siScr. After incubation period, cellular RNA was collected using the same method followed by RT-PCR analysis.

2.3.6 *In-vitro* cell viability assay

Cells were seeded at a density of 1×10^4 cells per well in 96-well plates with culture medium containing 10% FBS for 24 h. After 24 h, the cells were treated with different concentrations of nanoparticles (200-400 µg/ml) for 48 h. Following this treatment period, 10 µl of Thiazolyl Blue Tetrazolium Bromide (Sigma) at a concentration of 5 mg/ml in sterile PBS was added to each well and incubated for 4 h at 37°C in 5% CO_2. After removing the supernatant, 100 µL of DMSO was added to dissolve the formazan crystals, resulting in the formation of a purple-colored product. The absorbance of this product was measured using a Tecan plate reader at 570 nm. The

cell viability was calculated as a percentage of the absorbance in the treated cells compared with that of untreated cells, as follows:

Viability (%) = (A_g - A_{blank})/(A_c - A_{blank}) × 100

Where A_g is the absorbance of each group, A_c is the absorbance of the control group and A_{blank} is the absorbance of cell culture medium.

2.3.7 Cellular apoptosis assay

For apoptosis assays, 1×10^5 cells per well were seeded into 6-well plates in two separate sets. One set was incubated in a normal incubator while the other was placed in the hypoxic chamber for 48 h to induce hypoxia. After the respective incubation periods, the cells were exposed to EGFR Ab-siXBP1 NPs and EGFR Ab-siScr NPs maintained for an additional 48 h within the hypoxic chamber. The treatment groups consisted of control (cells only), cells treated with antibody-conjugated siXBP1 loaded nanoparticles, and cells treated with antibody-conjugated siScr-loaded nanoparticles. After 48 h of treatment, apoptosis was quantified using the FITC Annexin V Apoptosis Detection Kit I (cat. no. 556547; BD Biosciences) following the manufacturer's instructions. Cells were harvested and washed twice with PBS. Subsequently, 1×10^6 cells were resuspended in 100 µl of 1× binding buffer (diluted with ddH$_2$O), followed by the addition of 5 µl FITC and 5 µl PI to each tube. The samples were incubated for 30 min at room temperature in darkness. After staining, 500 µl of 1× binding buffer was added to each tube and analysed by flow cytometry. Similar experiments were conducted under non-hypoxic conditions.

2.3.8 Cell cycle analysis and colony formation assay

We utilized the Luminex Muse Cell Cycle Kit according to the manufacturer's instructions to evaluate the effect of XBP1 gene knockdown on the cell cycle progression of MDA-MB-231 cells. Initially, MDA-MB-231 cells were seeded at a density of 3×10^5 cells/mL in 6-well plates and incubated for 24 h. Subsequently, the cells were divided into three treatment groups: cells only, cells treated with 25 nM of EGFR Ab-siXBP1 nanoparticles, and cells treated with 25 nM of EGFR Ab-siScr nanoparticles. Following 48 h incubation period with the respective treatments, cells were trypsinized, washed with cold DPBS, and fixed with ice-cold 70% ethanol at -20°C for a minimum of 3 h. Following fixation, cells were washed with DPBS and suspended in 200 µL of Muse® Cell Cycle reagent for 30 min. at room temperature in darkness.

Subsequently, the distribution of cell cycle phases was quantified using the Muse Cell Analyzer (Luminex Corporation, Texas, USA).

Further, a colony formation assay was conducted to evaluate the impact of XBP1 gene knockdown on the proliferation rate of MDA-MB-231 cells. The cells were initially seeded at a low density of 500 cells/mL in 6-well plates containing culture medium supplemented with 10% FBS for 24h. After 24h, the cells were divided into three treatment groups: cells only (control), Cells treated with 25 nM of EGFR Ab-siXBP1 NPs and cells treated with 25 nM of EGFR Ab-siScr NPs and incubated for a duration of 10 days. After the incubation period, the cells were gently rinsed with PBS and fixed with 4% paraformaldehyde solution for 20 min. Subsequently, the fixed cells were stained with a 0.5% (w/v) crystal violet solution for 15 min. at room temperature. Following staining, excess dye was removed by thoroughly washing the cells with PBS. The formed colonies were then visualized and quantified using Image J software.

2.4 Results

2.4.1 Preparation and characterization of nanoparticles

In this study, lipid polymer hybrid nanoparticles were prepared via double emulsion solvent evaporation technique. The morphology of prepared nanoparticles was evaluated under SEM. Figure 2.1a revealed that the blank nanoparticles had a spherical shape with an average size 150±7.4 nm. From DLS measurements, the average size of blank nanoparticles, C-6 loaded nanoparticles and EGFP antibody-conjugated siRNA loaded nanoparticles was about 163 ±2.02 nm, 186.08±7.1 nm, and 178.9±9.2 nm, respectively (Table 2.3). These samples exhibited a positively charged surface, and their low polydispersity index (PDI) indicated that they were uniform in size and monodispersed.

To enhance the ability of the nanoparticles to target cancer cells, we attached targeting molecules, EGFR antibody to the surface of the nanoparticles. For conjugated samples, we observed a slight increase in size, changing from 186.08±7.1nm to 209.2±1.3nm. There was also a concurrent increase in PDI from 0.05±0.02 to 0.35±0.02 (Table 2.3). These changes fall within acceptable thresholds, indicating a homogeneous nanoparticle population [26]. In order to quantify the amount of EGFR antibody conjugated with the nanoparticles, a colorimetric Bradford protein assay was performed, with about 68.8% of EGFR antibody being successfully conjugated with the nanoparticles. This finding closely aligns with other reported studies [27].

We further assessed the cargo loading efficacy of these nanoparticles. As shown in Figure 2.1b, there was a typical fluorescence peak at 505nm wavelength of the C-6 observed in C-6 loaded nanoparticles, indicating the successful loading of C-6 within the nanoparticles. For C-6 NPs, the entrapment efficiency was calculated to be 73.37% (Table 2.3). For conjugated nanoparticles, the entrapment efficiency was reduced to 56.11% (Table 2.3), possibly attributed to losses incurred during the secondary centrifugation step carried out after antibody conjugation. Regarding siRNA, the highest loading efficiency of 94.92% was observed in siGFP nanoparticles. This could be attributed to the electrostatic interactions between the positively charged lipid compound and the negatively charged siRNA.

Table 2.3. Characterization of prepared PLGA lipid nanoparticles

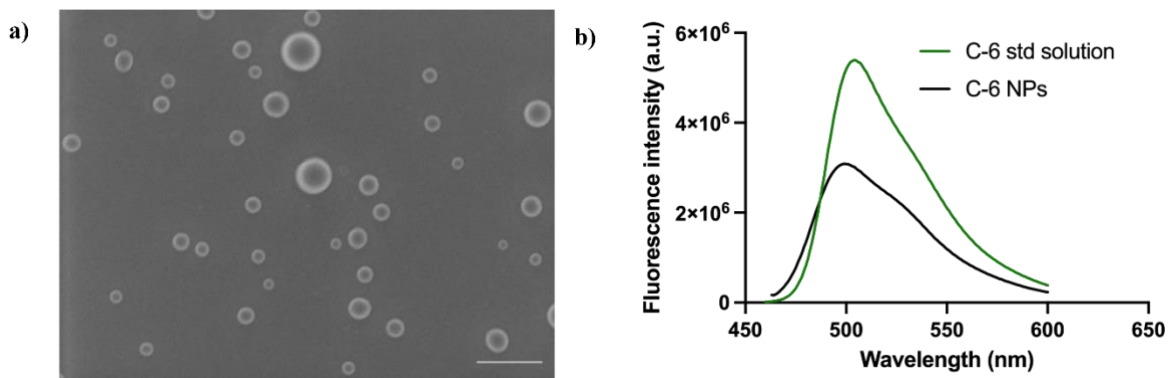| Samples	Particle size (nm)	PDI	Zeta Potential (mV)	Entrapment Efficiency (%)
Blank PLGA lipid nanoparticles	163 ±2.02	0.05±0.02	25.9±0.25	-
Coumarin-6 loaded nanoparticles (C-6 NPs)	186.08±7.1	0.06±0.03	19.4±0.37	73.37±1.7
EGFP siRNA loaded nanoparticles (siGFP NPs)	178.9±9.2	0.05±0.02	14.2±0.15	94.92±2.9
EGFR antibody-conjugated Coumarin-6 loaded nanoparticles (EGFR Ab-C-6 NPs)	209.2±1.3	0.25±0.03	-2.92±0.37	56.11±1.4
EGFR antibody-conjugated siXBP1 loaded nanoparticles (EGFR Ab-siXBP1 NPs)	226.7±8.7	0.35±0.02	-3.08±0.17	82.96±2.4
EGFR antibody-conjugated siScr loaded nanoparticles (EGFR Ab-Scr NPs)	208.9±4.5	0.14±0.05	-0.791±0.14	83.45±2.8

Figure 2.1: a) The SEM image of blank PLGA lipid nanoparticles (Scale bar = 200 nm); b) Fluorescence emission spectra of coumarin-6 solution (C-6 std solution) and coumarin-6 loaded nanoparticles (C-6 NPs)

2.4.2 *In-vitro* cellular uptake study

To achieve the targeting capability of our nanoparticles on TNBC cells, we conjugated the nanoparticles with EGFR antibody. This modification specifically targets the EGFR receptor, which is known to be overexpressed in approximately 50% of TNBC cells compared to other breast cancer subtypes [28]. This strategy was reported an effective targeting tool for TNBC cells, leading to increased cellular drug accumulation and enhanced treatment efficacy [29]. The targeting capability of antibody-conjugated nanoparticles was assessed by comparing the cellular uptake of EGFR Ab-C-6 NPs and non-targeted C-6 NPs in MDA-MB-231 cells at different incubation times. Figure 2.2a demonstrated the higher C-6 fluorescence signal from the cells treated by targeted nanoparticles compared with non-targeted ones. As shown in Figure 2.2b, the fluorescence intensity of C-6, measured via flow cytometry, demonstrated approximately 1.26-fold and 1.45-fold higher values for EGFR Ab-C-6 NPs compared to non-targeted counterparts at 1 h and 2 h incubation times, respectively. This enhanced internalization capability of targeted nanoparticles was probably attributed to the specific affinity interaction between anti-EGFR antibody and overexpressed EGFR on the surface of cancer cells.
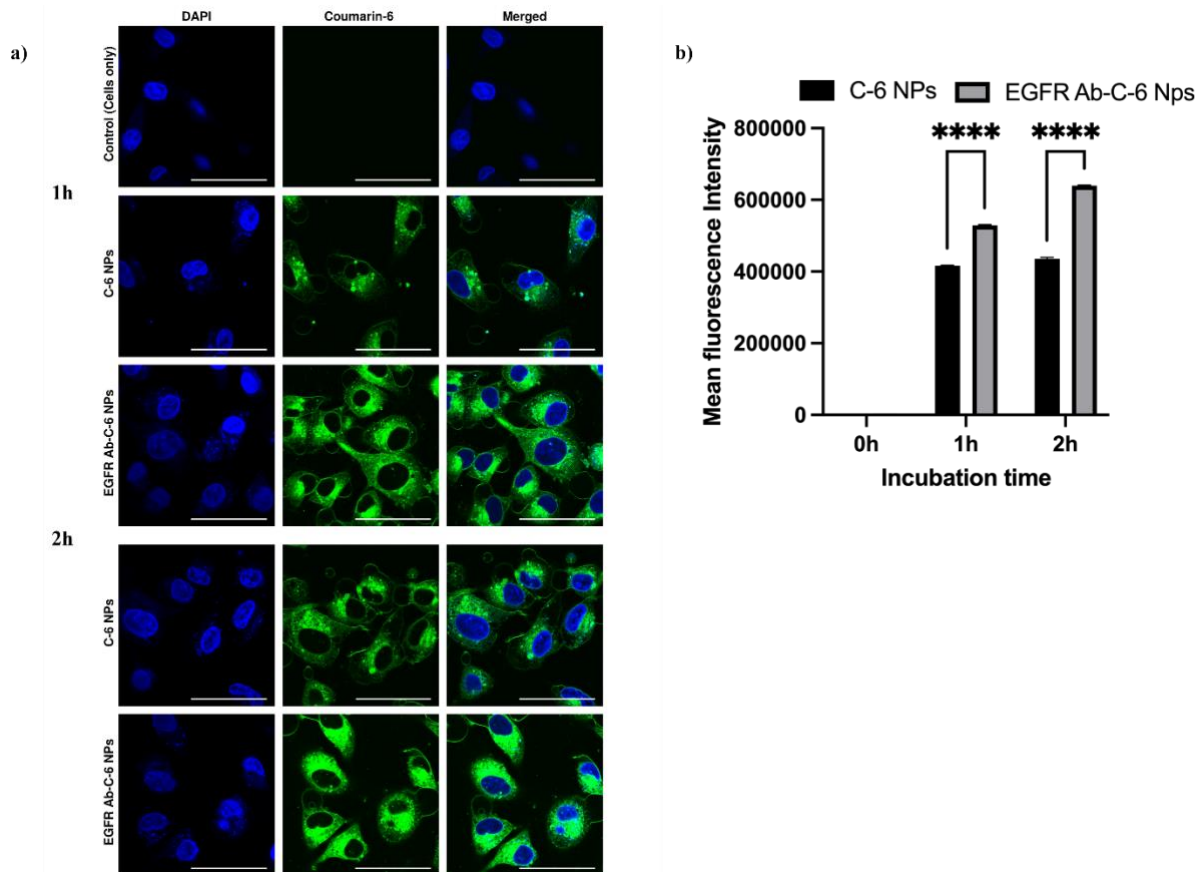
Figure 2.2: a) Confocal microscopic images of MDA-MB-231 cells after incubation with C-6 NPs and EGFR AB-C-6 NPs; The scale bar is 50 μm b) The mean fluorescence intensity of C-6 in MDA-MB-231 cells treated with C-6 NPs and EGFR AB-C-6 NPs measured by flow cytometry. Data represented as mean± s.e.m., (n=3). ****p ＜0.0001.

2.4.3 Assessment on *In-vitro* EGFP and XBP1 knockdown via nanoparticles

We first assessed XBP1 gene expression in two breast cancer cell lines, MDA-MB-231 and MCF-7, along with a normal breast cell line, HMEC. As illustrated in Figure. 2.3a, a significantly higher XBP1 mRNA expression was observed in MDA-MB-231 cells compared to MCF-7 and HMEC cell lines. Existing literature indicates that hypoxia triggers the activation of XBP1 expression, in conjunction with its co-regulator, HIF-1α, in TNBC tissues, thereby promotes cancer progression [11]. Thus, we investigated the effect of hypoxia on XBP1 expression in MDA-MB-231 cells. As shown in Figure 2.3b, XBP1 mRNA expression apparently increased under hypoxic conditions, which was further supported by western blot analysis (Figure 2.3c).

Following the confirmation of XBP1 gene expression levels in MDA-MB-231, we evaluated the efficacy of gene knockdown using our nanoparticles. We first validated the transfection feasibility of our nanoparticles targeting EGFP in HEK293 cells. Figure 2.3d demonstrates an apparent

decrease in EGFP fluorescence intensity in the cells treated with 100 µg/ml of siGFP NPs for 24 and 48 h compared with the control. Flow cytometry data further revealed reductions of 42.83% and 72% in EGFP intensity at 24h and 48h post-transfection, respectively (Figure 2.3e), indicating the nanoparticles are capable of effectively suppressing the EGFP gene expression. After confirming that our nanoparticles successfully delivered EGFP siRNA in HEK293 cells, we further assessed the transfection effectiveness of our formulation targeting XBP1 gene in MDA-MB-231. As shown in Figure 2.3f, the assessment of XBP1 mRNA expression levels was conducted under various treatment conditions, including EGFR Ab-siXBP1 NPs, EGFR Ab-Scr NPs, siXBP1 with RNAiMax and naked siXBP1 only. Among these treatments, we noted that approximately 75% reduction in XBP1 gene expression in MDA-MB-231 cells at 48 h after treatment with EGFR Ab-siXBP1 NPs. By contrast, the commercial transfection reagent (siXBP1 with RNAiMax) achieved only around 30% suppression of XBP1gene expression.
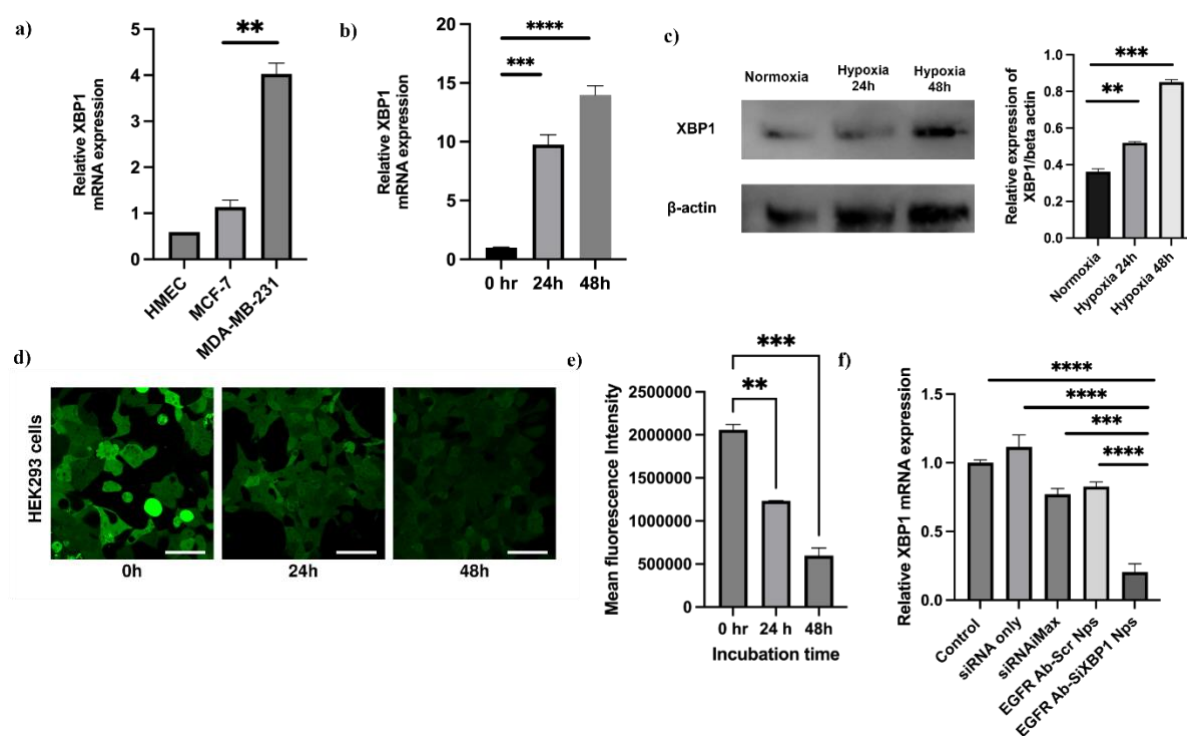
Figure 2.3: a) XBP1 mRNA expression in normal and breast cancer cell lines.; b) XBP1 mRNA expression in MDA-MB-231 under hypoxic conditions; c) Western blot and densitometric analysis of XBP1 protein expression in MDA-MB-231 cells under hypoxic conditions (d) Confocal microscopic images of HEK293-EGFP cells after the treatment with 100 µg/ml of siGFP NPs, the scale bar is 50 µm; e) The mean fluorescence intensity of EGFP positive cells; f) XBP1 mRNA expression in MDA-MB-231 cells after treatment with 25 nM of naked siRNA, 200 µg/ml of EGFR Ab-siXBP1 NPs (contains 25nM siRNA), 200 µg/ml of EGFR Ab-Scr NPs

(contains 25nM siRNA), and siXBP1 with RNAiMax (25nM). Data represented as mean ± SEM; n =3; **p ＜0.01; ***p ＜0.001; ****p ＜0.001

2.4.4 Investigation of cellular apoptosis after the *XBP1* gene knockdown

Before assessing the effect of XBP1 gene knockdown on cellular apoptosis, we first examined the cellular toxicity of our nanoparticles in MDA-MB-231 cells via MTT assay. As shown in Figure 2.4a, no significant change in cell viability was observed when treated with blank PLGA lipid NPs at concentrations of 200 µg/ml (the concentration used for gene delivery) and even at a higher concentration of 400 µg/ml, compared with the control group. This observation indicates that our nanoparticles are unlikely to adversely impact the viability of MDA-MB-231 cells in our study.

As illustrated in Figure 2.3c, hypoxia induces an upregulation in XBP1 protein expression levels. In line with this observation, we further assessed the XBP1 gene knockdown efficacy of the nanoparticles under hypoxic conditions, which are representative of the TNBC cell environment. As shown in Figure 2.4b, cells treated with EGFR Ab-siXBP1 NPs demonstrated a significant reduction of approximately 90% in XBP1 mRNA expression. Consistent with the decrease in mRNA levels, the expression level of XBP1 proteins was also reduced, as illustrated in Figure 2.4c.

Furthermore, an apoptosis and necrosis assay were conducted to determine the impact of XBP1 gene silencing on the cell death pathways. As displayed in Figure 2.4f and j, the cells treated with EGFR Ab-siXBP1 NPs under normal conditions exhibited low-level apoptosis and necrosis, only being 7±1.9%. This indicated that XBP1 gene knockdown showed negligible cytotoxicity to cancer cells under normal conditions. However, a higher percentage of dead cells was observed when the EGFR Ab-siXBP1 NP treatment occurred under hypoxic conditions, being 34 ± 2.4% (Figure 2.4i and j). Correspondingly, the percentage of healthy cells in this group reduced to about 66 ± 2.6%, compared to the control group (98.37 ± 1.2%, Figure 2.4j). Collectively, these findings suggest that the percentage of dead cells following XBP1 gene knockdown increases nearly threefold when cells are exposed to a hypoxic microenvironment compared to normal conditions.
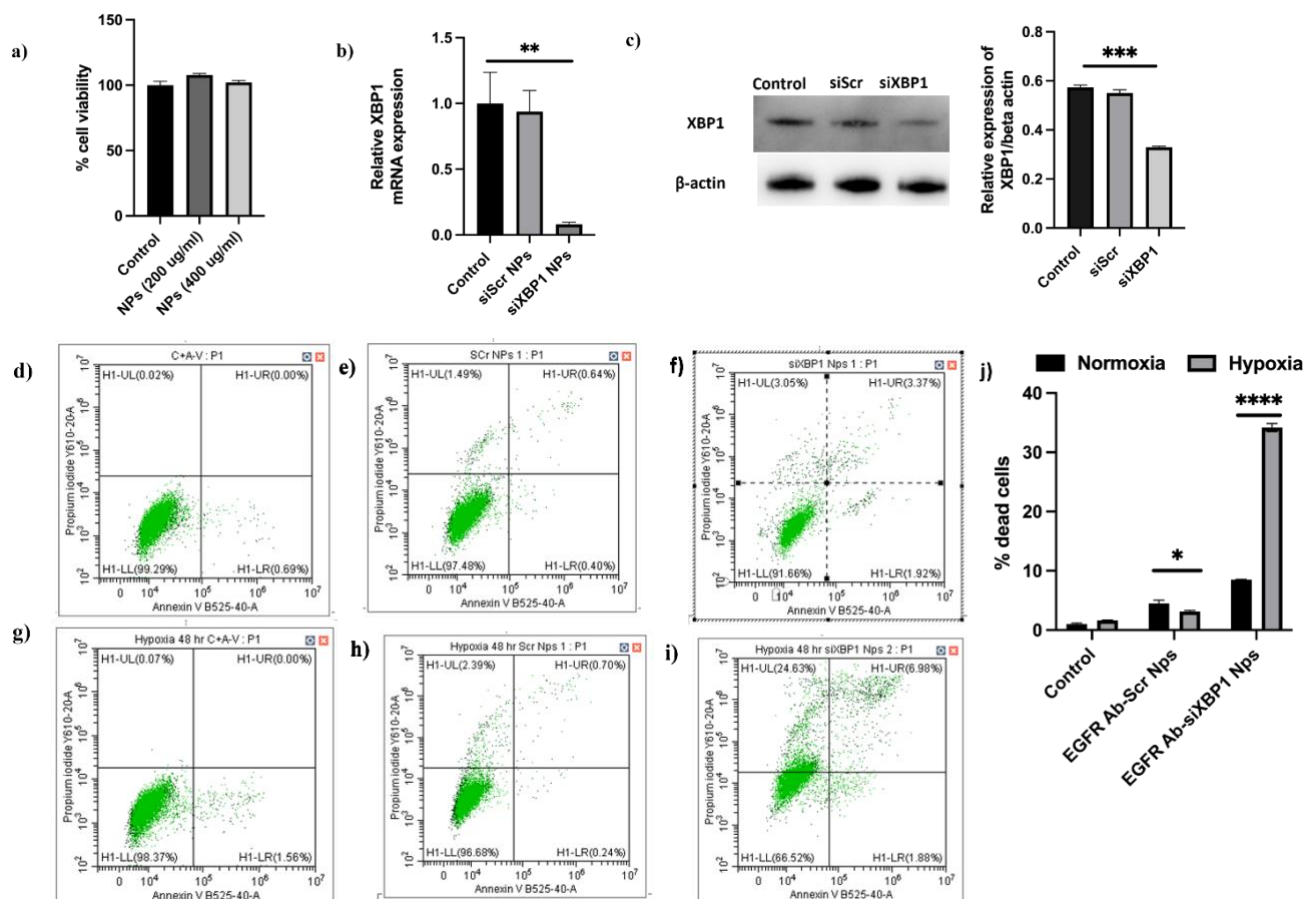
Figure 2.4: a) Cell viability of MDA-MB-231 cells after treatment with different concentrations of blank PLGA lipid nanoparticles; b) XBP1 mRNA expression in MDA-MB-231 cells after treatment with 200 μg/ml of EGFR Ab-siXBP1 NPs and EGFR Ab-Scr NPs under hypoxic conditions; c) Western blot and densitometric analysis of XBP1 protein expression level after the same treatments; (d-i) FITC-Annexin V/PI flow cytometry plots of MDA-MB-231cells after different treatments indicated in the figures; (j) Represent % of dead cells based on flow cytometry plots. Data represented as mean ± SEM; n =3; *p $<$0.1; ****p $<$0.001

2.4.5 Cell cycle analysis and colony formation assay

Further, to analyze whether XBP1 knockdown-induced apoptosis of MDA-MB-231 cells was mediated through cell cycle arrest, we further examined the effects of our treatment on cell cycle distribution. Figure 2.5a displayed the cell cycle distribution of the control group (cells only), cells treated with 25 nM of EGFR Ab-siXBP1 NPs and cells treated with 25 nM of EGFR Ab-siScr NPs, respectively. The flow cytometry analysis (Figure 2.5b) of the cell cycle after 48h of incubation showed that the nanoparticles used did not cause any cell cycle arrest at the concentration of 25nM.

Next, we tested the effect of EGFR Ab-siXBP1 NPs on the colony forming ability of MDA-MB-231 cells. As depicted in Figure 2.5c & d, treatment with EGFR Ab-siXBP1 NPs appeared to reduce the colony-forming ability of MDA-MB-231 cells compared to EGFR Ab-siScr Nps and the control group. However, the observed reduction was not statistically significant.
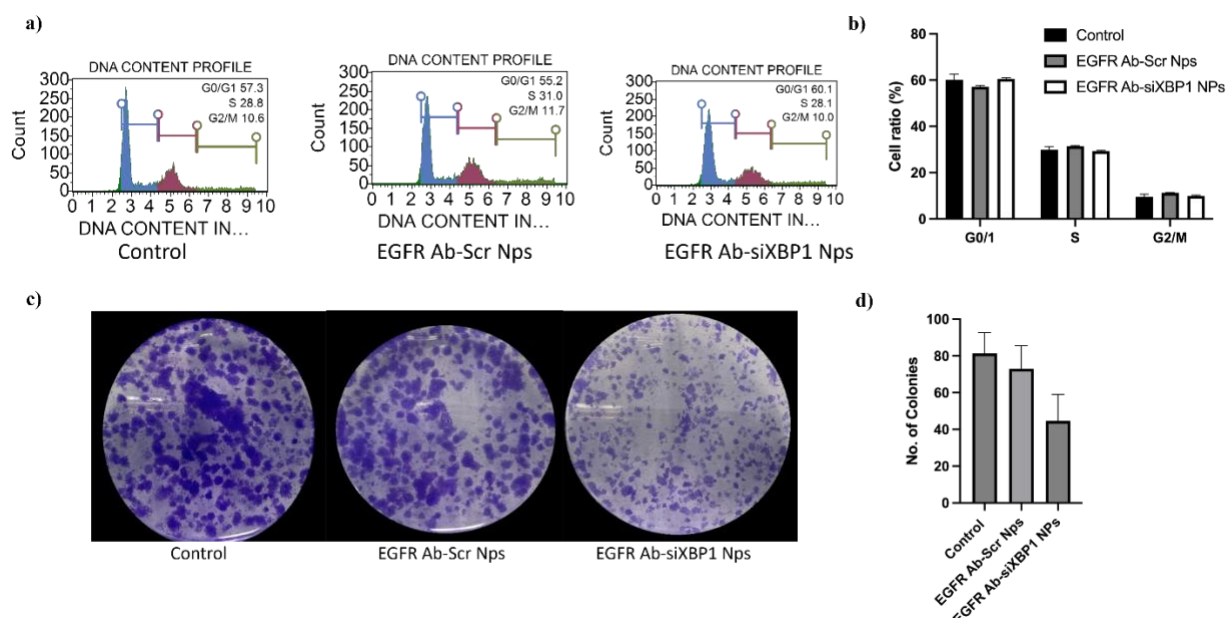
Figure 2.5: (a) MDA-MB-231 cell cycle distribution after treatment with 25 nM of EGFR Ab-siXBP1 NPs and EGFR Ab-Scr NPs; (b) The percentage of MDA-MB-231 cells at G0/G1, S and G2/M phases after treatment with NPs. (n = 3, Mean ± SEM); (c) Colony formation capacity of MDA-MB-231 cells after treatment with 25 nM of EGFR Ab-siXBP1 NPs and EGFR Ab-Scr NPs; (d) Counted number of colonies in each well. Data represented as mean ± SEM; n =3;

2.5 Discussion

TNBC, marked by the absence of ER, PR, and HER2 expression, displays insensitivity to endocrine therapy and HER2-targeted treatments, which led to a major challenge in developing a safe and effective treatment for TNBC [30, 31]. Recent studies have discovered the critical role of the unfolded protein response (UPR) regulator XBP1in fostering tumorigenesis and recurrence specifically in TNBC, making it a potential therapeutic target to treat TNBC [12]. The primary obstacle for targeting XBP1 in TNBC cells was mainly focused on achieving both efficient gene knockdown and specificity for TNBC cells [31]. To address this issue, this study focused on developing and investigating the effectiveness of PLGA lipid nanoparticles in knocking down XBP1 specifically in TNBC cells.

We successfully developed and characterized the lipid-polymer nanoparticles. We optimized their size, zeta potential, and surface morphology to ensure their suitability for targeted delivery. We

achieved a high entrapment efficiency of siRNA in our nanoparticles, a critical factor for effective gene silencing. Furthermore, the successful conjugation of EGFR antibodies to these nanoparticles enables their enhanced cellular uptake activity in TNBC cells, as demonstrated in Figure 2.2. This enhanced cellular uptake aligns with prior research reporting the effectiveness of EGFR-conjugated nanoparticles in targeting to breast cancer cells [32]. Importantly, our findings in Figure 2.4a demonstrate that these nanoparticles did not induce toxicity in MDA-MB-231 cells. This delivery system has demonstrated higher XBP1 transfection efficacy in MDA-MB-231 cells compared with commercial alternatives (Figure 2.3f). These nanoparticles resulted in approximately 75% XBP1 gene knockdown in MDA-MB231 cells at 48 h post-transfection, whereas commercial transfection reagents achieved only around 30% reduction of XBP1 gene expression. These results were consistent with other reported research, where approximately 80-85% XBP1 gene knockdown efficacy was achieved using antibody-conjugated siXBP1-loaded nanoparticles [23, 33]. We particularly focused on the gene silencing efficacy under hypoxic environment, a condition known to induce cancer cell metabolic adaptation, survival, and therapy resistance. Our results revealed that our nanoparticles achieved a significant reduction in XBP1 mRNA expression of approximately 90% even under the challenging hypoxic environment (Figure 2.4b).

Apoptosis is a crucial pathway leading to the cancer cell death specifically under hypoxic condition. We found out that XBP1 silencing did not alter cell apoptosis under normal conditions (Figure 2.4d-f), which aligns with previously reported studies [23, 33]. However, in hypoxic conditions where XBP1 expression is upregulated (Figure 2.3b), we noted a significant increase in apoptosis upon XBP1 gene silencing, with nearly a threefold increase in the number of apoptotic cells compared to normoxic conditions (Figure 2.4j). This observation is consistent with the findings reported by another research group that investigated XBP1's role in tumor survival under hypoxia conditions [34].

Unexpectedly, our study did not reveal any significant cell cycle arrest in response to nanoparticle treatment (Figure 2.5 a & b), consistent with prior research indicating that XBP1 silencing in TNBC does not typically induce alterations in the cell cycle [23]. Additionally, while we observed a slight decrease in the colony-forming ability of MDA-MB-231 cells (Figure 2.5 c & d), this reduction did not attain statistical significance, implying that other factors beyond XBP1 gene knockdown may influence long-term proliferative capacity in TNBC cells.

To sum up, our study demonstrated the in vitro XBP1 gene silencing efficacy by using the targeted nanoparticles loaded with siRNA, thus promoting apoptosis in challenging hypoxic conditions. These findings provide a strong foundation for advancing a safe and innovative TNBC treatment. Future investigations should prioritize in vivo studies to validate the efficacy and safety of this approach, bringing it one step closer to clinical applications.

As this thesis progresses, Chapters 3 and 4 will explore other challenging aspects of cancer progression, specifically in lung cancer. In Chapters 3 & 4, the focus shifts towards targeting inflammation, a critical driver of lung cancer, using berberine-loaded and NFκB, decoy ODNs-loaded nanoparticles. Given these objectives, it is relevant to discuss whether siRNA could play a role in achieving similar therapeutic outcomes in lung cancer by silencing key genes associated with inflammation and tumor growth. Inflammation-related markers, such as Interleukin (IL)-6 and IL-8, have been successfully targeted with siRNA in several cancer models. For example, Allahyari *et al.* used siRNA to simultaneously silence IL-6 and CD-73, significantly reducing tumor growth by mitigating the inflammatory environment that supports tumor progression [38]. Similarly, another study demonstrated that siRNA-mediated knockdown of IL-8 in prostate cancer reduced tumor cell migration and invasion, showcasing the broader applicability of siRNA in modulating the inflammatory cytokines that drive cancer progression [39].

In Chapter 4, where the focus is on inhibiting NFκB, a key transcription factor in inflammation-mediated cancer progression, siRNA offers a unique opportunity to achieve targeted gene silencing. Since NFκB regulates the expression of numerous genes involved in inflammation and cancer cell survival, siRNA targeting NFκB, or other downstream effectors, could further reduce the pro-tumorigenic environment associated with lung cancer [40]. Employing siRNA alongside other therapies, radiotherapy or chemotherapy, could amplify the therapeutic impact by concurrently reducing inflammation and inhibiting key survival pathways within tumor cells [41, 42].

Overall, the versatility of siRNA in gene silencing across different cancer types and pathways presents a compelling case for its broader application beyond TNBC.

Conflict of interest statement

The authors declare no conflicts of interest in this work.

2.6 References

1. Almansour, N.M., Triple-Negative Breast Cancer: A Brief Review About Epidemiology, Risk Factors, Signaling Pathways, Treatment and Role of Artificial Intelligence. Frontiers in Molecular Biosciences, 2022. 9.

2. Sun, Z., et al., The quest for nanoparticle-powered vaccines in cancer immunotherapy. J Nanobiotechnology, 2024. 22(1): p. 61.

3. Almansour, N.M., Triple-Negative Breast Cancer: A Brief Review About Epidemiology, Risk Factors, Signaling Pathways, Treatment and Role of Artificial Intelligence. Front Mol Biosci, 2022. 9: p. 836417.

4. Triple-Negative Breast Cancer: Symptoms, Treatment, Research. 2023: Breast cancer research foundation.

5. Li, Y., et al., Recent advances in therapeutic strategies for triple-negative breast cancer. J Hematol Oncol, 2022. 15(1): p. 121.

6. Wu, Q., et al., Multi-drug resistance in cancer chemotherapeutics: mechanisms and lab approaches. Cancer Lett, 2014. 347(2): p. 159-66.

7. Tao, J.J., K. Visvanathan, and A.C. Wolff, Long term side effects of adjuvant chemotherapy in patients with early breast cancer. Breast, 2015. 24 Suppl 2(0 2): p. S149-53.

8. Cheng, Y.J., et al., Long-Term Cardiovascular Risk After Radiotherapy in Women With Breast Cancer. J Am Heart Assoc, 2017. 6(5).

9. Chen, S., et al., The emerging role of XBP1 in cancer. Biomed Pharmacother, 2020. 127: p. 110069.

10. He, Y., et al., Emerging roles for XBP1, a sUPeR transcription factor. Gene Expr, 2010. 15(1): p. 13-25.

11. Shi, W., et al., Unravel the molecular mechanism of XBP1 in regulating the biology of cancer cells. J Cancer, 2019. 10(9): p. 2035-2046.

12. Chen, X., et al., XBP1 promotes triple-negative breast cancer by controlling the HIF1α pathway. Nature, 2014. 508(7494): p. 103-107.

13. Srivastava, N., et al., Hypoxia: syndicating triple negative breast cancer against various therapeutic regimens. Front Oncol, 2023. 13: p. 1199105.

14. Romero-Ramirez, L., et al., XBP1 is essential for survival under hypoxic conditions and is required for tumor growth. Cancer Res, 2004. 64(17): p. 5943-7.

15. McCarthy, N., Hypoxia and XBP1S. Nature Reviews Cancer, 2014. 14(5): p. 295-295.

16. Charbe, N.B., et al., Small interfering RNA for cancer treatment: overcoming hurdles in delivery. Acta Pharmaceutica Sinica B, 2020. 10(11): p. 2075-2109.

17. Zhao, Y., et al., XBP1 regulates the protumoral function of tumor-associated macrophages in human colorectal cancer. Signal Transduction and Targeted Therapy, 2021. 6(1): p. 357.

18. Byrd, A.E., I.V. Aragon, and J.W. Brewer, MicroRNA-30c-2* limits expression of proadaptive factor XBP1 in the unfolded protein response. J Cell Biol, 2012. 196(6): p. 689-98.

19. Tiemann, K. and J.J. Rossi, RNAi-based therapeutics-current status, challenges and prospects. EMBO Mol Med, 2009. 1(3): p. 142-51.

20. Ngamcherdtrakul, W. and W. Yantasee, siRNA therapeutics for breast cancer: recent efforts in targeting metastasis, drug resistance, and immune evasion. Transl Res, 2019. 214: p. 105-120.

21. Yao, Y., et al., Nanoparticle-Based Drug Delivery in Cancer Therapy and Its Role in Overcoming Drug Resistance. Front Mol Biosci, 2020. 7: p. 193.

22. Wang, L., B. Griffel, and X. Xu, Synthesis of PLGA-Lipid Hybrid Nanoparticles for siRNA Delivery Using the Emulsion Method PLGA-PEG-Lipid Nanoparticles for siRNA Delivery. Methods Mol Biol, 2017. 1632: p. 231-240.

23. Jensen, D.K., et al., Design of an inhalable dry powder formulation of DOTAP-modified PLGA nanoparticles loaded with siRNA. J Control Release, 2012. 157(1): p. 141-8.

24. Sivadasan, D., et al., Polymeric Lipid Hybrid Nanoparticles (PLNs) as Emerging Drug Delivery Platform-A Comprehensive Review of Their Properties, Preparation Methods, and Therapeutic Applications. Pharmaceutics, 2021. 13(8).

25.   Zhang, L., et al., Systemic Delivery of Aptamer-Conjugated XBP1 siRNA Nanoparticles for Efficient Suppression of HER2+ Breast Cancer. ACS Applied Materials & Interfaces, 2020. 12(29): p. 32360-32371.

26.   Zhang, L., et al., Development of targeted therapy therapeutics to sensitize triple-negative breast cancer chemosensitivity utilizing bacteriophage phi29 derived packaging RNA. Journal of Nanobiotechnology, 2021. 19(1): p. 13.

27.   Nielsen, T.O., et al., Immunohistochemical and clinical characterization of the basal-like subtype of invasive breast carcinoma. Clin Cancer Res, 2004. 10(16): p. 5367-74.

28.   Rio, D.C., et al., Purification of RNA using TRIzol (TRI reagent). Cold Spring Harb Protoc, 2010. 2010(6): p. pdb prot5439.

29.   Danaei, M., et al., Impact of Particle Size and Polydispersity Index on the Clinical Applications of Lipidic Nanocarrier Systems. Pharmaceutics, 2018. 10(2).

30.   Fang, F., et al., EGFR-targeted hybrid lipid nanoparticles for chemo-photothermal therapy against colorectal cancer cells. Chemistry and Physics of Lipids, 2023. 251: p. 105280.

31.   Masuda, H., et al., Role of epidermal growth factor receptor in breast cancer. Breast Cancer Res Treat, 2012. 136(2): p. 331-45.

32.   Acharya, S., F. Dilnawaz, and S.K. Sahoo, Targeted epidermal growth factor receptor nanoparticle bioconjugates for breast cancer therapy. Biomaterials, 2009. 30(29): p. 5737-50.

33.   Foulkes, W.D., I.E. Smith, and J.S. Reis-Filho, Triple-negative breast cancer. N Engl J Med, 2010. 363(20): p. 1938-48.

34.   Yin, L., et al., Triple-negative breast cancer molecular subtyping and treatment progress. Breast Cancer Res, 2020. 22(1): p. 61.

35.   Gao, J., et al., The promotion of siRNA delivery to breast cancer overexpressing epidermal growth factor receptor through anti-EGFR antibody conjugation by immunoliposomes. Biomaterials, 2011. 32(13): p. 3459-70.

36.   Zhang, L., et al., Systemic Delivery of Aptamer-Conjugated XBP1 siRNA Nanoparticles for Efficient Suppression of HER2+ Breast Cancer. ACS Appl Mater Interfaces, 2020. 12(29): p. 32360-32371.

37.   Romero-Ramirez, L., et al., XBP1 Is Essential for Survival under Hypoxic Conditions and Is Required for Tumor Growth. Cancer Research, 2004. 64(17): p. 5943-5947.

38.   Allahyari, S.E., et al., Simultaneous inhibition of CD73 and IL-6 molecules by siRNA-loaded nanoparticles prevents the growth and spread of cancer. Nanomedicine: Nanotechnology, Biology and Medicine, 2021. 34: p. 102384.

39.   Aalinkeel, R., et al., Nanotherapy silencing the interleukin-8 gene produces regression of prostate cancer by inhibition of angiogenesis. Immunology, 2016. 148(4): p. 387-406.

40.   Qin, B. and K. Cheng, Silencing of the IKKε gene by siRNA inhibits invasiveness and growth of breast cancer cells. Breast Cancer Research, 2010. 12(5): p. R74.

41.   Li, N., et al., Small interfering RNA targeting NF-κB attenuates lipopolysaccharide-induced acute lung injury in rats. BMC Physiol, 2016. 16(1): p. 7.

42.   Zheng, M., et al., Growth inhibition and radiosensitization of glioblastoma and lung cancer cells by small interfering RNA silencing of tumor necrosis factor receptor-associated factor 2. Cancer Res, 2008. 68(18): p. 7570-8.

Chapter 3. Berberine-loaded liquid crystalline nanostructure inhibits cancer progression in adenocarcinomic human alveolar basal epithelial cells *in vitro*

Meenu Mehta[1,2,3], Vamshikrishna Malyla[1,2,3], Keshav R Paudel[2,4], Dinesh K Chellapppan[5], Philip M Hansbro[2,4], Brian G Oliver[4,6], Kamal Dua[1,2,3]

[1]Discipline of Pharmacy, Graduate School of Health, University of Technology Sydney, Sydney, NSW 2007, Australia
[2]Centre for Inflammation, Centenary Institute, Sydney, NSW 2050, Australia
[3]Faculty of Health, Australian Research Centre in Complementary and Integrative Medicine, University of Technology Sydney, Ultimo, NSW 2007, Australia.
[4]School of Life Sciences, University of Technology Sydney, Sydney, NSW 2007, Australia
[5]Department of Life Sciences, School of Pharmacy, International Medical University, Bukit Jalil 57000, Kuala Lumpur, Malaysia
[6]Woolcock Institute of Medical Research, University of Sydney, Sydney, New South Wales, Australia

Abstract

Metastasis represents the leading cause of death in lung cancer patients. C-X-C Motif Chemokine Ligand 8 (CXCL-8), Chemokine (C-C motif) ligand 20 (CCL-20) and heme oxygenase -1 (HO-1) play an important role in cancer cell proliferation and migration. Berberine is an isoquinoline alkaloid isolated from several herbs in the Papaveraceae family that exhibits anti-inflammatory, anticancer and antidiabetic properties. Therefore, the aim of the present study is to investigate the inhibitory potential of berberine monoolein-loaded liquid crystalline nanoparticles (Berberine-LCNs) against cancer progression. Berberine-LCNs were prepared by mixing berberine, monoolein and poloxamer 407 (P407) using ultrasonication method. A549 cells were treated with or without 5 µM dose of berberine LCNs for 24 hrs and total cellular protein was extracted and further analysed for the protein expression of CCl-20, CXCL-8 and HO-1 using human oncology array kit. Our results showed that Berberine-LCNs significantly reduced the expression of CCl-20, CXCL-8 and HO-1 at dose of 5µM. Collectively, our findings suggest that Berberine-LCNs have inhibitory effect on inflammation/oxidative stress related cytokines i.e. CCL20, CXCL-8, and HO-1 which could be a novel therapeutic targets for the management of lung cancer.

Keywords: Berberine, Interleukins, Liquid crystalline nanoparticles, Inflammation, Lung Cancer

3.1 Introduction

Cancer is a multifaceted disease with a complicated molecular environment and altered cell pathways leading to an uncontrolled proliferation of cells [1]. Lung cancer is a leading cause of cancer death all over the globe. Around 1.8 million cancer deaths were recorded worldwide by lung cancer in 2020. According to the analysis, an estimated 28.4 million additional cancer cases are expected in 2040, representing a 47% increase from 2020 [2]. Lung cancer is classified histologically into small cell lung cancer (SCLC) and non-small cell lung cancer (NSCLC), with the latter accounting for 85% of all cases [3]. 90 percent of deaths from lung cancer were expected to be caused by tobacco smoke [4]. Tobacco smoke stimulates the epithelial cells and macrophages which triggers the inflammation and release of cytokines and chemokines such as tumor necrosis factor-alpha (TNF-α), transforming growth factor-beta (TGF-β), interleukin-1 (IL-1), IL-6, IL-8, C-X-C Motif Chemokine Ligand 9 (CXCL9), C-X-C Motif Chemokine Ligand 10 (CXCL 10) and Chemokine (C-C motif) ligand 20 (CCL20) [5, 6].

CCL20 is a CC (C-C motif) chemokine that attracts immature dendritic cells, effector/memory T-cells, and B-cells [7]. CCL20 activates CC chemokine receptor 6 (CCR6), and overexpression of both CCL20 and CCR6 promotes lung cancer cell proliferation, migration, and invasion [8]. CXCL8 (IL-8) belongs to the CXC chemokine family and categorised as a neutrophil chemoattractant with inflammatory action [9]. Furthermore, IL-8 has been linked to several other processes, including angiogenesis and lung cancer metastasis [10]. It has been established that CCL20 and CXCL8 synergise to promote cancer metastatic progression by inducing Epithelial-mesenchymal transition (EMT) via the phosphatidylinositol 3 kinase/ protein kinase B/extracellular signal-regulated protein kinase (PI3K/AKT-ERK1/2) signaling axis [11].

Cancer cells experience increased oxidative stress due to their high metabolic rate [12]. The role of hemeoxygenase-1 (HO-1) as a cytoprotective agent in tumor cells has been widely recognised in combating chemotherapeutic drug-induced oxidative stress and preventing apoptosis or autophagy in cancer cells [13]. In cancer cells, HO-1 overexpression enhances proliferation and survival. Furthermore, HO-1 promotes angiogenesis by altering the expression of angiogenic factors [14].

Plant-based compounds are target-specific and have minimal cytotoxicity, making them useful in the development of new therapeutic approaches for this complex disease [15]. Berberine belongs to the protoberberine alkaloids family and is found mostly in the root, stem, and bark of numerous plants. It is well known for its anticancer properties [16]. However, berberine's low bioavailability

(0.000354 mg/mL in water) and limited absorption are two major drawbacks, as only 0.5 percent of ingested berberine gets absorbed in the small intestine, and this number reduces to 0.35 percent when in systemic circulation [17]. One effective strategy for overcoming these drawbacks is to incorporate berberine into a nanostructure or carrier system, such as liquid crystalline nanoparticles (LCNs), which can efficiently deliver the substance to its target tissues [18].

Liquid crystalline nanoparticles (LCNs) received a lot of attention in the drug delivery domain due to their exceptional capacity to improve drug bioavailability and stability, minimize toxicity, and modulate the release of drugs after administration [18]. Moreover, liquid crystalline nanoparticles (LCNs) have effectively delivered various herbal compounds against diverse cancer types [19-21]. In a study by Loo et al., berberine was encapsulated into LCNs to improve its solubility and enhance its anticancer activity against human breast cancer cells. Results indicated that berberine LCNs exhibited increased cellular uptake and a significantly higher percentage of G0/G1 cell cycle distribution compared to free berberine when cells were exposed to a concentration of 2 μM [21]. Paudel et al. demonstrated that LCNs improved the sustained-release properties of naringenin. These naringenin-loaded LCNs efficiently reduced levels of pro-inflammatory markers, including IL-1β, IL-6, TNF-α, and IL-8. Moreover, the naringenin-loaded LCNs showed strong anticancer effects by inhibiting cell proliferation and migration in the A549 cell line [20]. Considering the significant role of IL-8, CCL-20, and HO-1 in cancer progression and recognizing the benefits of LCNs, our current study aimed to investigate the potential of berberine-loaded liquid crystalline nanoparticles (Berberine-LCNs) in inhibiting inflammation-mediated cancer progression in the lung cancer (A549) cell line.

3.2 Materials & Methods
3.2.1. Materials

Berberine hydrochloride, Monoolein, Poloxamer 407 (P407) were purchased from Sigma Chemicals Co, Germany. The oncology array kit was purchased from *In Vitro* Technologies Pvt Ltd, Australia. Dulbecco's modified Eagle's medium (DMEM), foetal bovine serum (FBS), penicillin and phosphate-buffered saline (PBS) were procured from Thermofisher Scientific Pvt Ltd. Additional chemical reagents and solvents were obtained from Sigma-Aldrich unless specified.

3.2.2. Methods

Cell Culture

Adenocarcinomic human alveolar basal epithelial cells (A549) cell lines (ATCC, USA) was obtained from Prof. Alaina Ammit, Woolcock Institute of Medical Research, Sydney, Australia. The cells were grown in a humified 37°C incubator with 5% CO_2 using Dulbecco's Modified Eagle's Medium (DMEM) supplemented with 10% fetal bovine serum, 1% penicillin, and streptomycin.

Preparation and charaterisation of Berberine-LCNs

Berberine-LCNs were formulated as previously mentioned [20]. Berberine-LCNs were prepared using ultrasonication method. Briefly, 200 mg of lipid (monoolein) and 20 mg of surfactant (poloxmer (P407)) were heated in separate glass vials in a water bath at 70°C. Then 5 mg of Berberine was added to the molten lipid and vortexed until complete dissolution. Then, the surfactant solution was added to the lipid-drug mixture and the resultant coarse dispersion was subjected to size reduction using a probe sonicator (Labsonic® P, Sartorius, Germany) at amplitude 80 and 5-s on and 5-s off-cycle for 5 min. The prepared nanoparticles were characterised for particle size, polydispersity index (PDI), and zeta potential using a Zetasizer Nano ZS (Malvern Instruments, Malvern, UK), with samples diluted 20-fold in distilled water prior to analysis. The entrapment efficiency of nanoparticles was also determined using ultracentrifugation method. All measurements were performed in triplicate at 25°C.

Human oncology protein array

A549 cells (1 x10^5 cells/well) were seeded in 6-well plates and treated for 24 hours with or without 5μM dose of Berberine-LCNs. Total cellular protein was extracted using radioimmunoprecipitation assay (RIPA) lysis buffer including a protease and phosphatase inhibitor cocktail and quantified using a bicinchoninic (BCA) protein assay kit. 350 μg of protein was utilized for both the control and treatment groups to perform an oncology array (R&D Systems, Minneapolis, MN). The experiment was performed as per manufacturer's protocol [22].

Statistical analysis

Results are presented as mean ± SEM from triplicate experiments. Statistical significance of data between 2 groups was determined using a 2-tailed Student's *t* test, using the 1-way ANOVA Graph Pad Prism software (version 8.2.1). Statistical differences were accepted at $P < 0.05$.

3.3 Results

Berberine LCNs were prepared as yellow-colored emulsions. The mean particle size, PDI and zeta potential of the nanoparticles were found to have 181.3±0.7 nm with PDI less than 0.1. The

zeta potential of prepared nanoparticles was negative, i.e. -5.19 ± 0.214. The entrapment efficiency of the formulation was determined using the ultracentrifugation method, and results showed that 75% of the berberine had been encapsulated within the nanoparticles.

From our preliminary 3-(4,5-dimethylthiazol-2-yl)-2,5-diphenyl tetrazolium bromide (MTT) cell-viability assay on A549 cells treated with Berberine-LCNs at a dose ranging 0.5-5 µM, we observed approximately 50% reduction in cell viability (****$p<0.0001$ vs media control) with 5 µM dose (data not shown). Therefore, we carried out further protein array experiment with 5 µM of Berberine-LCNs.

Our protein analysis data showed increased protein expression of CXCL-8, CCL-20 and HO-1 in A549 cells (without Berberine-LCNs treatment). The effect of Berberine-LCNs on CXCL-8, CCL-20 and HO-1 protein expression in A549 cells is shown in Fig. 1a-c. Results showed that Berberine-LCNs at a dose of 5 µM significantly downregulated the protein expression of CXCL-8 (Fig. 3.1a), CCL-20 (Fig. 3.1b) and HO-1 (Fig. 3.1c) as compared to control.
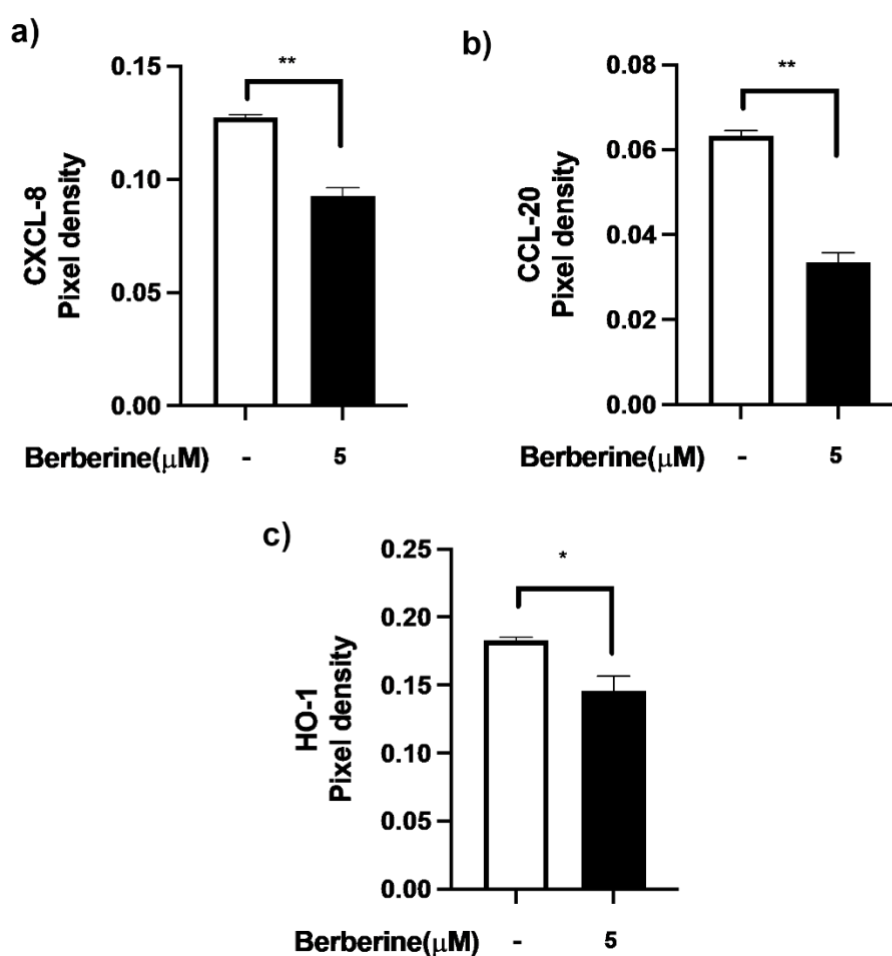
Fig. 3.1: Inhibition of proteins expression (a) CXCL-8, (b) CCL-20, (c) HO-1 upon treatment with Berberine-LCNs on A549 cells. Values are expressed as mean ± SEM (n=2); *p < 0.05, **P < 0.01* vs control (without Berberine-LCNs treatment). Analysis was performed by a 2-tailed Student's t-test.

3.4 Discussion

Our *in vitro* investigation in human lung adenocarcinoma cell line (A549) showed that 5 µM of Berberine-LCNs significantly inhibited the protein expression of CXCL-8, CCL-20, and HO-1. Although, we carried out protein array with 84 different lung cancer protein markers, only 21 proteins were significantly reduced by Berberine-LCNs and among these 21 proteins, 3 proteins; HO-1, CCL-20, CXCL-8 were particularly related with inflammation/oxidative stress induced lung cancer progression while other protein were related to epithelial-mesenchymal-transition pathway that facilitate metastasis/invasion of lung cancer cell.

CXCL-8 (also known as IL-8) is a potent growth factor for human lung cancer cells. A study performed in NSCLC cell line H460 and MOR/P found that anti-IL-8 neutralising antibody attenuate cell proliferation to 71% (H460) and 76% (MOR/P) respectively. Similarly, exogenous IL-8 stimulation results significant increase in cell proliferation [9]. Likewise, the production of CCL20 from A549 cells also induced proliferation and migration through activation of extracellular signal-regulated kinases and phosphoinositide 3-kinase signalling pathway suggesting CCL-20 as a potential therapeutic target for management of lung cancer (Fig. 3.2) [8]. The increase expression of HO-1 occurs in various tumours where HO-1 plays crucial role in rapid tumor proliferation due to its antioxidative and antiapoptotic effects. Among various lung cancer cell line (A549, NCI-H23, NCI-H157 and NCI-H460), the expression HO-1 was higher in A549 when compared to other cell lines. Using HO-1 inhibitor (ZnPP), Kim *et al.,* 2005 showed that HO-1 inhibition results in decrease A549 cell viability [13]. In our study, the significant inhibition of CXCL-8, CCL-20, and HO-1 protein expression clearly suggests that Berberine-LCNs can inhibit lung cancer proliferation and migration. Previous *in vitro* study of berberine free drug on A549 cells found that IC50 value of berberine to decrease the viability of the cells by 50% was 100µM, where investigators used 100 µM to further study cancer related protein and gene expression. The study revealed significant inhibition of various protein/genes related to cancer cell proliferation and migration [23]. Another study carried out by Li et al also used berberine free drug ranging 30-90 µM for 24 hrs in A549 cells. The study demonstrated significant reduction in the protein expression of matrix metalloproteinase-2 (MMP-2), B-cell lymphoma 2 (Bcl-2), BCL2 Associated X (Bax), Janus kinase 2 (Jak2), Vascular endothelial

growth factor (VEGF), Nuclear factor kappa B (NFκB)/p65 and Activator protein 1 (AP-1) at 90 μM [24]. It is worth noting that our 5 μM dose of Berberine-LCNs is approximately 20-fold less than previously published study but equally effective to a significant decrease in the protein expression of CXCL-8, CCL-20, and HO-1. This suggests that formulating berberine into LCNs offers additional benefits to achieve potent biological activity at a lower dose compared to using powder berberine. It is well known that powder berberine has low water solubility, dissolution rate, and oral bioavailability [17]. The potential reason for the better beneficial activity of our Berberine-LCNs formulation may be attributed to the increased cellular uptake of LCNs by A549 cells. The physicochemical characterisation/parameters and *in vitro* drug release of Berberine-LCNs were found in agreement with our previous studies involving similar LCNs encapsulating other phytoceuticals, rutin and naringenin. Moreover, we have also observed significant *in vitro* anticancer activity with those LCNs formulations [20, 25]. This overlay of the findings amongst various phytoceuticals berberine, rutin and naringenin, clearly highlights the validity and application of LCNs in lung cancer. However, there are a few limitations of our study. The TEM imaging and cellular uptake studies using microscopic techniques have not been performed in the current study, which will be part of our future direction. Moreover, we have performed only protein-based assay and therefore, our study opens a platform for us, as well as other researchers, to investigate if Berberine-LCNs inhibit key genes involved in lung cancer progression. Finally, the inhibition of proteins and genes *in vitro* by Berberine-LCNs can also be further validated using *in vivo* animal models. Taken together, our study suggests that advance drug delivery system such as LCNs offers versatility to target various disease such as lung cancer.
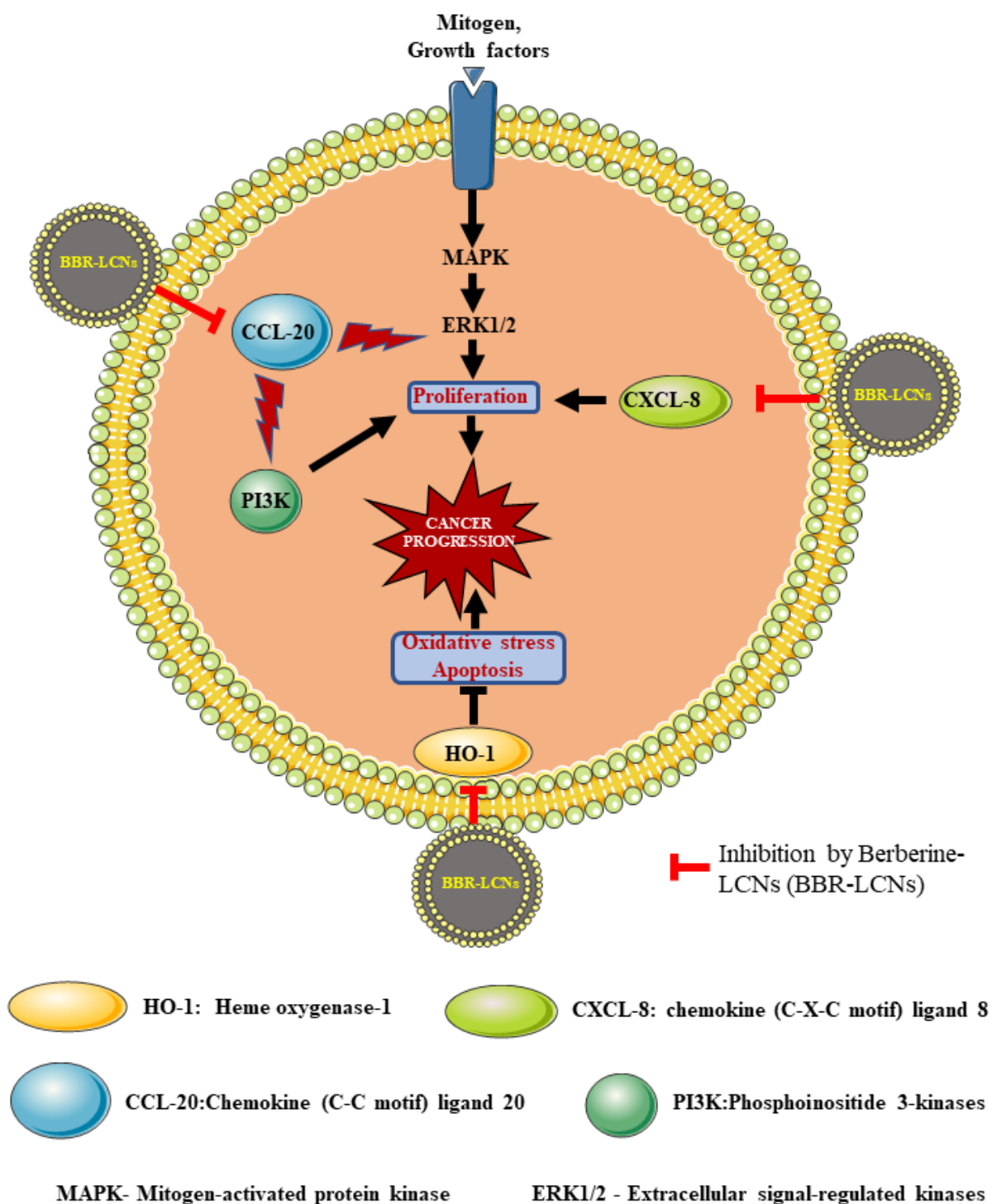
Figure 3.2: Uncontrolled cell proliferation and migration leads to lung cancer progression though overexpression of certain protein. Proliferation of A549 cell is mediated overexpression protein

such as CXCL-8 (IL-8) that acts as a growth factor. Proliferation and migration is also mediated by an overexpression of CCL-20 through activation of extracellular signal-regulated kinases (ERK1/2) and phosphoinositide 3-kinase (PI3K) signalling pathway. Similarly, overexpression of HO-1 protein protects cancer cell from oxidative damage and apoptosis and thus supports cancer cell survival. Berberine-LCNs inhibit A549 cell proliferation and migration by targeting these key proteins to halt lung cancer progression.

HO-1 - heme oxygenase-1; CXCL-8- chemokine (C-X-C motif) ligand 8; CCL-20 - chemokine (C-C motif) ligand 20; PI3K- Phosphoinositide 3-kinase; MAPK- Mitogen-activated protein kinase; ERK1/2 - Extracellular signal-regulated kinases; BBR-LCNs – Berberine loaded liquid crystalline nanoparticles

3.5 Conclusion

The enhanced therapeutic application of LCNs formulation over powder may be attributed to the improved physicochemical parameters that were favourable for enhanced therapeutic (anticancer) activity. The significant inhibition of CXCL-8, CCL-20, and HO-1 protein expression in A549 cells suggests that Berberine loaded nanoparticles could be a promising therapeutic alternative for the management of lung cancer. However, further *in vitro*, *in vivo* animal and human clinical studies with depth-mechanism are essential to validate the anti-cancer activity of Berberine-LCNs against lung cancer.

3.6 References

1. Sharma, P., et al., *Emerging trends in the novel drug delivery approaches for the treatment of lung cancer.* Chemico-Biological Interactions, 2019. **309**: p. 108720.

2. Sung, H., et al., *Global cancer statistics 2020: GLOBOCAN estimates of incidence and mortality worldwide for 36 cancers in 185 countries.* 2021. **71**(3): p. 209-249.

3. Sharma, P., et al., *Emerging trends in the novel drug delivery approaches for the treatment of lung cancer.* 2019. **309**: p. 108720.

4. Hurley, S., Winnall, WR, Greenhalgh, EM & Winstanley, MH. , *3.4 Lung cancer.* Tobacco in Australia: Facts and issues., ed. E. In Greenhalgh, Scollo, MM and Winstanley, MH. 2021, Melbourne: Cancer Council Victoria.

5. Takahashi, H., et al., *Tobacco smoke promotes lung tumorigenesis by triggering IKKβ- and JNK1-dependent inflammation.* 2010. **17**(1): p. 89-97.

6. Wang, G.-Z., et al., *Tobacco smoke induces production of chemokine CCL20 to promote lung cancer.* Cancer Letters, 2015. **363**(1): p. 60-70.

7. Schutyser, E., et al., *The CC chemokine CCL20 and its receptor CCR6.* 2003. **14**(5): p. 409-426.

8. Wang, B., et al., *Production of CCL20 from lung cancer cells induces the cell migration and proliferation through PI3K pathway.* J Cell Mol Med, 2016. **20**(5): p. 920-9.

9. Zhu, Y.M., et al., *Interleukin-8/CXCL8 is a growth factor for human lung cancer cells.* Br J Cancer, 2004. **91**(11): p. 1970-6.

10. Masuya, D., et al., *The intratumoral expression of vascular endothelial growth factor and interleukin-8 associated with angiogenesis in nonsmall cell lung carcinoma patients.* Cancer, 2001. **92**(10): p. 2628-38.

11. Cheng, X.-S., et al., *CCL20 and CXCL8 synergize to promote progression and poor survival outcome in patients with colorectal cancer by collaborative induction of the epithelial–mesenchymal transition.* Cancer Letters, 2014. **348**(1): p. 77-87.

12. Sosa, V., et al., *Oxidative stress and cancer: An overview.* Ageing Research Reviews, 2013. **12**(1): p. 376-390.

13. Kim, H.R., et al., *The role of heme oxygenase-1 in A549 human lung carcinoma cells.* 2005. **65**(9 Supplement): p. 404-404.

14. Chau, L.-Y., *Heme oxygenase-1: emerging target of cancer therapy.* Journal of Biomedical Science, 2015. **22**(1): p. 22.

15. Hardwick, J., et al., *Targeting cancer using curcumin encapsulated vesicular drug delivery systems.* 2021. **27**(1): p. 2-14.

16. Chen, Q.-Q., et al., *Berberine induces apoptosis in non-small-cell lung cancer cells by upregulating miR-19a targeting tissue factor.* Cancer management and research, 2019. **11**: p. 9005-9015.

17. Liu, Y.T., et al., *Extensive intestinal first-pass elimination and predominant hepatic distribution of berberine explain its low plasma levels in rats.* Drug Metab Dispos, 2010. **38**(10): p. 1779-84.

18. Madheswaran, T., et al., *Current potential and challenges in the advances of liquid crystalline nanoparticles as drug delivery systems.* Drug Discovery Today, 2019. **24**(7): p. 1405-1412.

19. Paudel, K.R., et al., *Rutin loaded liquid crystalline nanoparticles inhibit non-small cell lung cancer proliferation and migration in vitro.* Life Sciences, 2021. **276**: p. 119436.

20. Wadhwa, R., et al., *Anti-inflammatory and anticancer activities of Naringenin-loaded liquid crystalline nanoparticles in vitro.* J Food Biochem, 2021. **45**(1): p. e13572.

21. Loo, Y.S., et al., *Encapsulation of berberine into liquid crystalline nanoparticles to enhance its solubility and anticancer activity in MCF7 human breast cancer cells.* Journal of Drug Delivery Science and Technology, 2020. **57**: p. 101756.

22. Argentiero, A., et al., *Gene Expression Comparison between the Lymph Node-Positive and -Negative Reveals a Peculiar Immune Microenvironment Signature and a Theranostic Role for WNT Targeting in Pancreatic Ductal Adenocarcinoma: A Pilot Study.* Cancers (Basel), 2019. **11**(7).

23. Kalaiarasi, A., et al., *Plant Isoquinoline Alkaloid Berberine Exhibits Chromatin Remodeling by Modulation of Histone Deacetylase To Induce Growth Arrest and Apoptosis in the A549 Cell Line.* J Agric Food Chem, 2016. **64**(50): p. 9542-9550.

24. Li, J., et al., *Berberine hydrochloride inhibits cell proliferation and promotes apoptosis of non-small cell lung cancer via the suppression of the MMP2 and Bcl-2/Bax signaling pathways.* Oncology letters, 2018. **15**(5): p. 7409-7414.

25. Paudel, K.R., et al., *Rutin loaded liquid crystalline nanoparticles inhibit non-small cell lung cancer proliferation and migration in vitro.* Life Sci, 2021. **276**: p. 119436.

Chapter 4: Investigation of the anticancer potential of NFκB decoy oligonucleotide loaded polysaccharide nanoparticles in lung cancer cells

Meenu Mehta[1], Vinod Kumar Kannaujiya[2], Dikaia Xenaki[3], Brian Gregory George Oliver[3,4], Peter Richard Wich[2], Kamal Dua[5]

[1]School of Biomendical Engineering, University of Technology Sydney, Sydney, NSW 2007, Australia

[2]School of Chemical Engineering, University of New South Wales, Sydney, NSW 2052, Australia

[3]Woolcock Institute of Medical Research, University of Sydney, Sydney, New South Wales, Australia

[4]School of Life Sciences, University of Technology Sydney, Ultimo, NSW 2007, Australia

[5]Discipline of Pharmacy, Graduate School of Health, University of Technology Sydney, Sydney, NSW 2007, Australia

Abstract

Lung cancer continues to be a primary contributor to cancer-related deaths worldwide, characterized by aberrant cell proliferation and metastasis, often associated with chronic inflammation. Proinflammatory cytokines such as interleukin-6 (IL-6) and IL-8 have been implicated in lung cancer progression and are potential diagnostic biomarkers. NFκB, a master regulator linking inflammation and cancer, presents an attractive target for cancer therapy. However, challenges in the clinical application of NFκB decoy oligonucleotides (NFκB decoy ODNs) include poor cellular uptake and short half-life. To address these challenges, we developed polysaccharide-based nanoparticles (PNPs) loaded with NFκB decoy ODNs to target lung cancer. Results showed that PNPs exhibited a small particle size, positive zeta potential, and higher encapsulation efficiency (99%). *In-vitro* studies using A549 lung cancer cells revealed dose-dependent inhibition of proliferation by NFκB decoy ODN-loaded PNPs. Additionally, these nanoparticles significantly reduced levels of pro-inflammatory cytokines IL-6 and IL-8 in A549 cells. These findings suggest the therapeutic potential of NFκB decoy ODN-loaded PNPs in lung cancer treatment, warranting further investigation for clinical translation.

4.1 Introduction

Lung cancer continues to be the leading cause of cancer-related deaths worldwide [1]. Abnormal cell proliferation and metastasis/invasion are the key features of lung cancer cells [2]. One of the key factors driving lung cancer progression is the dysregulation of inflammatory signaling pathways, among which NFκB holds a pivotal role [3]. NFκB activation has been implicated in various aspects of cancer progression, including cell proliferation, survival, and metastasis [4]. Moreover, the buildup of pro-inflammatory cytokines, particularly interleukin 6 (IL-6) and interleukin 8 (IL-8) at the tumor site in cancerous tissues with increased NFκB activity, makes a significant contribution to the pro-tumorigenic microenvironment [5]. In this context, targeted inhibition of NFκB signaling emerges as a promising strategy for cancer therapy.

Oligodeoxynucleotides (ODNs) designed to mimic specific DNA sequences, known as decoy ODNs, offer a unique pharmacological approach to modulating NFκB activity [6]. By competitively binding to NFκB transcription factors, decoy ODNs can disrupt downstream signaling cascades, thereby suppressing the expression of pro-inflammatory genes implicated in cancer pathogenesis [7]. However, the clinical translation of decoy ODNs faces various challenges, including inefficient cellular uptake and susceptibility to enzymatic degradation [8].

To address these challenges, nanoparticle-based delivery systems have gathered significant interest as vehicles for enhancing the bioavailability and target specificity of therapeutic nucleic acids [7]. Polysaccharide-based nanoparticles (PNPs) represent a particularly attractive platform due to their biocompatibility, biodegradability, and ease of functionalization [9]. Dextran, a substance known since the 1940s for expanding blood volume, has lately gained attention for drug delivery purposes [10]. Recent research has explored the potential of dextran for drug delivery applications by means of chemical conjugation and functionalization. These processes provide dextran with favorable physicochemical characteristics and responsiveness to stimuli, facilitating controlled drug release behavior. Acetylated dextran (Ac-DEX) is one of the most studied dextran derivatives [11]. Cohen *et al* synthesized spermine-modified Ac-DEX nanoparticles for siRNA delivery in cancer cells. The findings demonstrated that these nanoparticles can efficiently encapsulate siRNA with high loading efficiency and inhibit luciferase expression in HeLa cells in a dose-dependent manner with minimal cytotoxicity [12]. Another study by Forester *et al.* revealed that dextran-based enhanced cellular uptake of siRNA in both mouse and human macrophages without causing toxicity. Results showed that nanoparticles preferentially accumulate in the liver, where they are mainly taken up by

macrophages and dendritic cells, suggesting their potential for targeted drug delivery to liver macrophages in diseases like liver cancer and fibrosis [13]

Utilizing the unique properties of PNPs, the present study explores their potential as carriers for NFκB decoy ODNs in lung cancer cells. Our aim is to deliver these therapeutic agents to lung cancer cells while protecting the cargo from degradation. Furthermore, we hypothesize that the successful delivery of NFκB decoy ODNs via PNPs will effectively inhibit NFκB signaling, thereby attenuating cancer cell proliferation and mitigating the pro-inflammatory cytokines (IL-6 & IL-8) associated with tumor progression.

4.2 Materials and Methods

4.2.1 Materials

NFκB decoy ODNs were procured from Sigma Aldrich Pvt Ltd. Spermine acetalated dextrose was synthesized in school of chemical Engineering, UNSW lab. MTT (3-[4,5-dimethylthiazol-2-yl]-2,5-diphenyl tetrazolium bromide), sodium dodecyl sulphate (SDS), hydrochloric acid, were procured from Sigma-Aldrich, St. Louis, MO, USA. Dulbecco's modified Eagle's medium (DMEM), foetal bovine serum (FBS), penicillin and phosphate-buffered saline (PBS) were procured from Thermofisher Scientific Pvt Ltd. All other reagents were of analytical grade and were used without further purification.

4.2.2 Methods

Preparation of NFκB decoy ODNs loaded polysaccharide-based nanoparticles (PNPs)

NFκB decoy ODNs loaded PNPs were prepared using double emulsion solvent evaporation method [13]. 10 mg of acetalated polysaccharide was dissolved in 800 µL of ice-cold dichloromethane (DCM) (Organic phase) in a round bottom cell culture tube and stored on ice. Subsequently, 130 µL of double-stranded ODNs (100 µM) solution in Tris buffer was introduced into the organic phase, followed by sonication for 10 seconds using a probe sonicator (UW 70, power MS 72/D, cycle 70%) to create the primary emulsion. Following this, 4 mL of a polyvinyl alcohol (PVA) solution (3% in PBS) was introduced to the initial dextran emulsion and sonicated for another 30 seconds to prepare a secondary emulsion (water-in-oil-in-water). The secondary emulsion was vigorously stirred overnight to evaporate the organic solvent. The prepared nanoparticles were purified using ultracentrifugation (45,000 x g, 20 min), and the resulting pellet was rinsed twice with 3 mL dd-H2O (pH 8). Lastly, 100 µL of PVA solution (0.3%) was added as

a cryoprotectant prior to lyophilization, resulting in a white fluffy powder. Additionally, scramble-loaded nanoparticles and blank nanoparticles were prepared using the same procedure.

Characterization of nanoparticles

For particle size analysis, Nanoparticles were resuspended and diluted in PBS to a concentration of 30-40 µg/mL, then thoroughly sonicated and vortexed prior to measurement. Zeta potential analysis was conducted using the zetasizer Nano ZS (Malvern Instruments, UK) to assess NP stability. Zeta potential was determined via electrophoretic mobility, with 150 µg of NPs dispersed in 1 mL of distilled water. The resulting sample was loaded into a clear disposable zeta cell and automatically analyzed using the zetasizer at 25 °C.

Encapsulation efficiency (EE) determination

The Quant-iT™ RiboGreenR Assay was used to determine the encapsulation efficiency of nanoparticles. The amount of free ODNs present in supernatant after particle centrifugation was measured and compared to the initial used concentration of ODNs. Therefore, particles were ultracentrifuged and 10 µL of the particle supernatant were mixed with 90 µL PBS in a 96-well microplate (black, flat bottom). The pure ODNs was diluted in TE buffer to get standard curve. The RiboGreenR reagent was diluted 1:200 in PBS and 100 µL were added to each well. The reagent was allowed to incubate with the particles for 5 minutes in a light-protected environment before measuring the fluorescence of the reacted dye using a Tecan microplate reader. The fluorescence readings of the particles were then compared to those of the theoretically encapsulated amount of ODNs using Microsoft Excel.

$$\%EE = \frac{(\text{ODNs amount used for formulation} - \text{ODNs amount present in supernatant })}{\text{ODNs amount used for formulation}} x100$$

Cell Culture

A549 cells (human lung epithelial carcinoma) were generously provided by Prof. Alaina Ammit from the Woolcock Institute of Medical Research, Sydney, Australia. The A549 cells were cultured in DMEM supplemented with 10% heat-inactivated FBS at 37°C in a humidified atmosphere containing 5% CO2.

Cell Proliferation assay (MTT assay)

$4x10^4$ cells/ml were seeded at a 100µl per well. The plates are incubated at 37°C in 5% CO2 for 48 hours. The cells were washed twice with hanks and 100µl per well of quiescent media was

added (DMEM supplemented with 1% antibiotics and 1% FBS) for 24h. Media was removed, and cells were treated with various concentrations (0.75nM, 1.5nM, 3nM, 6 nM and 12nM) of NFkB formulation for 24 hrs. All stimulations were performed in triplicates. 1% FBS in DMEM was used as blank. After 24 hr of treatment with formulations 10 µl of MTT dye (5mg/ml in sterile PBS) per well was added. The plates were incubated for 2-6 hours at 37°C in 5% CO2. Plates were then examined microscopically to visualise colour changes inside of viable cells. 100 µl of 10% w/v Sodium Dodecyl Sulphate (SDS) in 0.01M HCL per well was added to stop the reaction. The plates were incubated overnight before absorbance was read at 570nm - 690nm on the Spectramax M2 spectrophotometer.

Determination of IL-6 & IL-8 release

4×10^4 cells/ml were seeded in 12-well plates in DMEM supplemented with 10% FBS. After 72 hours, unadhered cells were removed and cells were washed with hanks and quiesced for 24 h. Then, the cells were treated with NFkB and scramble loaded nanoparticles (6nM) with or without TNF-α (10 ng/ml) and incubated for 24h. After 24 h, cell-free supernatants were collected and stored at -20°C until further analysis. The levels of pro-inflammatory cytokines IL-6 and IL-8 released in the cell culture supernatants were evaluated using ELISA kits (R&D Systems) following the manufacturer's instructions.

4.3 Results

4.3.1 Preparation and characterization of ODNs loaded PNPs

NFkB decoy ODNs loaded PNPs were prepared as white fluffy powder. The mean particle size, PDI and zeta potential of the nanoparticles were measured and summarized in Table 4.1. The mean particle size of scramble and NFkB decoy ODNs loaded nanoparticles were found to have 177.7±2.7 nm and 187.3±1.47 nm respectively with PDI less than 0.25 for both preparations. The zeta potential of scramble and NFkB decoy ODNs loaded nanoparticles was found to be positive i.e. 12.4±0.48 and 11.8±0.32 respectively. Entrapment efficiency of the formulation was determined using Ribogreen assay kit and results showed that 99% of the ODNs has been encapsulated within the nanoparticles.

Table 4.1: Characterization parameters of scramble and NFkB decoy ODNs loaded nanoparticles

Parameters	Scramble loaded nanoparticles	NFkB decoy ODNs loaded nanoparticles
Z-average (nm)	177.7±2.7	187.3±1.47

Polydispersity Index (PDI)	0.20	0.22
Zeta Potential (mV)	12.4±0.48	11.8±0.32
Encapsulation Efficiency (%)	-	99.8

4.3.2 Cell Proliferation assay (MTT assay)

The effect of ODNs loaded nanoparticles on A549 cells proliferation was studied using MTT assay and presented in Figure 4.1. ODNs loaded nanoparticles at doses of 0.75nM, 1.5nM, 3nM, 6nM and 12nM reduced the cell viability to 15%, 21%, 31%, 44% and 55% respectively when compared to the control (untreated).
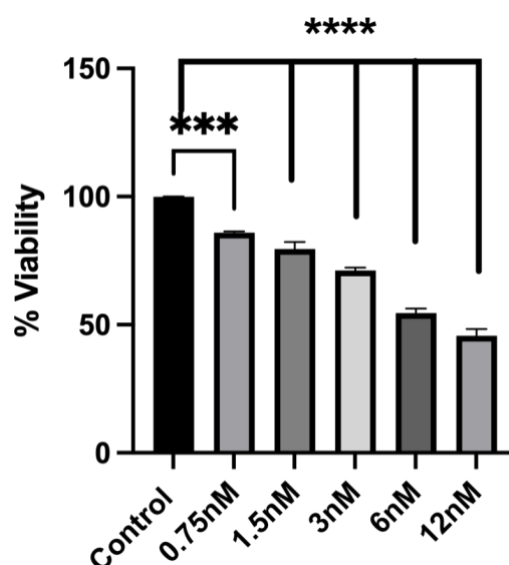
Figure 4.1: Effect of NFkB loaded ODNs loaded PNPs on A549 cells proliferation; n=3 independent experiments; ***$p<0.001$; ****$p<0.0001$ vs control (without nanoparticles treatment).

4.3.3 Determination of IL-6 & IL-8 release

As shown in Figures 4.2a & 4.2b, when the A549 cells were stimulated with TNF-α, there was a clear increase in IL-6 and IL-8 levels compared to the control condition (media + 1% FBS). ELISA results demonstrated that there was a significant reduction in IL-6 (Figure. 4.2a) & IL-8 levels (Figure 4.2 b) when A549 cells were treated with ODNs formulation at 6 nM concentration, as compared to the negative control (TNF-α). However, when compared to the negative control, scramble-loaded nanoparticles also exhibited a reduction in IL-6 and IL-8 levels. However, this reduction was not statistically significant for IL-8.
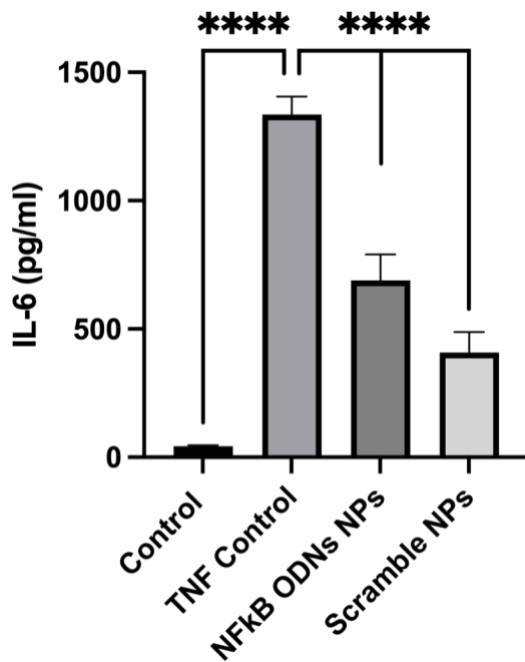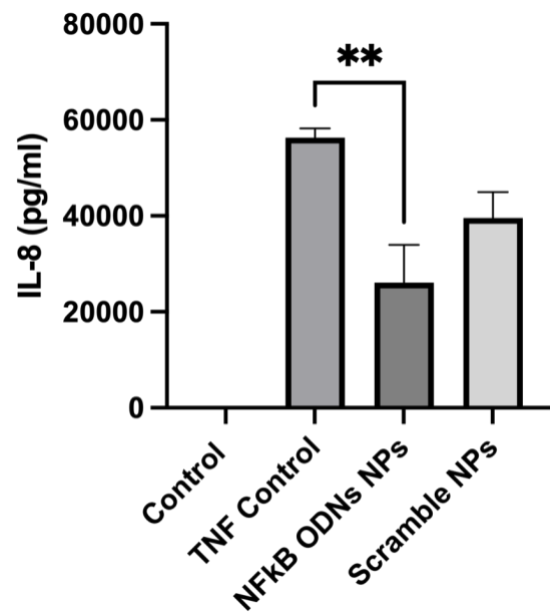
Figure 4.2: Inhibition of protein expression of a) IL-6 and b) IL-8 upon treatment with NFκB decoy ODNs and scramble loaded nanoparticles; Results are presented as mean ± SEM of n = 3 independent experiments. **** p<0.0001, **p<0.01

4.4 Discussion

The successful development of effective therapeutic strategies against lung cancer is a great concern, given its high mortality rates worldwide. In this study, we aimed to explore the potential of polysaccharide-based nanoparticles (PNPs) loaded with NFκB decoy ODNs as a promising therapeutic approach for lung cancer treatment. NFκB is a key regulator of inflammation and has been linked to the development of numerous cancers, including lung cancer [14]. Various studies have documented the use of decoy ODNs for cancer treatment [15, 16]. However, the inability of negatively charged nucleic acids to cross cell membrane barriers, as well as degradation by cellular enzymes, is the main barrier to the clinical application of nucleic acid therapies [8]. To overcome this barrier, various delivery systems and transfection agents have been investigated; however, some of them are associated with toxicity and immunogenicity [17, 18].

Polysaccharide-based nanoparticles emerged as a novel delivery system capable of delivering oligonucleotides to cancer cells with minimal toxicity [9]. Therefore, in the current study we have encapsulated NFκB decoy ODNs into polysaccharide-based nanoparticles for targeting lung cancer. The prepared PNPs exhibited favorable characteristics, including a uniform

particle size distribution, positive zeta potential. Encapsulation efficiency analysis revealed that an impressive 99.8% of the ODNs were successfully encapsulated within the nanoparticles, highlighting the effectiveness of the encapsulation process. This high encapsulation efficiency is crucial for ensuring the therapeutic efficacy of the loaded cargo and minimizing potential off-target effects.

Previous research has shown that lung cancer cells express IL-6 and IL-8, which promote cancer cell proliferation [5]. They promote tumorigenesis by directly acting on lung epithelial cells through NFκB signaling [19]. Decoy ODNs represents an ideal pharmacological tool for selectively inhibiting NFκB activation [7]. In our cell proliferation assays using A549 lung cancer cells, NFκB decoy ODNs loaded PNPs demonstrated a dose-dependent inhibition of cell viability (Figure 4.1). Specifically, at a concentration of 6nM, there was a nearly 50% inhibition of cellular proliferation, prompting us to select this dose for further investigations. Interestingly, a previous study by Fang *et al*. reported that the IC50 of naked NFκB decoy ODNs to inhibit A549 cell proliferation using the MTT assay was 2mg/L [15]. This indicates that our formulation is more potent than naked NFkB decoy ODNs in inhibiting A549 cellular proliferation.

Further formulations were tested to check their anti-inflammatory potential in A549 cancer cell line. As shown in Figure 4.2, NFκB decoy ODNs loaded PNPs significantly reduced levels of pro-inflammatory cytokines i.e., IL-6 and IL-8 at a concentration of 6 nM. when compared to the TNF-α control. Notably, even the scramble-loaded nanoparticles also exhibited a reduction in IL-6 and IL-8 levels compared to the TNF-α-stimulated control, although not statistically significant for IL-8. This may be due to non-specific anti-inflammatory effect of the nanoparticles, possibly mediated by nanoparticles interaction with cellular pathways involved in cytokine regulation. While these results highlight the promising anti-inflammatory effects of NFκB decoy ODN-loaded nanoparticles, comparing their efficacy with other NFκB inhibitors (Bay 11-7082, Proteasome inhibitors, such as bortezomib) is also valuable [20]. Small molecule inhibitors Bay 11-7082 block IKK to inhibit NFκB, yet its lack of specificity raises toxicity concerns [21]. While proteasome inhibitors, such as bortezomib, inhibit NFκB indirectly by preventing IκB degradation, however, they are frequently associated with significant side effects like neuropathy [22]. In contrast, our nanoparticles bypass the proteasome, directly blocking NFκB's DNA, which could minimize systemic toxicity while maintaining efficacy. Further, commercially available inhibitors like curcumin and aspirin also reduce NFκB activity but usually require high doses and act indirectly [23]. In

comparison, our decoy ODN-loaded PNPs provide a more targeted and potentially more effective approach at lower doses.

Despite these promising results, several limitations of the study should be acknowledged. Further studies are needed to investigate the long-term safety and efficacy of ODN-loaded nanoparticles in other lung cancer cell lines. Additionally, to better assess the baseline biocompatibility of the delivery system, future research should include cytotoxicity data for blank polysaccharide-based nanoparticles on A549 cells. The mechanisms underlying the observed effects on cell proliferation and cytokine release also require further elucidation to optimize the therapeutic potential of ODN-loaded nanoparticles for cancer therapy. While this study included comparisons with scramble-loaded nanoparticles, future studies should incorporate blank nanoparticles as an additional control to provide a more comprehensive evaluation of their effects on IL-6 and IL-8 protein expression. Furthermore, as these experiments were conducted in vitro using A549 cells, which may not fully represent the complex tumor microenvironment present in vivo, the efficacy of nanoparticles should be validated using in vivo models. Additionally, future work should include TEM imaging, nanoparticle uptake studies, and further safety assessments to fully characterize the nanoparticles and ensure their suitability for clinical applications.

To enhance the therapeutic impact of these nanoparticles, it is worth considering how targeting both inflammation and NFκB could provide a more robust approach to managing lung cancer progression. The role of inflammation in driving lung cancer progression, as highlighted in Chapter 3, and the central role of NFκB in regulating this inflammatory response, as demonstrated here, present a compelling case for a combined therapeutic strategy. Tumor progression mainly depends on pro-inflammatory cytokines like IL-6 and IL-8, which are controlled by NFκB signaling pathways [24]. By simultaneously targeting both NFκB and inflammation-related factors, it may be possible to disrupt the tumor-supportive microenvironment more comprehensively, hindering cancer growth and metastasis.

Moreover, studies have shown that inhibiting NFκB not only decreases pro-inflammatory cytokine production but also disrupts other critical pathways involved in angiogenesis and immune evasion [25]. Therefore, combining NFκB inhibition with strategies that target inflammation could enhance the overall therapeutic impact by addressing multiple mechanisms of tumor progression at once, offering a promising avenue for improving lung cancer treatment outcomes.

4.5 Conclusion

In conclusion, the findings of this study highlight the potential of NFκB decoy ODNs loaded polysaccharide-based nanoparticles as a promising therapeutic strategy for lung cancer treatment. The PNPs exhibited favorable characteristics in terms of particle size, zeta potential, and encapsulation efficiency, indicating their suitability as effective drug delivery carriers. Moreover, the ODNs loaded PNPs demonstrated dose-dependent inhibition of A549 lung cancer cell proliferation and a significant reduction in pro-inflammatory cytokine levels, suggesting their potential to suppress tumor progression and mitigate the inflammation associated with cancer. Further research is needed to explore their mechanism of action and assess their efficacy and safety *in-vivo*, with the goal of clinical translation.

4.6 References

1. Siegel, R.L., et al., Cancer statistics, 2022. CA: A Cancer Journal for Clinicians, 2022. 72(1): p. 7-33.

2. Larsen, J.E. and J.D. Minna, Molecular biology of lung cancer: clinical implications. Clin Chest Med, 2011. 32(4): p. 703-40.

3. Xia, Y., S. Shen, and I.M. Verma, NF-κB, an active player in human cancers. Cancer Immunol Res, 2014. 2(9): p. 823-30.

4. Liu, T., et al., NF-κB signaling in inflammation. Signal Transduct Target Ther, 2017. 2: p. 17023-.

5. Pine, S.R., et al., Increased levels of circulating interleukin 6, interleukin 8, C-reactive protein, and risk of lung cancer. J Natl Cancer Inst, 2011. 103(14): p. 1112-22.

6. Johari, B. and M. Moradi, Application of Transcription Factor Decoy Oligodeoxynucleotides (ODNs) for Cancer Therapy. Methods Mol Biol, 2022. 2521: p. 207-230.

7. Mehta, M., et al., Recent trends of NFκB decoy oligodeoxynucleotide-based nanotherapeutics in lung diseases. Journal of Controlled Release, 2021. 337: p. 629-644.

8. De Stefano, D., Oligonucleotides decoy to NF-kappaB: becoming a reality? Discovery medicine, 2011. 12(63): p. 97-105.

9. Liu, Z., et al., Polysaccharides-based nanoparticles as drug delivery systems. Advanced Drug Delivery Reviews, 2008. 60(15): p. 1650-1662.

10. Mehvar, R., Dextrans for targeted and sustained delivery of therapeutic and imaging agents. J Control Release, 2000. 69(1): p. 1-25.

11. Wang, S., et al., Acetalated dextran based nano- and microparticles: synthesis, fabrication, and therapeutic applications. Chemical Communications, 2021. 57(35): p. 4212-4229.

12. Cohen, J.L., et al., Acid-Degradable Cationic Dextran Particles for the Delivery of siRNA Therapeutics. Bioconjugate Chemistry, 2011. 22(6): p. 1056-1065.

13. Foerster, F., et al., Dextran-based therapeutic nanoparticles for hepatic drug delivery. Nanomedicine, 2016. 11(20): p. 2663-2677.

14. Park, M.H. and J.T. Hong, Roles of NF-κB in Cancer and Inflammatory Diseases and Their Therapeutic Approaches. Cells, 2016. 5(2).

15. Fang, Y., et al., Antitumor activity of NF-kB decoy oligodeoxynucleotides in a prostate cancer cell line. Asian Pac J Cancer Prev, 2011. 12(10): p. 2721-6.

16. Zhang, X., et al., STAT3-decoy oligodeoxynucleotide inhibits the growth of human lung cancer via down-regulating its target genes. Oncol Rep, 2007. 17(6): p. 1377-82.

17. Farahmand, L., B. Darvishi, and A.K. Majidzadeh, Suppression of chronic inflammation with engineered nanomaterials delivering nuclear factor κB transcription factor decoy oligodeoxynucleotides. Drug Deliv, 2017. 24(1): p. 1249-1261.

18. Roma-Rodrigues, C., et al., Gene Therapy in Cancer Treatment: Why Go Nano? Pharmaceutics, 2020. 12(3).

19. Rajasegaran, T., et al., Targeting Inflammation in Non-Small Cell Lung Cancer through Drug Repurposing. Pharmaceuticals, 2023. 16(3): p. 451.

20. Ramadass, V., T. Vaiyapuri, and V. Tergaonkar, Small Molecule NF-κB Pathway Inhibitors in Clinic. Int J Mol Sci, 2020. 21(14).

21. Rundall, B.K., C.E. Denlinger, and D.R. Jones, Combined histone deacetylase and NF-κB inhibition sensitizes non-small cell lung cancer to cell death. Surgery, 2004. 136(2): p. 416-425.

22. Davies, A.M., et al., Incorporating bortezomib into the treatment of lung cancer. Clinical Cancer Research, 2007. 13(15): p. 4647s-4651s.

23. Vadhan-Raj, S., et al., Curcumin Downregulates NF-kB and Related Genes in Patients with Multiple Myeloma: Results of a Phase I/II Study. Blood, 2007. 110(11): p. 1177-1177.

24. Zhao, H., et al., Inflammation and tumor progression: signaling pathways and targeted intervention. Signal Transduct Target Ther, 2021. 6(1): p. 263.

25. Kannaujiya, V.K., et al., Anticancer activity of NFκB decoy oligonucleotide-loaded nanoparticles against human lung cancer. Journal of Drug Delivery Science and Technology, 2023. 82: p. 104328.

Chapter 5: Conclusion and Future Perspectives

Breast and lung cancer remains a major global health concern due to limited treatment options and severe adverse effects of current therapies. Therefore, novel pharmacological interventions are urgently needed. Among several emerging drug molecules, plant-based and nucleic acid-based therapies show promise, but their clinical utility is hindered by poor pharmacokinetic properties. In response to this challenge, we engineered nanoparticle-mediated drug delivery platforms incorporating nucleic acids (siRNA & NFκB decoy ODNs) and phytochemicals (berberine). The subsequent *in-vitro* evaluation demonstrated their robust therapeutic effectiveness against breast and lung cancer cell-based models, underscoring their promising potential for clinical application. These developed drug delivery systems aim to overcome current treatment limitations and achieve more effective therapeutics against cancer.

The XBP1 gene, involved in TNBC aggressiveness, serves as a crucial factor for targeting breast cancer. siRNA therapy holds promise in silencing critical genes like XBP1, offering targeted treatment for TNBC patients. Lipid nanoparticles provide an efficient delivery platform for siRNA therapy, enhancing its effectiveness and minimizing off-target effects. Therefore, **Chapter 2** was designed to develop a targeted treatment approach for TNBC by developing EGFR antibody-conjugated siXBP1-loaded PLGA lipid nanoparticles. PLGA lipid nanoparticles were prepared via a double emulsion solvent evaporation technique. The prepared nanoparticles had a spherical shape with an average size of 150±7.4 nm. To achieve the targeting capability of our nanoparticles on TNBC cells, we conjugated the nanoparticles with an EGFR antibody. This modification targets the EGFR receptor, which is known to be overexpressed in approximately 50% of TNBC cells. We have achieved high siRNA entrapment efficiency (>70%), which was important for effective gene suppression. Confocal microscopy and flow cytometry confirmed the efficient uptake of EGFR antibody-conjugated nanoparticles by MDA-MB-231 cells. Transfection efficiency was evaluated using EGFP siRNA in HEK293 cells, showing a significant reduction in GFP expression and validating the gene-silencing potential. Next, the transfection efficacy of siXBP1-loaded nanoparticles to knock down the XBP1 gene in MDA-MB-231 cells was determined. Interestingly, the nanoparticles have successfully delivered XBP1 siRNA to MDA-MB-231 cells, resulting in significant gene suppression, even under challenging hypoxic conditions. The cellular toxicity of the nanoparticles in MDA-MB-231 cells was examined via MTT assay. Results showed no significant change in cell viability when treated with blank PLGA lipid NPs, even at a higher concentration. Furthermore, an apoptosis and necrosis assay were conducted to determine the

impact of XBP1 gene silencing on cell death pathways. Notably, gene silencing significantly promoted cell apoptosis under hypoxic conditions.

Inflammation serves as a potent driver in the development and progression of cancer. High levels of chemokines like CXCL-8 and CCL-20, along with overexpression of HO-1 in cancer cells, are linked to aggressive tumor behavior and resistance to chemotherapy in lung cancer patients. Therefore, targeting these proteins (CXCL-8, CCL-20, and HO-1) can be a promising therapeutic approach for lung cancer treatment. Additionally, plant-based compounds like berberine offer advantages over synthetic ones due to their natural origin and lower toxicity but are associated with limitations such as low solubility and poor bioavailability. Encapsulating these compounds into LCNs can enhance their solubility, bioavailability, and targeting capabilities, making them attractive options for combating inflammation-mediated lung cancer progression. Therefore, **Chapter 3** of the thesis investigated the potential of berberine-loaded LCNs in inhibiting inflammation-mediated lung cancer progression. Berberine, isolated from several herbs within the Papaveraceae family, exhibits significant anti-inflammatory and anticancer potential. This study involved encapsulating berberine into LCNs through ultrasonication, followed by characterization to check their size, zeta potential, and entrapment efficiency. TEM analysis revealed that nanoparticles were monodispersed, spherical and smooth-surfaced. The cell viability assay conducted on A549 cells using MTT revealed an IC50 value of 5 μM, which is significantly lower than that of berberine powder (100 μM). Additionally, protein analysis data showed that berberine-loaded LCNs significantly reduced the expression of inflammation-related key proteins (CXCL-8, CCL-20, and HO-1) involved in cancer progression at a much lower dose (5 μM) compared to berberine powder (90 μM). These findings suggest that formulating berberine into LCNs could enhance its biological activity while reducing dosage requirements.

Among emerging therapeutic strategies, targeting NFκB inhibition holds promise due to its role as a key regulator in the pathogenesis of non-small cell lung cancer (NSCLC). Elevated NFκB activity raises the accumulation of pro-inflammatory cytokines like IL-6 and IL-8 near tumor sites, create a microenvironment favourable to tumor growth. This underscores the potential of NFκB inhibition as a viable anti-cancer approach. Furthermore, Polysaccharide-based drug delivery systems have garnered notable attention due to their inherent biocompatibility, biodegradability, and easy chemical modification, making them promising candidates for advanced biomedical applications. Hence, **Chapter 4** focused on encapsulating NFκB decoy oligodeoxynucleotides (ASOs) into polysaccharide-based nanoparticles to assess

their efficacy in inhibiting inflammation-mediated cancer progression *in-vitro*. The nanoparticles were synthesized using a double emulsion solvent evaporation technique and characterized for size, zeta potential and entrapment efficiency. Small particle size (177 nm), positive zeta potential, and high encapsulation efficiency (>99%) ensure their suitability for targeted delivery to cancer cells. *In-vitro* MTT assays conducted on A549 cells revealed that NFκB decoy ASO-loaded nanoparticles significantly suppressed cellular proliferation in a dose-dependent manner. The developed formulation exhibited an IC50 value of 26.20 nM, markedly lower than naked NFκB decoy ASOs (2 mg/ml). Furthermore, the formulated nanoparticles effectively reduced levels of pro-inflammatory cytokines IL-6 and IL-8 at a significantly lower dose (6nM), offering the potential for alleviating chronic airway inflammation and inhibiting lung cancer progression. In conclusion, encapsulating NFκB decoy ODNs into nanoparticles presents a promising avenue for targeted therapy in NSCLC, with potential implications for improving patient outcomes and quality of life.

5.1 Future prospects

Although we obtained promising results from experiments conducted in the current project, some areas still need to be addressed. It is imperative to acknowledge the need for further exploration and validation to advance the field of cancer therapeutics.

Firstly, to ensure the robustness of our findings, it is imperative to validate our promising in vitro results across a broader spectrum of cell lines. While the MDA-MB-231 cell line serves as a representative model for TNBC, extending our research across other TNBC cell lines, such as MDA-MB-468 and MDA-MB-436, would enhance the credibility and applicability of our findings. Similarly, in lung cancer research, expanding beyond the A549 cell line to encompass other aggressive cell lines like H460 and H1299 would provide a more comprehensive understanding of the therapeutic interventions we propose.

Secondly, transitioning from *in-vitro* to *in-vivo* studies represents a crucial step in drug development. This shift is essential for gaining a comprehensive understanding of how developed nanoparticles will behave within complex biological systems. By utilizing *in-vivo* models, including patient-derived xenograft models, genetically engineered mouse models with relevant genetic alterations, and transgenic mouse models, we can assess drug metabolism, biodistribution, and immune response, which are crucial for evaluating the efficacy and safety of novel drugs. Additionally, these models provide more valuable insights into the potential challenges associated with clinical translation.

Thirdly, our research has led to the development of drug delivery systems, including lipid nanoparticles, polysaccharide nanoparticles, and liquid crystalline nanoparticles. Among the three delivery systems, lipid nanoparticles have shown better cellular uptake and targeted drug action, while future work should include TEM imaging, nanoparticle uptake studies, and further safety assessments to fully characterize the liquid crystalline and polysaccharide-based nanoparticles and ensure their suitability for clinical applications. Additionally, it is crucial to benchmark the efficacy of drug-loaded nanoparticles with standard chemotherapies, which for TNBC typically involve chemotherapy drugs like PTX and Dox, and for NSCLC include cisplatin and carboplatin. This way, we can more accurately determine their effectiveness, safety profiles, and potential for clinical application.

In summary, these future research directions, structured around validation across cell lines, comparison with standard treatments, and transition to *in-vivo* studies, are vital for advancing these delivery systems toward clinical translation, finally improving patient outcomes and contributing to the ongoing battle against cancer.

Appendix A

STATEMENT OF CONTRIBUTION

Mehta, M., Bui, T. A., Yang, X., Aksoy, Y., Goldys, E. M., & Deng, W. (2023). Lipid-Based Nanoparticles for Drug/Gene Delivery: An Overview of the Production Techniques and Difficulties Encountered in Their Industrial Development. ACS materials Au, 3(6), 600–619.

Mehta, M., Bui, T. A., Care. A., & Deng, W. (2024). Targeted polymer lipid hybrid nanoparticles for in-vitro siRNA therapy in triple-negative breast cancer. Journal of Drug Delivery Science and Technology, 98, p. 105911. https://doi.org/10.1016/j.jddst.2024.105911.

I attest that Higher Degree Research candidate Meenu was the primary contributor to the development of this publication.

Wei Deng   25/10/2024

Production Note:
Signature removed prior to publication.

Appendix B

ACKNOWLEDGEMENT OF CONTRIBUTION (CHAPTER 3)

The research outlined in this published chapter stems from research conducted by Meenu under the supervision of Dr Dua, Prof Hansbro and Prof Oliver. I (Meenu) would like to acknowledge the contribution of the following people to the work outlined in this chapter-

Vamshikrishna Malyla – investigation, data curation, writing (review and editing)

Keshav R Paudel – investigation, data curation, methodology, writing (review and editing)

Dinesh K Chellappan - conceptualisation, methodology, resources, writing (review and editing)

Philip M Hansbro – supervision, resources

Brian GG Oliver - writing (review and editing)

Kamal Dua – conceptualisation, supervision, writing (review and editing)

The formulation data of this study also forms part of the Bachelor of Pharmacy (Hons) dissertation (IMU, Malaysia): Formulation of Berberine hydrochloride loaded liquid crystalline nanoparticles for the therapeutic interventionin asthma – Project ID No. BP I-01/2019 (28) – Students involved: Lee Li Yen, Geena Hew Suet Yin.

Appendix C

ACKNOWLEDGEMENT OF CONTRIBUTION (CHAPTER 4)

Investigation of anticancer potential of NFκB decoy oligonucleotide loaded polysaccharide nanoparticles in lung cancer cells

The research outlined in this chapter (unpublished) stems from research conducted by Meenu under the supervision of Dr Dua and Dr Wich. I (Meenu) would like to acknowledge the contribution of the following people to the work outlined in this chapter:

Kamal Dua – conceptualisation, methodology, supervision, writing (review and editing), project administration

Peter Wich – conceptualisation, methodology, supervision, validation, resources, project administration

Brian Oliver – conceptualisation, methodology, supervision, validation, resources

Dikaia Xenaki - methodology, validation, formal analysis

Vinod Kumar Kannaujiya – investigation, data curation

Published work from the thesis

Review

Lipid-Based Nanoparticles for Drug/Gene Delivery: An Overview of the Production Techniques and Difficulties Encountered in Their Industrial Development

Meenu Mehta,[#] Thuy Anh Bui,[#] Xinpu Yang, Yagiz Aksoy, Ewa M. Goldys, and Wei Deng*

Read Online

ACCESS | Metrics & More | Article Recommendations

ABSTRACT: Over the past decade, the therapeutic potential of nanomaterials as novel drug delivery systems complementing conventional pharmacology has been widely acknowledged. Among these nanomaterials, lipid-based nanoparticles (LNPs) have shown remarkable pharmacological performance and promising therapeutic outcomes, thus gaining substantial interest in preclinical and clinical research. In this review, we introduce the main types of LNPs used in drug formulations such as liposomes, nanoemulsions, solid lipid nanoparticles, nanostructured lipid carriers, and lipid polymer hybrid nanoparticles, focusing on their main physicochemical properties and therapeutic potential. We discuss computational studies and modeling techniques to enhance the understanding of how LNPs interact with therapeutic cargo and to predict the potential effectiveness of such interactions in therapeutic applications. We also analyze the benefits and drawbacks of various LNP production techniques such as nanoprecipitation, emulsification, evaporation, thin film hydration, microfluidic-based methods, and an impingement jet mixer. Additionally, we discuss the major challenges associated with industrial development, including stability and sterilization, storage, regulatory compliance, reproducibility, and quality control. Overcoming these challenges and facilitating regulatory compliance represent the key steps toward LNP's successful commercialization and translation into clinical settings.

KEYWORDS: Manufacturing, Lipid-based nanoparticles, Delivery systems, Lipid-based nanoparticle synthesis, Industrial challenges
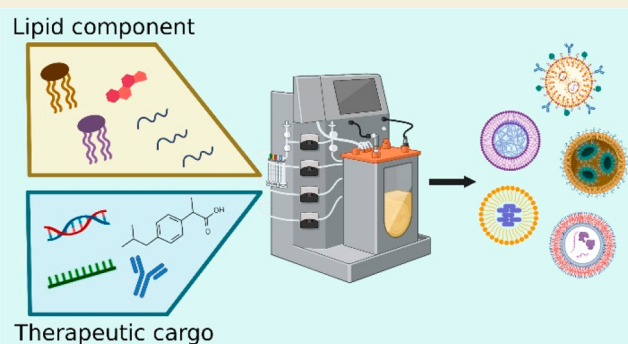
1. INTRODUCTION

Lipid-based nanoparticles (LNPs) are a highly adaptable class of nanocarriers that have gained widespread usage in medical research and pharmacology.[1] They can encapsulate various therapeutic agents including small molecules, nucleic acids and monoclonal antibodies for a diverse range of applications.[2,3] LNPs offer several benefits, such as safeguarding drugs from *in vivo* degradation, boosting their solubility and efficacy, enabling targeted drug delivery to the disease site, regulating drug release, and altering drug biodistribution.[4] These engineered nanocarriers hold the potential to overcome significant limitations of traditional therapeutic products such as inadequate efficacy, susceptibility to enzymatic degradation, low bioavailability, and off-target side effects.[1,5]

The potential for LNP-based pharmaceuticals has been increasingly recognized in recent years, with significant growth in both research and industrial sectors.[6] The LNP-based gene therapy market's value reached about $3.5 billion in 2021, with a projected compound annual growth rate of around 18.5% from 2021 to 2026.[7] The current market value of liposomal therapeutics used for cancer treatment (e.g., Doxil, DaunoX-

ome, Myocet, DepoCyt, Marqibo, Onivyde) was approximately $3.72 billion in 2021 and is anticipated to reach almost $7 billion by 2027.[8] In addition to cancer treatment, LNP-based therapies have gained FDA approval for treating other diseases, including COVID-19 vaccine (Spikevax , Comirnaty) and Amyloidosis (Onpattro), by delivering mRNA and siRNA, respectively.[9−11] Nevertheless, to be clinically relevant, LNP-based therapies must be produced through techniques that ensure stability during storage, compatibility with sterilization, quality control, and regulatory compliance.[4] These factors are crucial to the successful development and translation of LNP-based therapeutics for clinical applications.

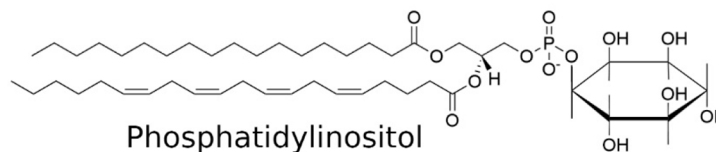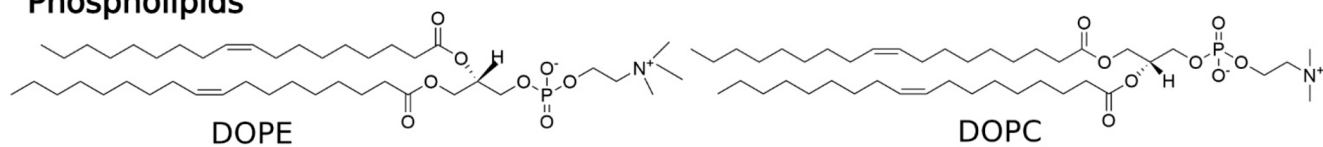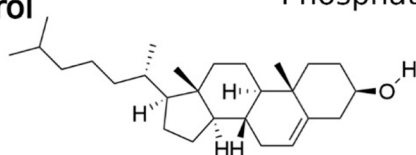**Figure 1.** Chemical structures of various components used in LNP formulations. These include phospholipids (1,2-dioleoyl-*sn*-glycero-3-phosphoethanolamine (DOPE), 1,2-dioleoyl-*sn*-glycero-3-phosphocholine (DOPC), and phosphatidylinositol), cholesterol, cationic and ionizable lipids (1,2-dioleoyl-3-trimethylammonium-propane (DOTAP), (1,2-dilinoleyloxy-3-dimethylaminopropane) (Dlin-MC3-DMA)), and PEG lipids (1,2-distearoyl-*sn*-glycero-3-phosphoethanolamine-*N*-[methoxy(polyethylene glycol)](DSPE-PEG), 1,2-distearoyl-*sn*-glycero-3-phosphoethanol-amine-*N*-[succinyl(polyethylene glycol)] (DSG-PEG)).

In addition to LNPs, metal–organic frameworks (MOFs) have emerged as a promising class of materials for drug delivery applications. MOFs possess unique porous properties that enable them to store and release molecules effectively, making them attractive candidates for drug delivery.[12] Zinc-based MOFs and chitosan/graphene oxide bionanocomposite beads efficiently loaded the antibiotic drug metronidazole, showing excellent releasing power.[13] Lipid-coated MOFs efficiently store dye molecules within the porous scaffold with the lipid bilayer preventing premature release. The lipid coating significantly improved nanoparticle stability, promising an innovative cancer therapy.[14]

Our review offers a comprehensive analysis of diverse LNP formulations, emphasizing their distinctive structural and physicochemical characteristics. We also briefly discuss computational modeling techniques such as molecular dynamics (MD) simulations, quantum mechanical calculations, and molecular docking studies in predicting the structural properties and dynamic behavior of LNPs.[15,16] Furthermore, we provide a thorough overview of the LNP manufacturing process, including both laboratory- and industrial-scale production. We also identify the crucial obstacles associated with the industrialization of LNP production that must be addressed to further the clinical implementation of LNPs in drug and gene delivery applications.

2. GENERAL CHARACTERISTICS OF LNPs

2.1. Main Components of LNPs

LNPs typically consist of four main lipid components: phospholipids and cholesterol, which are necessary for particle formation and stability; cationic or ionizable lipids, which enable binding with negatively charged nucleic acids, thereby increasing drug loading; and 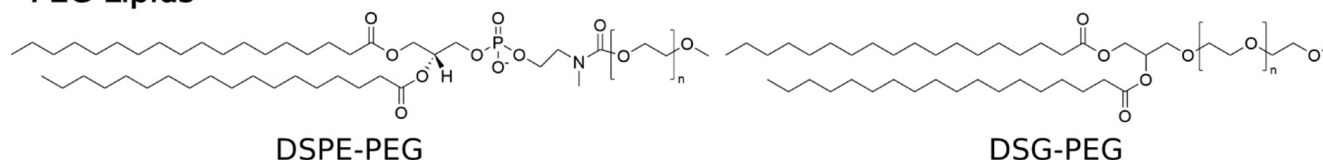PEGylated lipids, which contribute to enhanced particle stability and circulation time within the biological system[17] (Figure 1). Due to their biomimetic architecture and the similarity of their lipid components to those of cell membranes, LNPs can easily cross the cell membrane to deliver nanoparticle contents to the desired intracellular sites. After crossing the cell membrane, LNPs can take advantage of the low pH environment within the target cells, promoting endosomal escape and releasing the therapeutic cargo into the cytoplasm.[2]

2.2. Characteristics of LNPs

Understanding key factors related to LNP characteristics is essential before delving into LNP categories and synthesis methods. These factors include LNP size, surface charge, morphology, stability, loading efficacy, and entrapment efficiency.

Nanoparticle size plays a vital role in LNP properties, influencing stability, biodistribution, cellular uptake, and overall therapeutic efficacy.[18] Smaller LNPs (size <100 nm)
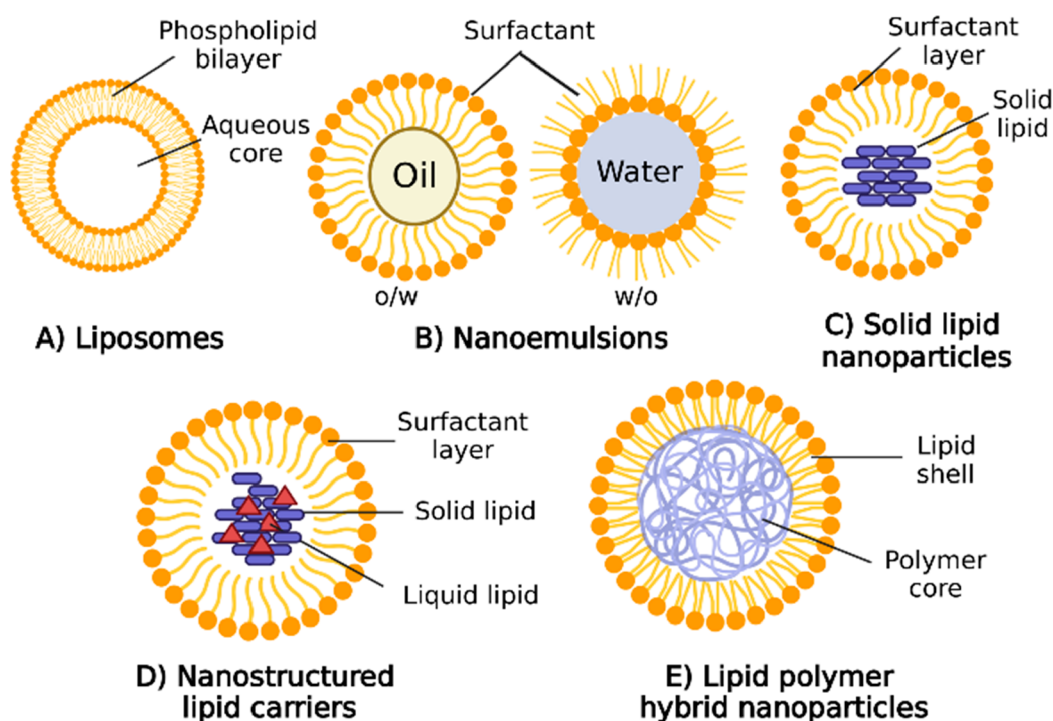
Figure 2. Schematic illustration depicts the structure of various LNP formulations used in drug delivery. (A) Liposomes are spherical vesicles with phospholipid bilayers, encapsulating hydrophilic drugs in their aqueous core and incorporating hydrophobic drugs within the lipid bilayers. (B) Nanoemulsions comprise oil droplets dispersed in an aqueous phase stabilized by surfactants, accommodating lipophilic drugs in the oil phase while preventing droplet aggregation. (C) Solid lipid nanoparticles (SLNs) consist of solid lipid matrices entrapping hydrophobic drugs, forming nanoscale particles with a lipid core. (D) Nanostructured lipid carriers (NLCs) are similar to SLNs but contain a combination of solid and liquid lipids, resulting in a more stable matrix and improved drug loading capacity. (E) Lipid polymer hybrid nanoparticles combine lipid-based and polymer-based components, offering the benefits of both systems. These nanoparticles can effectively encapsulate various types of drugs and exhibit enhanced stability and controlled release properties. Each type of LNP structure provides unique advantages and can be tailored for targeted drug delivery, enabling the encapsulation of a diverse range of therapeutic agents. Figure created with BioRender.com.

tend to exhibit enhanced cellular uptake and prolonged circulation time, while larger LNPs (size >100 nm) may offer higher drug loading capacity but reduced cellular uptake.[19] Dynamic Light Scattering (DLS) is the most preferred method for characterizing LNP sizes due to its effectiveness and convenience.[20,21]

Surface charge of LNPs, a critical parameter that indicates LNP stability in suspension, is commonly characterized through zeta potential measurements.[22] A highly positive or negative Zeta potential indicates a strong surface charge, which results in electrostatic repulsion between particles and enhancement of their stability in the dispersion. On the other hand, a Zeta potential close to zero suggests a low surface charge and a higher tendency for particle aggregation or coalescence, potentially leading to the destabilization of the LNP suspension.[23]

Surface morphology assessment of LNPs can be performed using transmission electron microscopy (TEM), scanning electron microscopy (SEM), and atomic force microscopy (AFM). These methods provide valuable insights into the physical structure and characteristics of the outer surface of the LNP.[24] A well-defined and smooth surface morphology is highly advantageous for LNPs in biological environments as it contributes to enhanced stability and mitigates the risk of opsonization, where serum proteins bind to the surface, triggering immune system clearance. This smooth surface minimizes unwanted interactions with biological components, promoting favorable LNP biodistribution and ensuring optimal

therapeutic efficacy.[25] On the other hand, LNPs with rough or irregular surface morphology may exhibit increased interactions with biological entities, potentially influencing LNP biodistribution patterns and impacting overall therapeutic effectiveness.[25]

LNP surface modification by PEGylation or targeting ligands can further influence the surface morphology of LNPs. For instance, these modifications can improve the stealth properties of LNPs, reducing recognition by the immune system and therefore extending drug circulation time for better drug delivery efficiency.[26] In short, accurate size, surface charge, and morphology determination of LNPs are crucial for optimizing LNP production and maintaining consistency in their properties. This precision plays a vital role in achieving a reliable and effective drug delivery using LNPs.

LNP stability, loading efficacy, and entrapment efficiency are critical factors in the development and optimization of LNP-based drug delivery systems. LNP stability refers to the capability of LNPs to preserve their physical and chemical properties over time under various conditions. These properties include shape, size, and lipid component integrity during long-term storage or exposure to different biological environments like blood, plasma, or varying pH conditions.[27] LNP drug loading capacity quantifies the total amount of drugs that can be loaded into the delivery system, while entrapment efficiency measures the effectiveness of the formulation process in retaining drug within the LNP.[18]

Table 1. LNPs in the Commercial Market and Clinical Trials

LNP subgroup	active substance	disease/applications	products	ref
liposomes	doxorubicin/ daunorubicin	cancer	Doxil, Myocet, Vixeos, DaunoXome, Transdrug	85–89
	other anticancer agents	cancer	Mepact, Depocyt, Marqibo, Onivyde	90–93
	paclitaxel	cancer	Abraxane	94–96
	amphotericin B	visceral leishmaniasis	Albecet, Ambisome, Amphotec	97–99
	vaccine	HAV viral vaccine	Epaxal, Inflexal	100, 101
	verteporfin	age-related macular degeneration	Visudyne	102
nanoemulsions	etomidate, profol	anesthetics	Etomidat-Lipuro, Diprivan	103, 104
	heparinoid	superficial thrombophlebitis	Nanoemulsions carrying heparinoid for topical delivery	105
	ibuprofen	pain relief	Topical delivery of ibuprofen-nanoemulsions	106
	cyclosporin A	immunosuppressants	Sandimmune and Sandimmun Neoral	107
	ritonavir	antiviral HIV-1 medicine in children	Norvir	108
	saquinavir	antiviral HIV-1 medicine in adult	Fortovase	108
solid lipid nanoparticles	mitoxantrone	hepatocarcinoma	Mitoxantrone-loaded polybutylcyanacrylate nanoparticles (DHAD-PBCA-NPs) (phase II clinical trial)	109
	doxorubicin	hepatocarcinoma	Doxorubicin Transdrug (DT) (Phase III clinical trial)	110
	oxiconazole	tinea fungal infection	Oxiconazole nitrate solid lipid nanoparticles loaded gel (Phase I clinical trial)	111
	halobetasol propionate	inflammation	Pluronic gel Halobetasol propionate-loaded lipid nanoparticles	112
			Duobril (Phase IV clinical trial)	113
	siRNA targeting transthyretin gene	amyloidosis	Onpattro (Patisiran)	10
nanostructured lipid carriers	acitretin	psoriasis	Acitretin Precirol ATO 5/oleic acid/Tween 80 (Randomized Controlled Trial)	114
	all-trans retinoic acids	keratinization disorders	Oleic acid/Cetyl palmitate/Cineole/Limonene/Transcutol/Butylated hydroxytoluene/Tween 20/Tween 80	115
	self-amplifying RNA	COVID-19	THEMBA II T-CELL Vaccine (phase I/II clinical trial)	116, 117
	mRNA-1273	COVID-19	Spikevax	118
	BNT162b2 mRNA	COVID-19	Comirnaty	119
lipid polymer hybrid nanoparticle	docetaxel	pancreatic cancer	Docetaxel polymeric nanoparticle (phase I clinical trial)	120, 121
	docetaxel	lung cancer with KRAS mutation	BIND-014 (Docetaxel Nanoparticles for Injectable Suspension) (phase II clinical trial)	122
	docetaxel	prostate cancer	BIND-014 (Docetaxel Nanoparticles for Injectable Suspension) (phase II clinical trial)	123

2.3. Computational Modeling of LNPs: Insights into Structure, Behavior, and Interactions

Computational modeling of LNPs utilizes computer-based methods such as MD simulations, quantum mechanical calculations, and molecular docking studies to analyze and predict the behavior, structure, and interactions of LNPs at the molecular level.[28,29] Among these, MD simulations have emerged as the primary method for studying LNPs. This technique was initially introduced by Chaban and Khandelia to characterize the molecular structure of lipid droplets, which consisted of varying fractions of cholesteryl oleate and triolein.[30] Using coarse-grained MD simulations, this group investigated the structure and transport properties of lipid droplets. Their findings revealed that cholesterol is uniformly distributed within the lipid droplet, and the extent of phospholipid coverage does not impact this distribution.[31]

Computational modeling is also a powerful tool for investigating the interaction between LNPs and different drug formulations.[32] Metwally and colleagues employed MD simulations to predict curcumin loading efficiency in solid LNPs.[33] The authors also used docking calculations to determine the binding energies between curcumin and solid LNPs. By establishing a correlation between the docking binding energy of the drug and LNPs and the entrapment

efficiencies in LNPs, this method offers valuable insights into drug loading capacity. Altogether, combination of bioinformatics and computational modeling could assist in selecting the best drug/carrier combinations for further investigation.[33]

In summary, computational tools can be used to optimize LNP formulations, screen potential drug candidates, and predict their behavior in biological environments, complementing experimental investigations in LNP research.[32,34] The following section will provide further insights into the application of computational modeling to study different types of LNPs.

3. MAIN TYPES OF LNPs

LNPs can be categorized into five subgroups: liposomes, lipid nanoemulsions, solid lipid nanoparticles, nanostructured lipid carriers, and lipid–polymer hybrid nanoparticles (Figure 2). This section offers an outline of the structural elements, physicochemical characteristics, computational modeling studies, and clinical applications of these LNP subgroups.

3.1. Liposomes

Liposomes, first discovered in 1965 by Bangham and colleagues, are self-assembling nanosized lipid vesicles comprising one or more concentric phospholipid bilayers

that enclose discrete aqueous spaces.[35] Liposomes were quickly recognized for their potential as drug delivery systems due to their ability to carry a diverse range of therapeutic drugs, with hydrophilic drugs contained within their aqueous core and hydrophobic drugs integrated into the lipid bilayer.[36,37] Additionally, liposomes can also carry other macromolecules such as different types of imaging agents, nucleic acids, and proteins, thus making them an extremely versatile drug delivery platform.[4] Liposomes can be synthesized into unilamellar or multilamellar vesicles, with sizes varying from 20 to 1000 nm, depending on the specific formulations and synthesis procedures.[2] Particle size is an important parameter for the pharmaceutical applications of liposomes. Small unilamellar liposomes (≤100 nm) exhibit higher encapsulation efficiency, improved drug half-life, and the ability to evade the immune system upon administration.[38]

MD simulations have been instrumental in understanding liposome characteristics, including vesicle formation and conformational stability.[39−41] Furthermore, these simulations have been utilized to enhance liposome thermal stability by formulating them with different phospholipid components.[40]

In the context of PEGylation, MD simulations have shed light on its impact on the drug-loading efficiency in lipid membranes. Dzieciuch et al. conducted a study using MD simulations to investigate the interaction between a hydrophobic molecule, p-THPP, and lipid bilayers. Their findings revealed that in PEGylated membranes, p-THPP wraps around the PEG corona, resulting in increased exposure to the solvent when compared to zwitterionic membranes.[42] PEGylation enhances hydrophobicity and protects drug molecules like hematoporphyrin under physiological conditions.[42] However, MD simulations revealed that PEGylation may not always improve the targeting efficiency. For example, a research group studied an activated endothelium targeting peptide's effectiveness in directing liposomes to vascular endothelium.[43] Upon peptide anchorage to a PEGylated liposome, MD simulations did not show evidence of improved targeting capability, as the ligand was embedded within the PEG layer, reducing its exposure to the solvent.

Additionally, computational prodrug design methodology has been applied to explore various active pharmaceutical ingredients for optimizing drug encapsulation and release from liposomes.[30] By leveraging computational simulations, this approach showcases the promise of guiding the design and advancement of liposome-based drug delivery systems, thereby providing improved therapeutic efficacy and controlled drug release.

Liposomes are widely recognized as a versatile drug delivery system with advantages such as rapid absorption, improved drug bioavailability, reduced toxicity, and protection against hydrolysis and oxidation.[4] However, their clinical applications face challenges due to short half-lives, low biostability, and the risk of drug leakage.[44] To address these limitations, strategies have been developed, including targeted liposomes with surface-attached ligands and "stealth" liposomes enclosed with biocompatible polymers like PEG to evade the immune response.[45−47] For example, a preclinical study demonstrated successful delivery of therapeutic agents for glioblastoma across the blood-brain barrier using ApoE-functionalized liposomal nanoplatform based on artesunate-phosphatidylcholine (ARTPC) encapsulated with Temozolomide.[48]

Thanks to the rapid development of liposome formulations in both the research community and the industry area, there has been a wide range of liposome drugs approved and applied in medical practice. For example, Doxil is the first FDA-approved liposomal drug containing doxorubicin (DOX) which is used to treat solid tumors.[49,50] Following the successful application of Doxil, various liposome-formulated drugs have been approved for disease treatments[2] (Table 1).

3.2. Nanoemulsions

Nanoemulsions are another type of LNP that consist of spherical biphasic liquid droplets ranging in size from 50 to 500 nm.[51,52] They are composed of an internally dispersed oil phase covered by an external continuous phase. Nanoemulsions can be prepared as oil-in-water (o/w) or water-in-oil (w/o) droplets to carry either hydrophobic or hydrophilic active compounds, respectively.[53] To stabilize these small droplets, different types of emulsifiers, such as surfactants, phospholipids, proteins, polysaccharides or polymers such as poly(vinyl alcohol), can be added during the synthesis procedure.[54,55] These surfactants, whether ionic or nonionic, prevent droplet aggregation through electrostatic repulsion or steric hindrance, hydration, and thermal fluctuation interactions.[55,56]

Nanoemulsions have a colloidal structure that enables solubilization and encapsulation of hydrophobic drugs, reducing adverse effects.[57] They are mainly used for topical drug delivery (Table 1) but have potential for other modes of administration like intravenous, ocular, intranasal, and oral delivery.[58−61] Nanoemulsions find applications in the food industry as flavoring, coloring, nutraceutical, or preservative agents.[53] They offer advantages as drug delivery systems, skincare materials, or food additives due to their cost-effectiveness, improved drug bioavailability, physical stability, and nontoxic nature.[60] However, they may be thermodynamically unstable, requiring surfactants, and can be influenced by environmental factors like pH and temperature, making them less suitable for clinical applications compared to other types of lipid nanoparticles.[61]

MD simulations are commonly used to explore the dynamic behavior, interactions, and stability of nanoemulsions at molecular levels under different conditions. For instance, Pirhadi and Amani used the MD simulations to study a siRNA-loaded nanoemulsion with benzakonium chloride as a surfactant, cyclohexane as the oil phase, and ethanol as the cosurfactant.[62] MD simulations revealed oil molecules in the hydrophobic core, increasing the nanoemulsion size, while benzalkonium chloride's polar terminal groups were mainly on the surface. In another study, MD simulations were used to predict the interactions between polymeric surfactant and seven different hydrophobic drugs within nanoemulsions for improved drug solubilization and stability.[63] Besides MD simulations, mesoscale simulations, like dissipative particle dynamics, extend the scope to study larger scales and timeframes, providing a comprehensive understanding of nanoemulsion systems' collective behavior and stability.[64] In summary, these simulations aid in developing efficient and stable nanoemulsion formulations for drug delivery, cosmetics, and food technology.[65]

3.3. Solid Lipid Nanoparticles

Solid lipid nanoparticles (SLNs) were initially formulated as small spherical particles with a solid lipid core at room temperature, and subsequent advancements have led to the development of flat ellipsoidal or disc-like shapes, exhibiting sizes between 50 and 100 nm.[18,66,67] Within SLNs, the active

substance can be added to the lipid core or lipid shell or dispersed within the whole lipid matrix. The solid lipid core of SLNs is a new method to improve particle stability compared to liposomes.[68] The incorporation of cationic lipids into SLN shell formulations can enhance cellular internalization of the particles, potentially improving tumor targeting, blood-brain barrier penetration, and gene transfection efficiency.[69] Additionally, the outer shell of SLNs can be modified with macromolecules such as oligosaccharides, proteins, specific ligands, and antibodies to enhance their specificity at desired therapeutic sites.[70−73]

SLNs carrying several therapeutic agents including antioxidants, anticancer agents, nucleic acids, antibiotics, cytokines, and other hydrophobic drugs have currently been examined in clinical trials[69] (Table 1). Additional research is needed to comprehensively investigate the therapeutic capabilities of SLNs as drug carriers.

Using computational modeling, specifically MD simulations, offers valuable insights into the physicochemical properties and behavior of SLNs at the molecular level.[74] These simulations explore the dynamic behavior and interactions of lipid molecules within SLNs, shedding light on their stability, structural changes, and drug encapsulation efficiency under various conditions.[75] MD simulations were employed to investigate the structure and conformational differences of tripalmitin SLNs and the morphology of SLN.[76] Additionally, docking simulations were utilized to predict the loading of therapeutic agents into the SLN core. These computational modeling methods offer advantages in optimizing SLN formulations for specific applications by predicting drug release profiles, biodistribution, and cellular uptake.

From the pharmaceutical aspect, SLNs have both advantages and disadvantages compared to other types of drug carriers. SLNs offer several technical advantages such as drug protection from chemical and enzymatic degradation, improved physical stability, ease of scale-up production, omission of the need for organic solvents, ease of sterilization process, and ability to codelivery two active agents.[68,77−79] They also have great potential for various routes of administration.[80] This material also has reputation for being biodegradable and biocompatible.[81]

However, SLNs are facing the main technological issues of limited drug loading efficiency, short shelf life due to cold storage requirements, poor long-term drug retention, low drug loading capacity, polydispersity, and high operative temperature.[69,82,83] Indeed, specific values for these parameters can vary significantly depending on various factors, including formulation composition, lipid type, encapsulated drug, storage conditions, and intended application. For instance, the entrapment efficiency of Pomegranate extract within SLN has been reported within only 25.15−63.5%.[84] Therefore, researchers and manufacturers must carefully optimize these parameters to address the challenges and ensure the stability and efficacy of SLNs for specific applications.

3.4. Nanostructured Lipid Carriers

As mentioned earlier, solid lipid nanoparticles (SLNs) have a key weakness in limited drug loading capacity.[124] To address this challenge, researchers have introduced the second generation of SLNs, known as nanostructured lipid carriers (NLCs), which incorporate both solid and liquid lipids in their cores, resulting in a more disordered lipid structure. This structural characteristic allows for higher drug loading capacity and improved drug release kinetics compared to SLNs.[125,126] The ratio between solid lipid (e.g., cetyl palmitate), liquid oil (e.g., caprylic triglyceride), and surfactant (e.g., polysorbate 80) plays a critical role in determining the entrapment efficiency and stability of therapeutic agents in vivo.[127] NLCs can be modified with ligands or polymers for targeted delivery of hydrophilic and hydrophobic drugs.[79] As efficient carriers, RNA- and pDNA-loaded NLCs enable gene therapy and personalized medicine, modulating gene expression, and delivering therapeutic proteins. These lipid-based nanoparticles offer versatile platforms for nucleic-acid−based therapies to treat genetic diseases and cancers.

MD simulations offer valuable insights into the physicochemical properties and behavior of NLCs.[74] For instance, the self-assembly behavior of mixed NLC systems containing Rhodamine, Miglyol 812, Tween 80, and Gelucire 44/14 was investigated by using MD simulations.[128] The results demonstrated that raising the temperature to 358 K improved the stability of the NLCs, leading to enhanced component compaction. Furthermore, this study has shown that adding oil to the lipid formulation creates an imperfect core, effectively increasing the drug loading capacity of the NLCs.

NLCs offer advantages over other LNP formulations such as improved drug-loading capacity, controlled release, and enhanced stability for drug delivery.[129,126] They are biocompatible and biodegradable, making them ideal drug carriers. NLCs have shown promise in increasing oral drug availability and have been studied in clinical trials for various pharmaceuticals, including COVID-19 mRNA vaccines, anticancer agents, antioxidants, and antiviral agents[127,130−132] (Table 1). They also hold potential for gene therapy, chemotherapy, and applications in the food and cosmetic industry.[133] However, challenges like low drug loading efficiency and particle stability may affect their drug-delivery effectiveness.[129] Further research is required to tackle these challenges and unlock the full potential of NLCs in therapeutic and biomedical applications.

3.5. Lipid Polymer Hybrid Nanoparticles

Lipid polymer hybrid nanoparticles (LPNs) are another major type of lipid nanoparticle that combines the advantages of lipids and polymers for various biomedical applications.[117] LPNs have polymer cores that contain therapeutic substances and lipid/lipid-PEG shells as a "stealth" coating for improved in vivo circulation.[134] This unique structural composition offers optimal biocompatibility and physical stability, making them an ideal vehicle for drug delivery.[117] LPNs have been successfully used to encapsulate various pharmaceuticals, including nucleic acids, for sustained release and improved stability. Furthermore, incorporating functional groups on the polymer surface facilitates the targeted drug delivery to specific cells or tissues.

Density functional theory (DFT) simulations, one of the computational modeling methods, were utilized to gain a better understanding of the interaction mechanism between the anticancer drug doxorubicin (DOX) and the polymers within LNPs.[135] The study aimed to improve the therapeutic efficacy of doxorubicin (DOX) in lipid nanoparticles (LPNs). By analysis of the DOX-loaded LPNs, researchers found that polymers interacted strongly with DOX at various sites, forming stable complexes. The simulations indicated energetically favorable binding, suggesting a potential for enhancing oral bioavailability.
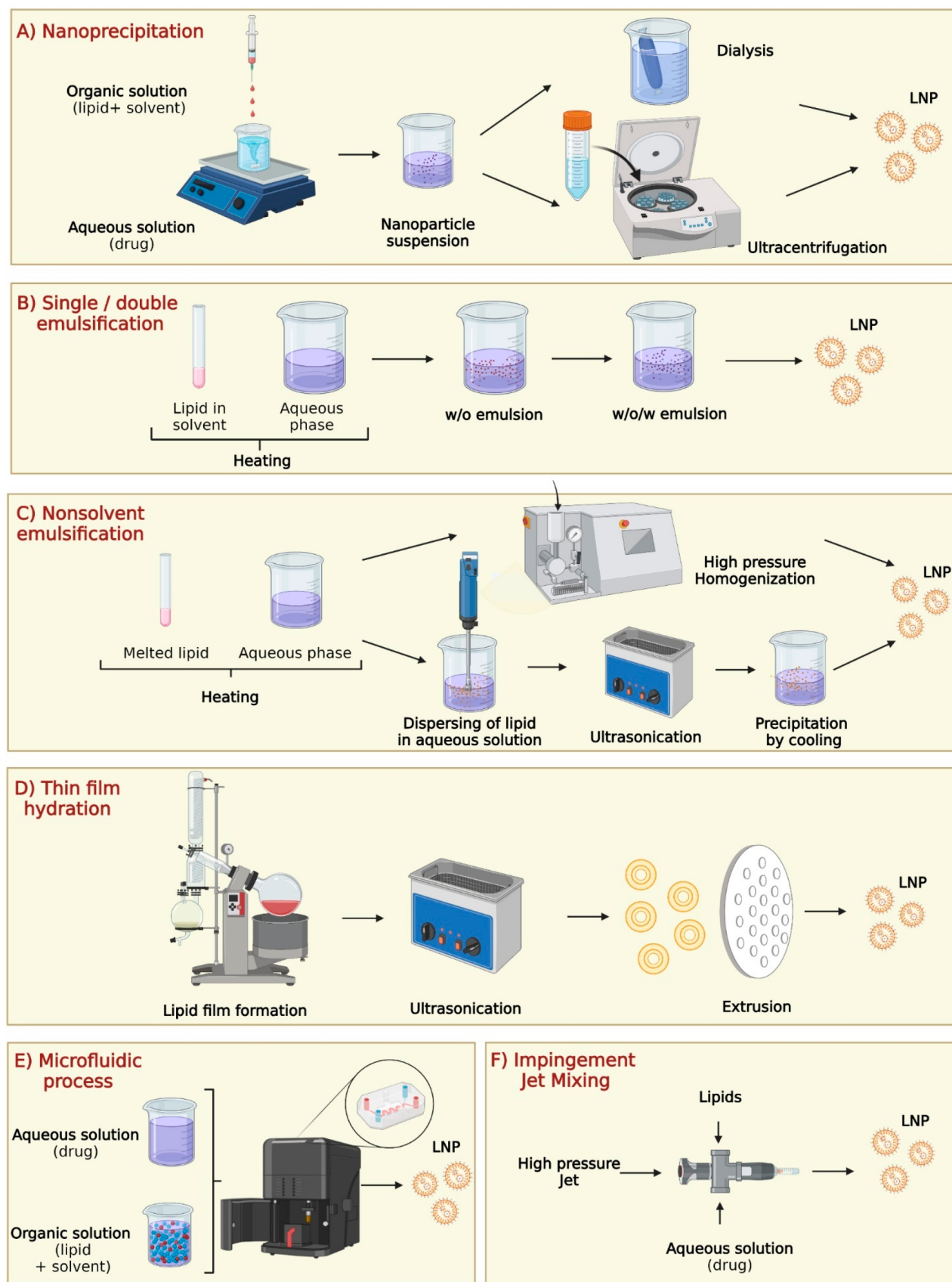
Figure 3. LNP synthesis processes in laboratory and industry environments: (A) Nanoprecipitation, (B) single/double emulsification, (C) nonsolvent emulsification, (D) thin film hydration, (E) microfluidic process, and (F) impingement jet mixer. Created with BioRender.com.

LPNs are gaining recognition as an advanced substitute for traditional liposomal and polymeric drug delivery systems due to their wide range of advantages, encompassing applications in combinatorial/active targeted drug deliveries, cancer gene therapy, vaccine development, and novel diagnostic imaging methods.[136] Encouraging results from Phase I and II clinical trials demonstrate the potential of LPNs in delivering the anticancer drug Docetaxel, particularly for lung, pancreatic, and prostate cancers[120−123] (Table 1). Nevertheless, LPNs encounter certain challenges, such as potential polymer component toxicity and difficulties in achieving consistent particle size and shape.[18] Ongoing research endeavors aim to address these obstacles and further advance LPNs for use in diverse biomedical applications. Despite the challenges, LPNs exhibit great promise for drug delivery due to their distinctive properties and versatility in addressing various biomedical needs.

4. LNP SYNTHESIS METHODS

Nanoparticle synthesis typically involves two methods: bottom-up and top-down approaches. The bottom-up approach nucleates atomic-sized materials into nanoparticles using gas phase synthesis, block copolymer synthesis, Turkeyvich method, and microbial synthesis.[135,136] The top-down approach physically dismantles bulk materials into nanosized fragments using milling, spark ablation, and laser ablation.[72] For LNPs, the synthesis primarily follows a wet chemistry bottom-up approach due to their distinctive colloidal structure.[137] This section provides an overview of the main LNP synthesis methods, including nanoprecipitation, single/double emulsification, nonsolvent emulsification, thin film hydration, microfluidic process, and impingement jet mixing technology[137] (Figure 3).

The choice of the LNP synthesis method plays a crucial role in determining their therapeutic applications, as it directly influences their physicochemical properties, drug loading efficiency, stability, and behavior in vivo. Each LNP synthesis method yields nanoparticles with distinct characteristics that directly impact their performance in various therapeutic applications.[137]

4.1. Nanoprecipitation

The nanoprecipitation method was first developed by Fessi et al. in 1989 and has been mainly used for encapsulating hydrophobic drugs (Figure 3A).[21] This technique relies on a precipitation mechanism, wherein two miscible solvents, the organic phase and aqueous phase, are continuously mixed under moderate magnetic stirring to facilitate the spontaneous formation of LNPs. The organic phase consists of film-forming polymers, drug molecules, polymers, lipophilic surfactants, and organic solvents, while the aqueous phase contains water and stabilizer.[134] The polymers utilized for LNP production can fall into two categories: nonbiodegradable, such as Eudragit, and biodegradable, such as polylactide (PLA), polylactide-*co*-glycolide (PLGA), and poly-*ε*-caprolactone (PCL).[138−141]

After particle formation, the organic solvent is removed from the formulation using methods like dialysis, ultracentrifugation, rotary evaporation, and freeze-drying.[143] Dialysis, the most popular method for solvent removal, involves placing the LNP formulation in a dialysis bag or tubing with a semipermeable membrane, allowing the solvent to diffuse out into a buffer solution until desired solvent removal level is achieved.[144] Ultracentrifugation uses high centrifugal forces to pellet LNPs based on size and density, leaving free lipids and unincorporated drugs in the supernatant.[145] Rotary evaporation evaporates the solvent under reduced pressure and elevated temperatures, collecting the solvent separately and leaving behind a concentrated LNP suspension.[146] Freeze-drying freezes the LNP suspension and removes the solvent through sublimation under vacuum, resulting in a dry, solid LNP powder.[147] These methods are crucial for LNP formulation development, ensuring highly concentrated and purified LNPs for diverse biomedical applications.

The size and drug encapsulation efficiency of LNPs prepared by nanoprecipitation can be significantly affected by various parameters, such as the stirring rate, aqueous/organic phase ratio, and concentration of lipid/surfactant/drug.[21] The formation of inhomogeneous and incomplete saturated lipid solutions may interfere with spontaneous nucleation during small particle formation, resulting in varied LNP sizes.[21,142] Additionally, incomplete mixing of aqueous and organic solutions before precipitation can lead to unevenly small LNP sizes.[143] Therefore, it is crucial to thoroughly characterize the size and surface morphology of the produced LNPs before any testing or application.

Incomplete mixing during nanoprecipitation is a critical challenge that contributes to batch-to-batch variation and compromises the overall quality of the LNPs.[144] To overcome these issues, careful optimization of the mixing process is essential. By controlling crucial mixing parameters such as speed, duration, and solvent ratio, it is possible to achieve better homogenization of lipids and drug molecules.[142] This fine-tuning ensures a more uniform distribution, resulting in consistent and efficient LNP formulations across different batches. Addressing these challenges in nanoprecipitation is vital to enhance the reproducibility and quality of LNPs, making them more suitable for large-scale production and expanding their potential in various therapeutic applications.[144]

4.2. Single/Double Emulsification

The single oil/water solvent emulsification method, invented by Gasko, is a commonly used technique for preparing LNPs carrying hydrophobic drugs (Figure 3B).[145] It involves low melting lipids like stearic acid and Compritol 888 ATO, surfactants such as Epikuron 200 and Tween 80, emulsifiers like polysorbate 20 and polysorbate 600, and water.[146] The solvent mixture is preheated, water is added, and then the mixture is emulsified to create oil-in-water emulsions. These emulsions are transferred to cold water with continuous stirring for LNP crystallization.

Another approach to synthesizing LNPs is the solvent-based emulsification method, which can be achieved through emulsion-solvent evaporation, solvent diffusion, solvent displacement, or solvent injection.[147]

In this method, lipids and poorly water-soluble drugs are dissolved in an organic solvent and emulsified with an aqueous solution to create oil-in-water emulsions. The emulsion is then evaporated under agitation to remove the organic solvent, followed by centrifugation. However, residual solvent toxicity can be a concern, especially if the lipid solubility in the solvent remains low.[27]

The double emulsification technique is developed for preparing hydrophilic-loaded LNPs. In this method, an aqueous solution is emulsified in melted lipid solvents to create a primary water-in-oil (w/o) emulsion. Next, the primary oil-in-water (o/w) emulsion is dispersed as droplets
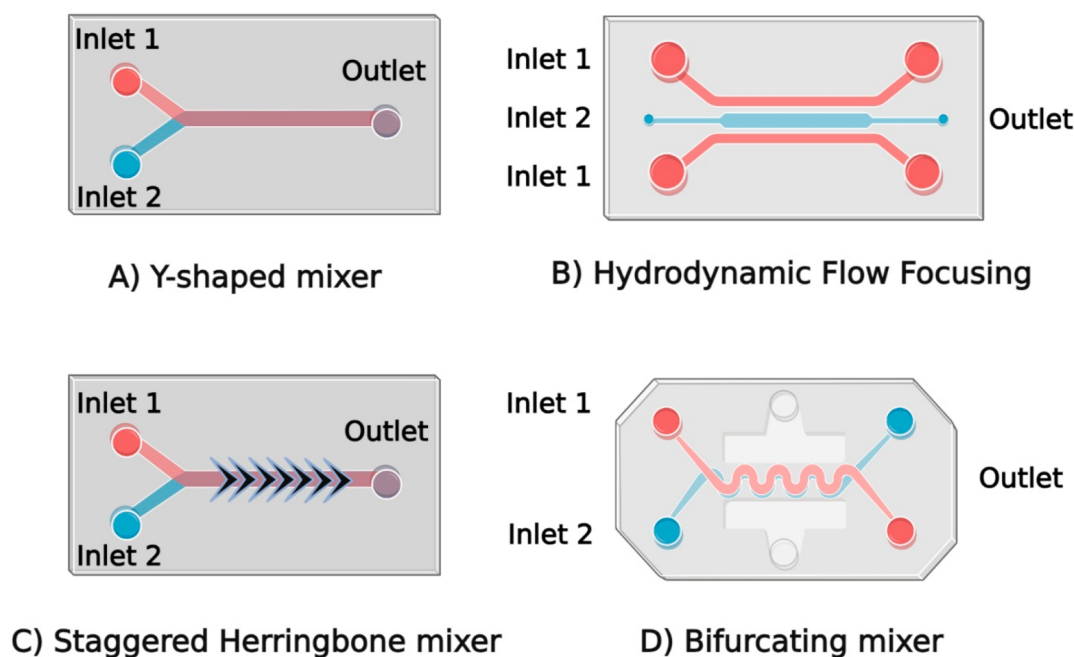
Figure 4. Different designs of microchips used in microfluidic devices: (A) Y-shaped mixer, (B) hydrodynamic flow focusing, (C) staggered herringbone mixer, and (D) bifurcating mixer. Created with BioRender.com.

in another aqueous solution containing a hydrophilic emulsifier, resulting in the formation of a double water-in-oil-in-water (w/o/w) emulsion using either sonication or membrane emulsification.[148] Typically, two surfactants are used in this process: one hydrophobic surfactant to stabilize the interface of the water-in-oil (w/o) internal emulsion and one hydrophilic surfactant for the external interface of the oil globules. Microemulsion methods can produce LNPs loaded with various drug compounds, such as Baclofen, Idarubicin, Ketoprofen, Nevirapine, and Tobramycin.[2,149]

Although the emulsification technique offers the advantage of low mechanical energy input, it also has several drawbacks, including a low dispersing degree, emulsion instability, lipid insolubility in organic solvents, and the need for additional solvent removal procedures.[150,151] In line with LNPs prepared using nanoprecipitation and microfluidic methods, it is crucial to incorporate a solvent removal step in the synthesis process to mitigate the potential toxicity associated with any residual solvents in the produced LNPs.[152]

4.3. Nonsolvent Emulsification

Nonsolvent emulsification techniques offer a solvent-free approach to create oil-in-water emulsions using melted lipids as the liquid phase (Figure 3C).[142] High-pressure homogenization and ultrasonication are commonly used methods for this purpose. In the homogenization process, melted lipids are mixed with drugs and a preheated aqueous phase containing surfactants. The mixture undergoes high-pressure homogenization for several cycles to achieve the desired nanoparticle size.[153,154] Alternatively, ultrasonication involves homogenizing the aqueous phase with surfactants and melted lipids using high-speed stirring, followed by ultrasonication to break down large particles into smaller droplets.[155]

However, the nonsolvent emulsification technique involves complex procedures and multistep processes, leading to a potential batch-to-batch variation. Variations in homogenization/sonication time, lipid surfactant ratio, drug concentra-

tions, and lipid/surfactant type can result in different particle sizes, polydispersion indices, zeta potential, and drug entrapment efficiency in the lipid nanoparticles, leading to variable product outcomes.[156,157] To ensure consistent product quality, the careful optimization of these parameters is essential.

4.4. Thin Film Hydration

Thin film hydration is a widely used method in both laboratory and industrial settings for producing lipid nanoparticles (Figure 3D). In this process, lipids are dissolved and mixed in an organic solvent to achieve homogeneity, and then the solvent is removed through rotary evaporation, forming a thin lipid film on the flask's sides.[146] After hydrating the lipid suspension, it is passed through a filter with uniform pore sizes several times, resulting in uniform-sized lipid nanoparticles.[146] Various parameters, such as applied pressure, temperatures, membrane pore size, extrusion force, and the number of cycles, can affect the mean size and polydispersity of the nanoparticles produced.[2] The extrusion process is favored due to its lower energy requirements, reduced risk of contamination, and narrower particle size distribution achieved with consistent filters. Industry-utilized extruders like LIPEX and LiposoFast LF-50 have successfully produced liposomes with diverse payloads, including proteins, peptides, small molecules, and larger molecules.[93]

4.5. Microfluidic Process

The microfluidic process is widely acknowledged as a highly successful method for the industrial production of diverse lipid nanoparticles.[158] This method is fundamentally based on nanoprecipitation due to the precisely controlled mixing of lipid and drug solutions in microchannels.[159] The rapid mixing at the microscale in microfluidic devices enables more uniform and reproducible nanoparticle formation compared with traditional bulk mixing methods. Additionally, the small dimensions of microfluidic channels offer advantages in terms of heat and mass transfer, resulting in improved size control and homogeneity of LNPs.[160] The microfluidic

approach allows for precise tuning of formulation process parameters, such as flow rates, concentrations, and mixing ratios, to optimize LNP characteristics.[159] By controlling these parameters, researchers can tailor the size, drug loading capacity, and stability of LNPs for specific therapeutic applications.

In a microfluidic device, lipid fluids are controlled in microchannels with dimensions in the tens of microns.[96] There are two primary types of microfluidic devices used for producing LNPs: chip-based platforms, which involve the controlled mixing of organic and aqueous solvents within a specifically designed chip, and capillary-based platforms, where the organic solvent is introduced through a central tube surrounded by multiple tubes for rapid dilution with the exiting aqueous solution.[161]

In the upcoming section, our focus will be on chip-based mixers, which utilize diverse micromixer designs to produce LNPs (Figure 4).

4.5.1. T- or Y-Mixer. Chip-based platforms use a variety of microchannel designs for LNP production. The flat microchannel, which contains T- and Y-shaped microchannels, is the earliest and simplest microchip to produce LNPs (Figure 4A). Upon introducing the lipid and buffer solutions at the inlets, LNPs form at the liquid interface through molecular diffusion-based organic solvent dilution.[161,162] T- or Y-shaped mixing is a rapid mixing method requiring high flow rates (40 to 60 mL/min) to produce high volumes of LNPs (>100 μL).[163] Although this flat microchannel method offers high throughput and straightforward device fabrication, it faces challenges in scaling down to the small volumes required for discovery experiments. Additionally, the limited control over LNP size, ranging from 30 to 250 nm, may not produce the ideal LNPs.[161]

To address the limitations in throughput volume and LNP size control, alternative mixer devices have been explored for LNP preparation.

4.5.2. Hydrodynamic Flow Focusing. Hydrodynamic flow focusing (HFF) is one of the most used micromixer designs (Figure 4B). HFF devices have 2D and 3D structures, where the former belongs to chip-based platforms and the latter is a capillary-based platform.[144] For the 2D HFF, fluids are injected simultaneously via three inlets. The organic phase containing the precursor ingredients of the nanoparticles is introduced to the central stream, and the aqueous phase streams squeeze the central channel perpendicular and create a narrowly focused stream, generating rapid diffusion-based mixing.[144,164] In a 2D HFF, the laminar flow condition develops interfacial force. Small-size LNPs (<150 nm) are produced by adjusting operating parameters which could influence the interface of the aqueous and organic phases.[1,3] A comparison study demonstrated that an HFF device could generate small siRNA-LNPs with an average size of 38 nm. The 20% enhanced encapsulation efficiency with gene silencing *in vitro* has been shown compared to vortex mixing.[6] However, the low throughput (<10 mL/h) limits the application of 2D HFF, and the lipid aggregation happening at the wall of the microfluidic channel affects the particle size control and results in channel blocking.[4,165]

To further investigate the HFF, a 3D HFF was developed by DeVoe's group.[166] This multicapillary-arrayed device contains seven small capillary arrays embedded in one larger capillary where the lipid stream inlet was in the middle, and an aqueous solution was injected into the outer channel. This 3D HFF can produce consistently uniformed liposomes with four-time increase in throughput compared to the conventional 2D HFF.[166] However, the main drawback of this multicapillary arrayed 3D HFF device is the complicated manufacturing operation with costly equipment.[167] Meanwhile, when forming the smallest LNPs using the HFF technique, the high flow rate ratio will dilute the sample concentration, which may affect the following *in vivo* experiment.[163] Those issues limit the application of HFF; thus, this mixer is not extensively used as other microfluidic devices.

4.5.3. Staggered Herringbone Micromixer. Several passive mixers have been reported to enhance production efficiency by increasing the contact area between the aqueous and solvent phases.[4] One such mixer is the staggered herringbone micromixer (SHM), featuring an asymmetric herringbone groove pattern in microchannel (Figure 4C).[139] The herringbone structure disrupts the laminar flow, leading to chaotic advection and rapid, controlled mixing (<10 ms) to form homogeneous and small LNPs (30 nm) with high reproducibility.[4,144,163] However, the low throughput of the SHM (<100 mL/h) limits its full clinical potential as the demand for LNPs in clinical applications grows, making it a significant bottleneck in scaling up LNP production for large-scale therapeutic use.[165]

We introduce the groundbreaking parallelized microfluidic device (PMD), a revolutionary system that ushers in a new era of scalable LNP production. From the early discovery phase with milliliter per hour rates to the clinically relevant milliliter per hour rates, the PMD offers an impressive 100-fold enhancement over single microfluidic channels, addressing the pressing need for efficient and versatile manufacturing processes in the field of LNP synthesis. With ladder geometry and SHM mixing channels (1×, 10×, and 128×), the PMD enables precise scalability.[165] Additionally, individual flow resistors ensure uniform fluid distribution, enhancing formulation consistency.[165] Validation studies confirm remarkable therapeutic potential, surpassing conventional bulk mixing methods in *in vivo* siRNA and mRNA delivery. The success of the SHM led to NanoAssemblr platforms, offering user-friendly and rapid solutions for scalable LNP production, advancing nanomedicine for clinical applications.[168]

4.5.4. Bifurcating Mixer. The NxGen™ mixer by NanoAssemblr is a groundbreaking advancement designed for the large-scale production of LNPs.[169] It overcomes LNP scale-up reproducibility challenges, achieving over 25 times the throughput of the classic mixer without compromising identical particle formation conditions, ensuring highly reproducible outcomes across various particle types. Its innovative chip design features numerous bifurcating mixers, inducing chaotic flow and rapid mixing, enabling LNP production at exceptional rates of up to 200 mL/min while maintaining LNP encapsulation rate and polydispersity control (Figure 4D).

The NxGen mixer promises rapid and efficient large-scale LNP manufacturing. It is indispensable for researchers and pharmaceutical companies seeking scalable, high-throughput LNP production, advancing therapeutic developments, and personalized medicine. This mixer revolutionizes LNP formulation, bridging the gap from the laboratory to real-world clinical applications.[4]

4.6. Impingement Jet Mixer

Impingement jet mixing (IJM), also referred to as the tea stirrer, is an innovative microfluidic mixing technique for the small-scale production of mRNA-LNPs[170] (Figure 3F). It is a device that creates a high-velocity stream of fluid being directed toward another stream of fluid, resulting in intense mixing and shearing forces that can effectively homogenize the two fluids.[171] To produce LNPs, the IJM is first used to mix lipids with an aqueous solution containing the drug or therapeutic agent of interest. The high-pressure jet forces the lipids to form small droplets that are then stabilized by surfactants, resulting in the formation of LNPs. The size and properties of the resulting nanoparticles can be controlled by adjusting the processing parameters of the mixer such as the pressure and flow rate of the fluids.

Starting from the small size of the confined IJM, the IJM can be easily scaled up based on the original design, making it a valuable tool in pharmaceutical manufacturing, particularly during pandemics such as COVID-19. IJM systems have been widely used for mRNA-COVID-19 vaccine production by several companies, such as Knauer and Pfizer. At Knauer, the IJM system utilizes 400 pounds of pressure to combine a lipid solvent solution with an mRNA solution, effectively forcing the fluids to mix.[172] Pfizer successfully replicated the quarter-sized mixers and implemented a parallelization of 100 static mixers, enabling continuous synthesis and significantly increasing vaccine productivity at the Kalamazoo site to 100 million doses per month.[173] To automate the process, a computer system was implemented to control the flow rate and pressure. Overall, IJM is a powerful tool for producing uniform and stable LNPs for drug delivery applications.

4.7. Scaling-Up LNP Production by Microfluidic Devices

Microfluidic technologies can be utilized to achieve the scaled-up production of LNPs for industrial applications. To achieve this purpose, in microfluidic systems, strategies like pilling-up, numbering-up, or parallelization of microfluidic devices are employed.[162]

Pilling-up involves stacking multiple microfluidic devices in series, increasing throughput and production capacity, which enhances overall production efficiency.[110] Numbering-up, on the other hand, entails running multiple identical microfluidic devices in parallel, multiplying the production rate and enabling higher LNP yields within the same time frame.[110] Parallelization takes the integration of multiple microfluidic devices, optimized for specific LNP synthesis steps, into a single production platform, resulting in a streamlined workflow and improved overall LNP production.[110] For example, a research group introduced iLiNP (invasive lipid nanoparticle production device), a microfluidic device comprising five-layered microchannels created by stacking glass-iLiNP devices and later parallelized (numbering-up) to achieve mass LNP production. The iLiNP system efficiently produces LNPs in the size range of 20 to 60 nm at a flow rate of 20−50 mL/min, demonstrating comparable performance to commercially available microfluidic systems like NanoAssemblr.[111]

By implementing these strategies, researchers and industry can overcome the limitations of single microfluidic devices and achieve significant scale-up improvements in LNP production, making them more viable for large-scale applications.

5. MAIN CHALLENGES ASSOCIATED WITH THE INDUSTRIAL DEVELOPMENT OF LNPs

LNPs have shown immense promise as therapeutic nano-carriers, creating high demand across diverse fields, especially in the pharmaceutical industry. Nevertheless, traditional manufacturing approaches pose significant challenges in scaling up nanomedicine production, limiting their clinical development.[27] Furthermore, the substantial costs associated with commercial manufacturing act as a recognized barrier, hindering the smooth transition from bench research to clinical application.[27]

In this section, we will delve into the primary challenges associated with the industrial production of LNPs, encompassing aspects such as stability, sterilization, storage, regulatory compliance, and quality control of synthesized LNPs.

5.1. Stability and Sterilization

Stability is a crucial requirement in the industrial production of LNP formulations, and it can be influenced by lipid polymorphism, which refers to phase transformations.[113,174] Different methods and lipid types used in LNPs can lead to polymorphism, potentially compromising their stability.[175] For instance, exposure to radiation and high temperatures can trigger lipid polymorphism, resulting in LNP instability.[27] Polymorphism has been observed in triglycerides and fatty acids prepared using the hot homogenization method.[175]

During preparation or storage, triglycerides in LNPs may convert from their α-form to the more stable β-form, leading to the formation of polymorphic crystalline aggregates and reduced amorphous zones in the carrier matrix, which can result in drug leakage.[176] The kinetics of triglyceride polymorphic transitions depend on chain length, with longer-chain triglycerides crystallizing more slowly than shorter-chain ones.[177] As a result, LNP formulations composed of long-chain triglycerides tend to be more stable than those containing short-chain triglycerides. Proper consideration of lipid polymorphism is vital for achieving stable LNP formulations during industrial production.

Sterilizing LNPs during industrial production poses a significant challenge due to potential destabilization caused by conventional methods.[116] For instance, γ radiation commonly used for sterilization can lead to lipid oxidation and chain scission, affecting LNP stability and efficacy.[178] Autoclaving may trigger phase transitions and thermal stress, further destabilizing LNPs.[179] Filtration and aseptic processing may cause aggregation or deformation due to shear stress.[180] To address this, alternative sterilization methods like UV irradiation, ethylene oxide sterilization, and mild sterile filtration have been explored.[121] However, each method has limitations and requires careful optimization for each LNP formulation. Thus, selecting an appropriate sterilization method remains critical for ensuring the stability and efficacy of LNPs during industrial production.

5.2. Storage

Industrial production of LNPs poses significant challenges due to their inherent instability and susceptibility to physical and chemical changes during storage. These alterations can have adverse effects on drug encapsulation, release properties, and overall stability, leading to issues like aggregation, changes in particle size distribution, drug leakage, and decreased stability.[27] Additionally, lipid oxidation during storage can impact particle surface charge, drug release properties, and

Table 2. Toxicity of LNP-Based Marketed Drugs

Marketed formulation	active drug	toxicity symptoms	ref
Doxil	doxorubicin	hand-foot syndrome, stomatitis, skin toxicity (facial swelling, itching), hypersensitivity reactions, mild myelosuppression and alopecia, dyspnea	200−202
Myocet	doxorubicin	neutropenia, mild cardiotoxic	203
Abelcet, Amphotec, AmBisome	amphotericin B	nephrotoxicity, hypersensitivity reactions such as rash, flushing, facial edema, bronchospasm, persistent fever and rigors, hypokalemia	204−206
Linhaliq/Pulmaquin	ciprofloxacin	dyspnea, bronchospasm, hemoptysis, cough, taste disorders.	207
Daunoxome	daunorubicin	hematological toxicity such as neutropenia, back pain	208, 209
Visudyne	verteporfin	back pain, chest pain, dyspnea, dizziness, rash	210
Arikace	amikacin	ototoxicity including deafness, dizziness, vertigo, dysphonia, pneumonitis, laryngitis	211, 212
Ambraxane	paclitaxel	neutropenia, hypersensitivity reactions, neuropathy, severe myelosuppression	213

stability, potentially resulting in the formation of toxic byproducts that can compromise therapeutic efficacy.[122]

Moreover, interactions with container materials, such as leaching of ions, absorption of surfactants, and changes in pH, can further influence LNP stability.[181] Due to these issues, most LNP formulations have a relatively short shelf life of less than one year.[182] Efforts to overcome these obstacles and extend the shelf life of LNPs are essential for successful commercialization and widespread clinical use of these promising nanocarriers.

To tackle these challenges, several strategies have been devised, encompassing lyophilization, incorporation of stabilizing agents like antioxidants or chelators to prevent oxidation and aggregation, utilization of excipients as buffers, osmolytes, or cryoprotectants, and specialized packaging materials to prevent container interactions.[181,183] Freezing and lyophilization are commonly used techniques for long-term storage of lipid-based formulations.[184,185] However, lyophilization can be costly and time-consuming, potentially leading to drug damage due to stresses from crystallization and vacuum dehydration, thereby compromising LNP stability unless cryoprotectants are included.[186,187]

Studies have shown that incorporating 5% (w/v) sucrose or trehalose (cryoprotectants) in LNP-mRNA formulations stored in liquid nitrogen can preserve mRNA in vivo efficacy for up to 3 months.[187] Pfizer's COVID-19 mRNA vaccines are stored in freezing conditions with added sucrose, and Moderna uses Tris-HCl buffer as a hydroxyl radical scavenger, providing additional stabilization for LNP-based mRNA vaccines.[188,189] Implementing these strategies holds promise in extending the LNP shelf life and enhancing the stability of LNPs, thereby advancing their successful utilization in various therapeutic applications.

Existing LNP-formulated drugs often necessitate ultracold storage temperatures.[190] For instance, during the COVID-19 pandemic, mRNA-LNP vaccines like Comirnaty (BNT162b2) and Spikevax (mRNA-1273) require storage at ultracold temperatures (−80 and −20 °C, respectively) to ensure their safety and efficacy as per regulatory guidelines.[182] Consequently, the distribution and storage of these vaccines require advanced packaging technologies and specialized containers capable of withstanding ultralow temperatures and minimizing breakage during transportation.[191]

To address these challenges, Corning researchers have introduced Valor glass vials specifically designed for delivering LNP-based mRNA vaccines.[192] Valor glass vials are made from aluminosilicate glass, providing superior strength and resistance to breakages, even in extremely cold conditions. These vials are produced using the ion exchange method, reducing cracks, breakage, and particulate contamination, while an inner coating diminishes friction and aesthetic flaws. These vials comply with USP Type I hydrolytic criteria and exhibit low extractable concentrations, ensuring a high product quality.

Moreover, SiO2Materials Science, a U.S.-based pharmaceutical company, has developed a novel container for LNP-mRNA vaccine storage. This SiO_2 primary container combines a cyclic olefin polymer with nanolayer glass as the inner layer, achieved through plasma-enhanced chemical vapor deposition. This innovative SiO_2 vial demonstrates exceptional resistance to physical, thermal, and chemical stress over its lifespan, eliminating concerns of breakage or leakage.[193]

In conclusion, optimizing the long-term storage of LNPs requires careful consideration and fine-tuning of storage conditions and packaging to ensure their enduring stability and effectiveness.[190,194] Moreover, special attention should be devoted to shelf life during formulation design to facilitate the widespread use of LNP products, such as mRNA-LNP vaccines.[184] While challenges related to LNP storage persist, ongoing research and innovation are essential to surmounting these hurdles and making LNP-formulated drugs more accessible and efficacious.

Conclusively, to improve the long-term storage of LNPs, careful consideration and optimization of storage conditions and packaging are required to ensure their stability and efficacy.[80,180] Additionally, more attention should be given to shelf life in formulation design to facilitate large-scale use of LNP products such as mRNA-LNP vaccines.[182,194] While challenges associated with LNP storage remain, continued research and innovation are necessary to overcome these obstacles and make LNP-formulated drugs more accessible and effective.

5.3. Regulatory Compliance

In addition to the challenges in research and development, it is anticipated that the regulatory approval process can pose an additional barrier for unfeasible LNP-based technologies, especially considering the diverse range of compounds that can be delivered by LNPs.[195] Regulatory bodies such as the Food and Drug Administration (FDA) and European Medicines Agency (EMA) require LNPs to meet quality, safety, and efficacy standards before approval.[196] During the preclinical development stage, cell and animal studies are conducted to evaluate the toxicological effects of the LNP formulation. If considered safe, then approval (via an FDA "Investigational New Drug" or EMA 'European Investigational Medicinal Product Dossier' form) is required to begin phase 1 clinical trial. This meticulous regulatory scrutiny ensures the safety and effectiveness of LNPs in therapeutic applications.

To ensure regulatory compliance, toxicology evaluations play a crucial role, particularly concerning LNPs, as their

accumulation in healthy tissues can lead to cytotoxicity and genotoxicity (Table 2). This may be due to the cationic lipid components utilized in LNP formulations. For instance, first-generation monoalkyl cationic lipid, stearyl amine, has been shown to cause hemolysis and hemagglutination of human erythrocytes.[81] Another commonly used cationic lipid, DOTAP, has the propensity to bind to serum proteins, lipoproteins, and the extracellular matrix, leading to aggregation or premature drug release.[197,198] Similarly, LNPs containing YSK05, a pH-sensitive cationic lipid used for delivering short interfering RNA (siRNA), exhibited rapid interactions with cell surfaces, leading to concentration-dependent toxicity in human A375 and A375-SM melanoma cell lines.[199] Addressing these toxicological concerns is vital for the safe and effective use of LNPs in therapeutic applications.

Following government approval for clinical use, LNP-based drugs undergo comprehensive testing in clinical trial phases 1−3.[214] These trials involve evaluation in healthy individuals, patients with the target disease, and a larger population, with additional approvals needed between phases 2 and 3. Throughout each stage, the regulatory agency thoroughly assesses safety and efficacy data, potential side effects, dosing regimen, and overall safety profile to make informed decisions on authorizing the drug for commercial use. These rigorous evaluations ensure that LNP-based drugs meet the highest standards of safety and effectiveness before they become available for widespread clinical application.

Adhering to government regulatory standards is crucial to ensure patient safety and enable the therapeutic application of LNP-based drugs.[195] In certain situations, approval can be expedited, as seen during the rapid authorization of LNP-formulated mRNA vaccines amidst the SARS-CoV-2 health emergency.[215] Additionally, large pharmaceutical companies hold an advantage in the LNP field, leveraging prior regulatory approvals and successful R&D pipelines.[216] However, the typical FDA and EMA approval process for new drugs takes around 6−9 months, considering the FDA's requirement to approve or reject a drug within 10 months after phase 3 trial completion. Consequently, staggered approval of LNP-based drugs can be attributed to research and technical limitations.

A notable example is Patisiran (Onpattro), an FDA-approved medication for treating fatal hereditary polyneuropathy. Its R&D pipeline involved the design and screening of more than 300 ionizable lipids, evaluating suitable LNP size, encapsulation efficiency, surface charge, and injection site for targeted siRNA delivery. This exhaustive study showcases significant advancements in LNP research while emphasizing the considerable effort needed for successful regulatory approval.[10,217]

Ensuring regulatory compliance for LNPs is paramount to guarantee their safety and effectiveness in therapeutic applications. Manufacturers must adhere to established quality standards, conduct rigorous characterization studies and toxicology evaluations, and meet specific regulatory criteria for clinical trials before LNPs can be authorized for use.[195] This comprehensive approach is essential to ensure that LNPs meet the necessary safety and efficacy standards, providing confidence in their therapeutic potential.

5.4. Quality Control

The significance of quality control in LNP industrial production cannot be overstated as it is pivotal to ensure the safety, efficacy, and consistent therapeutic performance of these products. Manufacturers must adhere to stringent quality control procedures throughout the entire production process to guarantee that the final LNP product aligns with the required specifications and standards. An essential aspect of quality control involves a thorough validation of the manufacturing process itself, verifying its reproducibility, consistency, and adherence to the required quality benchmarks. To achieve this, manufacturers should implement a robust quality management system, incorporating regular audits, inspections, and comprehensive documentation to ensure compliance with regulatory requirements.[218]

Characterizing LNPs through quality control is crucial, involving the assessment of physicochemical properties like particle size, polydispersity index (PDI), surface charge, morphology, and stability.[4] These attributes termed critical quality attributes (CQAs) for liposome drug products, significantly impact the safety and performance of LNPs, necessitating stringent control and monitoring during production.[219] Meeting regulatory requirements, LNPs should have a PDI value of ≤0.30.[220] However, the conventional batch process often yields large, heterogeneous particles (>100 nm), necessitating additional steps like extrusion, sonication, and homogenization to reduce particle sizes, leading to challenges in quality control and batch-to-batch consistency. Variations in lipid and component batches can further compound inconsistencies in the final product, aggravated by production condition differences, such as temperature, pressure, and mixing parameters. This approach's scalability to larger volumes poses challenges in quality control and increased variability.[221,222]

Alternatively, continuous processing, such as microfluidic mixing, offers better control over product quality and performance.[223,224] The incorporation of turbidity probes and UV−vis spectrometers with predictive algorithms enables real-time monitoring and feedback, swiftly detecting and rectifying deviations from the desired specifications during production. The scalability achieved through pilot-scale mixing process scaling-out ensures enhanced reproducibility and facilitates scaled-up production.[225]

In conclusion, achieving superior quality control in industrial LNP production requires a comprehensive approach involving robust process validation and meticulous characterization. By adhering to required specifications and standards, manufacturers can confidently deliver safe, effective, and reliable LNP-based therapies to patients.

6. FUTURE PROSPECTS AND CONCLUSION

This review has delved into the clinical potential of various types of LNPs and their production processes at both laboratory and industrial scales. To enable widespread clinical application, addressing challenges is crucial, such as developing efficient scaling-up methods such as continuous flow synthesis to increase yield and reduce costs.

Harmonizing regulatory policies for LNP use in clinical settings at a global level is essential. Consistency in regulations can foster the development and approval of new LNP-based therapies, especially for rare diseases that require international collaboration.[226] The International Council for Harmonization of Technical Requirements for Pharmaceuticals for Human Use (ICH) guidelines provide a framework for new drug development, and mutual recognition agreements between regulatory agencies facilitate the approval process for drugs approved in other countries.[196]

In conclusion, LNPs hold significant promise for improving drug delivery. Different types of LNPs and preparation methods offer distinct advantages and challenges, necessitating careful consideration when designing drug delivery systems. While clinical trials have demonstrated the effectiveness of LNPs, further improvements in their industrial development are needed to ensure safe and efficient drug delivery.

■ AUTHOR INFORMATION

Corresponding Author

Wei Deng — *School of Biomedical Engineering, Faculty of Engineering and Information Technology, University of Technology Sydney, Ultimo, NSW 2007, Australia;* ⦿ orcid.org/0000-0002-9413-0978; Email: wei.deng@uts.edu.au

Authors

Meenu Mehta — *School of Biomedical Engineering, Faculty of Engineering and Information Technology, University of Technology Sydney, Ultimo, NSW 2007, Australia;* ⦿ orcid.org/0000-0001-8174-5781

Thuy Anh Bui — *School of Biomedical Engineering, Faculty of Engineering and Information Technology, University of Technology Sydney, Ultimo, NSW 2007, Australia;* ⦿ orcid.org/0000-0002-7282-9227

Xinpu Yang — *School of Biomedical Engineering, Faculty of Engineering and Information Technology, University of Technology Sydney, Ultimo, NSW 2007, Australia*

Yagiz Aksoy — *Cancer Diagnosis and Pathology Group, Kolling Institute of Medical Research, Royal North Shore Hospital, St Leonards NSW 2065 Australia - Sydney Medical School, University of Sydney, Sydney, NSW 2006, Australia*

Ewa M. Goldys — *Graduate School of Biomedical Engineering, ARC Centre of Excellence in Nanoscale Biophotonics, Faculty of Engineering, UNSW, Sydney, NSW 2052, Australia*

Complete contact information is available at:
https://pubs.acs.org/10.1021/acsmaterialsau.3c00032

Author Contributions

#M.M. and T.A.B. contributed equally to this work. **Meenu Mehta** conceptualization, writing original draft, writing-reviewing and editing; **Thuy Anh Bui** conceptualization, writing original draft, writing-reviewing and editing; **Xinpu Yang** writing original draft about Microfluidic devices, **Yagiz Aksoy** writing-reviewing and editing; **Ewa M. Goldys** reviewing and editing; **Wei Deng** funding acquisition, conceptualization, writing original draft, writing-reviewing and editing.

Notes

The authors declare no competing financial interest.

■ ACKNOWLEDGMENTS

■ REFERENCES

(1) Gurevich, E. V.; Gurevich, V. V. Beyond traditional pharmacology: new tools and approaches. *Br. J. Pharmacol.* **2015**, *172* (13), 3229−3241.

(2) Tenchov, R.; Bird, R.; Curtze, A. E.; Zhou, Q. Lipid Nanoparticles—From Liposomes to mRNA Vaccine Delivery, a Landscape of Research Diversity and Advancement. *ACS Nano* **2021**, *15* (11), 16982−17015.

(3) Mittal, D.; Kaur, G.; Singh, P.; Yadav, K.; Ali, S. A. Nanoparticle-Based Sustainable Agriculture and Food Science: Recent Advances and Future Outlook. *Frontiers in Nanotechnology* **2020**, *2*, Review.

(4) Shah, S.; Dhawan, V.; Holm, R.; Nagarsenker, M. S.; Perrie, Y. Liposomes: Advancements and innovation in the manufacturing process. *Adv. Drug Deliv Rev.* **2020**, *154−155*, 102−122.

(5) Beck, H.; Harter, M.; Hass, B.; Schmeck, C.; Baerfacker, L. Small molecules and their impact in drug discovery: A perspective on the occasion of the 125th anniversary of the Bayer Chemical Research Laboratory. *Drug Discov Today* **2022**, *27* (6), 1560−1574.

(6) Forbes, N.; Hussain, M. T.; Briuglia, M. L.; Edwards, D. P.; Horst, J. H. T.; Szita, N.; Perrie, Y. Rapid and scale-independent microfluidic manufacture of liposomes entrapping protein incorporating in-line purification and at-line size monitoring. *Int. J. Pharm.* **2019**, *556*, 68−81.

(7) Verma, M.; Ozer, I.; Xie, W.; Gallagher, R.; Teixeira, A.; Choy, M. The landscape for lipid-nanoparticle-based genomic medicines. *Nat. Rev. Drug Discov* **2023**, *22*, 349.

(8) Wang, Y.; Grainger, D. W. Regulatory Considerations Specific to Liposome Drug Development as Complex Drug Products. *Frontiers in Drug Delivery* **2022**, *2*, 901281.

(9) Wang, Z.; Cui, K.; Costabel, U.; Zhang, X. Nanotechnology-facilitated vaccine development during the coronavirus disease 2019 (COVID-19) pandemic. *Exploration (Beijing)* **2022**, *2* (5), 20210082.

(10) Akinc, A.; Maier, M. A.; Manoharan, M.; Fitzgerald, K.; Jayaraman, M.; Barros, S.; Ansell, S.; Du, X.; Hope, M. J.; Madden, T. D.; et al. The Onpattro story and the clinical translation of nanomedicines containing nucleic acid-based drugs. *Nat. Nanotechnol* **2019**, *14* (12), 1084−1087.

(11) Guo, S.; Li, K.; Hu, B.; Li, C.; Zhang, M.; Hussain, A.; Wang, X.; Cheng, Q.; Yang, F.; Ge, K.; et al. Membrane-destabilizing ionizable lipid empowered imaging-guided siRNA delivery and cancer treatment. *Exploration (Beijing)* **2021**, *1* (1), 35−49.

(12) Kumar, G.; Kant, A.; Kumar, M.; Masram, D. T. Synthesis, characterizations and kinetic study of metal organic framework nanocomposite excipient used as extended release delivery vehicle for an antibiotic drug. *Inorg. Chim. Acta* **2019**, *496*, 119036.

(13) Kumar, G.; Chaudhary, K.; Mogha, N. K.; Kant, A.; Masram, D. T. Extended Release of Metronidazole Drug Using Chitosan/Graphene Oxide Bionanocomposite Beads as the Drug Carrier. *ACS Omega* **2021**, *6* (31), 20433−20444.

(14) Wuttke, S.; Braig, S.; Preiß, T.; Zimpel, A.; Sicklinger, J.; Bellomo, C.; Rädler, J. O.; Vollmar, A. M.; Bein, T. MOF nanoparticles coated by lipid bilayers and their uptake by cancer cells. *Chem. Commun. (Camb)* **2015**, *51* (87), 15752−15755.

(15) Róg, T.; Girych, M.; Bunker, A. Mechanistic Understanding from Molecular Dynamics in Pharmaceutical Research 2: Lipid Membrane in Drug Design. *Pharmaceuticals* **2021**, *14* (10), 1062.

(16) Hathout, R. M.; Metwally, A. A. Towards better modelling of drug-loading in solid lipid nanoparticles: Molecular dynamics, docking experiments and Gaussian Processes machine learning. *Eur. J. Pharm. Biopharm.* **2016**, *108*, 262−268.

(17) Cheng, X.; Lee, R. J. The role of helper lipids in lipid nanoparticles (LNPs) designed for oligonucleotide delivery. *Adv. Drug Deliv Rev.* **2016**, *99* (Pt A), 129−137.

(18) Puri, A.; Loomis, K.; Smith, B.; Lee, J. H.; Yavlovich, A.; Heldman, E.; Blumenthal, R. Lipid-based nanoparticles as pharmaceutical drug carriers: from concepts to clinic. *Crit Rev. Ther Drug Carrier Syst* **2009**, *26* (6), 523−580.

(19) Xu, L.; Wang, X.; Liu, Y.; Yang, G.; Falconer, R. J.; Zhao, C.-X. Lipid Nanoparticles for Drug Delivery. *Advanced NanoBiomed Research* **2022**, *2* (2), 2100109.

(20) Mora-Huertas, C. E.; Fessi, H.; Elaissari, A. Polymer-based nanocapsules for drug delivery. *Int. J. Pharm.* **2010**, *385* (1−2), 113−142.

(21) Martínez Rivas, C. J.; Tarhini, M.; Badri, W.; Miladi, K.; Greige-Gerges, H.; Nazari, Q. A.; Galindo Rodríguez, S. A.; Román, R.; Fessi, H.; Elaissari, A. Nanoprecipitation process: From encapsulation to drug delivery. *Int. J. Pharm.* **2017**, *532* (1), 66−81.

(22) Rasmussen, M. K.; Pedersen, J. N.; Marie, R. Size and surface charge characterization of nanoparticles with a salt gradient. *Nat. Commun.* **2020**, *11* (1), 2337.

(23) Smith, M. C.; Crist, R. M.; Clogston, J. D.; McNeil, S. E. Zeta potential: a case study of cationic, anionic, and neutral liposomes. *Anal Bioanal Chem.* **2017**, *409* (24), 5779−5787.

(24) Ruozi, B.; Belletti, D.; Tombesi, A.; Tosi, G.; Bondioli, L.; Forni, F.; Vandelli, M. A. AFM, ESEM, TEM, and CLSM in liposomal characterization: a comparative study. *Int. J. Nanomedicine* **2011**, *6*, 557−563.

(25) Zhigaltsev, I. V.; Cullis, P. R. Morphological Behavior of Liposomes and Lipid Nanoparticles. *Langmuir* **2023**, *39* (9), 3185−3193.

(26) Knop, K.; Hoogenboom, R.; Fischer, D.; Schubert, U. S. Poly(ethylene glycol) in drug delivery: pros and cons as well as potential alternatives. *Angew. Chem., Int. Ed. Engl.* **2010**, *49* (36), 6288−6308.

(27) Battaglia, L.; Gallarate, M. Lipid nanoparticles: state of the art, new preparation methods and challenges in drug delivery. *Expert Opin Drug Deliv* **2012**, *9* (5), 497−508.

(28) Yu, F.; Miao, Y.; Wang, M.; Liu, Q.; Yuan, L.; Geng, R.; Qiu, Q.; Ni, C.; Kay, M. Predicting nanoemulsion formulation and studying the synergism mechanism between surfactant and cosurfactant: A combined computational and experimental approach. *Int. J. Pharm.* **2022**, *615*, 121473.

(29) Balouch, M.; Storchmannova, K.; Stepanek, F.; Berka, K. Computational Prodrug Design Methodology for Liposome Formulability Enhancement of Small-Molecule APIs. *Mol. Pharmaceutics* **2023**, *20* (4), 2119−2127.

(30) Chaban, V. V.; Khandelia, H. Distribution of neutral lipids in the lipid droplet core. *J. Phys. Chem. B* **2014**, *118* (38), 11145−11151.

(31) Chaban, V. V.; Khandelia, H. Lipid structure in triolein lipid droplets. *J. Phys. Chem. B* **2014**, *118* (35), 10335−10340.

(32) Chan, C.; Du, S.; Dong, Y.; Cheng, X. Computational and Experimental Approaches to Investigate Lipid Nanoparticles as Drug and Gene Delivery Systems. *Curr. Top Med. Chem.* **2021**, *21* (2), 92−114.

(33) Metwally, A. A.; Hathout, R. M. Computer-Assisted Drug Formulation Design: Novel Approach in Drug Delivery. *Mol. Pharmaceutics* **2015**, *12* (8), 2800−2810.

(34) Yadav, D. K.; Kumar, S.; Choi, E. H.; Chaudhary, S.; Kim, M. H. Computational Modeling on Aquaporin-3 as Skin Cancer Target: A Virtual Screening Study. *Front Chem.* **2020**, *8*, 250.

(35) Bangham, A. D.; Standish, M. M.; Watkins, J. C. Diffusion of univalent ions across the lamellae of swollen phospholipids. *J. Mol. Biol.* **1965**, *13* (1), 238−252.

(36) Wang, H. F.; Ran, R.; Liu, Y.; Hui, Y.; Zeng, B.; Chen, D.; Weitz, D. A.; Zhao, C. X. Tumor-Vasculature-on-a-Chip for Investigating Nanoparticle Extravasation and Tumor Accumulation. *ACS Nano* **2018**, *12* (11), 11600−11609.

(37) Has, C.; Sunthar, P. A comprehensive review on recent preparation techniques of liposomes. *J. Liposome Res.* **2020**, *30* (4), 336−365.

(38) Harashima, H.; Sakata, K.; Funato, K.; Kiwada, H. Enhanced hepatic uptake of liposomes through complement activation depending on the size of liposomes. *Pharm. Res.* **1994**, *11* (3), 402−406.

(39) Parchekani, J.; Allahverdi, A.; Taghdir, M.; Naderi-Manesh, H. Design and simulation of the liposomal model by using a coarse-grained molecular dynamics approach towards drug delivery goals. *Sci. Rep* **2022**, *12* (1), 2371.

(40) Lemaalem, M.; Hadrioui, N.; Derouiche, A.; Ridouane, H. Structure and dynamics of liposomes designed for drug delivery: coarse-grained molecular dynamics simulations to reveal the role of lipopolymer incorporation. *RSC Adv.* **2020**, *10* (7), 3745−3755.

(41) Jambeck, J. P.; Eriksson, E. S.; Laaksonen, A.; Lyubartsev, A. P.; Eriksson, L. A. Molecular Dynamics Studies of Liposomes as Carriers for Photosensitizing Drugs: Development, Validation, and Simulations with a Coarse-Grained Model. *J. Chem. Theory Comput* **2014**, *10* (1), 5−13.

(42) Dzieciuch, M.; Rissanen, S.; Szydlowska, N.; Bunker, A.; Kumorek, M.; Jamroz, D.; Vattulainen, I.; Nowakowska, M.; Rog, T.; Kepczynski, M. PEGylated Liposomes as Carriers of Hydrophobic Porphyrins. *J. Phys. Chem. B* **2015**, *119* (22), 6646−6657.

(43) Lehtinen, J.; Magarkar, A.; Stepniewski, M.; Hakola, S.; Bergman, M.; Rog, T.; Yliperttula, M.; Urtti, A.; Bunker, A. Analysis of cause of failure of new targeting peptide in PEGylated liposome: molecular modeling as rational design tool for nanomedicine. *Eur. J. Pharm. Sci.* **2012**, *46* (3), 121−130.

(44) Wagner, A.; Vorauer-Uhl, K. Liposome technology for industrial purposes. *Journal of drug delivery* **2011**, *2011*, 1.

(45) Sercombe, L.; Veerati, T.; Moheimani, F.; Wu, S. Y.; Sood, A. K.; Hua, S. Advances and Challenges of Liposome Assisted Drug Delivery. *Front Pharmacol* **2015**, *6*, 286.

(46) Immordino, M. L.; Dosio, F.; Cattel, L. Stealth liposomes: review of the basic science, rationale, and clinical applications, existing and potential. *Int. J. Nanomedicine* **2006**, *1* (3), 297−315.

(47) Lee, Y.; Thompson, D. H. Stimuli-responsive liposomes for drug delivery. *Wiley Interdiscip Rev. Nanomed Nanobiotechnol* **2017**, *9* (5), e1450 DOI: 10.1002/wnan.1450.

(48) Ismail, M.; Yang, W.; Li, Y.; Chai, T.; Zhang, D.; Du, Q.; Muhammad, P.; Hanif, S.; Zheng, M.; Shi, B. Targeted liposomes for combined delivery of artesunate and Temozolomide to resistant glioblastoma. *Biomaterials* **2022**, *287*, 121608.

(49) Barenholz, Y.; Haran, G. Method of amphophilic drug loading into liposomes by pH gradient, US Patent 1993, 5 192 549. Gabizon, A.; Catane, R.; Uziely, B.; Kaufman, B.; Safra, T.; Cohen, R.; Martin, F.; Huang, A.; Barenholz, Y. Prolonged circulation time and enhanced accumulation in malignant exudates of doxorubicin encapsulated in polyethylene glycol-coated liposomes. *Cancer Res.* **1994**, *54*, 987−992.

(50) Barenholz, Y. C. Doxil®—The first FDA-approved nano-drug: Lessons learned. *Journal of controlled release* **2012**, *160* (2), 117−134.

(51) Tadros, T.; Izquierdo, P.; Esquena, J.; Solans, C. Formation and stability of nano-emulsions. *Adv. Colloid Interface Sci.* **2004**, *108−109*, 303−318.

(52) Gupta, A. Nanoemulsions. In *Nanoparticles for Biomedical Applications*, Chung, E. J.; Leon, L., Rinaldi, C., Eds.; Elsevier, 2020; Ch. 21, pp 371−384.

(53) Aswathanarayan, J. B.; Vittal, R. R. Nanoemulsions and Their Potential Applications in Food Industry. *Frontiers in Sustainable Food Systems* **2019**, *3*, 95.

(54) Kralova, I.; Sjöblom, J. Surfactants Used in Food Industry: A Review. *J. Dispersion Sci. Technol.* **2009**, *30* (9), 1363−1383.

(55) Ikeuchi-Takahashi, Y.; Kobayashi, A.; Ishihara, C.; Matsubara, T.; Matsubara, H.; Onishi, H. Influence of Polysorbate 60 on Formulation Properties and Bioavailability of Morin-Loaded Nano-emulsions with and without Low-Saponification-Degree Polyvinyl Alcohol. *Biol. Pharm. Bull.* **2018**, *41* (5), 754−760.

(56) Silva, H. D.; Cerqueira, M. A.; Vicente, A. A. Influence of surfactant and processing conditions in the stability of oil-in-water nanoemulsions. *Journal of Food Engineering* **2015**, *167*, 89−98.

(57) Wilson, R. J.; Li, Y.; Yang, G.; Zhao, C.-X. Nanoemulsions for drug delivery. *Particuology* **2022**, *64*, 85−97.

(58) Ammar, H. O.; Salama, H. A.; Ghorab, M.; Mahmoud, A. A. Development of dorzolamide hydrochloride in situ gel nanoemulsion for ocular delivery. *Drug Dev. Ind. Pharm.* **2010**, *36* (11), 1330−1339.

(59) Kumar, M.; Misra, A.; Babbar, A. K.; Mishra, A. K.; Mishra, P.; Pathak, K. Intranasal nanoemulsion based brain targeting drug delivery system of risperidone. *Int. J. Pharm.* **2008**, *358* (1−2), 285−291.

(60) Jaiswal, M.; Dudhe, R.; Sharma, P. K. Nanoemulsion: an advanced mode of drug delivery system. *3 Biotech* **2015**, *5* (2), 123−127.

(61) Hormann, K.; Zimmer, A. Drug delivery and drug targeting with parenteral lipid nanoemulsions - A review. *J. Controlled Release* **2016**, *223*, 85−98.

(62) Pirhadi, S.; Amani, A. Molecular dynamics simulation of self-assembly in a nanoemulsion system. *Chemical Papers* **2020**, *74* (8), 2443−2448.

(63) Pyrhönen, J.; Bansal, K. K.; Bhadane, R.; Wilén, C.-E.; Salo-Ahen, O. M. H.; Rosenholm, J. M. Molecular Dynamics Prediction Verified by Experimental Evaluation of the Solubility of Different Drugs in Poly(decalactone) for the Fabrication of Polymeric Nanoemulsions. *Advanced NanoBiomed Research* **2022**, *2* (1), 2100072.

(64) Hong, Z.; Xiao, N.; Li, L.; Xie, X. Investigation of nanoemulsion interfacial properties: A mesoscopic simulation. *Journal of Food Engineering* **2020**, *276*, 109877.

(65) Glotzer, S. C.; Paul, W. Molecular and Mesoscale Simulation Methods for Polymer Materials. *Annu. Rev. Mater. Res.* **2002**, *32* (1), 401−436.

(66) Polchi, A.; Magini, A.; Mazuryk, J.; Tancini, B.; Gapinski, J.; Patkowski, A.; Giovagnoli, S.; Emiliani, C. Rapamycin Loaded Solid Lipid Nanoparticles as a New Tool to Deliver mTOR Inhibitors: Formulation and in Vitro Characterization. *Nanomaterials (Basel)* **2016**, *6* (5), 87.

(67) Shah, R. M.; Mata, J. P.; Bryant, G.; Campo, L.; Ife, A.; Karpe, A. V.; Jadhav, S. R.; Eldridge, D. S.; Palombo, E. A.; Harding, I. H. Structure Analysis of Solid Lipid Nanoparticles for Drug Delivery: A Combined USANS/SANS Study. *Particle & Particle Systems Characterization* **2019**, *36* (1), 1800359.

(68) Duan, Y.; Dhar, A.; Patel, C.; Khimani, M.; Neogi, S.; Sharma, P.; Siva Kumar, N.; Vekariya, R. L. A brief review on solid lipid nanoparticles: part and parcel of contemporary drug delivery systems. *RSC Adv.* **2020**, *10* (45), 26777−26791.

(69) Geszke-Moritz, M.; Moritz, M. Solid lipid nanoparticles as attractive drug vehicles: Composition, properties and therapeutic strategies. *Mater. Sci. Eng. C Mater. Biol. Appl.* **2016**, *68*, 982−994.

(70) Qiu, S.; Liang, D.; Guo, F.; Deng, T.; Peng, T.; Gao, Y.; Zhang, X.; Zhong, H. Solid lipid nanoparticles modified with amphipathic chitosan derivatives for improved stability in the gastrointestinal tract. *Journal of Drug Delivery Science and Technology* **2018**, *48*, 288−299.

(71) Kuo, Y. C.; Chung, J. F. Physicochemical properties of nevirapine-loaded solid lipid nanoparticles and nanostructured lipid carriers. *Colloids Surf. B Biointerfaces* **2011**, *83* (2), 299−306.

(72) Venishetty, V. K.; Komuravelli, R.; Kuncha, M.; Sistla, R.; Diwan, P. V. Increased brain uptake of docetaxel and ketoconazole loaded folate-grafted solid lipid nanoparticles. *Nanomedicine* **2013**, *9* (1), 111−121.

(73) Kuo, Y. C.; Liang, C. T. Inhibition of human brain malignant glioblastoma cells using carmustine-loaded catanionic solid lipid nanoparticles with surface anti-epithelial growth factor receptor. *Biomaterials* **2011**, *32* (12), 3340−3350.

(74) Abdel-Mageed, H. M.; Abd El Aziz, A. E.; Mohamed, S. A.; AbuelEzz, N. Z. The tiny big world of solid lipid nanoparticles and nanostructured lipid carriers: an updated review. *J. Microencapsul* **2022**, *39* (1), 72−94.

(75) Hathout, R. M.; Metwally, A. A. Towards better modelling of drug-loading in solid lipid nanoparticles: Molecular dynamics, docking experiments and Gaussian Processes machine learning. *Eur. J. Pharm. Biopharm* **2016**, *108*, 262−268.

(76) Pink, D. L.; Loruthai, O.; Ziolek, R. M.; Wasutrasawat, P.; Terry, A. E.; Lawrence, M. J.; Lorenz, C. D. On the Structure of Solid Lipid Nanoparticles. *Small* **2019**, *15* (45), No. e1903156.

(77) Gastaldi, L.; Battaglia, L.; Peira, E.; Chirio, D.; Muntoni, E.; Solazzi, I.; Gallarate, M.; Dosio, F. Solid lipid nanoparticles as vehicles of drugs to the brain: current state of the art. *Eur. J. Pharm. Biopharm* **2014**, *87* (3), 433−444.

(78) Soares, S.; Fonte, P.; Costa, A.; Andrade, J.; Seabra, V.; Ferreira, D.; Reis, S.; Sarmento, B. Effect of freeze-drying, cryoprotectants and storage conditions on the stability of secondary structure of insulin-loaded solid lipid nanoparticles. *Int. J. Pharm.* **2013**, *456* (2), 370−381.

(79) Mehnert, W.; Mäder, K. Solid lipid nanoparticles: production, characterization and applications. *Adv. Drug Deliv Rev.* **2001**, *47* (2−3), 165−196.

(80) Shegokar, R.; Singh, K. K.; Muller, R. H. Production & stability of stavudine solid lipid nanoparticles-from lab to industrial scale. *Int. J. Pharm.* **2011**, *416* (2), 461−470.

(81) Farhood, H.; Gao, X.; Son, K.; Yang, Y. Y.; Lazo, J. S.; Huang, L.; Barsoum, J.; Bottega, R.; Epand, R. M. Cationic liposomes for direct gene transfer in therapy of cancer and other diseases. *Ann. N.Y. Acad. Sci.* **1994**, *716*, 23−34 discussion 34−25.

(82) Araujo, V. H. S.; Delello Di Filippo, L.; Duarte, J. L.; Spósito, L.; Camargo, B. A. F.; da Silva, P. B.; Chorilli, M. Exploiting solid lipid nanoparticles and nanostructured lipid carriers for drug delivery against cutaneous fungal infections. *Crit Rev. Microbiol* **2021**, *47* (1), 79−90.

(83) Hao, J.; Wang, F.; Wang, X.; Zhang, D.; Bi, Y.; Gao, Y.; Zhao, X.; Zhang, Q. Development and optimization of baicalin-loaded solid lipid nanoparticles prepared by coacervation method using central composite design. *Eur. J. Pharm. Sci.* **2012**, *47* (2), 497−505.

(84) Badawi, N.; El-Say, K.; Attia, D.; El-Nabarawi, M.; Elmazar, M.; Teaima, M. Development of Pomegranate Extract-Loaded Solid Lipid Nanoparticles: Quality by Design Approach to Screen the Variables Affecting the Quality Attributes and Characterization. *ACS Omega* **2020**, *5* (34), 21712−21721.

(85) Ostrosky-Zeichner, L.; Marr, K. A.; Rex, J. H.; Cohen, S. H. Amphotericin B: Time for a New "Gold Standard". *Clin. Infect. Dis.* **2003**, *37* (3), 415.

(86) FDA approves DaunoXome as first-line therapy for Kaposi's sarcoma. Food and Drug Administration. *J. Int. Assoc Physicians AIDS Care* **1996**, *2* (5), 50−51.

(87) Guo, P.; Hsu, T. M.; Zhao, Y.; Martin, C. R.; Zare, R. N. Preparing amorphous hydrophobic drug nanoparticles by nanoporous membrane extrusion. *Nanomedicine (Lond)* **2013**, *8* (3), 333−341.

(88) FDA Fast Track Designation for Myocet for Metastatic Breast Cancer. *Oncology Times* **2010**, *32* (3), 24.

(89) FDA Approves Onivyde Combo Regimen for Advanced Pancreatic Cancer. *Oncology Times* **2015**, *37* (22), 8.

(90) Venkatakrishnan, K.; Liu, Y.; Noe, D.; Mertz, J.; Bargfrede, M.; Marbury, T.; Farbakhsh, K.; Oliva, C.; Milton, A. Pharmacokinetics and pharmacodynamics of liposomal mifamurtide in adult volunteers with mild or moderate hepatic impairment. *Br. J. Clin. Pharmacol.* **2014**, *77* (6), 998−1010.

(91) Galmarini, C. M.; Mackey, J. R.; Dumontet, C. Nucleoside analogues and nucleobases in cancer treatment. *Lancet Oncol* **2002**, *3* (7), 415−424.

(92) O'Brien, S.; Schiller, G.; Lister, J.; Damon, L.; Goldberg, S.; Aulitzky, W.; Ben-Yehuda, D.; Stock, W.; Coutre, S.; Douer, D.; et al. High-dose vincristine sulfate liposome injection for advanced, relapsed, and refractory adult Philadelphia chromosome-negative acute lymphoblastic leukemia. *J. Clin Oncol* **2013**, *31* (6), 676−683.

(93) Berger, N.; Sachse, A.; Bender, J.; Schubert, R.; Brandl, M. Filter extrusion of liposomes using different devices: comparison of liposome size, encapsulation efficiency, and process characteristics. *Int. J. Pharm.* **2001**, *223* (1−2), 55−68.

(94) Gradishar, W. J.; Tjulandin, S.; Davidson, N.; Shaw, H.; Desai, N.; Bhar, P.; Hawkins, M.; O'Shaughnessy, J. Phase III trial of nanoparticle albumin-bound paclitaxel compared with polyethylated castor oil-based paclitaxel in women with breast cancer. *J. Clin Oncol* **2005**, *23* (31), 7794−7803.

(95) Yardley, D. A. nab-Paclitaxel mechanisms of action and delivery. *J. Controlled Release* **2013**, *170* (3), 365−372.

(96) Ran, R.; Sun, Q.; Baby, T.; Wibowo, D.; Middelberg, A. P.; Zhao, C.-X. *J. C. E. S. Multiphase microfluidic synthesis of micro-and nanostructures for pharmaceutical applications* **2017**, *169*, 78−96.

(97) Adedoyin, A.; Bernardo, J. F.; Swenson, C. E.; Bolsack, L. E.; Horwith, G.; DeWit, S.; Kelly, E.; Klasterksy, J.; Sculier, J. P.; DeValeriola, D.; et al. Pharmacokinetic profile of ABELCET

(amphotericin B lipid complex injection): combined experience from phase I and phase II studies. *Antimicrob. Agents Chemother.* **1997**, *41* (10), 2201−2208.

(98) Stone, N. R.; Bicanic, T.; Salim, R.; Hope, W. Liposomal Amphotericin B (AmBisome((R))): A Review of the Pharmacokinetics, Pharmacodynamics, Clinical Experience and Future Directions. *Drugs* **2016**, *76* (4), 485−500.

(99) Clemons, K. V.; Stevens, D. A. Comparison of fungizone, Amphotec, AmBisome, and Abelcet for treatment of systemic murine cryptococcosis. *Antimicrob. Agents Chemother.* **1998**, *42* (4), 899−902.

(100) Bovier, P. A. Epaxal: a virosomal vaccine to prevent hepatitis A infection. *Expert Rev. Vaccines* **2008**, *7* (8), 1141−1150.

(101) Herzog, C.; Hartmann, K.; Kunzi, V.; Kursteiner, O.; Mischler, R.; Lazar, H.; Gluck, R. Eleven years of Inflexal V-a virosomal adjuvanted influenza vaccine. *Vaccine* **2009**, *27* (33), 4381−4387.

(102) Cheng, X.; Gao, J.; Ding, Y.; Lu, Y.; Wei, Q.; Cui, D.; Fan, J.; Li, X.; Zhu, E.; Lu, Y.; et al. Multi-Functional Liposome: A Powerful Theranostic Nano-Platform Enhancing Photodynamic Therapy. *Adv. Sci. (Weinh)* **2021**, *8* (16), No. e2100876.

(103) Mayer, M.; Doenicke, A.; Nebauer, A. E.; Hepting, L. Propofol and etomidate-Lipuro for induction of general anesthesia. Hemodynamics, vascular compatibility, subjective findings and postoperative nausea. *Anaesthesist* **1996**, *45* (11), 1082−1084.

(104) Patel, H. H.; P, M.; Patel, P. M.; Roth, D. M. *General Anesthetics and Therapeutic Gases*; McGraw Hill.

(105) Bakshi, P.; Jiang, Y.; Nakata, T.; Akaki, J.; Matsuoka, N.; Banga, A. K. Formulation Development and Characterization of Nanoemulsion-Based Formulation for Topical Delivery of Heparinoid. *J. Pharm. Sci.* **2018**, *107* (11), 2883−2890.

(106) Salim, N.; Jose García-Celma, M.; Escribano, E.; Nolla, J.; Llinàs, M.; Basri, M.; Solans, C.; Esquena, J.; Tadros, T. F. Formation of Nanoemulsion Containing Ibuprofen by PIC Method for Topical Delivery. *Materials Today: Proceedings* **2018**, *5*, S172−S179.

(107) Stahelin, H. F. The history of cyclosporin A (Sandimmune) revisited: another point of view. *Experientia* **1996**, *52* (1), 5−13.

(108) Dickman, D. A. *Process Chemistry Development of the HIV Protease Inhibitor Drug Kaletra: A Mixture of Ritonavir and Lopinavir* **2022**, 57.

(109) Zhou, Q.; Sun, X.; Zeng, L.; Liu, J.; Zhang, Z. A randomized multicenter phase II clinical trial of mitoxantrone-loaded nanoparticles in the treatment of 108 patients with unresected hepatocellular carcinoma. *Nanomedicine* **2009**, *5* (4), 419−423.

(110) Holtze, C. Large-scale droplet production in microfluidic devices—an industrial perspective. *J. Phys. D: Appl. Phys.* **2013**, *46* (11), 114008.

(111) Maeki, M.; Okada, Y.; Uno, S.; Sugiura, K.; Suzuki, Y.; Okuda, K.; Sato, Y.; Ando, M.; Yamazaki, H.; Takeuchi, M. Mass production system for RNA-loaded lipid nanoparticles using piling up microfluidic devices. *Applied Materials Today* **2023**, *31*, 101754.

(112) Carvajal-Vidal, P.; Gonzalez-Pizarro, R.; Araya, C.; Espina, M.; Halbaut, L.; Gomez de Aranda, I.; Garcia, M. L.; Calpena, A. C. Nanostructured lipid carriers loaded with Halobetasol propionate for topical treatment of inflammation: Development, characterization, biopharmaceutical behavior and therapeutic efficacy of gel dosage forms. *Int. J. Pharm.* **2020**, *585*, 119480.

(113) Luzzati, V.; Tardieu, A.; Gulik-Krzywicki, T. Polymorphism of lipids. *Nature* **1968**, *217* (5133), 1028−1030.

(114) Agrawal, Y.; Petkar, K. C.; Sawant, K. K. Development, evaluation and clinical studies of Acitretin loaded nanostructured lipid carriers for topical treatment of psoriasis. *Int. J. Pharm.* **2010**, *401* (1−2), 93−102.

(115) Charoenputtakun, P.; Pamornpathomkul, B.; Opanasopit, P.; Rojanarata, T.; Ngawhirunpat, T. Terpene composited lipid nanoparticles for enhanced dermal delivery of all-trans-retinoic acids. *Biol. Pharm. Bull.* **2014**, *37* (7), 1139−1148.

(116) El-Salamouni, N. S.; Farid, R. M.; El-Kamel, A. H.; El-Gamal, S. S. Effect of sterilization on the physical stability of brimonidine-loaded solid lipid nanoparticles and nanostructured lipid carriers. *Int. J. Pharm.* **2015**, *496* (2), 976−983.

(117) Hadinoto, K.; Sundaresan, A.; Cheow, W. S. Lipid-polymer hybrid nanoparticles as a new generation therapeutic delivery platform: A review. *Eur. J. Pharm. Biopharm.* **2013**, *85* (3, Part A), 427−443.

(118) Baden, L. R.; El Sahly, H. M.; Essink, B.; Kotloff, K.; Frey, S.; Novak, R.; Diemert, D.; Spector, S. A.; Rouphael, N.; Creech, C. B.; et al. Efficacy and Safety of the mRNA-1273 SARS-CoV-2 Vaccine. *N Engl J. Med.* **2021**, *384* (5), 403−416.

(119) Polack, F. P.; Thomas, S. J.; Kitchin, N.; Absalon, J.; Gurtman, A.; Lockhart, S.; Perez, J. L.; Perez Marc, G.; Moreira, E. D.; Zerbini, C.; et al. Safety and Efficacy of the BNT162b2 mRNA Covid-19 Vaccine. *N Engl J. Med.* **2020**, *383* (27), 2603−2615.

(120) Song, S. Y.; Kim, K. P.; Jeong, S. Y.; Park, J.; Park, J.; Jung, J.; Chung, H. K.; Lee, S. W.; Seo, M. H.; Lee, J. S.; et al. Polymeric nanoparticle-docetaxel for the treatment of advanced solid tumors: phase I clinical trial and preclinical data from an orthotopic pancreatic cancer model. *Oncotarget* **2016**, *7* (47), 77348−77357.

(121) Vetten, M. A.; Yah, C. S.; Singh, T.; Gulumian, M. Challenges facing sterilization and depyrogenation of nanoparticles: effects on structural stability and biomedical applications. *Nanomedicine* **2014**, *10* (7), 1391−1399.

(122) Packer, M.; Gyawali, D.; Yerabolu, R.; Schariter, J.; White, P. A novel mechanism for the loss of mRNA activity in lipid nanoparticle delivery systems. *Nat. Commun.* **2021**, *12* (1), 6777.

(123) Autio, K. A.; Dreicer, R.; Anderson, J.; Garcia, J. A.; Alva, A.; Hart, L. L.; Milowsky, M. I.; Posadas, E. M.; Ryan, C. J.; Graf, R. P.; et al. Safety and Efficacy of BIND-014, a Docetaxel Nanoparticle Targeting Prostate-Specific Membrane Antigen for Patients With Metastatic Castration-Resistant Prostate Cancer: A Phase 2 Clinical Trial. *JAMA Oncol* **2018**, *4* (10), 1344−1351.

(124) Lobovkina, T.; Jacobson, G. B.; Gonzalez-Gonzalez, E.; Hickerson, R. P.; Leake, D.; Kaspar, R. L.; Contag, C. H.; Zare, R. N. In vivo sustained release of siRNA from solid lipid nanoparticles. *ACS Nano* **2011**, *5* (12), 9977−9983.

(125) Salvi, V. R.; Pawar, P. Nanostructured lipid carriers (NLC) system: A novel drug targeting carrier. *Journal of Drug Delivery Science and Technology* **2019**, *51*, 255−267.

(126) Chauhan, I.; Yasir, M.; Verma, M.; Singh, A. P. Nanostructured Lipid Carriers: A Groundbreaking Approach for Transdermal Drug Delivery. *Adv. Pharm. Bull.* **2020**, *10* (2), 150−165.

(127) Izza, N.; Suga, K.; Okamoto, Y.; Watanabe, N.; Bui, T. T.; Wibisono, Y.; Fadila, C. R.; Umakoshi, H. Systematic Characterization of Nanostructured Lipid Carriers from Cetyl Palmitate/Caprylic Triglyceride/Tween 80 Mixtures in an Aqueous Environment. *Langmuir* **2021**, *37* (14), 4284−4293.

(128) Ortiz, A. C.; Yanez, O.; Salas-Huenuleo, E.; Morales, J. O. Development of a Nanostructured Lipid Carrier (NLC) by a Low-Energy Method, Comparison of Release Kinetics and Molecular Dynamics Simulation. *Pharmaceutics* **2021**, *13* (4), 531.

(129) Beloqui, A.; Solinis, M. A.; Rodriguez-Gascon, A.; Almeida, A. J.; Preat, V. Nanostructured lipid carriers: Promising drug delivery systems for future clinics. *Nanomedicine* **2016**, *12* (1), 143−161.

(130) Carvajal-Vidal, P.; Fabrega, M. J.; Espina, M.; Calpena, A. C.; Garcia, M. L. Development of Halobetasol-loaded nanostructured lipid carrier for dermal administration: Optimization, physicochemical and biopharmaceutical behavior, and therapeutic efficacy. *Nanomedicine* **2019**, *20*, 102026.

(131) Cirri, M.; Maestrini, L.; Maestrelli, F.; Mennini, N.; Mura, P.; Ghelardini, C.; Di Cesare Mannelli, L. Design, characterization and in vivo evaluation of nanostructured lipid carriers (NLC) as a new drug delivery system for hydrochlorothiazide oral administration in pediatric therapy. *Drug Deliv* **2018**, *25* (1), 1910−1921.

(132) Sun, M.; Nie, S.; Pan, X.; Zhang, R.; Fan, Z.; Wang, S. Quercetin-nanostructured lipid carriers: characteristics and anti-breast cancer activities in vitro. *Colloids Surf. B Biointerfaces* **2014**, *113*, 15−24.

(133) Jaiswal, P.; Gidwani, B.; Vyas, A. Nanostructured lipid carriers and their current application in targeted drug delivery. *Artif Cells Nanomed Biotechnol* **2016**, *44* (1), 27−40.

(134) Zhang, L. I.; Zhang, L. Lipid-Polymer Hybrid Nanoparticles: Synthesis, Characterization and Applications. *Nano LIFE* **2010**, *01* (01n02), 163−173.

(135) Shafique, M.; Ur Rehman, M.; Kamal, Z.; Alzhrani, R. M.; Alshehri, S.; Alamri, A. H.; Bakkari, M. A.; Sabei, F. Y.; Safhi, A. Y.; Mohammed, A. M.; et al. Formulation development of lipid polymer hybrid nanoparticles of doxorubicin and its in-vitro, in-vivo and computational evaluation. *Front Pharmacol* **2023**, *14*, 1025013.

(136) Hadinoto, K.; Sundaresan, A.; Cheow, W. S. Lipid-polymer hybrid nanoparticles as a new generation therapeutic delivery platform: a review. *Eur. J. Pharm. Biopharm* **2013**, *85* (3 Pt A), 427−443.

(137) Musielak, E.; Feliczak-Guzik, A.; Nowak, I. Synthesis and Potential Applications of Lipid Nanoparticles in Medicine. *Materials (Basel)* **2022**, *15* (2), 682.

(138) Bazylińska, U.; Lewińska, A.; Lamch, L.; Wilk, K. A. Polymeric nanocapsules and nanospheres for encapsulation and long sustained release of hydrophobic cyanine-type photosensitizer. *Colloids Surf., A* **2014**, *442*, 42−49.

(139) Siqueira-Moura, M. P.; Primo, F. L.; Espreafico, E. M.; Tedesco, A. C. Development, characterization, and photocytotoxicity assessment on human melanoma of chloroaluminum phthalocyanine nanocapsules. *Mater. Sci. Eng. C Mater. Biol. Appl.* **2013**, *33* (3), 1744−1752.

(140) Mazzarino, L.; Travelet, C.; Ortega-Murillo, S.; Otsuka, I.; Pignot-Paintrand, I.; Lemos-Senna, E.; Borsali, R. Elaboration of chitosan-coated nanoparticles loaded with curcumin for mucoadhesive applications. *J. Colloid Interface Sci.* **2012**, *370* (1), 58−66.

(141) Katara, R.; Majumdar, D. K. Eudragit RL 100-based nanoparticulate system of aceclofenac for ocular delivery. *Colloids Surf. B Biointerfaces* **2013**, *103*, 455−462.

(142) Dong, Y.; Ng, W. K.; Shen, S.; Kim, S.; Tan, R. B. Solid lipid nanoparticles: continuous and potential large-scale nanoprecipitation production in static mixers. *Colloids Surf. B Biointerfaces* **2012**, *94*, 68−72.

(143) Riewe, J.; Erfle, P.; Melzig, S.; Kwade, A.; Dietzel, A.; Bunjes, H. Antisolvent precipitation of lipid nanoparticles in microfluidic systems - A comparative study. *Int. J. Pharm.* **2020**, *579*, 119167.

(144) Streck, S.; Neumann, H.; Nielsen, H. M.; Rades, T.; McDowell, A. Comparison of bulk and microfluidics methods for the formulation of poly-lactic-co-glycolic acid (PLGA) nanoparticles modified with cell-penetrating peptides of different architectures. *International journal of pharmaceutics: X* **2019**, *1*, 100030.

(145) Gupta, A.; Eral, H. B.; Hatton, T. A.; Doyle, P. S. Nanoemulsions: formation, properties and applications. *Soft Matter* **2016**, *12* (11), 2826−2841.

(146) Ganesan, P.; Narayanasamy, D. Lipid nanoparticles: Different preparation techniques, characterization, hurdles, and strategies for the production of solid lipid nanoparticles and nanostructured lipid carriers for oral drug delivery. *Sustainable Chemistry and Pharmacy* **2017**, *6*, 37−56.

(147) Battaglia, L.; Trotta, M.; Gallarate, M.; Carlotti, M. E.; Zara, G. P.; Bargoni, A. Solid lipid nanoparticles formed by solvent-in-water emulsion-diffusion technique: development and influence on insulin stability. *J. Microencapsul* **2007**, *24* (7), 672.

(148) Vandergraaf, S.; Schroen, C.; Boom, R. Preparation of double emulsions by membrane emulsification?a review. *J. Membr. Sci.* **2005**, *251* (1−2), 7−15.

(149) Gibaud, S.; Attivi, D. Microemulsions for oral administration and their therapeutic applications. *Expert Opin Drug Deliv* **2012**, *9* (8), 937−951.

(150) Trotta, M.; Debernardi, F.; Caputo, O. Preparation of solid lipid nanoparticles by a solvent emulsification-diffusion technique. *Int. J. Pharm.* **2003**, *257* (1−2), 153−160.

(151) Sjöström, B.; Bergenståhl, B. Preparation of submicron drug particles in lecithin-stabilized o/w emulsions I. Model studies of the precipitation of cholesteryl acetate. *Int. J. Pharm.* **1992**, *88* (1−3), 53−62.

(152) Trotta, M.; Gallarate, M.; Pattarino, F.; Morel, S. Emulsions containing partially water-miscible solvents for the preparation of drug nanosuspensions. *J. Controlled Release* **2001**, *76* (1−2), 119−128.

(153) Gamal, A.; Gad, S.; Gardouh, A. Formulation and pharmacokinetic evaluation of rifampicin solid lipid nanoparticles. *J. Res. Pharmacy* **2020**, *24*, 539.

(154) Roumi, S.; Tabrizi, M. H.; Eshaghi, A.; Abbasi, N. Teucrium polium extract-loaded solid lipid nanoparticles: A design and in vitro anticancer study. *J. Food Biochem* **2021**, *45* (9), No. e13868.

(155) Subramanian, P. Lipid-Based Nanocarrier System for the Effective Delivery of Nutraceuticals. *Molecules* **2021**, *26* (18), 5510.

(156) Das, S.; Ng, W. K.; Kanaujia, P.; Kim, S.; Tan, R. B. Formulation design, preparation and physicochemical characterizations of solid lipid nanoparticles containing a hydrophobic drug: effects of process variables. *Colloids Surf. B Biointerfaces* **2011**, *88* (1), 483−489.

(157) Khairnar, S. V.; Pagare, P.; Thakre, A.; Nambiar, A. R.; Junnuthula, V.; Abraham, M. C.; Kolimi, P.; Nyavanandi, D.; Dyawanapelly, S. Review on the Scale-Up Methods for the Preparation of Solid Lipid Nanoparticles. *Pharmaceutics* **2022**, *14* (9), 1886.

(158) Ding, S.; Anton, N.; Vandamme, T. F.; Serra, C. A. Microfluidic nanoprecipitation systems for preparing pure drug or polymeric drug loaded nanoparticles: an overview. *Expert Opin Drug Deliv* **2016**, *13* (10), 1447−1460.

(159) Liu, Y.; Yang, G.; Hui, Y.; Ranaweera, S.; Zhao, C. X. Microfluidic Nanoparticles for Drug Delivery. *Small* **2022**, *18* (36), No. e2106580.

(160) Pourabed, A.; Younas, T.; Liu, C.; Shanbhag, B. K.; He, L.; Alan, T. High throughput acoustic microfluidic mixer controls self-assembly of protein nanoparticles with tuneable sizes. *J. Colloid Interface Sci.* **2021**, *585*, 229−236.

(161) Maeki, M.; Kimura, N.; Sato, Y.; Harashima, H.; Tokeshi, M. Advances in microfluidics for lipid nanoparticles and extracellular vesicles and applications in drug delivery systems. *Adv. Drug Delivery Rev.* **2018**, *128*, 84−100.

(162) Maeki, M.; Uno, S.; Niwa, A.; Okada, Y.; Tokeshi, M. Microfluidic technologies and devices for lipid nanoparticle-based RNA delivery. *J. Controlled Release* **2022**, *344*, 80−96.

(163) Shepherd, S. J.; Issadore, D.; Mitchell, M. J. Microfluidic formulation of nanoparticles for biomedical applications. *Biomaterials* **2021**, *274*, 120826.

(164) Baby, T.; Liu, Y.; Middelberg, A. P.; Zhao, C.-X. *J. C. E. S. Fundamental studies on throughput capacities of hydrodynamic flow-focusing microfluidics for producing monodisperse polymer nanoparticles* **2017**, *169*, 128−139.

(165) Shepherd, S. J.; Warzecha, C. C.; Yadavali, S.; El-Mayta, R.; Alameh, M. G.; Wang, L. L.; Weissman, D.; Wilson, J. M.; Issadore, D.; Mitchell, M. J. Scalable mRNA and siRNA Lipid Nanoparticle Production Using a Parallelized Microfluidic Device. *Nano Lett.* **2021**, *21* (13), 5671−5680.

(166) Hood, R. R.; DeVoe, D. L.; Atencia, J.; Vreeland, W. N.; Omiatek, D. M. A facile route to the synthesis of monodisperse nanoscale liposomes using 3D microfluidic hydrodynamic focusing in a concentric capillary array. *Lab Chip* **2014**, *14* (14), 2403−2409.

(167) Ahn, G. Y.; Choi, I.; Ryu, T. K.; Ryu, Y. H.; Oh, D. H.; Kang, H. W.; Kang, M. H.; Choi, S. W. Continuous production of lipid nanoparticles by multiple-splitting in microfluidic devices with chaotic microfibrous channels. *Colloids Surf. B Biointerfaces* **2023**, *224*, 113212.

(168) Abstiens, K.; Goepferich, A. M. Microfluidic manufacturing improves polydispersity of multicomponent polymeric nanoparticles. *Journal of Drug Delivery Science and Technology* **2019**, *49*, 433−439.

(169) Precision Nanosystems. *NxGen TM - A Disruptive Technology Enabling Transformative Medicine.* https://www.precisionnanosystems.com/platform-technologies/nxgen.

(170) Hao, Y.; Seo, J. H.; Hu, Y.; Mao, H. Q.; Mittal, R. Flow physics and mixing quality in a confined impinging jet mixer. *AIP Adv.* **2020**, *10* (4), 045105.

(171) Tao, J.; Chow, S. F.; Zheng, Y. Application of flash nanoprecipitation to fabricate poorly water-soluble drug nanoparticles. *Acta Pharm. Sin B* **2019**, *9* (1), 4−18.

(172) Knauer. *Impingement Jets Mixing Skids for high-flow production of nanoparticles (LNP, microemulsions, etc.)*, 2022. https://www.knauer.net/en/Systems-Solutions/LNP_lipid_nanoparticles/impingement-jets-mixing-skids-for-high-flow-production-of-nanoparticles (accessed 21 Mar 2023).

(173) Warne, N.; Ruesch, M.; Siwik, P.; Mensah, P.; Ludwig, J.; Hripcsak, M.; Godavarti, R.; Prigodich, A.; Dolsten, M. Delivering 3 billion doses of Comirnaty in 2021. *Nat. Biotechnol.* **2023**, *41* (2), 183−188.

(174) Siekmann, B.; Westesen, K. Thermoanalysis of the recrystallization process of melt-homogenized glyceride nanoparticles. *Colloids Surf., B* **1994**, *3* (3), 159−175.

(175) Battaglia, L.; Gallarate, M. Lipid nanoparticles: state of the art, new preparation methods and challenges in drug delivery. *Expert Opinion on Drug Delivery* **2012**, *9* (5), 497−508.

(176) Souto, E. B.; Müller, R. H. Cosmetic features and applications of lipid nanoparticles (SLN, NLC). *Int. J. Cosmet Sci.* **2008**, *30* (3), 157−165.

(177) Bunjes, H.; Westesen, K.; Koch, M. H. J. Crystallization tendency and polymorphic transitions in triglyceride nanoparticles. *Int. J. Pharm.* **1996**, *129* (1), 159−173.

(178) Youshia, J.; Kamel, A. O.; El Shamy, A.; Mansour, S. Gamma sterilization and in vivo evaluation of cationic nanostructured lipid carriers as potential ocular delivery systems for antiglaucoma drugs. *Eur. J. Pharm. Sci.* **2021**, *163*, 105887.

(179) Gokce, E. H.; Sandri, G.; Bonferoni, M. C.; Rossi, S.; Ferrari, F.; Guneri, T.; Caramella, C. Cyclosporine A loaded SLNs: evaluation of cellular uptake and corneal cytotoxicity. *Int. J. Pharm.* **2008**, *364* (1), 76−86.

(180) Hou, X.; Zaks, T.; Langer, R.; Dong, Y. Lipid nanoparticles for mRNA delivery. *Nat. Rev. Mater.* **2021**, *6* (12), 1078−1094.

(181) Ma, G. J.; Yoon, B. K.; Sut, T. N.; Yoo, K. Y.; Lee, S. H.; Jeon, W. Y.; Jackman, J. A.; Ariga, K.; Cho, N. J. Lipid coating technology: A potential solution to address the problem of sticky containers and vanishing drugs. *View* **2022**, *3* (3), 20200078.

(182) Schoenmaker, L.; Witzigmann, D.; Kulkarni, J. A.; Verbeke, R.; Kersten, G.; Jiskoot, W.; Crommelin, D. J. A. mRNA-lipid nanoparticle COVID-19 vaccines: Structure and stability. *Int. J. Pharm.* **2021**, *601*, 120586.

(183) Jakubek, Z. J.; Chen, S.; Zaifman, J.; Tam, Y. Y. C.; Zou, S. Lipid Nanoparticle and Liposome Reference Materials: Assessment of Size Homogeneity and Long-Term −70 degrees C and 4 degrees C Storage Stability. *Langmuir* **2023**, *39* (7), 2509−2519.

(184) Hansen, L.; Daoussi, R.; Vervaet, C.; Remon, J.-P.; De Beer, T. Freeze-drying of live virus vaccines: a review. *Vaccine* **2015**, *33* (42), 5507−5519.

(185) Jakubek, Z. J.; Chen, S.; Zaifman, J.; Tam, Y. Y. C.; Zou, S. Lipid Nanoparticle and Liposome Reference Materials: Assessment of Size Homogeneity and Long-Term −70 and 4 °C Storage Stability. *Langmuir* **2023**, *39* (7), 2509−2519.

(186) Chen, J.; Chen, J.; Xu, Q. Current Developments and Challenges of mRNA Vaccines. *Annu. Rev. Biomed Eng.* **2022**, *24*, 85−109.

(187) Zhao, P.; Hou, X.; Yan, J.; Du, S.; Xue, Y.; Li, W.; Xiang, G.; Dong, Y. Long-term storage of lipid-like nanoparticles for mRNA delivery. *Bioactive Materials* **2020**, *5* (2), 358−363.

(188) Kim, J.; Eygeris, Y.; Gupta, M.; Sahay, G. Self-assembled mRNA vaccines. *Adv. Drug Deliv Rev.* **2021**, *170*, 83−112.

(189) https://www.ema.europa.eu/en/documents/product-information/covid-19-vaccine-moderna-epar-product-information_en.pdf (accessed 15 April 2023).

(190) Kim, B.; Hosn, R. R.; Remba, T.; Yun, D.; Li, N.; Abraham, W.; Melo, M. B.; Cortes, M.; Li, B.; Zhang, Y.; et al. Optimization of

storage conditions for lipid nanoparticle-formulated self-replicating RNA vaccines. *J. Controlled Release* **2023**, *353*, 241−253.

(191) Ramakanth, D.; Singh, S.; Maji, P. K.; Lee, Y. S.; Gaikwad, K. K. Advanced packaging for distribution and storage of COVID-19 vaccines: a review. *Environmental Chemistry Letters* **2021**, *19* (5), 3597−3608.

(192) Kramer, D. *A Revolutionary Glass Package Designed Specifically for Pharmaceutical Use.* https://www.corning.com/worldwide/en/products/pharmaceutical-technologies/valor-glass/revolutionary-glass-package-valor-pharmaceutical.html (accessed 15 April 2023).

(193) Weikart, C.; Langer, R. *A New Hybrid Material for Packaging COVID-19 Vaccines and Other Biologics: Combining the Best of Glass and Plastic*, October 28, 2020. https://www.americanpharmaceuticalreview.com/Featured-Articles/569163-A-New-Hybrid-Material-for-Packaging-COVID-19-Vaccines-and-Other-Biologics-Combining-the-Best-of-Glass-and-Plastic/ (accessed 15 April 2023).

(194) Ball, R. L.; Bajaj, P.; Whitehead, K. A. Achieving long-term stability of lipid nanoparticles: examining the effect of pH, temperature, and lyophilization. *Int. J. Nanomedicine* **2017**, *12*, 305−315.

(195) Foulkes, R.; Man, E.; Thind, J.; Yeung, S.; Joy, A.; Hoskins, C. The regulation of nanomaterials and nanomedicines for clinical application: current and future perspectives. *Biomater. Sci.* **2020**, *8* (17), 4653−4664.

(196) Bawa, R.; Audette, G. F.; Reese, B. *Handbook of Clinical Nanomedicine: Law, Business, Regulation, Safety, and Risk*; Jenny Stanford Publishing, 2016.

(197) Dokka, S.; Toledo, D.; Shi, X.; Castranova, V.; Rojanasakul, Y. Oxygen radical-mediated pulmonary toxicity induced by some cationic liposomes. *Pharm. Res.* **2000**, *17* (5), 521−525.

(198) Lv, H.; Zhang, S.; Wang, B.; Cui, S.; Yan, J. Toxicity of cationic lipids and cationic polymers in gene delivery. *J. Controlled Release* **2006**, *114* (1), 100−109.

(199) AlBaloul, A. Y.; Sato, Y.; Maishi, N.; Hida, K.; Harashima, H. Two Modes of Toxicity of Lipid Nanoparticles Containing a pH-Sensitive Cationic Lipid on Human A375 and A375-SM Melanoma Cell Lines. *BPB Reports* **2019**, *2* (4), 48−55.

(200) Uziely, B.; Jeffers, S.; Isacson, R.; Kutsch, K.; Wei-Tsao, D.; Yehoshua, Z.; Libson, E.; Muggia, F. M.; Gabizon, A. Liposomal doxorubicin: antitumor activity and unique toxicities during two complementary phase I studies. *Journal of Clinical Oncology* **1995**, *13* (7), 1777−1785.

(201) Skubitz, K. M.; Skubitz, A. P. Mechanism of transient dyspnea induced by pegylated-liposomal doxorubicin (Doxil). *Anti-cancer drugs* **1998**, *9* (1), 45−50.

(202) Chanan-Khan, A.; Szebeni, J.; Savay, S.; Liebes, L.; Rafique, N.; Alving, C.; Muggia, F. Complement activation following first exposure to pegylated liposomal doxorubicin (Doxil®): possible role in hypersensitivity reactions. *Annals of Oncology* **2003**, *14* (9), 1430−1437.

(203) Nagykálnai, T. [Non-pegylated doxorubicin (Myocet®) as the less cardiotoxic alternative of free doxorubicin]. *Magy Onkol* **2010**, *54* (4), 359−367.

(204) Wong-Beringer, A.; Jacobs, R. A.; Guglielmo, B. J. Lipid Formulations of Amphotericin B: Clinical Efficacy and Toxicities. *Clinical Infectious Diseases* **1998**, *27* (3), 603−618.

(205) Cook, G.; Franklin, I. M. Adverse drug reactions associated with the administration of amphotericin B lipid complex (Abelcet). *Bone Marrow Transplantation* **1999**, *23* (12), 1325−1326.

(206) Walsh, T. J.; Finberg, R. W.; Arndt, C.; Hiemenz, J.; Schwartz, C.; Bodensteiner, D.; Pappas, P.; Seibel, N.; Greenberg, R. N.; Dummer, S.; et al. Liposomal amphotericin B for empirical therapy in patients with persistent fever and neutropenia. *New England Journal of Medicine* **1999**, *340* (10), 764−771.

(207) *Linhaliq withdrawal assessment report*; European Medical Agency, 2019. https://www.ema.europa.eu/en/documents/withdrawal-report/withdrawal-assessment-report-linhaliq_en.pdf (accessed 28 July 2023).

(208) Money-Kyrle, J. F.; Bates, F.; Ready, J.; Gazzard, B. G.; Phillips, R. H.; Boag, F. C. Liposomal daunorubicin in advanced Kaposi's sarcoma: a phase II study. *Clin Oncol (R Coll Radiol)* **1993**, 5 (6), 367−371.

(209) Cabriales, S.; Bresnahan, J.; Testa, D.; Espina, B. M.; Scadden, D. T.; Ross, M.; Gill, P. S. Extravasation of liposomal daunorubicin in patients with AIDS-associated Kaposi's sarcoma: a report of four cases. *Oncol Nurs Forum* **1998**, 25 (1), 67−70.

(210) Bressler, N. M. Photodynamic Therapy of Subfoveal Choroidal Neovascularization in Age-Related Macular Degeneration With Verteporfin: Two-Year Results of 2 Randomized Clinical Trials—TAP Report 2. *Archives of Ophthalmology* **2001**, *119* (2), 198−207.

(211) Morita, A.; Namkoong, H.; Yagi, K.; Asakura, T.; Hosoya, M.; Tanaka, H.; Lee, H.; Ogawa, T.; Kusumoto, T.; Azekawa, S.; et al. Early-phase adverse effects and management of liposomal amikacin inhalation for refractory Mycobacterium avium complex lung disease in real-world settings. *Infection and Drug Resistance* **2022**, *Volume 15*, 4001−4011.

(212) Schiffelers, R.; Storm, G.; Bakker-Woudenberg, I. Liposome-encapsulated aminoglycosides in pre-clinical and clinical studies. *J. Antimicrob. Chemother.* **2001**, *48* (3), 333−344.

(213) *ABRAXANE for Injectable Suspension (paclitaxel protein-bound particles for injectable suspension) (albumin-bound)*; FDA. https://www.accessdata.fda.gov/drugsatfda_docs/label/2012/021660s031lbl.pdf (accessed 28 July 2023).

(214) Bawa, R. Regulating nanomedicine - can the FDA handle it? *Curr. Drug Deliv* **2011**, 8 (3), 227−234.

(215) Haynes, B. F. A New Vaccine to Battle Covid-19. *N Engl J. Med.* **2021**, *384* (5), 470−471.

(216) Wang, Y.; Grainger, D. W. Regulatory considerations specific to liposome drug development as complex drug products. *Frontiers in Drug Delivery* **2022**, 2, 10.

(217) Let's talk about lipid nanoparticles. *Nat. Rev. Mater.* **2021**, *6* (2), 99.

(218) Roces, C. B.; Lou, G.; Jain, N.; Abraham, S.; Thomas, A.; Halbert, G. W.; Perrie, Y. Manufacturing Considerations for the Development of Lipid Nanoparticles Using Microfluidics. *Pharmaceutics* **2020**, *12* (11), 1095.

(219) Aftaab, S. U.; Ali, S. A. *Liposome Drug Products: Chemistry, Manufacturing, and Controls; Human Pharmacokinetics and Bioavailability; and Labeling Documentation. Guidance for Industry*; FDA, 2021 (acccessed 3 Apr 2023).

(220) Chen, M.; Liu, X.; Fahr, A. Skin penetration and deposition of carboxyfluorescein and temoporfin from different lipid vesicular systems: In vitro study with finite and infinite dosage application. *Int. J. Pharm.* **2011**, *408* (1−2), 223−234.

(221) Amrani, S.; Tabrizian, M. Characterization of Nanoscale Loaded Liposomes Produced by 2D Hydrodynamic Flow Focusing. *ACS Biomater Sci. Eng.* **2018**, *4* (2), 502−513.

(222) Roberts, S. A.; Parikh, N.; Blower, R. J.; Agrawal, N. SPIN: rapid synthesis, purification, and concentration of small drug-loaded liposomes. *J. Liposome Res.* **2018**, *28* (4), 331−340.

(223) Kimura, N.; Maeki, M.; Sato, Y.; Ishida, A.; Tani, H.; Harashima, H.; Tokeshi, M. Development of a Microfluidic-Based Post-Treatment Process for Size-Controlled Lipid Nanoparticles and Application to siRNA Delivery. *ACS Appl. Mater. Interfaces* **2020**, *12* (30), 34011−34020.

(224) Smiatek, J.; Jung, A.; Bluhmki, E. Towards a Digital Bioprocess Replica: Computational Approaches in Biopharmaceutical Development and Manufacturing. *Trends Biotechnol* **2020**, *38* (10), 1141−1153.

(225) Valencia, P. M.; Farokhzad, O. C.; Karnik, R.; Langer, R. Microfluidic technologies for accelerating the clinical translation of nanoparticles. *Nat. Nanotechnol* **2012**, 7 (10), 623−629.

(226) Scioli Montoto, S.; Muraca, G.; Ruiz, M. E. Solid Lipid Nanoparticles for Drug Delivery: Pharmacological and Biopharmaceutical Aspects. *Front Mol. Biosci* **2020**, 7, 587997.
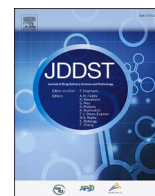
Targeted polymer lipid hybrid nanoparticles for *in-vitro* siRNA therapy in triple-negative breast cancer

Meenu Mehta [a], Thuy Anh Bui [a], Andrew Care [b], Wei Deng [a,*]

[a] *School of Biomedical Engineering, University of Technology Sydney, Ultimo, NSW, 2007, Australia*
[b] *School of Life Sciences, University of Technology Sydney, Ultimo, New South Wales, 2007, Australia*

ARTICLE INFO

ABSTRACT

Triple-negative breast cancer (TNBC) is an aggressive subtype of breast cancer, characterised by a lack of hormone receptors and HER2 expression, resulting in limited treatment options and poor patient outcomes. This study explores a novel therapeutic approach using PLGA lipid nanoparticles loaded with siXBP1 and conjugated with an epidermal growth factor receptor (EGFR) antibody. This nanncarrier will silence the XBP1 gene, which is crucial for the progression and survival of TNBC, particularly in hypoxic conditions. The conjugation of nanoparticles with the EGFR antibody improves their targeting ability to TNBC cells, as confirmed by confocal microscopy and flow cytometry. The fluorescence intensity of the targeted nanoparticles was 1.45 times higher than that of the non-targeted counterparts. These nanoparticles efficiently delivered siRNA to TNBC cells, resulting in substantial XBP1 gene silencing efficacy of 75 %. Under hypoxic conditions, this gene silencing effect significantly promoted apoptosis by nearly threefold compared to normoxic conditions. These findings provide valuable insights into targeted therapies for TNBC and pave the way for further *in vivo* investigations to advance this approach toward clinical applications.

1. Introduction

Among all breast cancer subtypes, triple-negative breast cancer (TNBC) stands out as the most aggressive, comprising approximately 15 % of cases. It is characterized by the absence of human epidermal growth factor receptors 2 (HER2), progesterone receptors, and estrogen receptors [1]. TNBC is associated with a high recurrence rate and limited survival, with a 40 % mortality rate within five years of diagnosis [1][]. After metastasis, the average survival time is just 12.2 months, and the postoperative recurrence rate is approximately 25 % [2]. Chemoradiotherapy stands as the standard of care for TNBC, yet its constraints involve drug toxicity, resistance, and late morbidity linked to high-dose radiation [3]. Due to the lack of targeted therapies specific to TNBC, there is a pressing need for innovative approaches to enhance patient outcomes [4–6].

To address this challenge, XBP1 emerges as a key driver of TNBC tumor growth and recurrence, primarily by regulating the ER stress response and unfolded protein pathways, impacting cell survival, proliferation, and chemoresistance [7,8]. Elevated XBP1 expression is frequently associated with TNBC, promoting these detrimental effects and contributing to a poor prognosis and treatment resistance [9].

Notably, a connection between XBP1 and reduced TNBC responsiveness to standard treatments is well-established [9]. Analysis of 193 TNBC patient samples revealed shorter relapse-free survival in cases with an elevated XBP1 signature [10].

Hypoxia-inducing factor 1α (HIF-1α) is known to be hyperactivated in the hypoxic microenvironment of human tumors including TNBC [11]. XBP1 has been identified to regulate tumorigenicity by controlling the HIF-1α pathway [10,12]. It can boost the stability and activity of HIF-1α, resulting in the activation of genes that support angiogenesis, glycolysis and cell survival [10,13]. XBP1 knockdown may offer a promising therapeutic approach in TNBC, particularly in hypoxic conditions. However the challenge remains in achieving precise and efficient gene silencing within TNBC cells due to limited drug delivery options.

Given significant roles of XBP1 in driving TNBC tumor growth and recurrence, specific XBP1 inhibition in TNBC tumor is a potential therapeutic approach which relies on two key challenges: basis of genetic approach and efficiency delivery vehicles specific to target cells. In the context of XBP1 gene knockdown, small interfering RNA (siRNA) offers a promising strategy for targeted gene silencing in TNBC treatment. By leveraging the RNA interference (RNAi) pathway, siRNA can selectively

---

* Corresponding author.
  E-mail address: wei.deng@uts.edu.au (W. Deng).

downregulate crucial genes, inhibiting tumor growth and overcoming treatment resistance [14]. Regarding delivery vehicles, nanoparticle-based drug delivery systems, including lipid nanoparticles with polymers like Poly (lactic-co-glycolic acid) (PLGA), are advantageous for cancer therapy [15,16]. They are noted for their biocompatibility, controlled drug release, and capacity to encapsulate diverse therapeutic agents, such as siRNA [17,18]. Within PLGA lipid nanoparticle, the lipid component ensures stability, biocompatibility, and enhanced cellular uptake via intracellular delivery of therapeutic contents, while the PLGA polymer enables controlled release and safeguards the encapsulated siRNA cargo [19].

The goal of this study was to devise a targeted therapeutic strategy for triple-negative breast cancer (TNBC) by engineering epidermal growth factor receptor (EGFR) antibody conjugated siXBP1 loaded PLGA lipid nanoparticles. We selected the EGFR antibody due to its elevated expression in TNBC, aiming to enhance siRNA delivery specificity [20].

To achieve this goal, we first characterized the synthesized nanoparticles for their particle size, zeta potential, and surface morphology, ensuring suitability for TNBC targeted delivery. Next, we examined the cellular uptake of the EGFR antibody-conjugated PLGA lipid nanoparticles in TNBC cells (MDA-MB-231) using confocal microscopy and flow cytometry as assessment of nanoparticle internalization. We confirmed EGFP gene silencing in HEK293-EGFP cells by encapsulating EGFP siRNA for confocal microscopy analysis prior to validation of XBP1 gene silencing in MDA-MB-231 cells with siXBP1-loaded PLGA lipid nanoparticles by qRT-PCR and Western Blot. Finally, we evaluated the effect of XBP1 gene knockdown with EGFR antibody-siXBP1-loaded PLGA lipid nanoparticles on cell survival and apoptosis in MDA-MB-231 cells under hypoxic conditions, highlighting the potential of our nanoparticles as a promising therapeutic approach for TNBC.

2. Materials and methods

2.1. Materials

Poly(D,L-lactide-co-glycolide) acid terminated, lactide:glycolide 50:50 (PLGA) (719,870-5G), Mw 24,000–38000, Poly vinyl alcohol (PVA) (P8136), MW 30,000–70,000, Coumarin-6 (C-6) (442,631-1G) were purchased from Sigma-Aldrich Pty Ltd (Australia). DOTAP (890890 P-200 mg) and 1,2-distearoyl-*sn*-glycero-3-phosphoethanol-amine-N-[maleimide(polyethylene glycol)-2000] (ammonium salt) (DSPE-PEG2000-Mal) (880126p-25mg) were purchased from Avanti Polar Lipids. Chloroform (C2432–500 mL), Dichloromethane (270,997-1 L), Phosphate buffered saline (P4417-50 TAB) were also purchased from Sigma-Aldrich Pty Ltd (Sydney, Australia). Human anti-EGFR antibody (cetuximab, C225) was purchased from Assay Matrix Pty Ltd (Melbourne, Australia). Scramble siRNA (siScr -SIC001) was purchased from Merck, Australia and siRNA targeting EGFP (siGFP-51-01-05-06) was purchased from Integrated DNA Technologies, Australia. siRNA targeting XBP1 (s14913), Lipofectamine RNAiMax transfection reagent (13,778,075), Opti-Minimal Essential Medium (Opti-MEM; reduced serum medium; product, 31,985,062), Pierce™ Coomassie (Bradford Protein Assay Kit) (23,200) were purchased from (Thermo Fisher Scientific, Australia). MTT (3-[4,5-dimethylthiazol-2-yl]-2,5-diphenyl tetrazolium bromide), Dimethyl sulfoxide (DMSO), DAPI were purchased from Sigma-Aldrich, St. Louis, MO, USA. FITC Annexin V Apoptosis Detection Kit I (cat. no. 556547) was purchased from BD Biosciences (San Jose, CA, USA). The antibodies to XBP1 and β-actin were purchased from Abcam. All the remaining chemical reagents and solvents were purchased from Sigma-Aldrich unless stated.

2.2. Cell culture

MDA-MB-231 and MCF-7 cell lines were a kind gift from Prof. Majid Ebrahimi Warkiani lab, School of Biomedical Engineering, University of

Table 1
Composition of different PLGA lipid nanoparticles.

S. No.	Formulation	Cargo amount	PLGA/DOTAP ratio (w/w)	PVA (% w/v)	DSPE-PEG2000-Mal (mg)
1.	Blank PLGA lipid nanoparticles	–	7:3	1	0.3
2.	Coumarin-6 loaded nanoparticles (C-6 NPs)	17.5 μg	7:3	1	0.3
3.	EGFP siRNA loaded nanoparticles (siEGFP NPs)	100 pmole	7:3	1	0.3
4.	Scramble siRNA loaded nanoparticles (Scr NPs)	200 pmole	7:3	1	0.3
5.	siXBP1 (siRNA) loaded nanoparticles	200 pmole	7:3	1	0.3

Technology Sydney, Australia. These cells were cultured in Dulbecco's Modified Eagle's Medium (DMEM) (Sigma-Aldrich Pty Ltd, Australia) with 10 % heat-inactivated Fetal Bovine Serum (Thermo Fisher Scientific, Australia) at 37 °C at 5 % CO_2 in a humidified atmosphere. Human mammary epithelial cells (HMEC) and Human embryonic kidney 293 cells expressing EGFP (HEK 293-EGFP) were a kind gift from Prof. Ewa Goldys lab, School of Biomedical Engineering, University of New South Wales, Australia. HMEC were cultured in HMEC growth medium while HEK 293-EGFP cells were cultured in DMEM with10 % heat-inactivated Fetal Bovine Serum under standard conditions (37 °C, 5 % CO_2) in a humidified incubator. All cells were frequently tested for the presence of mycoplasma, and all experiments were carried out in mycoplasma negative cells.

2.3. Methods

2.3.1. Preparation of PLGA lipid nanoparticles

PLGA lipid nanoparticles were prepared using the double emulsion-solvent evaporation technique [18]. The formulation was optimized including the particle size, zeta potential and polydispersity index (PDI) based on DOTAP/PLGA ratio, sonication time and polyvinyl alcohol (PVA) concentration. In brief, 200 pmole of siRNA was added dropwise to 500 μl of PLGA/DOTAP mixture (mole ratio of 7:3) in dichloromethane (DCM). This mixture was emulsified using probe sonication over an ice bath at 40 % amp for 30 s (3 times) to form the primary emulsion. Subsequently, 6 ml of 1 % (w/v) PVA containing 0.3 mg of DSPE-PEG2000-Mal was added to the primary emulsion, followed by sonication at 40 % amp for 30 s (3 times) over an ice bath. This process resulted in the formation of the secondary water-in-oil-in-water emulsion, which was left under agitation for 3 h at room temperature to evaporate organic solvent. Afterwards, the dispersion was centrifuged for 12 min at 4 °C and 18,000×*g*. The supernatant was discarded, and the pellet containing the nanoparticles was re-dispersed in phosphate buffer saline (PBS). This process of centrifugation and re-dispersion was repeated three times to ensure the removal of PVA before further characterisation. We employed the same method to prepare various types of PLGA lipid nanoparticles, by encapsulating different cargoes (coumarin-6 (a dye), EGFP siRNA, scramble siRNA). The formulation details are listed in Table 1.

2.3.1.1. Antibody conjugation to nanoparticles. Antibody conjugation to nanoparticles was achieved through a thiol-maleimide reaction [21]. Initially, 10 μl EGFR antibody (1 mg/ml stock solution in PBS) was diluted with 990 μl of PBS (pH 7.4). Simultaneously, 1 mg of N-Succinimidyl S-Acetylthioacetate (SATA) was dissolved in 0.5 ml of dimethyl sulphoxide (DMSO) just before the reaction. The EGFR antibody solution was then mixed with SATA solution at a molar ratio of 8:1 (SATA: antibody) and incubated at room temperature for 30 min. To facillitate

SATA crosslinking with maleimide groups, the sulfhydryl groups were deacetylated by mixing the SATA/antibody solution with 100 μl of hydroxylamine solution (0.5 M Hydroxylamine, 25 mM EDTA in PBS, pH 7.2–7.5) and incubated for 1 h at room temperature. Subsequently, conjugation was initiated by combining nanoparticles with the SATA/antibody solution at a molar ratio of 1:10 (nanoparticles: SATA/antibody solution) and incubated at room temperature for 2 h, followed by overnight incubation at 4 °C. Unbound antibody was removed through centrifugation, and the nanoparticle pellet was redispersed in PBS for further applications.

2.3.1.2. Quantification of EGFR antibody conjugated onto the surface of nanoparticles. The amount of EGFR antibody conjugated to the nanoparticle surface was confirmed by Bradford assay, which was based on the binding of coomassie brilliant blue dye (Bradford reagent) to proteins, resulting in a color change proportional to the protein concentration. Following the manufacturer's protocol, various concentrations of the protein standard solution, ranging from 25 μg/mL to 2000 μg/mL, were prepared in PBS buffer. Next, 5 μL of each standard or nanoparticle suspension was carefully transferred to the appropriate wells of a microplate. Subsequently, 250 μL of the Bradford reagent was added to

Table 2
Primer sequences used for qRT-PCR.

Primer	Sequence
XBP1 - Forward	5′- AGGAGTTAAGACAGCGCTTGGGGATGGAT-3′
XBP1 - Reverse	5′-CTGAATCTGAAGAGTCAATACCGCCAGAAT-3′
Beta actin – Forward	5′-CCTGTACGCCAACACAGTGC-3′
Beta actin – Reverse	5′-ATACTCCTGCTT GCTGATCC-3′

siRNA concentration used in the nanoparticle preparation.

In details, various concentrations of pure siRNA solution (ranging from 5 ng/mL to 200 ng/mL) were prepared using TE buffer. Subsequently, 20 μL pure siRNA solution and the supernatant were added to wells of a microplate, followed by thorough pipetting. The microplate was incubated for 20 min at room temperature, shielded from light. After incubation, fluorescence was measured using a microplate reader (Ex/Em: 480 nm/535 nm). The concentration of siRNA in the supernatant was determined by comparing it to the standard curve of a free siRNA solution. The entrapment efficiency was calculated using the following equation:

$$\%EE = \frac{(\text{RNA amount used for formulation} - \text{RNA amount present in supernatant })}{\text{RNA amount used for formulation}} \times 100$$

each well, and the plate was incubated for 10 min at room temperature. The absorbance was measured at 595 nm using a Tecan plate reader. The amount of conjugated antibody was determined by assessing the absorbance intensity and subsequently calculating its concentration using the standard curve of free protein solution.

2.3.2. Nanoparticle characterization

Particle size, polydispersity index (PDI), and zeta potential measurements were carried out using Dynamic Light Scattering (Malvern Zetasizer Nano ZS). Before analysis, the nanoparticle suspension was resuspended, sonicated, and vortexed. For particle size and PDI measurement, diluted samples were placed in clear disposable cuvettes, while zeta cells were utilized for zeta potential measurement. All measurements were performed in triplicate at 25 °C. The surface morphology of nanoparticles was examined by using Scanning Electron Microscopy (SEM, Zeiss Supra 55 VP). For SEM imaging, nanoparticles were suspended in nuclease-free water (100 μl/ml) and sonicated for 30 s. A drop of this suspension was deposited on a silicon wafer and allowed to air dry for 24 h under ambient conditions. The silicon wafer was then attached to a stub using double-sided carbon tape. To ensure conductivity, the nanoparticles were sputtered with gold/palladium using the Leica Coater prior to image acquisition.

2.3.3. Entrapment efficiency (EE)

The amount of coumarin-6 (C-6) encapsulated within the nanoparticles was determined by assessing the fluorescence intensity of the C-6-loaded nanoparticles (C-6 NPs) (Ex/Em: 450 nm/505 nm) and subsequently calculating its concentration using the standard curve derived from a free C-6 solution.

The entrapment efficiency of siRNA loaded inside the nanoparticles was determined using RediPlate 96 Ribogreen RNA Kit (Thermo Fisher Scientific, Australia). The RiboGreen® reagent specifically reacts with free siRNA, producing a fluorescent compound with an emission maximum at 535 nm ($\lambda ex = 485$ nm). Thus, to assess entrapment efficiency, the prepared nanoparticle suspension was centrifuged and the supernatant was collected. The unloaded siRNA in the supernatant was then measured using the Ribogreen RNA Kit and compared to the initial

2.3.4. Cellular uptake activity

Cellular uptake activity was assessed by using C-6 NPs and EGFR antibody conjugated C-6 nanoparticles (EGFR Ab-C-6 NPs). Briefly, 5×10^4 MDA-MB-231 cells were cultured overnight in glass-bottom petri dishes and incubated with nanoparticle suspension (200 μg/ml) for 1 and 2 h, respectively. Subsequently, the cells were thoroughly washed with DPBS (pH 7.4) three times to eliminate any unbound nanoparticles and then fixed using 4 % paraformaldehyde (100 μl) at room temperature. After fixation, the cells were stained with DAPI (Sigma) reagent, and the internalization of nanoparticles was visualized using a Nikon A1 inverted confocal microscope system. Additionally, flow cytometry analysis was performed after the nanoparticle incubation. The cells were washed, trypsinized, collected, and their fluorescence was quantitatively analyzed using a CytoFLEX LX flow cytometer (Beckman Coulter).

2.3.5. XBP1 expression level in normal vs breast cancer cell lines and under hypoxia conditions

To evaluate XBP1 gene expression, we selected two breast cancer cell lines, MDA-MB-231 and MCF-7, along with one normal mammary epithelial cell line (HMEC). To induce hypoxia, MDA-MB-231 cells were placed in hypoxic chamber for 24 h or 48 h. After each incubation period, RNA and proteins were isolated from cells and analyzed for XBP1 gene expression.

2.3.5.1. RNA extraction. RNA samples were isolated using the Trizol® method [22]. Initially, the cells underwent a brief wash in PBS, followed by transfer into nuclease-free Eppendorf tubes. Subsequently, they were centrifuged at 12,000×*g* at 4 °C for 10 min. The resulting cell pellets were then combined with 1 ml of Trizol® (Invitrogen), and 300 μl was added, after which the mixture was incubated at room temperature for 3 min. After this, the samples were subjected to phase separation by centrifuging at 12,000×*g* at 4 °C for 10 min. The upper aqueous layer, containing the RNA, was carefully transferred to new tubes containing 600 μl of ice-cold isopropanol (Sigma, Australia). RNA precipitation was facilitated by centrifuging for 30 min at 12,000×*g* and 4 °C. The RNA pellets were briefly washed in 1 ml of 70 % ethanol and again centrifuged at 12,000×*g* at 4 °C for 10 min. Following this step, the ethanol
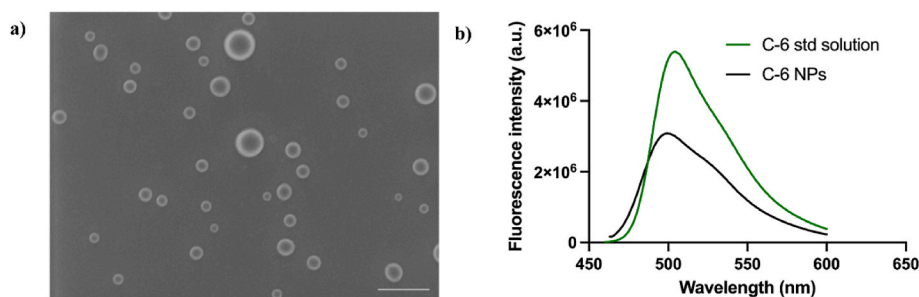
Fig. 1. a) The SEM image of blank PLGA lipid nanoparticles (Scale bar = 200 nm); b) Fluorescence emission spectra of coumarin-6 solution (C-6 std solution) and coumarin-6 loaded nanoparticles (C-6 NPs).

was removed, and the RNA pellet was dried on a 37 °C heat block for 5 min. Finally, the resulting RNA pellet was resuspended in 40 μl of nuclease-free water. RNA concentration was measured via absorbance at 260 nm by Nanodrop™ One Microvolume UV–Vis spectrophometer (Thermo Fisher Scientific, Australia).

2.3.5.2. qRT-PCR. All the primers utilized in the quantitative PCR reactions for this study were purchased from Sigma-Aldrich. In summary, a quantity of RNA samples less than 1 μg was employed for both cDNA conversion and the qPCR reaction, employing the Luna® Universal One-Step RT-qPCR Kit from New England Biolabs. The qPCR reactions were conducted according to the manufacturer's protocol. The primer sequences used for these reactions are detailed in Table 2.

2.3.5.3. Protein extraction. Cell samples were gathered in RIPA Lysis buffer, which included Halt™ Protease Inhibitor Cocktail (Thermo Fisher Scientific, Australia). They were left to incubate on ice for 20 min before undergoing a short 15-s sonication. Subsequently, the cell lysates were subjected to centrifugation at $12,000 \times g$ at 4 °C for 20 min to eliminate cellular debris. The protein concentration of each sample was assessed via absorbance at 280 nm using the NanoDrop™ Microvolume UV–Vis Spectrophotometer (Thermo Fisher Scientific, Australia).

2.3.5.4. Western blot assay. Briefly, 30 μg of each protein lysate was combined with 5 μl of NuPAGE LDS Sample Buffer and heated at 70 °C for 10 min. All prepared samples were subsequently loaded into NuPAGE 4–12 % Bis-Tris 1.5 mm Mini Protein Gels secured within the XCell SureLock™ Mini-Cell. The loaded protein samples were then separated in 1 × NuPAGE MOPS SDS Running Buffer at 125 V for 90 min.

After the gel electrophoresis, the protein samples were transferred onto a 0.2 μm PVDF Transfer Membrane using the XCell Blot Module and 1 × NuPAGE Transfer Buffer at 30 V for 120 min. The membranes were subsequently immersed in a blocking solution (3 % w/v Bovine Serum Albumin from Sigma in TTBS buffer, which consists of 0.01 M Tris Base, 0.05 M NaCl, and 0.1 % Tween20) for 1 h at room temperature to prevent non-specific binding.

Membrane incubation with primary antibodies (XBP1 or Beta-actin from Abcam, each at a 1:1000 dilution in TTBS) was carried out at 4 °C overnight. After three 5-min washes in TTBS buffer, the membranes were incubated in an anti-rabbit horse peroxidase-conjugated secondary antibody (CST, diluted at 1:5000 in TTBS) on an orbital shaker at room temperature. Following this, the membranes were washed in TTBS buffer for 5 min each and then visualized using Pierce™ ECL Western Blotting Substrate (Thermo Fisher Scientific, Australia) under a ChemiDoc MP System (Biorad, USA).

2.3.6. Assessment on in vitro EGFP and XBP1 knockdown via siRNA-loaded nanoparticles

HEK293-EGFP cells were cultured at a density of 5×10^4 in glass-bottom petri dishes and then incubated with the siGFP-loaded

nanoparticle suspension (10 nM) for 24 and 48 h. Subsequently, the cells were imaged under a confocal microscope to assess EGFP fluorescence signal. Additionally, flow cytometry analysis was performed as indicated in the above section.

MDA-MB-231 cells were seeded at a density of 1×10^5 cells per well in a 6-well plate and incubated for 24 h. Following this, the cells were treated with various conditions for an additional 48 h. The treatment conditions included: cells only, free siRNA alone, siRNA transfected with RNAiMax transfection reagent, EGFR antibody conjugated siXBP1-loaded nanoparticles (EGFR Ab-siXBP1 NPs) and EGFR antibody conjugated siScr-loaded nanoparticles (EGFR Ab-Scr NPs). All these samples contain 25 nM siXBP1 or siScr. After incubation period, cellular RNA was collected using the same method followed by RT-PCR analysis.

2.3.7. In-vitro cell viability assay

Cells were seeded at a density of 1×10^4 cells per well in 96-well plates with culture medium containing 10 % FBS for 24 h. After 24 h, the cells were treated with different concentrations of nanoparticles (200–400 μg/ml) for 48 h. Following this treatment period, 10 μl of Thiazolyl Blue Tetrazolium Bromide (Sigma) at a concentration of 5 mg/ml in sterile PBS was added to each well and incubated for 4 h at 37 °C in 5 % CO$_2$. After removing the supernatant, 100 μL of DMSO was added to dissolve the formazan crystals, resulting in the formation of a purple-colored product. The absorbance of this product was measured using a Tecan plate reader at 570 nm. The cell viability was calculated as a percentage of the absorbance in the treated cells compared with that of untreated cells, as follows:

$$\text{Viability (\%)} = (A_g - A_{blank})/(A_c - A_{blank}) \times 100$$

Where A_g is the absorbance of each group, A_c is the absorbance of the control group and A_{blank} is the absorbance of cell culture medium.

2.3.8. Cellular apoptosis assay

For apoptosis assays, 1×10^5 cells per well were seeded into 6-well plates in two separate sets. One set was incubated in normal incubator while the other was placed in hypoxic chamber for 48 h to induce hypoxia. After the respective incubation periods, the cells were exposed to EGFR Ab-siXBP1 NPs and EGFR Ab-siScr NPs maintained for an additional 48 h within the hypoxic chamber. The treatment groups consisted of control (cells only), cells treated with antibody-conjugated siXBP1 loaded nanoparticles, and cells treated with antibody-conjugated siScr-loaded nanoparticles. After 48 h of treatment, apoptosis was quantified using the FITC Annexin V Apoptosis Detection Kit I (cat. no. 556547; BD Biosciences) following the manufacturer's instructions. Cells were harvested and washed twice with PBS. Subsequently, 1×10^6 cells were resuspended in 100 μl of 1 × binding buffer (diluted with ddH$_2$O), followed by the addition of 5 μl FITC and 5 μl PI to each tube. The samples were incubated for 30 min at room temperature in darkness. After staining, 500 μl of 1 × binding buffer was added to each tube and analyzed by flow cytometry. Similar experiments were conducted under non-hypoxic conditions.

Table 3
Characterization of prepared PLGA lipid nanoparticles.

Samples	Particle size (nm)	PDI	Zeta Potential (mV)	Entrapment Efficiency (%)
Blank PLGA lipid nanoparticles	163 ± 2.02	0.05 ± 0.02	25.9 ± 0.25	–
Coumarin-6 loaded nanoparticles (C-6 NPs)	186.08 ± 7.1	0.06 ± 0.03	19.4 ± 0.37	73.37 ± 1.7
EGFP siRNA loaded nanoparticles (siGFP NPs)	178.9 ± 9.2	0.05 ± 0.02	14.2 ± 0.15	94.92 ± 2.9
EGFR antibody-conjugated Coumarin-6 loaded nanoparticles (EGFR Ab-C-6 NPs)	209.2 ± 1.3	0.25 ± 0.03	−2.92 ± 0.37	56.11 ± 1.4
EGFR antibody-conjugated siXBP1 loaded nanoparticles (EGFR Ab-siXBP1 NPs)	226.7 ± 8.7	0.35 ± 0.02	−3.08 ± 0.17	82.96 ± 2.4
EGFR antibody- conjugated siScr loaded nanoparticles (EGFR Ab-Scr NPs)	208.9 ± 4.5	0.14 ± 0.05	−0.791 ± 0.14	83.45 ± 2.8

3. Results

3.1. Preparation and characterization of nanoparticles

In this study, lipid polymer hybrid nanoparticles were prepared via double emulsion solvent evaporation technique. The morphology of prepared nanoparticles was evaluated under SEM. Fig. 1a revealed that the blank nanoparticles had a spherical shape with an average size 150 ± 7.4 nm. From DLS measurements, the average size of blank nanoparticles, C-6 loaded nanoparticles and EGFP siRNA loaded nanoparticles was about 163 ± 2.02 nm, 186.08 ± 7.1 nm, and 178.9 ± 9.2 nm, respectively (Table 3). These samples exhibited a positively charged surface, and their low polydispersity index (PDI) indicated that they were uniform in size and monodispersed.

To enhance the ability of the nanoparticles to target cancer cells, we attached targeting molecules, EGFR antibody to the surface of the nanoparticles. For conjugated samples, we observed a slight increase in size, changing from 186.08 ± 7.1 nm to 209.2 ± 1.3 nm. There was also a concurrent increase in PDI from 0.05 ± 0.02 to 0.35 ± 0.02 (Table 3).

These changes fall within acceptable thresholds, indicating a homogeneous nanoparticle population [23]. In order to quantify the amount of EGFR antibody conjugated with the nanoparticles, a colorimetric Bradford protein assay was performed, with about 68.8 % of EGFR antibody being successfully conjugated with the nanoparticles. This finding closely aligns with other reported studies [24].

We further assessed the cargo loading efficacy of these nanoparticles. As shown in Fig. 1b, there was a typical fluorescence peak at 505 nm wavelength of the C-6 observed in C-6 loaded nanoparticles, indicating the successful loading of C-6 within the nanoparticles. For C-6 NPs, the entrapment efficiency was calculated to be 73.37 % (Table 3). For conjugated nanoparticles, the entrapment efficiency was reduced to 56.11 % (Table 3), possibly attributed to losses incurred during the secondary centrifugation step carried out after antibody conjugation. Regarding siRNA, the highest loading efficiency of 94.92 % was observed in siGFP nanoparticles. This could be attributed to the electrostatic interactions between the positively charged lipid compound and the negatively charged siRNA.
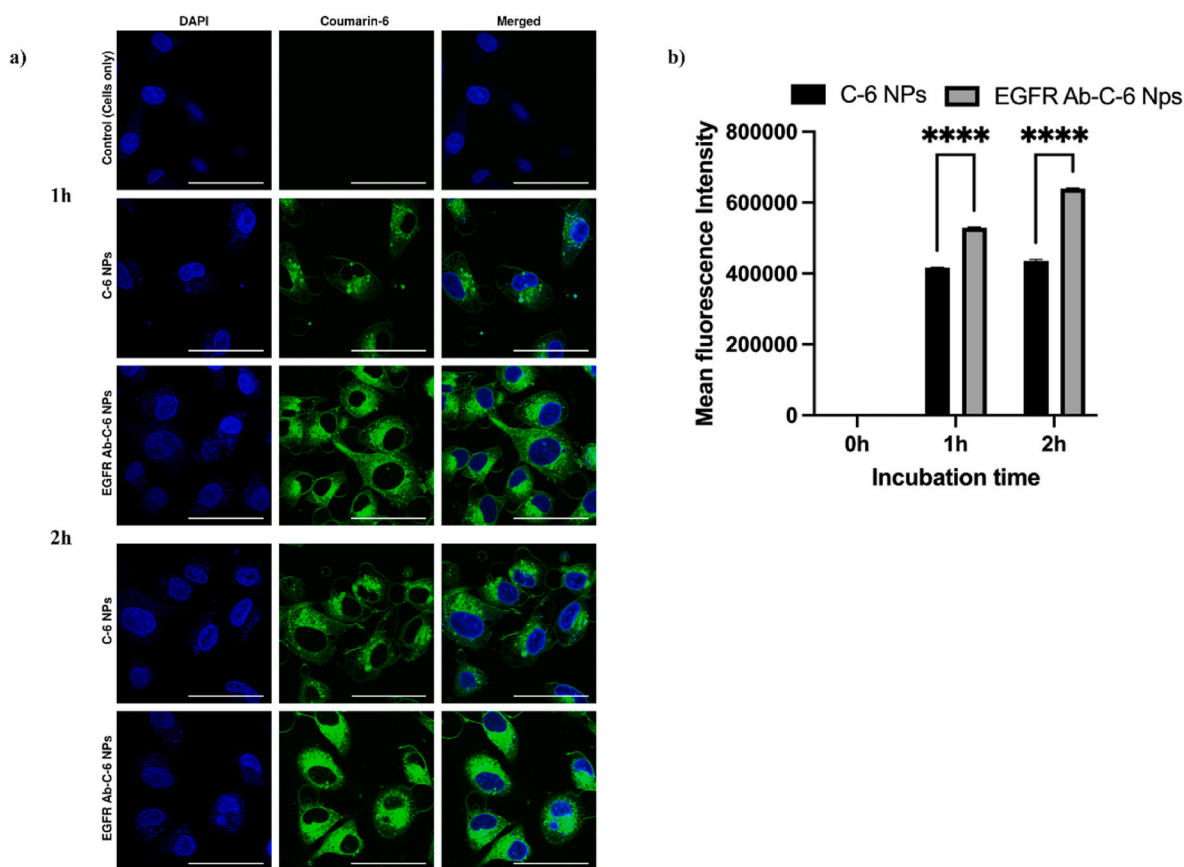

Fig. 2. a) Confocal microscopic images of MDA-MB-231 cells after incubation with C-6 NPs and EGFR AB-C-6 NPs; The scale bar is 50 μm b) The mean fluorescence intensity of C-6 in MDA-MB-231 cells treated with C-6 NPs and EGFR AB-C-6 NPs measured by flow cytometry. Data represented as mean ± s.e.m., (n = 3). ****p < 0.0001.
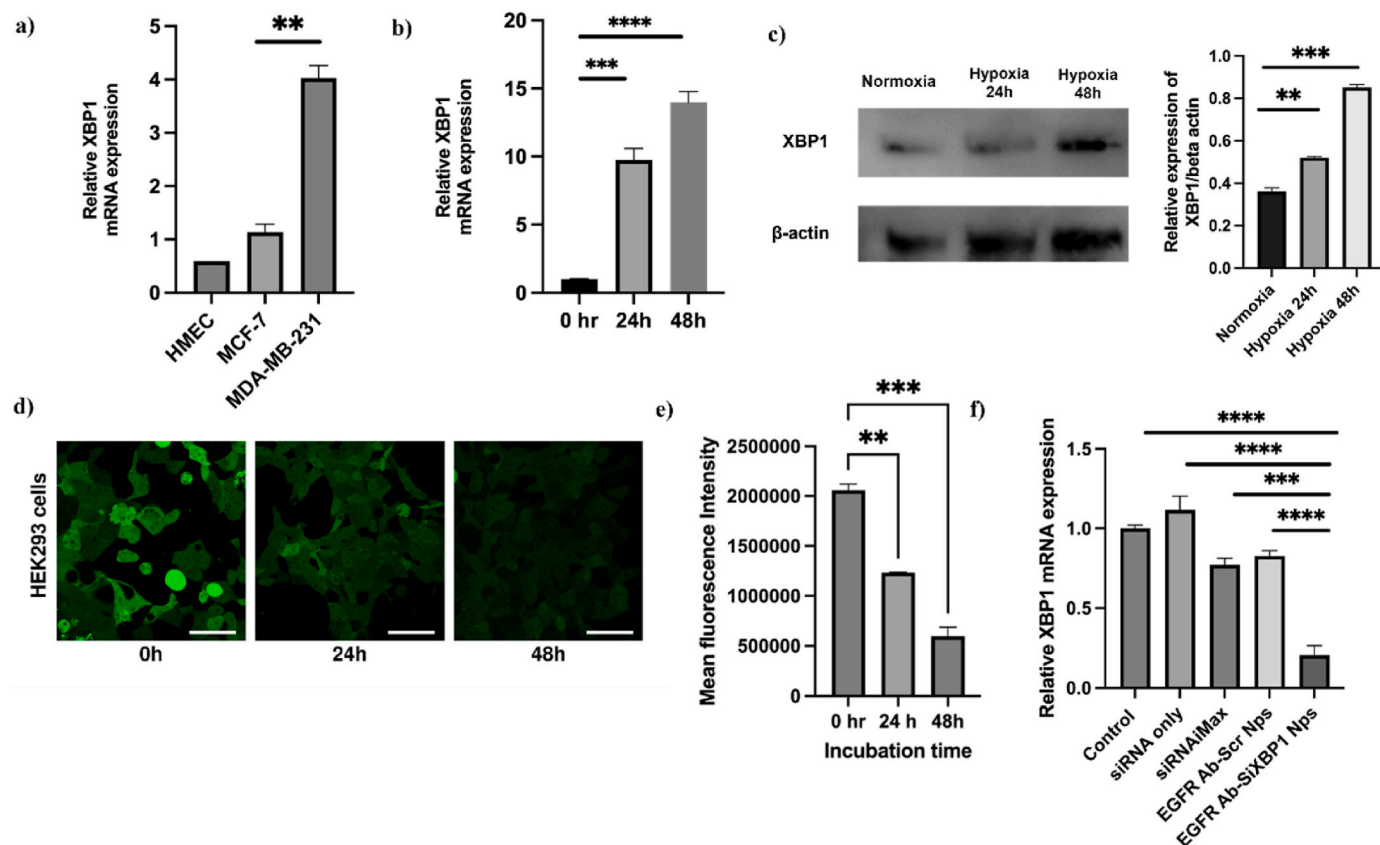
Fig. 3. a) XBP1 mRNA expression in normal and breast cancer cell lines.; b) XBP1 mRNA expression in MDA-MB-231 under hypoxic conditions; c) Western blot and densitometric analysis of XBP1 protein expression in MDA-MB-231 cells under hypoxic conditions (d) Confocal microscopic images of HEK293-EGFP cells after the treatment with 100 μg/ml of siGFP NPs, the scale bar is 50 μm; e) The mean fluorescence intensity of EGFP positive cells; f) XBP1 mRNA expression in MDA-MB-231 cells after treatment with 25 nM of naked siRNA, 200 μg/ml of EGFR Ab-siXBP1 NPs (contains 25 nM siRNA), 200 μg/ml of EGFR Ab-Scr NPs (contains 25 nM siRNA), and siXBP1 with RNAiMax (25 nM). Data represented as mean ± SEM; n = 3; **$p < 0.01$; ***$p < 0.001$; ****$p < 0.001$.

3.2. In-vitro cellular uptake study

To achieve the targeting capability of our nanoparticles on TNBC cells, we conjugated the nanoparticles with EGFR antibody. This modification specifically targets the EGFR receptor, which is known to be overexpressed in approximately 50 % of TNBC cells compared to other breast cancer subtypes [25]. This strategy was reported an effective targeting tool for TNBC cells, leading to increased cellular drug accumulation and enhanced treatment efficacy [26]. The targeting capability of antibody conjugated nanoparticles was assessed by comparing the cellular uptake of EGFR Ab-C-6 NPs and non-targeted C-6 NPs in MDA-MB-231 cells at different incubation times. Fig. 2a demonstrated the higher C-6 fluorescence signal from the cells treated by targeted nanoparticles compared with non-targeted ones. As shown in Fig. 2b, the fluorescence intensity of C-6, measured via flow cytometry, demonstrated approximately 1.26-fold and 1.45-fold higher values for EGFR Ab-C-6 NPs compared to non-targeted counterparts at 1 h and 2 h incubation times, respectively. This enhanced internalization capability of targeted nanoparticles was probably attributed to the specific affinity interaction between anti-EGFR antibody and overexpressed EGFR on the surface of cancer cells.

3.3. Assessment on in-vitro EGFP and XBP1 knockdown via nanoparticles

We first assessed XBP1 gene expression in two breast cancer cell lines, MDA-MB-231 and MCF-7, along with a normal breast cell line, HMEC. As illustrated in Fig. 3a, a significantly higher XBP1 mRNA expression was observed in MDA-MB-231 cells compared to MCF-7 and HMEC cell lines. Existing literature indicates that hypoxia triggers the activation of XBP1 expression, in conjunction with its co-regulator, HIF-1α, in TNBC tissues, thereby promotes cancer progression [10]. Thus, we investigated the effect of hypoxia on XBP1 expression in MDA-MB-231 cells. As shown in Fig. 3b, XBP1 mRNA expression apparently increased under hypoxic conditions, which was further supported by Western blot analysis (Fig. 3c).

Following the confirmation of XBP1 gene expression levels in MDA-MB-231, we evaluated the efficacy of gene knockdown using our nanoparticles. We first validated the transfection feasibility of our nanoparticles targeting EGFP in HEK293 cells. Fig. 3d demonstrates an apparent decrease in EGFP fluorescence intensity in the cells treated with 100 μg/ml of siGFP NPs for 24 and 48 h compared with the control. Flow cytometry data further revealed reductions of 42.83 % and 72 % in EGFP intensity at 24 h and 48 h post-transfection, respectively (Fig. 3e), indicating the nanoparticles are capable of effectively suppressing the EGFP gene expression. After confirming that our nanoparticles successfully delivered EGFP siRNA in HEK293 cells, we further assessed the transfection effectiveness of our formulation targeting XBP1 gene in MDA-MB-231. As shown in Fig. 3f, the assessment of XBP1 mRNA expression levels was conducted under various treatment conditions, including EGFR Ab-siXBP1 NPs, EGFR Ab-Scr NPs, siXBP1 with RNAiMax and naked siXBP1 only. Among these treatments, we noted that approximately 75 % reduction in XBP1 gene expression in MDA-MB-231 cells at 48 h after treatment with EGFR Ab-siXBP1 NPs. By contrast, the commercial transfection reagent (siXBP1 with RNAiMax) achieved only around 30 % suppression of XBP1gene expression.
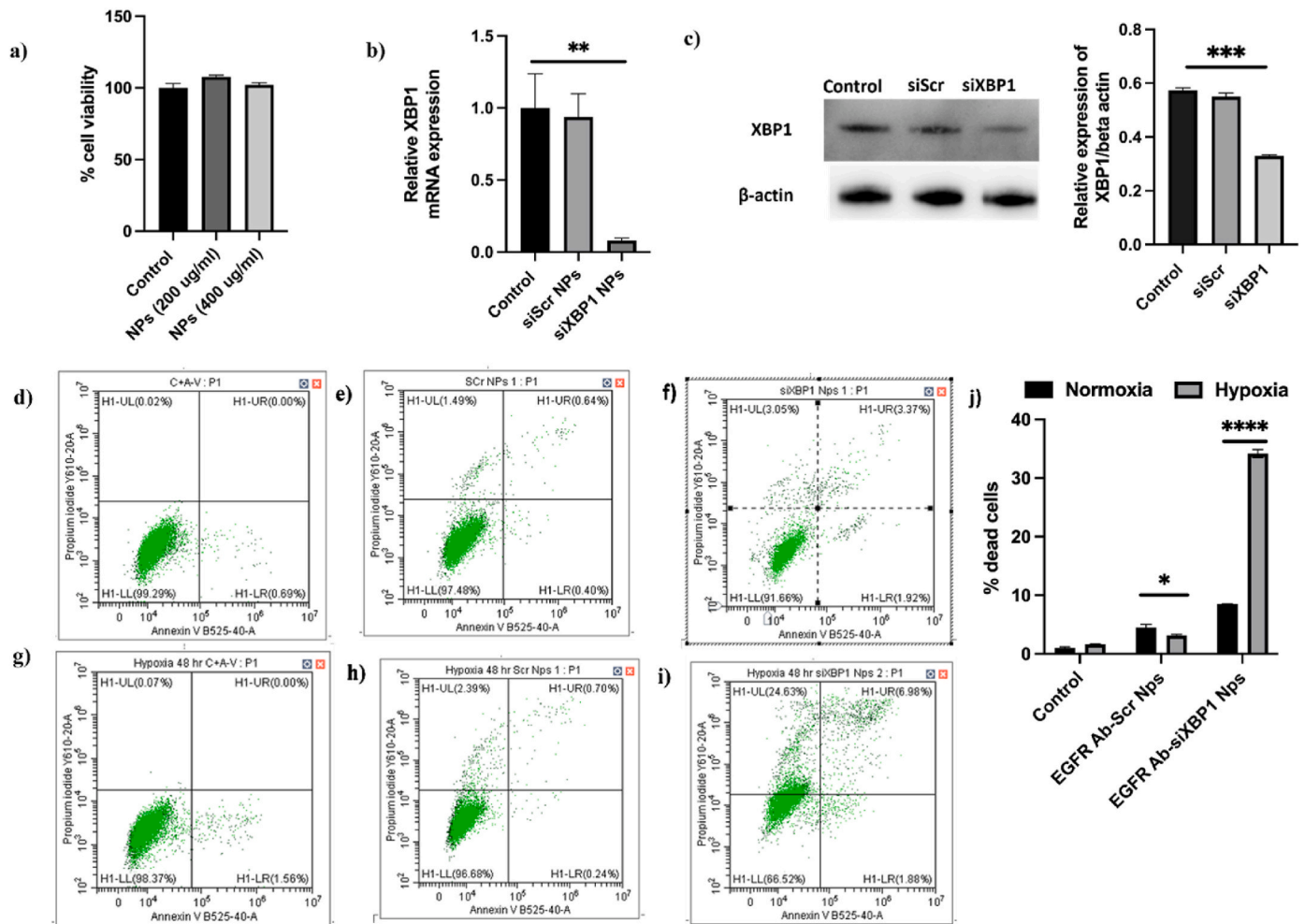
Fig. 4. a) Cell viability of MDA-MB-231 cells after treatment with different concentrations of blank PLGA lipid nanoparticles; b) XBP1 mRNA expression in MDA-MB-231 cells after treatment with 200 μg/ml of EGFR Ab-siXBP1 NPs and EGFR Ab-Scr NPs under hypoxic conditions; c) Western blot and densitometric analysis of XBP1 protein expression level after the same treatments; (d–i) FITC-Annexin V/PI flow cytometry plots of MDA-MB-231 cells after different treatments indicated in the figures; (j) Represent % of dead cells based on flow cytometry plots. Data represented as mean ± SEM; n = 3; *p < 0.1; ****p < 0.001.

3.4. Investigation of cellular apoptosis after the XBP1 gene knockdown

Before assessing the effect of XBP1 gene knockdown on cellular apoptosis, we first examined the cellular toxicity of our nanoparticles in MDA-MB-231 cells via MTT assay. As shown in Fig. 4a, no significant change in cell viability was observed when treated with blank PLGA lipid NPs at concentrations of 200 μg/ml (the concentration used for gene delivery) and even at a higher concentration of 400 μg/ml, compared with the control group. This observation indicates that our nanoparticles are unlikely to adversely impact the viability of MDA-MB-231 cells in our study.

As illustrated in Fig. 3c, hypoxia induces an upregulation in XBP1 protein expression levels. In line with this observation, we further assessed the XBP1 gene knockdown efficacy of the nanoparticles under hypoxic conditions, which are representative of the TNBC cell environment. As shown in Fig. 4b, cells treated with EGFR Ab-siXBP1 NPs demonstrated a significant reduction of approximately 90 % in XBP1 mRNA expression. Consistent with the decrease in mRNA levels, the expression level of XBP1 proteins was also reduced, as illustrated in Fig. 4c.

Furthermore, an apoptosis and necrosis assay were conducted to determine the impact of XBP1 gene silencing on the cell death pathways. As displayed in Fig. 4f and j, the cells treated with EGFR Ab-siXBP1 NPs under normal conditions exhibited low-level apoptosis and necrosis,

only being 7 ± 1.9 %. This indicated that XBP1 gene knockdown showed negligible cytotoxicity to cancer cells under normal conditions. However, the higher percentage of dead cells was observed when the EGFR Ab-siXBP1 NP treatment occurred under hypoxic conditions, being 34 ± 2.4 % (Fig. 4i and j). Correspondingly, the percentage of healthy cells in this group reduced to about 66 ± 2.6 %, compared to the control group (98.37 ± 1.2 %, Fig. 4j). Collectively, these findings suggest that the percentage of dead cells following XBP1 gene knockdown increases nearly threefold when cells are exposed to a hypoxic microenvironment compared to normal conditions.

4. Discussion

TNBC, marked by the absence of ER, PR, and HER2 expression, display insensitivity to endocrine therapy and HER2-targeted treatments, which led to a major challenge in developing a safe and effective treatment for TNBC [27,28]. Recent studies have discovered the critical role of the unfolded protein response (UPR) regulator XBP1 in fostering tumorigenesis and recurrence specifically in TNBC, making it a potential therapeutic target to treat TNBC [10]. The primary obstacle for targeting XBP1 in TNBC cells was mainly focused on achieving both efficient gene knockdown and specificity for TNBC cells [28]. To address this issue, this study focused on developing and investigating the effectiveness of PLGA lipid nanoparticles in knocking down XBP1 specifically in TNBC

cells.

We successfully developed and characterized the lipid-polymer nanoparticles. We optimized their size, zeta potential, and surface morphology to ensure their suitability for targeted delivery. We achieved a high entrapment efficiency of siRNA in our nanoparticles, a critical factor for effective gene silencing. Furthermore, the successful conjugation of EGFR antibodies to these nanoparticles enables their enhanced cellular uptake activity in TNBC cells, as demonstrated in Fig. 2. This enhanced cellular uptake aligns with prior research reporting the effectiveness of EGFR-conjugated nanoparticles in targeting to breast cancer cells [29]. Importantly, our findings in Fig. 4a demonstrate that these nanoparticles did not induce toxicity in MDA-MB-231 cells. This delivery system has demonstrated higher XBP1 transfection efficacy in MDA-MB-231 cells compared with commercial alternatives (Fig. 3f). These nanoparticles (25 nM) resulted in approximately 75 % XBP1 gene knockdown in MDA-MB-231 cells at 48 h post-transfection, whereas commercial transfection reagents achieved only around 30 % reduction of XBP1 gene expression. These results were consistent with other reported research, where approximately 80–85 % XBP1 gene knockdown efficacy was achieved using antibody-conjugated siXBP1-loaded nanoparticles [30,31]. We particularly focused on the gene silencing efficacy under hypoxic environment, a condition known to induce cancer cell metabolic adaptation, survival, and therapy resistance [10]. Our results revealed that our nanoparticles achieved a significant reduction in XBP1 mRNA expression of approximately 90 % even under the challenging hypoxic environment (Fig. 4b).

Apoptosis is a crucial pathway leading to the cancer cell death specifically under hypoxic condition. We found out that XBP1 silencing did not alter cell apoptosis under normal conditions (Fig. 4d–f), which aligns with previously reported studies [30,31]. However, in hypoxic conditions where XBP1 expression is upregulated (Fig. 3b), we noted a significant increase in apoptosis upon XBP1 gene silencing, with nearly a threefold increase in the number of apoptotic cells compared to normoxic conditions (Fig. 4j). This observation is consistent with the findings reported by another research group who investigated XBP1's role in tumor survival under hypoxia conditions [32].

5. Conclusion

To sum up, our study demonstrated the *in vitro* XBP1 gene silencing efficacy by using the targeted nanoparticles loaded with siRNA, thus promoting apoptosis in the challenging hypoxic conditions. These findings provide a strong foundation for advancing a safe and innovative TNBC treatment. Future investigations should prioritize *in vivo* studies to validate the efficacy and safety of this approach, bringing it one step closer to clinical applications.

CRediT authorship contribution statement

Meenu Mehta: Writing – review & editing, Writing – original draft, Validation, Methodology, Investigation, Formal analysis, Data curation, Conceptualization. **Thuy Anh Bui:** Writing – review & editing, Visualization, Investigation, Formal analysis, Data curation. **Andrew Care:** Writing – review & editing, Visualization, Supervision, Resources, Project administration. **Wei Deng:** Writing – review & editing, Visualization, Supervision, Resources, Project administration, Funding acquisition.

Declaration of competing interest

The authors declare that they have no known competing financial interests or personal relationships that could have appeared to influence the work reported in this paper.

Data availability

Data will be made available on request.

References

[1] N.M. Almansour, Triple-negative breast cancer: a brief review about epidemiology, risk factors, signaling pathways, treatment and role of artificial intelligence, Front. Mol. Biosci. 9 (2022).

[2] M. Bou Zerdan, et al., Triple negative breast cancer: updates on classification and treatment in 2021, Cancers 14 (5) (2022).

[3] Y. Li, et al., Recent advances in therapeutic strategies for triple-negative breast cancer, J. Hematol. Oncol. 15 (1) (2022) 121.

[4] Q. Wu, et al., Multi-drug resistance in cancer chemotherapeutics: mechanisms and lab approaches, Cancer Lett. 347 (2) (2014) 159–166.

[5] J.J. Tao, K. Visvanathan, A.C. Wolff, Long term side effects of adjuvant chemotherapy in patients with early breast cancer, Breast 24 (0 2) (2015) S149–S153. Suppl 2.

[6] Y.J. Cheng, et al., Long-Term cardiovascular risk after radiotherapy in women with breast cancer, J. Am. Heart Assoc. 6 (5) (2017).

[7] S. Chen, et al., The emerging role of XBP1 in cancer, Biomed. Pharmacother. 127 (2020) 110069.

[8] Y. He, et al., Emerging roles for XBP1, a sUPeR transcription factor, Gene Expr. 15 (1) (2010) 13–25.

[9] W. Shi, et al., Unravel the molecular mechanism of XBP1 in regulating the biology of cancer cells, J. Cancer 10 (9) (2019) 2035–2046.

[10] X. Chen, et al., XBP1 promotes triple-negative breast cancer by controlling the HIF1α pathway, Nature 508 (7494) (2014) 103–107.

[11] N. Srivastava, et al., Hypoxia: syndicating triple negative breast cancer against various therapeutic regimens, Front. Oncol. 13 (2023) 1199105.

[12] L. Romero-Ramirez, et al., XBP1 is essential for survival under hypoxic conditions and is required for tumor growth, Cancer Res. 64 (17) (2004) 5943–5947.

[13] N. McCarthy, Hypoxia and XBP1S, Nat. Rev. Cancer 14 (5) (2014) 295, 295.

[14] N.B. Charbe, et al., Small interfering RNA for cancer treatment: overcoming hurdles in delivery, Acta Pharm. Sin. B 10 (11) (2020) 2075–2109.

[15] W. Ngamcherdtrakul, W. Yantasee, siRNA therapeutics for breast cancer: recent efforts in targeting metastasis, drug resistance, and immune evasion, Transl. Res. 214 (2019) 105–120.

[16] Y. Yao, et al., Nanoparticle-based drug delivery in cancer therapy and its role in overcoming drug resistance, Front. Mol. Biosci. 7 (2020) 193.

[17] L. Wang, B. Griffel, X. Xu, Synthesis of PLGA-lipid hybrid nanoparticles for siRNA delivery using the emulsion method PLGA-PEG-lipid nanoparticles for siRNA delivery, Methods Mol. Biol. 1632 (2017) 231–240.

[18] D.K. Jensen, et al., Design of an inhalable dry powder formulation of DOTAP-modified PLGA nanoparticles loaded with siRNA, J. Contr. Release 157 (1) (2012) 141–148.

[19] D. Sivadasan, et al., Polymeric lipid hybrid nanoparticles (PLNs) as emerging drug delivery platform-A comprehensive review of their properties, preparation methods, and therapeutic applications, Pharmaceutics 13 (8) (2021).

[20] T.O. Nielsen, et al., Immunohistochemical and clinical characterization of the basal-like subtype of invasive breast carcinoma, Clin. Cancer Res. 10 (16) (2004) 5367–5374.

[21] J.H. Mortensen, et al., Targeted antiepidermal growth factor receptor (cetuximab) immunoliposomes enhance cellular uptake in vitro and exhibit increased accumulation in an intracranial model of glioblastoma multiforme, J Drug Deliv 2013 (2013) 209205.

[22] D.C. Rio, et al., Purification of RNA using TRIzol (TRI reagent), Cold Spring Harb. Protoc. 2010 (6) (2010) pdb prot5439.

[23] M. Danaei, et al., Impact of particle size and polydispersity index on the clinical applications of lipidic nanocarrier systems, Pharmaceutics 10 (2) (2018).

[24] F. Fang, et al., EGFR-targeted hybrid lipid nanoparticles for chemo-photothermal therapy against colorectal cancer cells, Chem. Phys. Lipids 251 (2023) 105280.

[25] H. Masuda, et al., Role of epidermal growth factor receptor in breast cancer, Breast Cancer Res. Treat. 136 (2) (2012) 331–345.

[26] S. Acharya, F. Dilnawaz, S.K. Sahoo, Targeted epidermal growth factor receptor nanoparticle bioconjugates for breast cancer therapy, Biomaterials 30 (29) (2009) 5737–5750.

[27] W.D. Foulkes, I.E. Smith, J.S. Reis-Filho, Triple-negative breast cancer, N. Engl. J. Med. 363 (20) (2010) 1938–1948.

[28] L. Yin, et al., Triple-negative breast cancer molecular subtyping and treatment progress, Breast Cancer Res. 22 (1) (2020) 61.

[29] J. Gao, et al., The promotion of siRNA delivery to breast cancer overexpressing epidermal growth factor receptor through anti-EGFR antibody conjugation by immunoliposomes, Biomaterials 32 (13) (2011) 3459–3470.

[30] L. Zhang, et al., Systemic delivery of aptamer-conjugated XBP1 siRNA nanoparticles for efficient suppression of HER2+ breast cancer, ACS Appl. Mater. Interfaces 12 (29) (2020) 32360–32371.

[31] L. Zhang, et al., Development of targeted therapy therapeutics to sensitize triple-negative breast cancer chemosensitivity utilizing bacteriophage phi29 derived packaging RNA, J. Nanobiotechnol. 19 (1) (2021) 13.

[32] L. Romero-Ramirez, et al., XBP1 is essential for survival under hypoxic conditions and is required for tumor growth, Cancer Res. 64 (17) (2004) 5943–5947.

SHORT COMMUNICATION

Journal of **Food Biochemistry**

WILEY

Berberine loaded liquid crystalline nanostructure inhibits cancer progression in adenocarcinomic human alveolar basal epithelial cells in vitro

Meenu Mehta[1,2,3] (iD) | Vamshikrishna Malyla[1,2,3] (iD) | Keshav R. Paudel[2,4] (iD) | Dinesh Kumar Chellappan[5] (iD) | Philip M. Hansbro[2,4] (iD) | Brian G. Oliver[4,6] (iD) | Kamal Dua[1,2,3] (iD)

[1]Discipline of Pharmacy, Graduate School of Health, University of Technology Sydney, Sydney, New South Wales, Australia

[2]Centre for Inflammation, Centenary Institute, Sydney, New South Wales, Australia

[3]Faculty of Health, Australian Research Centre in Complementary and Integrative Medicine, University of Technology Sydney, Ultimo, New South Wales, Australia

[4]School of Life Sciences, University of Technology Sydney, Sydney, New South Wales, Australia

[5]Department of Life Sciences, School of Pharmacy, International Medical University, Kuala Lumpur, Malaysia

[6]Woolcock Institute of Medical Research, University of Sydney, Sydney, New South Wales, Australia

Correspondence
Kamal Dua, Discipline of Pharmacy, Graduate School of Health, University of Technology Sydney, Ultimo NSW 2007, Australia.
Email: Kamal.Dua@uts.edu.au

Abstract

Metastasis represents the leading cause of death in lung cancer patients. C-X-C Motif Chemokine Ligand 8 (CXCL-8), Chemokine (C-C motif) ligand 20 (CCL-20) and heme oxygenase −1 (HO-1) play an important role in cancer cell proliferation and migration. Berberine is an isoquinoline alkaloid isolated from several herbs in the Papaveraceae family that exhibits anti-i nflammatory, anticancer and antidiabetic properties. Therefore, the aim of present study is to investigate the inhibitory potential of ber-berine monoolein loaded liquid crystalline nanoparticles (berberine-LCNs) against cancer progression. Berberine-LCNs were prepared by mixing berberine, monoolein and poloxamer 407 (P407) using ultrasonication method. A549 cells were treated

with or without 5 μM dose of berberine LCNs for 24 hr and total cellular protein was extracted and further analyzed for the protein expression of CCl-20, CXCL-8 and HO-1 using human oncology array kit. Our results showed that berberine-LCNs significantly reduced the expression of CCl-20, CXCL-8 and HO-1 at dose of 5μM. Collectively, our findings suggest that berberine-LCNs have inhibitory effect on in-flammation/oxidative stress related cytokines i.e. CCL20, CXCL-8, and HO-1 which could be a novel therapeutic target for the management of lung cancer.